

Document No. 69SD4372

January 15, 1970

# GRAVITY GRADIENT STABILIZATION SYSTEM

for the

## APPLICATIONS TECHNOLOGY SATELLITE



**N70-34278**

FACILITY FORM 602	(ACCESSION NUMBER)	(THRU)
	241	1
	(PAGES)	(CODE)
	CR-109849	21
(NASA CR OR TMX OR AD NUMBER)		(CATEGORY)

**FINAL TECHNICAL REPORT**  
**Hardware Development and Test**  
**VOLUME II**

**Book 2**

**GENERAL ELECTRIC**

Reproduced by  
**NATIONAL TECHNICAL  
INFORMATION SERVICE**  
Springfield, Va., 22151

DOCUMENT NO. 69SD4372  
JANUARY 15, 1970

FINAL REPORT  
FOR THE  
APPLICATIONS TECHNOLOGY SATELLITE  
GRAVITY GRADIENT  
STABILIZATION SYSTEM  
VOLUME II  
HARDWARE DEVELOPMENT AND TEST

CONTRACT NO. NAS 5-9042  
FOR THE  
NATIONAL AERONAUTICS AND SPACE ADMINISTRATION  
R.W. WIRTH  
ATS TECHNICAL OFFICER

APPROVED BY:   
R.E. CLAYTON  
ATS-E PROGRAM MANAGER

**GENERAL  ELECTRIC**

SPACE SYSTEMS ORGANIZATION  
Valley Forge Space Center  
P. O. Box 8555 • Philadelphia, Penna. 19101

# TABLE OF CONTENTS

<u>Section</u>		<u>Page</u>
1	GRAVITY GRADIENT STABILIZATION SYSTEMS	
	DESIGN AND DEVELOPMENT . . . . .	1-1
1.1	Volume II Contents . . . . .	1-1
1.2	Hardware Summary . . . . .	1-1
1.3	Deliverable Hardware End Items . . . . .	1-12
1.3.1	Thermal Model . . . . .	1-12
1.3.2	Dynamic Model . . . . .	1-13
1.3.3	Engineering Units . . . . .	1-14
1.3.4	Prototype Units . . . . .	1-14
1.3.5	Flight System . . . . .	1-14
1.4	Field and Flight Support . . . . .	1-15
2	BOOM SUBSYSTEM . . . . .	2-1
2.1	Introduction . . . . .	2-1
2.2	Engineering Development . . . . .	2-5
2.2.1	Major Subcontract . . . . .	2-5
2.2.2	Interface Considerations . . . . .	2-5
2.2.3	150-Foot Rod Considerations . . . . .	2-8
2.2.4	Motor Selection . . . . .	2-9
2.2.5	Potentiometer Boom Length Indicator . . . . .	2-9
2.2.6	Boom Electrical Isolation . . . . .	2-10
2.2.7	Tip Target Configuration . . . . .	2-10
2.2.8	Release Monitor . . . . .	2-10
2.2.9	Design Details . . . . .	2-11
2.2.10	Test Program . . . . .	2-17
2.2.11	Damper Boom Digitation Program . . . . .	2-43
2.2.12	Summary and Conclusion of Development Program . . . . .	2-48
2.3	Qualification Tests Primary Boom . . . . .	2-51
2.3.1	Component Qualification Primary Boom . . . . .	2-51
2.3.2	System Qualification, Primary Boom . . . . .	2-51
2.4	Flight Acceptance, Primary Boom . . . . .	2-53
2.4.1	ATS-A . . . . .	2-53
2.4.2	ATS-D . . . . .	2-54
2.4.3	ATS-E . . . . .	2-55
2.5	Qualification Tests, Damper Boom . . . . .	2-56
2.5.1	Component Qualification, Damper Boom . . . . .	2-57
2.5.2	System Qualification, Damper Boom . . . . .	2-57

## TABLE OF CONTENTS (CONT'D)

<u>Section</u>	<u>Page</u>
2.6 Flight Acceptance, Damper Boom. . . . .	2-58
2.6.1 ATS-A . . . . .	2-58
2.6.2 ATS-D . . . . .	2-58
2.6.3 ATS-E . . . . .	2-59
 3 COMBINATION PASSIVE DAMPER . . . . .	 3-1
3.1 Purpose of the CPD . . . . .	3-1
3.2 Engineering Development . . . . .	3-2
3.2.1 CPD Unit Nomenclature . . . . .	3-2
3.2.2 CPD Description . . . . .	3-2
3.2.3 Details of Major Subsystems . . . . .	3-13
3.2.4 Test Equipment . . . . .	3-71
3.2.5 Test Results . . . . .	3-75
3.2.6 Other Significant Test Results . . . . .	3-79
3.2.7 Testing General . . . . .	3-81
3.2.8 Conclusions and Recommendations of Engineering Development . . . . .	 3-85
3.2.9 Chronological Summary of CPD Design . . . . .	3-86
3.2.10 Drawings and Specifications . . . . .	3-91
3.3 Qualification Tests . . . . .	3-93
3.3.1 Component Qualification . . . . .	3-94
3.3.2 System Qualification . . . . .	3-94
3.4 Flight Acceptance . . . . .	3-95
3.4.1 ATS-A . . . . .	3-95
3.4.2 ATS-D . . . . .	3-95
3.4.3 ATS-E . . . . .	3-96
3.5 Reference List . . . . .	3-96
3.5.1 Component History Documents . . . . .	3-96
3.5.2 Quarterly Progress Reports . . . . .	3-97
3.5.3 Other Pertinent Documents . . . . .	3-97
 4 TV CAMERA SYSTEM . . . . .	 4-1
4.1 Introduction . . . . .	4-1
4.2 Engineering Development . . . . .	4-1
4.2.1 General . . . . .	4-1
4.2.2 Electrical . . . . .	4-4
4.2.3 Mechanical . . . . .	4-14
4.2.4 Engineering Test Program . . . . .	4-18
4.2.5 Summary and Conclusions of TV Camera Development . . . . .	 4-26



## TABLE OF CONTENTS (CONT'D)

<u>Section</u>	<u>Page</u>
4.3 Qualification Tests, TV Camera . . . . .	4-27
4.3.1 Component Qualification . . . . .	4-27
4.3.2 System Qualification . . . . .	4-28
4.4 Flight Acceptance Tests, TV Camera . . . . .	4-28
4.4.1 ATS-A . . . . .	4-29
4.4.2 ATS-D . . . . .	4-29
4.4.3 ATS-E . . . . .	4-30
 5 SOLAR ASPECT SENSOR . . . . .	 5-1
5.1 Introduction . . . . .	5-1
5.1.1 Purpose . . . . .	5-1
5.1.2 Description . . . . .	5-1
5.1.3 Principle of Operation. . . . .	5-2
5.2 Engineering Development. . . . .	5-8
5.2.1 Source Selection. . . . .	5-8
5.2.2 Operating Characteristics . . . . .	5-8
5.2.3 Mechanical Considerations . . . . .	5-12
5.2.4 Electrical Considerations . . . . .	5-13
5.2.5 Engineering Test Program . . . . .	5-14
5.2.6 Conclusions . . . . .	5-29
5.3 Qualification . . . . .	5-29
5.3.1 Component Qualification . . . . .	5-30
5.4 Flight Acceptance . . . . .	5-30
5.5 Applicable Documents. . . . .	5-33
5.6 List of Reference . . . . .	5-35
 6 Power Control Unit. . . . .	 6-1
6.1 Purpose and Function . . . . .	6-1
6.2 Engineering Development . . . . .	6-2
6.2.1 Mechanical Considerations . . . . .	6-2
6.2.2 Electrical Considerations . . . . .	6-5
6.2.3 Optimization Program . . . . .	6-14
6.2.4 Engineering Tests and Results . . . . .	6-17
6.3 Qualification . . . . .	6-44
6.3.1 Component Qualification . . . . .	6-45
6.3.2 System Qualification . . . . .	6-45
6.4 Flight Acceptance . . . . .	6-45

## TABLE OF CONTENTS (CONT'D)

<u>Section</u>	<u>Page</u>
7	RF ATTITUDE SENSOR . . . . . 7-1
7.1	Introduction . . . . . 7-1
7.2	Electrical Design . . . . . 7-2
7.2.1	75.76 MHz IF Amplifier . . . . . 7-4
7.2.2	IF Filter . . . . . 7-6
7.2.3	IF Amplifier - Detector . . . . . 7-7
7.2.4	Video Filter . . . . . 7-8
7.2.5	Limiters . . . . . 7-10
7.2.6	Acquisition Control . . . . . 7-10
7.2.7	Sweep Circuit . . . . . 7-12
7.2.8	Frequency Multiplier . . . . . 7-14
7.2.9	2.56 MHz Oscillator . . . . . 7-22
7.2.10	Digital Processing . . . . . 7-24
7.2.11	256 Divider and Phase Detector . . . . . 7-26
7.2.12	Video Telemetry Circuit . . . . . 7-31
7.2.13	Power Supply. . . . . 7-35
7.3	Mechanical Design . . . . . 7-37
7.3.1	RF Assembly. . . . . 7-41
7.3.2	RF Support . . . . . 7-41
7.3.3	Varactor Chain . . . . . 7-41
7.3.4	Base plate . . . . . 7-42
7.3.5	Cover . . . . . 7-42
7.3.6	Modules . . . . . 7-42
7.3.7	Equipment Plates . . . . . 7-44
7.3.8	Equipment Plate Subassemblies . . . . . 7-44
8	QUALITY CONTROL AND TEST . . . . . 8-1
9	RELIABILITY . . . . . 9-1
9-1	Introduction and Summary . . . . . 9-1
9.2	Summary of Significant Activities and Accomplishments . . . . . 9-2
9.3	Systems Reliability Assessment . . . . . 9-5
9.4	Discussion of Test Failure History . . . . . 9-6
10	MATERIALS AND PROCESSES . . . . . 10-1

## TABLE OF CONTENTS (CONT'D)

<u>Section</u>	<u>Page</u>
11	MANUFACTURING . . . . . 11-1
	11.1 Controlled Environmental Area . . . . . 11-1
	11.2 Materials Laboratory . . . . . 11-1
	11.3 Electronics Shop . . . . . 11-1
	11.4 Machine Shop. . . . . 11-2
12	PARTS PROGRAM . . . . . 12-1
13	NEW TECHNOLOGIES . . . . . 13-1
	13.1 Angle Indicator . . . . . 13-2
	13.2 Angle Indicator Readout Device . . . . . 13-3
	13.3 CPD Clutch Mechanism . . . . . 13-3

## LIST OF ILLUSTRATIONS

<u>Figure</u>		<u>Page</u>
1-1	ATS Gravity Gradient Hardware. . . . .	1-4
1-2	Packaging Arrangement for the ATS-A System. . . . .	1-5
2-1	STEM Principle . . . . .	2-2
2-2	Primary Boom Assembly (1/2 system) . . . . .	2-4
2-3	Damper Boom with Linear Actuator at Right . . . . .	2-4
2-4	Gravity Gradient Rod Sample. . . . .	2-11
2-5	Primary Boom Assembly Schematic (1/2 system). . . . .	2-12
2-6	Primary Boom Package Locations Showing Scissoring Pivots . . . . .	2-14
2-7	Scissoring Linkage Seal, Primary Boom System . . . . .	2-16
2-8	Damper Boom Schematic . . . . .	2-21
2-9	Damper Boom Ball Lock Release Scheme . . . . .	2-22
2-10	Boom Straightness Measuring Tank (left), Boom Deployment Track (right) . . . . .	2-28
2A-1	Damper Boom Straightness Profile . . . . .	2-66
3-1	Combination Passive Damper Schematic . . . . .	3-3
3-2	Combination Passive Damper for ATS. . . . .	3-3
3-3	Combination Passive Damper Package Elevation View . . . . .	3-4
3-4	Combination Passive Damper Package Plan View . . . . .	3-5
3-5	CPD Engineering Unit Assembled (Cover Removed) and T-1 Damper Boom Package in Place . . . . .	3-11
3-6	Details of CPD Engineering Unit 1 . . . . .	3-11
3-7	Baseplate and Caging Mechanism of CPD Engineering Unit 1 with Damper Boom Package in Place . . . . .	3-12
3-8	Caging Cable and Baseplate (with Pyrotechnic Device 2) After Uncaging Operation, CPD Engineering Unit 1 . . . . .	3-13
3-9	Flux Density Measurements . . . . .	3-15
3-10	Flux Density Measurements Effect of Pole Pieces. . . . .	3-15
3-11	Magnetic Arrangement of Single and Double Penetration. . . . .	3-17
3-12	Force on Diamagnetic Specimen in Non-Uniform Field . . . . .	3-22
3-13	Eddy Current Damper Suspension System Schematic . . . . .	3-22
3-14	Diamagnetic Suspension Characteristic . . . . .	3-25
3-15	Suspension Load Capacity vs. Initial Air Gap Setting. . . . .	3-27
3-16	Torque Angle Characteristics for Bismuth and Various Thicknesses of Pyrolytic Graphite . . . . .	3-28
3-17	Definition of Magnet Side . . . . .	3-29
3-18	Energy Dissipation by Eddy Current and Hysteresis in Torsional Restraint vs. Amplitude of Oscillation (ATS-A Eddy Current Damper) . . . . .	3-35

# LIST OF ILLUSTRATIONS (CONT'D)

<u>Figure</u>		<u>Page</u>
3-19	Passive Hysteresis Damper for ATS-D/E Configuration (Engineering Unit No. 2). . . . .	3-38
3-20	Passive Hysteresis Damper Details. . . . .	3-39
3-21	Passive Hysteresis Damper Suspension System, ATS-D/E Configuration . . . . .	3-40
3-22	Wire Attachment to End Flexure. . . . .	3-40
3-23	Idealized Damping Curves for Original PHD and VTHD (Torsional Restrain Omitted) . . . . .	3-41
3-24	CPD Clutch Mechanism. . . . .	3-49
3-25	Force vs. Displacement for Square Fluted Diaphragm (0.014 in. beryllium copper) . . . . .	3-51
3-26	Two-Way Clutch Solenoid Specification Sheet. . . . .	3-52
3-27	CPD Solenoid Section . . . . .	3-53
3-28	Force vs. Travel Test Results for Engineering Solenoid Unit .	3-54
3-29	Deep Indentation at Edge of V-Groove Caused by Detent Ball in ECD Mode . . . . .	3-56
3-30	Encoder Disc for Angle Indicator . . . . .	3-58
3-31	Angle Indicator Head Assembly . . . . .	3-60
3-32	Typical Angle Indicator Bit Circuit . . . . .	3-60
3-33	Angle Indicator Assembly in Test Fixture. . . . .	3-61
3-34	Angle Indicator Assembly Exploded View . . . . .	3-61
3-35	Angle Indicator Thermal Test Results (Average of Two Modules) . . . . .	3-64
3-36	Original Encoder Disc Design. . . . .	3-66
3-37	New Encoder Disc Design . . . . .	3-66
3-38	Caging Cable Calibration Results . . . . .	3-69
3-39	Eddy Current Caging Torque Test Results . . . . .	3-69
3-40	Advanced Damping Test Fixture (ADTF) . . . . .	3-73
3-41	Low Order Force Fixture (LOFF) . . . . .	3-74
4-1	TV Camera System (l to r) Electronics, Camera and Mounting Bracket (Engineering Unit 5101) . . . . .	4-3
4-2	Electronics Unit Details . . . . .	4-2
4-3	Camera (Engineering Unit 5101) . . . . .	4-4
4-4	Vidicon Heater Current vs. Telemetry Output Voltage . . .	4-7
4-5	Vidicon Target Supply Voltage vs. Telemetry Output Voltage .	4-7
4-6	Temperature vs. Telemetry Output Voltage . . . . .	4-8
4-7	TV Camera Model 0431F Block Diagram . . . . .	4-8
4-8	TV Camera Schematic (Lear Siegler Dwg. 124901). . . . .	4-9
4-9	TV Camera Assembly (GE Dwg. 47D209695). . . . .	4-15
4-10	Control Unit Assembly (GE Dwg. 47D207485) . . . . .	4-19

# LIST OF ILLUSTRATIONS (CONT'D)

<u>Figure</u>		<u>Page</u>
5-1	Solar Aspect Sensor Electronics (r) and Typical Detector	5-1
5-2	SAS Detector Orientation . . . . .	5-2
5-3	Sensor Pictorial Representation . . . . .	5-3
5-4	Solar Aspect Sensor Logic Diagram. . . . .	5-5
5-5	SAS Detector Alignment Geometry . . . . .	5-9
5-6	Crosscoupling Effects on Bit Output. . . . .	5-10
5-7	SAS Termination Circuit . . . . .	5-13
5-8	Optical Alignment Setup. . . . .	5-15
5-9	Nulling Circuit. . . . .	5-16
5-10	Reticle 1 AGC and B1 Test Results . . . . .	5-17
5-11	Reticle 1, Bit 2 Test Results . . . . .	5-17
5-12	Reticle 1, Bits 4 and 5 Test Results . . . . .	5-18
5-13	Reticle 1, Bits 6, 7, and 8 Test Results . . . . .	5-18
5-14	Transition Edge Error vs. True Transition Position (Reticle 1, Bit 1) . . . . .	5-19
5-15	Transition Edge Error vs. Transition Position (Reticle 1, Bit 2) . . . . .	5-19
5-16	Transition Edge Error vs. True Transition Position (Reticle 1, Bits 3 and 4). . . . .	5-20
5-17	Translation Edge Error vs. True Translation Position (Reticle 1, Bits 5, 6, 7, and 8) . . . . .	5-20
5-18	SAS Detector and Test Fixture . . . . .	5-24
5-19	Sensed Angle Geometry. . . . .	5-25
5-20	Theoretical Value vs. Actual Readout . . . . .	5-26
5-21	SAS Solar-Vacuum Test in 5- by 6-foot Chamber . . . . .	5-28
5-22	Test Profile Temperature Excursion . . . . .	5-28
5B-1	GE 5000-watt Xenon Compact Arc Lamp . . . . .	A2-2
5B-2	Solar Cell Relative Spectral Response . . . . .	A2-2
5B-3	Fused Quartz Index of Refraction . . . . .	A2-3
5B-4	Product of Solar Spectrum and Silicon Solar Cell Response . . . . .	A2-4
5B-5	Product of Xenon Spectrum . . . . .	A2-4
5C-1	SAS Test Console. . . . .	A3-2
5C-2	Detector Simulation Circuit . . . . .	A3-3
5C-3	AGC Cell Output Simulation . . . . .	A3-3
5C-4	Diode Leakage Measuring Circuit . . . . .	A3-4
5C-5	Output Current Measuring Circuit . . . . .	A3-5
5C-6	Detector Monitoring Circuit . . . . .	A3-5

# LIST OF ILLUSTRATIONS (CONT'D)

<u>Figure</u>		<u>Page</u>
6-1	Power Control Unit, Prototype Hardware . . . . .	6-3
6-2	PCU Wiring Boards for the First Flight Unit Shown During Assembly. . . . .	6-4
6-3	Power Control Unit Schematic (GE Dwg. 47J207904) . . . .	6-7
6-4	Thermal Test Chamber Temperature. . . . .	6-18
6-5	Thermal Test Power Supply Module Temperature . . . .	6-19
6-6	Thermal Test, R53 Temperature . . . . .	6-19
6-7	Thermal Test, R20 Heat Sink Temperature . . . . .	6-20
6-8	Thermal Test, Field Driver Scissor B Temperature . . .	6-20
6-9	Thermal Test, Q22 Heat Sink Temperature (Armature Scissor B) . . . . .	6-21
6-10	Thermal Test, R24 Heat Sink Temperature. . . . .	6-21
6-11	PCU Mounting Surface Temperature vs. Time. . . . .	6-23
6-12	Squib Driver A9 Output Transistor Temperature vs. Time .	6-23
6-13	Hysteresis Driver Transistor Q2 Temperature vs. Time . .	6-24
6-14	Hysteresis Driver Q1 Transistor Temperature vs. Time . .	6-24
6-15	A18 Field Driver Scissor B Temperature vs. Time . . . .	6-25
6-16	Temperature of Heat Sink Beside Q22 (Output of Mod A19) vs. Time . . . . .	6-25
6-17	A19 Scissor B Armature Driver Transistor Temperature vs. Time . . . . .	6-26
6-18	R53 (Detector Lamp Circuit) Resistor Temperature vs. Time . . . . .	6-26
6-19	Solenoid Driver Transistor Saturation Voltage vs. Input Voltage Hysteresis Damper . . . . .	6-29
6-20	Solenoid Driver Transistor Saturation Voltage vs. Input Voltage, Rod B Emergency . . . . .	6-29
6-21	Hysteresis Damper Solenoid Driver Test Circuit. . . . .	6-32
6-22	Motor Field Driver Transistor Saturation Voltage vs. Input Voltage, Rod B Field Driver. . . . .	6-35
6-23	Field Driver Test Circuit . . . . .	6-36
6-24	Line Voltage Drop Determining Circuit . . . . .	6-37
6-25	Motor Armature Driver Saturation Voltage vs. Input Voltage Rod A Motor Armature Driver . . . . .	6-39
6-26	-5 Volt Power Supply vs. Load at Nominal Voltage . . . .	6-41
6-27	-5 Volt Power Supply Output vs. Input Voltage (650-ohm Load) . . . . .	6-41
6-28	Squib Driver Pulse Width vs. Input Voltage . . . . .	6-43
6-29	Squib Driver Load Current vs. Input Voltage . . . . .	6-43
6-30	Squib Driver Delay Time vs. Input Voltage. . . . .	6-44

# LIST OF ILLUSTRATIONS (CONT'D)

<u>Figure</u>		<u>Page</u>
7-1	RF Attitude Sensor Mockup . . . . .	7-3
7-2	RF Attitude Sensor Block Diagram . . . . .	7-3
7-3	75.76 MHz IF Schematic . . . . .	7-5
7-4	Receiver IF Filter . . . . .	7-6
7-5	Last IF Amplifier-Detector . . . . .	7-7
7-6	10 kHz Filter . . . . .	7-9
7-7	Limiters Schematic . . . . .	7-11
7-8	Acquistion Control . . . . .	7-12
7-9	Sweep Circuit . . . . .	7-13
7-10	Multiplier Block Diagram . . . . .	7-15
7-11	X2 Circuit Schematic . . . . .	7-16
7-12	X4 Circuit Schematic . . . . .	7-18
7-13	X6 Circuit Schematic . . . . .	7-19
7-14	227.8 Mc Amplifier Circuit Schematic . . . . .	7-21
7-15	2.56 Mc Oscillator and Buffer . . . . .	7-23
7-16	Digital Data Collection . . . . .	7-25
7-17	Data Timing Diagram . . . . .	7-25
7-18	8-Bit Counter Schematic . . . . .	7-27
7-19	8-Bit Counter Logic . . . . .	7-29
7-20	256 Dividers and Phase Detectors . . . . .	7-32
7-21	3-Channel Summer . . . . .	7-33
7-22	Chopper Amplifier . . . . .	7-34
7-23	Power Supply . . . . .	7-38
7-24	RF Attitude Sensor Packaging . . . . .	7-39
9-1	Mathematical Model - Basic Gravity Gradient Stabilization Mission . . . . .	9-7
9-2	Mathematical Model - Gravity Gradient Experiment (ATS-A), Initial Stabilization Assumed . . . . .	9-8
11-1	Typical Dynamic Units . . . . .	11-3
11-2	Thermal Model Units . . . . .	11-4
11-3	Assembly of Flight 2 CPD in Clean Area . . . . .	11-5
11-4	Typical PCU Wiring Board Featuring Cordwood Modular Construction . . . . .	11-6
11-5	Working Model of CPD Caging Arrangement . . . . .	11-6
13-1	Boom Angle Indicator . . . . .	13-5
13-2	Encoder Disc . . . . .	13-5
13-3	CPD Clutch Mechanism . . . . .	13-6



**SECTION 4**  
**TV CAMERA SYSTEM**

## TV CAMERA SYSTEM FACT SHEET

### DESIGNER:

General Electric Company Space Division

### SUBCONTRACTOR:

Lear-Siegler, Inc., ; Anaheim, California

### CONTROLLING DOCUMENTS:

Specification	SVS-7310
Outline Drawing	47D207010, Control Unit 47D207011, Camera Unit
Assembly Drawing	47J209695, Camera Unit 47D207485, Control Unit
Schematic	LSI Model 0431F Television Camera (Figure

### PERFORMANCE REQUIREMENTS:

Picture - black and white

Scan - 525 horizontal lines (15,750 Hz)

30 frames per second

Field of View -  $64^{\circ}$  by  $48^{\circ}$  (in a 4 to 3 raster)

Power - 9.6 watts regulated at -24 vdc,  $\pm 2\%$

Weight - 10 lb (including camera, control unit and cabling)

Sun shutter - automatically protect vidicon from solar radiation damage

### UNIT DESIGNATION:

5101*	Engineering Unit
5102*	Engineering Unit
5103	Engineering Unit
5104	Qualification Unit
5105	Qualification Spacecraft Unit
5106	Qualification Spacecraft Unit
5107	Flight Unit 1 (Flown on ATS-A)
5110	Flight Unit 1 (Flown on ATS-A)
5109	Flight Unit 2 (Flown on ATS-D)
5108	Flight Unit 3 (Flown on ATS-E)

\*These cameras were placed on life test following the engineering test program.

## SECTION 4

### TV CAMERA SYSTEM

#### 4.1 INTRODUCTION

The primary purpose of the Television Camera System (TVCS) was to observe in-orbit thermal bending and dynamic characteristics of the gravity gradient primary booms. The camera also provided vehicle attitude information, derived from the earth's image, to aid the in-flight calibration of the earth sensor. The TVCS was designed to meet the requirements of Specification SVS-7310. Lear Siegler, Inc. of Anaheim, California was the vendor.

This section describes the engineering development, qualification, and acceptance of the flight equipment.

#### 4.2 ENGINEERING DEVELOPMENT

##### 4.2.1 BACKGROUND

The following discussion is a brief history of the background relative to the TVCS design:

In August of 1964, GE requested formal quotations from five potential vendors of TV Camera Systems against a Component Specification, SVS-7310, and a Work Statement, 9744-WS-001. The only vendor to submit a bid was Lear-Siegler, Inc., of Anaheim, California.

A subsequent revision of the specification, requiring the use of high reliability parts, resulted in a higher quotation, and a further revision, deleting the hi-rel parts but requesting LSI to burn-in their standard parts, LSI had to write specifications for each of their commercial parts, and a still higher quotation resulted. Included in these last two bids was a critical review of the camera circuits with redesign necessary for reliability and stability, if necessary. In addition LSI assumed the responsibility for the mounting brackets.

Prior to the fourth quotation two other significant events had transpired. First, GE recognized that the standard LSI Model 0431C Camera would not accomplish the system requirements. (That is, that the information acquired from the final TV video presentation was calculated to be a two-inch detector threshold for relative boom tip displacement and an absolute boom tip displacement of  $\pm 2$  inches relative to the camera boresight, which in turn would be related to the spacecraft principal axes during installation and alignment at Hughes Aircraft Company.)

GE then studied the use of a slow scan television camera system, as reported in the fifth monthly progress report, (Document No. 64SD4390) and the second quarterly progress report (Document No. 65SD4201).

However, the specific recommendation to use a slow scan system (reference: GE letter 4730-127-GGEP, dated 19 January 1965) was modified by NASA/GSFC's reluctance to depart from a standard scan system because of incompatibilities with existing ground station equipment.

NASA/GSFC then directed GE to restrict the video output to 3.5 mHz, which further reduced the resolution and tip displacement capabilities.

A contract was negotiated and agreed upon between GE and LSI in April, 1965.

The camera to be supplied by LSI was their standard 0431C Camera, modified to include the video filter and the telemetry requirements of SVS-7310, and with certain potentiometers and overstressed parts replaced. This camera was designated LSI Model 0431F; the TVCS is shown in Figures 4-1 through 4-3.

The camera design compromised the original system requirements relative to the accuracy of positioning the boom tip targets in space.



Figure 4-1. TV Camera System (Engineering Unit 5101) Showing (l to r) Electronics, Camera and Bracket Support

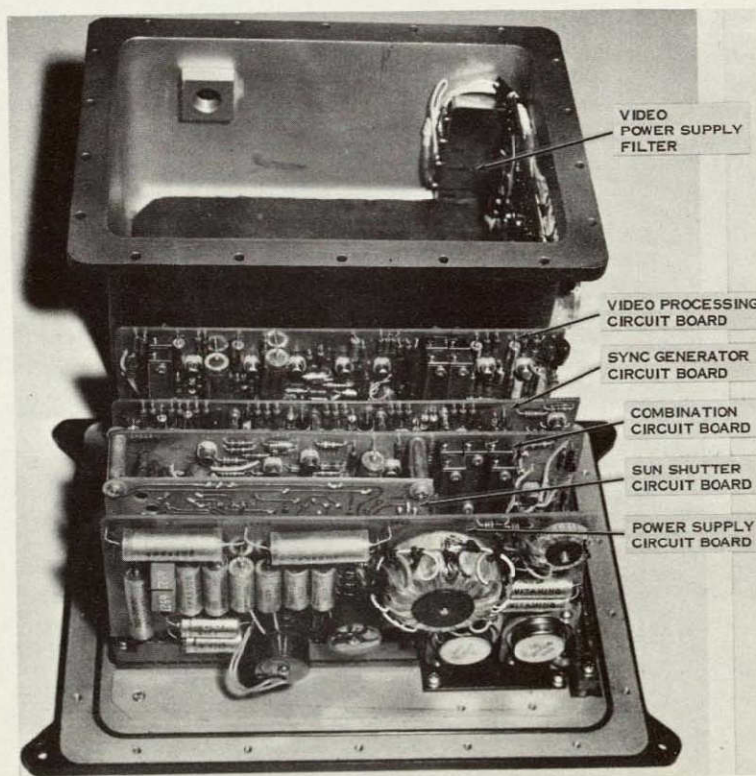


Figure 4-2. Electronics Unit Details



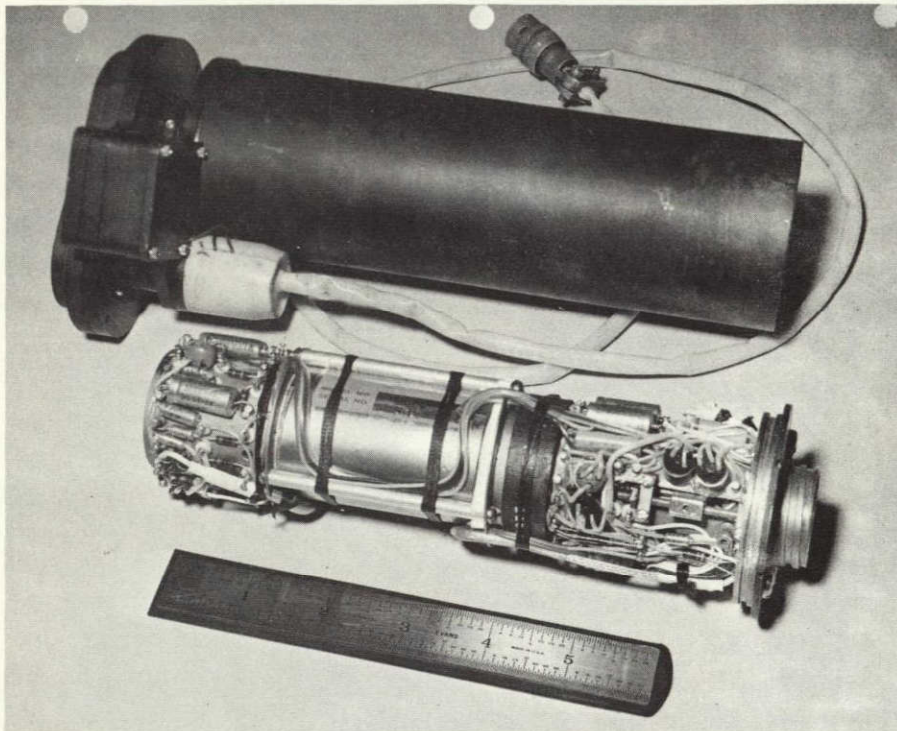


Figure 4-3. TV Camera (Engineering Unit 5101)

#### 4.2.2 ELECTRICAL

##### 4.2.2.1 Characteristics

The Model 0431F Television System consists of the following major circuits and assemblies:

1. Vidicon
2. Video amplifier and processor
3. Synchronizing generator
4. Deflection generators
5. Power converter
6. Shutter logic
7. Telemetry

#### 4.2.2.1.1 Vidicon

To reduce the weight and volume of the camera, an electrostatic-focus, electromagnetic-deflection ruggedized vidicon is utilized. It is an RCA Model 8567, with a reticle per GE Specification SVS-7310.

#### 4.2.2.1.2 Video Amplifier and Processor

The video preamplifier in the camera unit serves as an impedance match between the vidicon and the main video processing amplifier in the control unit. The preamplifier also raises the video output from the vidicon to a level sufficient to mask the noise generated in subsequent stages.

Video processing is straight-forward with blanking and synchronizing pulses inserted at appropriate points. The synchronizing, blanking, and pedestal levels remain fixed, independent of the video signal level. A low impedance video output is provided for either transmitting or monitoring purposes. A 3.5 mHz filter is in series with the video output to limit the content of the video signal.

#### 4.2.2.1.3 Synchronizing Generator

The synchronizing generator furnishes timing pulses, composite blanking pulses, composite sync pulses, and horizontal sync pulses for operating a keyed clamp.

The master oscillator is crystal-controlled at 31,500 Hz. This frequency is divided by 525 for the vertical sweep rate and by 2 for the horizontal. The countdown circuitry is designed for maximum stability with variations of temperature and supply voltage.

#### 4.2.2.1.4 Deflection Generators

Ample deflection voltages are provided for vidicon acceleration voltages up to 350 volts. Vertical linearity is better than  $\pm 2$  percent and is made essentially independent of picture size through the use of feedback. The horizontal deflection generator is a high-speed switch with controlled retrace. The resultant horizontal linearity is better than  $\pm 2$  percent. As a result of the precision sweep, the video output tends to remain constant across the scanned area of the tube.

#### 4.2.2.1.5 Power Converter

Input to the power converter is approximately 9.6 watts at 24 volts. A primary regulator adjusted to a nominal 20 volts drives a dc-to-dc converter to supply the necessary vidicon voltage as well as transistor circuit voltages. The power converter is synchronized to the horizontal line rate to prevent switching interference in the video signal.

#### 4.2.2.1.6 Shutter Logic

Input power to the shutter logic is approximately 0.2 watt continuous and approximately 1.2 watts during shutter actuation. The circuit is designed to perform the functions as called for in paragraph 3.5.8 of GE Specification SVS-7310.

#### 4.2.2.1.7 Telemetry

The four telemetry signals are provided to give information for protection and analysis of the TVCS performance during orbital flight. These telemetry points are Vidicon Filament Current, Vidicon Target Supply Voltage, Vidicon Faceplate Temperature and Series Regulator Temperature. Sample curves are shown in Figure 4-4 thru 4-6.

### 4.2.2.2 Theory of Operation

#### 4.2.2.2.1 General

The Model 0431F camera and camera control unit is a complete television signal generating system. The camera unit consists of the vidicon pickup tube, deflection assembly, video preamplifier, horizontal deflection, and blanking circuits. It also contains the sensor (light sensitive) for the sun shutter circuitry. The camera unit is connected to the control unit through two multiconductor cables.

The control unit contains the setup controls, vertical deflection generator, synchronizing generator, video processing amplifier, shutter logic and power converter. Access to all operating controls is gained by removal of the cover. Refer to block diagram, Figure 4-7, and schematic diagram, Figure 4-8, for discussion on theory of operation.



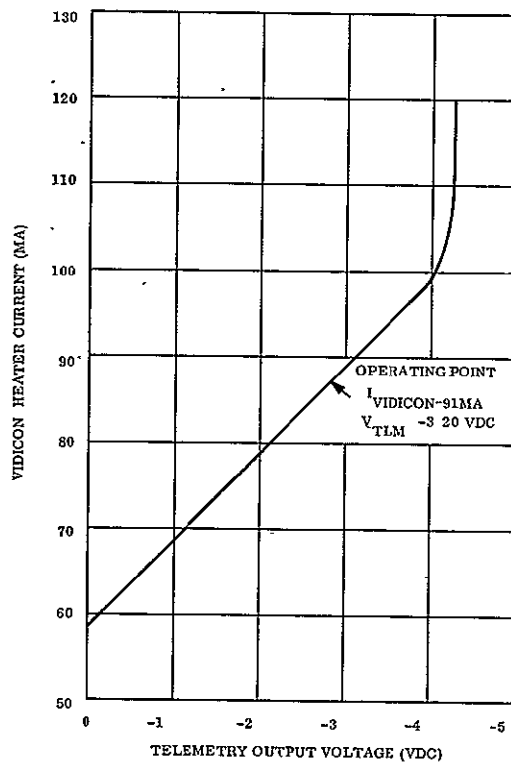


Figure 4-4. Vidicon Heater Current vs TLM Output Voltage

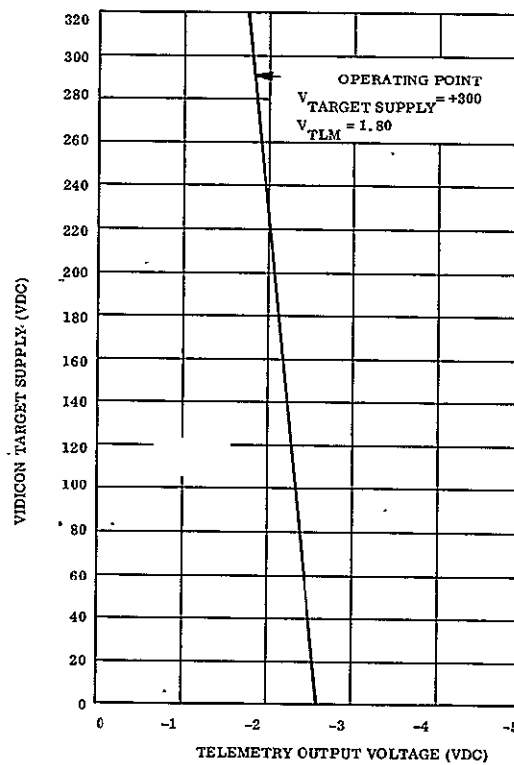


Figure 4-5. Vidicon Target Supply Voltage vs TLM Output Voltage

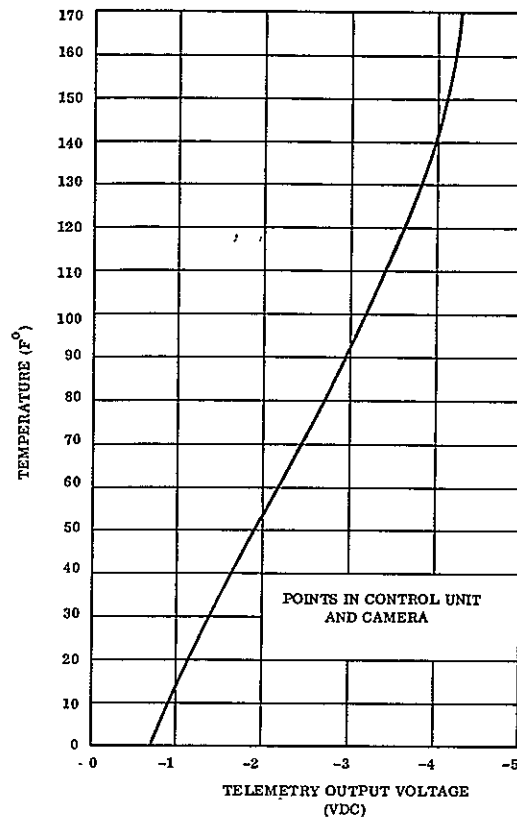


Figure 4-6. Temperature vs TLM Output Voltage

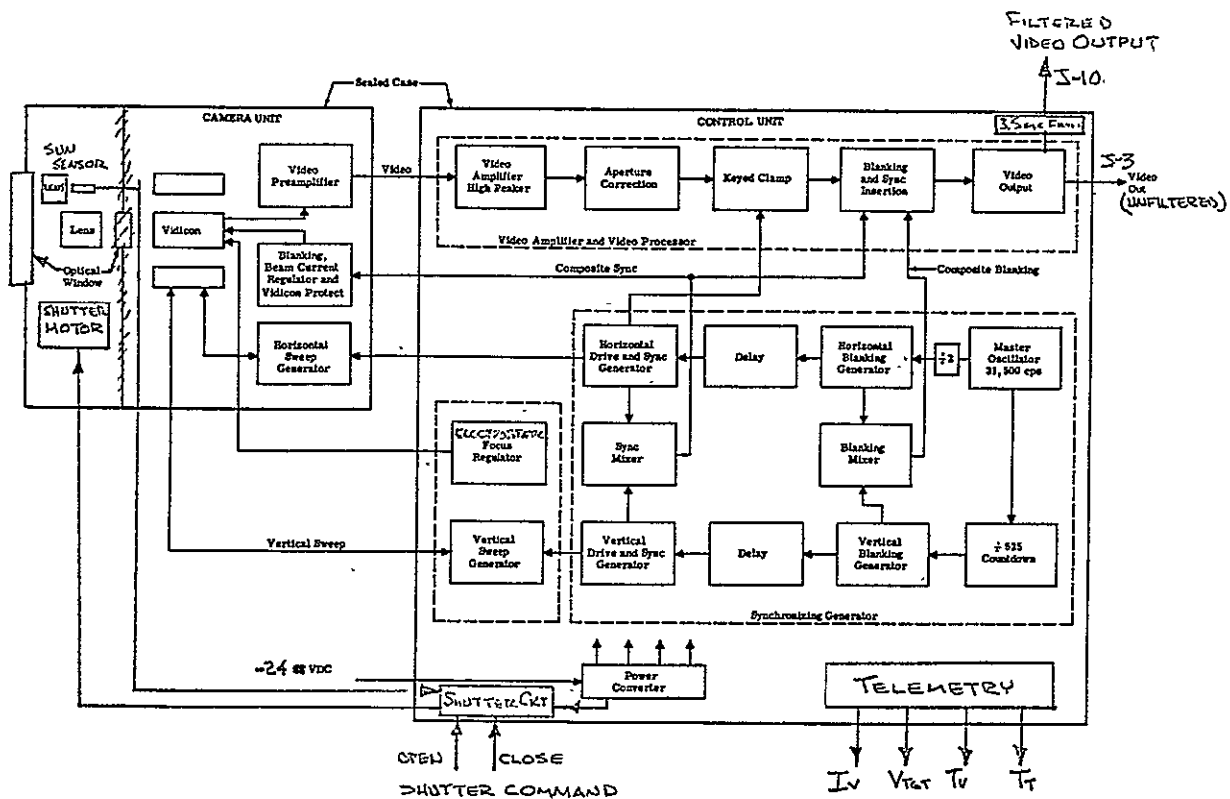


Figure 4-7. TV Camera Model 0431F Block Diagram

#### 4.2.2.2.2 Camera Unit

The camera unit contains the vidicon and its associated circuitry, and the horizontal deflection, blanking, beam current, and vidicon protect circuits.

The vidicon element voltages are supplied from the camera control unit. These voltages are  $\pm 500$  vdc to the mesh, and  $+300$  vdc to the wall and G2. Filament voltage is obtained from the  $+6$  vdc source. The Model 0431F camera incorporates "automatic target", which is obtained by applying  $300$  vdc to the target of the vidicon through R10 and R11. This becomes a constant current source supplied to the target. The signal generated at the output of the vidicon is essentially constant with widely changing light levels.

Horizontal sweep is generated by Q11, Q23, L1 and the horizontal deflection coil in the deflection yoke. The drive pulse to this circuit is supplied by the camera control unit and generated by the horizontal sync. Vertical sweep to the deflection yoke is obtained from the camera control unit.

The video preamplifier is a six-stage, direct coupled, wideband amplifier using keyed dc feedback for stabilization. Emitter follower Q4 offers a very high input impedance to the target of the vidicon. Direct coupled signal amplification is obtained by the grounded emitter-grounded base combination of Q5 and Q6. Further amplification is obtained by the emitter follower grounded base combination of Q7 and Q8. Output level of the video amplifier is approximately one volt peak-to-peak, dc feedback is accomplished by clamping the output during the horizontal blanking period. Q10 is keyed on during the horizontal flyback period by a signal from the horizontal deflection coil.

Vidicon beam current is cut off during horizontal and vertical retrace to prevent a signal from appearing at the target during this period. The vertical flyback signal to Q1 and the horizontal flyback signal to Q2 cut off the beam current regulator transistors Q2 and Q3 during this period. Beam current is controlled by adjusting the dc voltage level between the cathode and G1 of the vidicon through Q2 and Q3. Should the loss of either horizontal or vertical sweep occur, beam current to the vidicon will turn off Q2 or Q3, thereby raising the negative potential between cathode and G2 of the vidicon.

#### 4.2.2.2.3 Camera Control Unit

The camera control unit contains all the necessary circuitry to process the video generated at the camera. The synchronizing generator, vertical sweep generator, and power supply are also located in this unit.

Input video from the camera is amplified by Q101. This transistor stage amplifies the higher frequencies more than the lower frequencies to compensate for any loss due to the interconnecting cable between the camera and the control unit. Peaking is achieved in this stage by adjusting C103.

The aperture correction circuit (consisting of T101, C107, and R110) is driven by emitter follower Q102. The correction circuit is essentially a high-frequency, constant phase shift network and the amount of high frequency rise is adjustable by R110. Any insertion loss of this circuit is compensated by amplifier Q103. This stage also contains the video gain potentiometer R120 for setting video level.

Further amplification and video frequency response shaping is obtained in the next stage containing Q105.

Horizontal sync is utilized to restore the dc level of the video signal at the end of each horizontal line. The dc level that the clamp circuit (Q106 and T102) clamps to, is adjusted by the blanking level (setup) potentiometer R133. Mixed blanking is inserted in the video amplifier Q107 and Q108. Emitter follower output stage Q111 is the final stage of the video amplifier. Mixed sync is inserted in the video at this stage. The camera control unit video amplifier is designed to operate into a 75-ohm load.

All necessary sync pulses, sweeps, and blanking originate from the sync generator. The crystal controlled clock (Q201, and Q202) operates at 31,500 cps. Its output drives the first  $\div 7$  countdown and  $\div 2$  countdown. All countdown circuits are free-running multivibrators synchronized to some multiple of the clock frequency. Horizontal sync and blanking are generated by the  $\div 2$  circuit (Q216 and Q217).

Vertical Blanking and sync are generated by the succession of several divide circuits ( $\div 7$ ,  $\div 5$ ,  $\div 5$ , and  $\div 3$ ). Horizontal blanking width is adjusted by R290 which is in the horizontal blanking multivibrator circuit Q219 and Q220. Horizontal sync width is adjusted by R308 which is in the horizontal sync multivibrator circuit (Q302 and Q303). The horizontal front porch is a fixed value of approximately 1.5 microseconds and is essentially a delay of the  $\div 2$  circuit in relationship to horizontal blanking.

Vertical blanking is generated by multivibrator Q223 and Q224 driven by the last countdown circuit ( $\div 3$ ). Vertical front porch is made adjustable by delaying the output of the  $\div 3$  (in relationship to vertical blanking) to the vertical sync circuit (Q214 and Q215). Vertical front porch and vertical sync are adjusted by R296 and R297, respectively.

Vertical deflection is initiated by the vertical sync. Ramp generator Q112 utilizes the time constant of C124 and R145 and charges to some level determined by the vertical sync period. Vertical centering (R147) determines the dc level from which the ramp voltage starts. The remainder of the vertical deflection circuit is a dc-coupled amplifier whose output drives the vertical deflection coils in the camera yoke. Vertical size is adjusted by R156 which controls the amount of current through the yoke.

Horizontal drive pulses to the horizontal deflection circuit in the camera are generated by multivibrator Q121 and Q123. This multivibrator is driven by mixed sync. Centering and width are adjusted by R162 and R163 respectively. These potentiometers adjust the amount and phase of the yoke current.

The power converter supplies all the necessary voltages to the camera and camera control circuits, plus the high potentials required on the vidicon. This converter is a synchronized, regulated, dc-to-dc converter.

Input power of 24 vdc is regulated by dc regulator section Q405 through Q409 and the regulated output voltage of the regulator is adjusted by R424. Multivibrator Q401 and Q404 is synchronized at one-half the line rate by the horizontal sync pulse, assuring that any noise spikes generated by the power converter will appear during the horizontal blanking

period. Output from the multivibrator is amplified by Q402 and Q403. This amplified signal drives the switching transistors Q410 and Q411. Output from the transformer is rectified and filtered to produce the various dc voltages required.

The 24 vdc return is connected to the chassis of the TVCS, on the secondary of T402, in the power supply.

#### 4.2.3 MECHANICAL

##### 4.2.3.1 Camera

The TV Camera envelope drawing is 47D209695, Figure 4-9. This drawing lists all external dimensions. The camera is essentially an 8-inch long, 2.5-inch diameter tube with a connector on one end and a lens/shutter assembly on the other end. The shutter assembly is 1.6 inches long and about 4.5 inches by 3.7 inches high. Two brackets are mounted on the main camera barrel to provide for mounting of the camera to the spacecraft. The connector end of the camera is bolted to the tube by six #4 screws. The connector end plate supports the vidicon and the camera electronics with an aluminum tube (3 sections bolted together at flanged ends) supported at the connector end plate with set screws and epoxy. The tube flanges fit tightly in the electrically insulated barrel. The lens end of this inside tube fits around a concentric shoulder on the lens/shutter assembly which is bolted to the camera barrel by six screws. The vidicon is supported at the pin end by the socket and a set screw on one pin; and at the other end by a teflon compression ring, which fits tightly between the face of the vidicon and the lens assembly. The vidicon is supported in the middle by two tightly fitting teflon rings. The rings provide support between the O D of the vidicon and the I D of the inner camera support tube. All electronics parts are mounted on the outside of the inner tube.

The lens/shutter assembly is manufactured by Wollensak Division of the 3M Company, Rochester, N. Y.

As stated above, the lens/shutter is attached to the camera barrel with six screws. The assembly consists of the vidicon optics, the sun sensor and optics, an alignment window, and the sun shutter and movement. The basic optics are an 8 element f/2.8, 10mm focal

## 2. ASSY INSTRUCTIONS:

A. PROTECTIVE RUBBERIZED COATING ON BARREL TO BE REMOVED PRIOR TO BRACKET INSTALLATION.

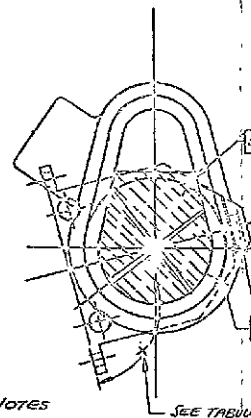
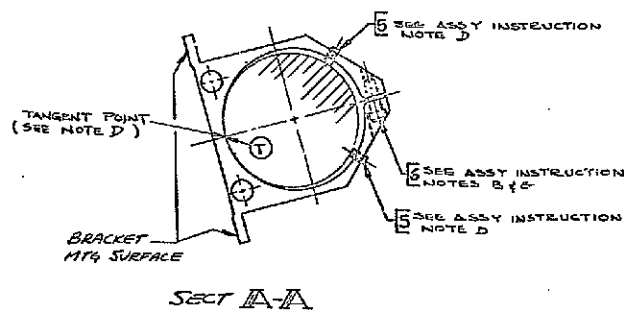
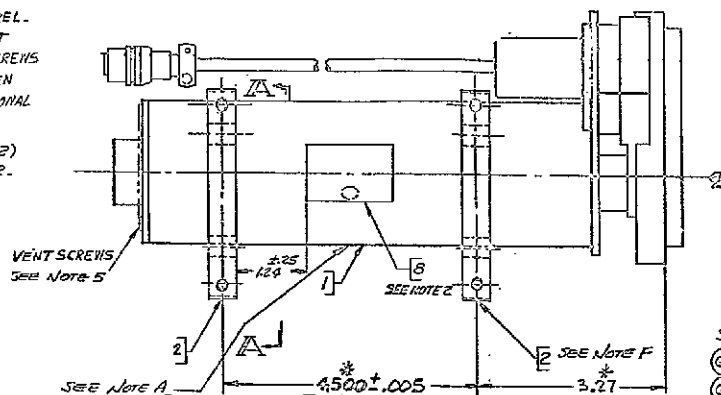
B. LOOSEN BOLT ITEM 6 UNTIL UPPER (SP.11) PART OF BRACKET IS IN AN UNRESTRAINED CONDITION.

C. LOCATE TWO BRACKETS ALONG CAMERA BARREL WITH PROPER ORIENTATION USING MOUNTING PLATE NUTCH-MARKED COORDINATED TOOLING TO ADJUST BRACKET SPACING. (REF HOLDING FIXTURE GE-101100HA)

D. WITH CAMERA BARREL RESTING ON TANGENT POINT (1) OF INTERNAL DIA. AND SET SCREWS (ITEM 5) WITH DRAWN SO THEY ARE NOT TOUCHING BARREL, TIGHTEN COIT (ITEM 6) TO 15 INCH POUNDS  $\pm 1$  INCH POUND.

E. ADJUST #8-32 SET SCREWS (ITEM 5) UNTIL THEY ARE JUST TOUCHING THE CAMERA BARREL. CHECK ANGLE "X", APPLY THREAD SEALANT AND ACTIVATOR (ITEMS 8 AND 7) TO SET SCREWS (ITEM 5) PER PROCESS SPEC. ITEM 4. TIGHTEN SET SCREWS (ITEM 5) ONE - HALF (1/2) ADDITIONAL TURN.

F. MOUNTING SURFACE OF BRACKETS (ITEM 2) TO BE MUTUALLY PARALLEL TO WITHIN .002.



### GENERAL NOTES:

1. DRAWING TOLERANCES PER 110A1604 APPLY.
2. MARK PER 110A1526, CLASS 10, IN ACCORDANCE WITH 47210808. LOCATE ITEM 8 APPROXIMATELY AS SHOWN ON ASSY 2.
3. DELETED
4. UNIT SHALL MEET THE REQUIREMENTS SPECIFIED IN SVS 7210 (LATEST REVISION).
5. DEBRASS UNIT IS PLACED IN BONDED STOCK ROOMS & DISCARDED VENT SCREWS (RTY 5) UNIT TO BE PACKAGED FOR 16845000. AFTER REMOVAL OF VENT SCREWS PRIOR TO PACKAGING, UNIT SHOULD NOT BE EXPOSED TO AN ENVIRONMENT OF MORE THAN 55% RELATIVE HUMIDITY.
6. STORAGE TEMP. SHOULD NOT EXCEED 1160°F.
7. UNLESS MARKED (X), DIMENSIONS ESTABLISH SPACE REQUIREMENTS MOUNTING AND OTHER INSTALLATION DATA, AND ARE FOR ENGINEERING REFERENCE. SEE ASSY INSTRUCTIONS IN ZONE G10 FOR DIMENSIONS MARKED \*.

SEE NOTES  
 (G1) ENG & PROTOTYPE  
 (G2) QUAL & FLIGHT

GR10	X
GR10	115°±0°30'
GR10	80°±0°30'

SHOWN IN G1663 CONFIGURATION

SEE SEPARATE PL & C/S

UNLESS OTHERWISE SPECIFIED DIMENSIONS ARE IN INCHES TOLERANCES ON: 2 PLACE DECIMALS $\pm .03$ ALL 3 PLACE DECIMALS $\pm .010$ SHIP FINISHES $\pm .005$		REV. NO. 15 DATE 1/1/63 BY 1001/1002 CHECKED 1001/1002 APPROVED 1001/1002	GENERAL ELECTRIC SPACECRAFT (A) DIV. 100 PHILA. PA. U.S.A. TV CAMERA, ASSEMBLY OF CONTRACT NO. NAS-5-9042 D 15227 47209695
REDUCED SIZE PRINT	47209695		

Figure 4-9. TV Camera Assembly  
(GE Dwg. 47209695)

length lens assembly with a manually adjustable aperture to f/16. This lens has an approximate 80 degree field of view. The sun sensor is located behind a 4 element, 85 degree field of view, lens assembly and the sensor is a photo diode. The sun sensor and associated electronics operate to protect the vidicon whenever the sun is within the field of view of the primary optics (vidicon) by sending a pulse to the sun shutter motor, which then actuates to position a blade in front of the vidicon optics. The sun shutter motor is a meter movement whose rest positions are either "full scale (opened) or "zero" (closed). It is held in either position by "magnetic detents". Small magnets at both limits of travel attach to the movement when actuated to either position in order to maintain that position when the command pulse is removed from the actuator circuit. The alignment window is mounted on the front end of the lens/shutter assembly. It is 1/4-inch thick quartz with an inconel coating on the "front-most" side. The coating has been eliminated from in front of the sun sensor optics (to provide increased sun sensor sensitivity) and in such a manner (in front of the vidicon optics) to provide alignment cross marks for initial alignment and alignment check of the camera to the vehicle. The quartz window also protects the lens systems from browning.

The camera weighs a maximum of four pounds. The aluminum parts of the camera barrel and connector end plate are gold plated and painted with black epoxy paint. The lens/shutter assembly is black anodized, dyed black. The two aluminum mounting brackets are painted black with epoxy paint.

#### 4.2.3.2 Control Unit

The TVCS Control Unit envelope drawing is GE No. 47D207485, Figure 4-10. As shown, the control unit is a rectangular box 5.7 inches wide by 9.0 inches long by 3.7 inches high. The maximum weight is 5.25 pounds. The base is a flat aluminum plate and the cover is a 5-sided aluminum casting, all walls are about 3/16-inch thick. The cover has a flange on it, which is bolted to the base with 18 screws. An "O" ring is located in the ground base, between the base and the cover, to provide damping between the two pieces. All connectors and the 3.5 mHz filter are located on the cover.



The five printed circuit boards containing the control unit electronic circuits are mounted in connectors located on the base plate. A 1/4 inch thick polyurethane cushion is cemented to the inside top of the cover to compress against the boards, and maintain their position during handling and while undergoing the launch environments of vibration and acceleration. The outer surface is painted black with epoxy paint. The basic aluminum is gold plated before painting.

#### 4.2.4 ENGINEERING TEST PROGRAM

The original engineering program intended to use three cameras, one for functional and temperature (and thermal vacuum) tests, one for an Engineering Qualification Program, and one for an Engineering Life Test Program. The intent of the above program was to verify the design, determine problems in design and to acquire life test data on a flight-type TVCS.

As time progressed during the program the Engineering Life Test TVCS delivery was delayed because the vendor's efforts were required for the prototype units. Since the testing was completed on the first two engineering units, it was decided to place them on a life test at GE and cancel the life test, at the vendor, scheduled for the third unit.

Following is a listing of the tests performed on each of the Engineering units:

##### Unit No. 1 (Serial No. 5101)

Functional	EMI
Temperature	Functional
Functional	Dipole
Thermal Vacuum	Life Testing
Functional	



Unit No. 2 (Serial No. 5102)

Functional	Sun Shutter Sensitivity
Corona	Thermal Vacuum
Functional	Functional
Vibration	Vibration
Functional	Functional
Thermal Vacuum	Solar Vacuum
Functional	Functional
Vibration	Life Testing
Functional	

Unit No. 3 (Serial No. 5103)

Functional
Vibration
Functional
Tip Target Location/Photograph Test
Functional

All testing was performed, in general, per Standing Instruction SI 237,013. Since this was an Engineering Program some deviations were made during the testing.

The results of testing Unit No. 5101 provided information on the problems to be anticipated at temperature -- the electronics was unstable at temperature extremes and the quality of the video changed. In most cases it was not a serious problem. However, at low temperature on the camera (vidicon) the dark current of the vidicon decreased to the point where, on some vidicons, the reticle was invisible. In order to minimize this problem, vidicons were selected for use on specific flights according to the vidicon dark current. EMI tests

run on Unit 5101 indicated that the camera met the requirements of Specification SVS-7310 and the ATS System EMI Specification. The dipole test also indicated that the TVCS would be no problem. The TVCS dipole was found to be less than 100 pole-centimeters.

At the completion of the testing of unit 5101, it was placed on a Bench Life Test. The test was run at room ambient temperature and pressure. During this test the video, power consumption and shutter operation were checked daily. At the time the TVCS was placed on the life test it had been operating for about 137 hours. After 1573 hours on life test, the video presentation became defocused and had to be readjusted to make it usable. The camera was then operated for an additional 936 hours before it again became defocused and had to be readjusted. The camera was then used for a series of exploratory dipole tests, to determine the optimum method for determining the dipole of a component with the TVCS configuration.

TVCS Unit 5102 was identical in configuration to Unit 5101, except that it was conformal coated (electronics piece parts). This unit was used as a "workhorse" in order to verify the validity of the mechanical and electrical design of the TVCS. It can be seen from the test list that it was subjected to an entire qualification program with the exception of humidity, acceleration and storage (temperature) tests. It was felt that these tests would be time consuming, expensive, and yield minimum usable results, so they were not performed. In addition to the testing noted above, additional testing of corona region determinations, comprehensive sun shutter performance, and solar vacuum temperature distributions were performed.

The corona testing was performed in the thermal-vacuum environment and provided information on the critical corona region.

This area was determined to be the pressure region between 2.0 mmHg and 0.3 mmHg. The camera and control unit were both unsealed units, and had vent holes to allow them to operate in space at pressures well below the critical region.

The sun shutter testing resulted in the following design changes:

1. Reversal of rest position on the shutter motor spring to maintain a closed position during vibration and acceleration environments.
2. Removal of resistors R611 and R634 in the motor drive circuit. R611 was removed to provide a stronger pulse to open the shutter when activated by the sun, and R634 was removed to provide twice the amount of drive current to actuate the shutter in all cases. These changes were made to prevent the shutter blade from "sticking" in the event that it came in contact with the housing because of warping during launch or because of thermal gradients.
3. The inconel coating on the quartz window was removed from in front of the sun sensor optics to increase the sensor sensitivity -- to increase the sun actuation angle to protect the vidicon from sun burn.
4. The sensitivity potentiometer in the sun sensor was also changed (setting) to increase the sun actuation angle and to decrease the deadband between the "close" and "open" angles.
5. Five resistors in the circuit were also reselected to provide for better sensitivity of the sun shutter actuation angle.
6. A 0.0142-inch hole was drilled in the blade support tube between the meter movement rotor and the blade to minimize any barometer effects which might occur in this previously sealed tube in a vacuum.
7. The vendor was directed to supply the meter movement vendor with the parts which mate to the meter movement and blade to minimize any possible misadjustment which might cause mechanical interference between the blade and the housing.

The solar vacuum tests were performed primarily to verify the TVCS thermal analysis.

The data acquired in this test indicated in all areas that the analysis was correct.

During solar vacuum and thermal vacuum testing many electronic piece parts failed to operate and testing had to be interrupted for repairs. The most frequent problems were encountered with the carbon potentiometers in the focus, beam current, and target voltage adjustment circuits. Since these potentiometers seemed to be affected by the vacuum environment, they were replaced with a higher quality potentiometer. The newer potentiometers operated very well in the vacuum environment.

In order to reduce the chance of other piece parts (resistors, capacitors, diodes transistors, etc.) failing, it was decided to burn-in TVCS Unit 5102 prior to the start of the official test cycle. Piece part failure was noted to be most frequent in the first 100 hours of operating life. After this time, failures became extremely rare. All flight, and the qualification, cameras were exposed to an approximately 75 hour burn-in test in the thermal vacuum chamber under Acceptance Test conditions of temperature and pressure. These tests proved successful in weeding-out the bad piece parts. After the tests the bad parts were replaced, the TVCS was readjusted for optimum performance and the official test cycle began.

The testing of the Engineering Units also indicated that the telemetry channels of vidicon heater current and vidicon target voltage would not provide a good picture of what these apparent values were, and would not provide good accurate diagnostic data if the TVCS failed to operate properly in orbit.

The nature of the circuit design and the points in the circuit at which the telemetry data is acquired is such that a failure or shift in the -6 volt supply could indicate trouble in either of the above telemetry functions. Since it was very difficult, short of a comprehensive redesign of the camera and electronics to get the exact telemetry information indicated, it was decided to use what was available and to use it in the best manner possible with a full realization of the shortcomings in the circuit configuration. The data analysis group was made aware of the telemetry situation and the data will be processed accordingly.

At this point all design modifications which were incorporated into the final TVCS design were completely tested on the Engineering units prior to their incorporation.

Thermal vacuum testing of Camera Unit 5102 revealed a grease problem. Two "O" rings used in the camera were greased to aid assembly of the camera parts. When the unit was exposed to the thermal vacuum test the grease migrated to the quartz window, video quality seriously degraded, and it appeared that the camera had defocused. As a result of this finding, the grease and "O" rings were removed from all flight (and qualification) cameras.

The most significant testing performed on TVCS Unit 5103 was the "Tip Target Location/ Photograph Test Series". These tests were performed as follows:

The TVCS was setup on the roof of GE Space Facility in Valley Forge, Penna. , and a boom tip target stand was setup 132 feet from the camera, at a 25 degree angle from the camera sighting axis. The stand was made to provide 20 discrete positions for the tip target. (ten in a horizontal direction and 10 in a vertical direction). The positions along the "X" stand were 6 inches apart.

The TVCS was powered and connected to a monitor. A photographic camera, utilizing 35 mm film, was setup to view and photograph the monitor. A series of 120 photographs were taken under the following conditions:

1. Tip target back lighted against a black background - sunlight used for lighting
2. Tip target back lighted against a white background - sunlight used for lighting
3. Same as 1, except front lighted
4. Same as 2, except front lighted
5. Tip target backlighted at night with 150 watt spot lamp at about 2 feet from target
6. Same as 5, except front lighted

Twenty photographs were taken under each of the above six conditions. The TV camera was set at f/11 for the day photos and f/8 for the night photos. The photographic camera was set to provide the best picture of the monitor. All film strips were given to the data analysis group at GESD for evaluation and practicing of data accumulation techniques.

Camera Units 5102 and 5103 were also used as a "tool" in trouble shooting problems encountered in the testing of flight cameras.

All detailed data and test summary results can be found in Component History Documents Book CLVII Volumes 1 thru 6.

#### 4.2.5 SUMMARY AND CONCLUSIONS OF TV CAMERA DEVELOPMENT

The TVCS engineering unit was subjected to a very complete and comprehensive test program. The test program was in some instances carried out in parallel with both the qualification and flight testing programs. This situation occurred because marginal performance conditions which passed on the engineering units (and were not evident as being marginal) failed on either the qualification or the flight units.

In general the engineering testing program was considered very successful. Even though many difficulties and failures were encountered, it is evident that it did uncover a majority of design, manufacturing, and workmanship problems, that could in most cases be corrected on prime hardware.

The testing program verified the fact that when high reliability and high quality electronic piece parts are not used, frequent failures will indeed occur. In three critical areas the piece parts were replaced with higher quality parts, but in the majority of the cases, no changes were made.

The testing program indicated that because of piece part drift (with time and temperature), a component burn-test could minimize these changes and help to weed out marginal piece parts. The burn-in test was used successfully on the component qualification and flight units. It also became evident that the TVCS would require retest and possible readjustment after storage for long periods of time.

It was evident the TVCS would not meet the original system requirements, but that it would be able to provide boom tip location data to within 6 inches of the actual position, and that the data derived from the earth's image would aid in the in-flight calibration of the earth sensors.

The TVCS was found to operate better at the higher temperatures than at the lower temperatures. This is, in general, because the reticle was blacker at the high temperatures. (The vidicon dark current increased with temperature to present a blacker reticle) the blacker



reticle provided easier data interpretation. The noise of the video increased at higher temperatures, however, it did not impair the video to the degree that it was unuseable.

Because the TVCS was basically a standard commercial component, it would probably not live the minimum specified life. Results of two engineering bench life tests indicated this conclusion.

It is felt that usable data would be obtained from the TVCS, however, the length of time this data would be available was undetermined.

#### 4.3 QUALIFICATION TESTS, TV CAMERA

Two prototype TV Camera Systems (designated as component and system qualified) were subjected to similar environments at more severe levels than the anticipated operating environments in order to establish confidence that the design was valid under extreme operating conditions. Following tests, the component qualified unit was not further dispositioned, but the system qualified units were included in the spacecraft qualification tests conducted by the vehicle contractor following the GE tests. A summary of these environments and references to the appropriate test reports are listed below. These documents are on file at GE and will be made available on request of the Contract Administrator for NASA programs.

##### 4.3.1 COMPONENT QUALIFICATION

Serial No. 5104

Part No. 47D209695 (Camera)

47D207485 (electronics)

Test Report 4315-QC-021 (1/11/67)

Failure Analysis Report 218-E-12

### Test Sequence

1. Prefunctional Burn-In
2. Functional
3. Humidity
4. Post Humidity
5. Vibration
6. Post Vibration
7. Acceleration
8. Post Acceleration

#### 4.3.2 SYSTEM QUALIFICATION

Serial No. 5105 and 5106

Part No. 47D209695 (Camera)

47D207485 (electronics)

Test Report 4315-QC-004 (8/11/66)

### Test Sequence

1. Functiona
2. Vibration
3. Functional & Post Vibration
4. Thermal-Vacuum
5. Functional, Post Thermal-Vacuum

#### 4.4 FLIGHT ACCEPTANCE TESTS, TV CAMERA

Each of the TV Camera Systems flight units were exposed to vibration and thermal-vacuum environments at levels anticipated during flight to verify that the design had not

degraded during manufacture. A summary of these environments and references to the applicable test reports are listed below. These documents are on file at GE and will be made available on request of the Contract Administrator for NASA programs.

#### 4.4.1 ATS-A (TWO TV CAMERA SYSTEMS WERE FLOWN ON THE ATS-A)

Serial No. 5107 and 5110

Part No. 47D209695 (Camera)

47D207485 (electronics)

Test Reports: 4315-QC-231 (1/25/67)

4315-QC-232 (1/25/67)

#### Test Sequence

1. Prefunctional Burn-In
2. Functional
3. Vibration
4. Post Vibration
5. Thermal-Vacuum
6. Post Thermal-Vacuum
7. Mating Test

#### 4.4.2 ATS-D

Serial No. 5109

Part No. 47D209695 (Camera)

47D207485 (electronics)

Test Report: 4315-QC-034 (5/5/67)

4315-QC-037 (6/16/67)

4315-QC-038 (8/30/67)

Failure Analysis Report, 297-E-47, 285-E-39, 288-E-40.

290-E-41, and 293-E-44.

Test Sequence:

- |                          |                    |
|--------------------------|--------------------|
| 1. Prefunctional Burn-In | 11. Functional     |
| 2. Functional            | 12. Vibration      |
| 3. Vibration             | 13. Post Vibration |
| 4. Post Vibration        | 14. Thermal-Vacuum |
| 5. Thermal-Vacuum        | 15. Rework         |
| 6. Rework                | 16. Vibration      |
| 7. Functional            | 17. Loose Particle |
| 8. Vibration             | 18. Functional     |
| 9. Rework                | 19. Thermal-Vacuum |
| 10. Loose Particle       | 20. Functional     |

4.4.3 ATS-E

Serial No. 5108

Part No. 47D209695 (Camera)

47D207485 (electronics)

Test Report: 4315-QC-025 (3/30/67)

1315-003 (8/14/68)

Failure Analysis Report 262-E-29 (10/23/66)

## Test Sequence

- |                          |  |
|--------------------------|--|
| 1. Prefunctional Burn-In | 10. Functional                                 |
| 2. Functional            | 11. Vibration                                  |
| 3. Vibration             | 12. Post-Vibration                             |
| 4. Post Vibration        | 13. Thermal-Vacuum                             |
| 5. Thermal-Vacuum        | 14. Post Thermal-Vacuum                        |
| 6. Functional            | 15. Shelf Life                                 |
| 7. Vibration             | 16. Shutter Input Power Source<br>Modification |
| 8. Post Vibration        | 17. Functional Test                            |
| 9. Thermal-Vacuum        |  |

### NOTE

Item 16 consisted of changing the input power leads from direct tie-in of the -24 vdc bus to the camera input power line. This was done to make the automatic sun shutter operate only during times that the camera power was commanded on. With power on continuously to the sun shutter circuit, the sun shutter operated (opened and closed) at the spin rate of the spacecraft during the orbit injection and station acquisition periods. This situation was undesirable since it caused an unnecessary number of shutter actuations, and consumed power while contributing nothing to the spacecraft mission.

**SECTION 5**  
**SOLAR ASPECT SENSOR**

## SOLAR ASPECT SENSOR FACT SHEET

### MANUFACTURER:

Adcole Corp., Waltham, Mass.

### CONTROLLING DOCUMENTS:

Specification	SVS-7306
Outline Drawing	47E207013
Standing Instruction	237012

### PERFORMANCE REQUIREMENTS:

Field of View -  $4\pi$  steradians

Resolution and Accuracy - Better than 1 degree in all operating environments

Operating Temperature - Detector  $-55^{\circ}\text{C}$  to  $+69^{\circ}\text{C}$   
Electronics  $0^{\circ}\text{C}$  to  $+40^{\circ}\text{C}$

Reliability - 3-year life at a 50% duty cycle

Power - 1 watt at 24 vdc

Weight - less than 5 lb

### UNIT DESIGNATION:

#### Electronics

P02	Qualification
P03	Flight Acceptance
F04	Flight Acceptance
F05	Flight Acceptance
F04	ATS-A Flight
F05	ATS-D Flight
F03	ATS-E Flight

#### Detectors

P021 - P025	Qualification
F031 - F035	Flight Acceptance
F041 - F045	Flight Acceptance
F051 - F055	Flight Acceptance
F041 - F045	ATS-A Flight
F051 - F055	ATS-D Flight
F031 - F035	ATS-E Flight

## SECTION 5

### SOLAR ASPECT SENSOR

#### 5.1 INTRODUCTION

##### 5.1.1 PURPOSE

The Solar Aspect Sensor (SAS) was designed to provide one form of attitude data of the ATS spacecraft. The SAS was manufactured by the Adcole Corporation of Waltham, Mass., to requirements specified by General Electric in Specification SVS-7306. This section describes the operation of the Solar Aspect Sensor, a history of the engineering development and testing that was expended in deriving the design, and a listing of the tests that were conducted to qualify and acceptance test the hardware.

##### 5.1.2 DESCRIPTION

Figure 5-1 depicts the single electronics unit and one of the five solar detectors which comprise the SAS. Each detector has a 128-degree by 128-degree square field of view; spherical ( $4\pi$  steradian) coverage is obtained with the detectors placed on the spacecraft as shown in

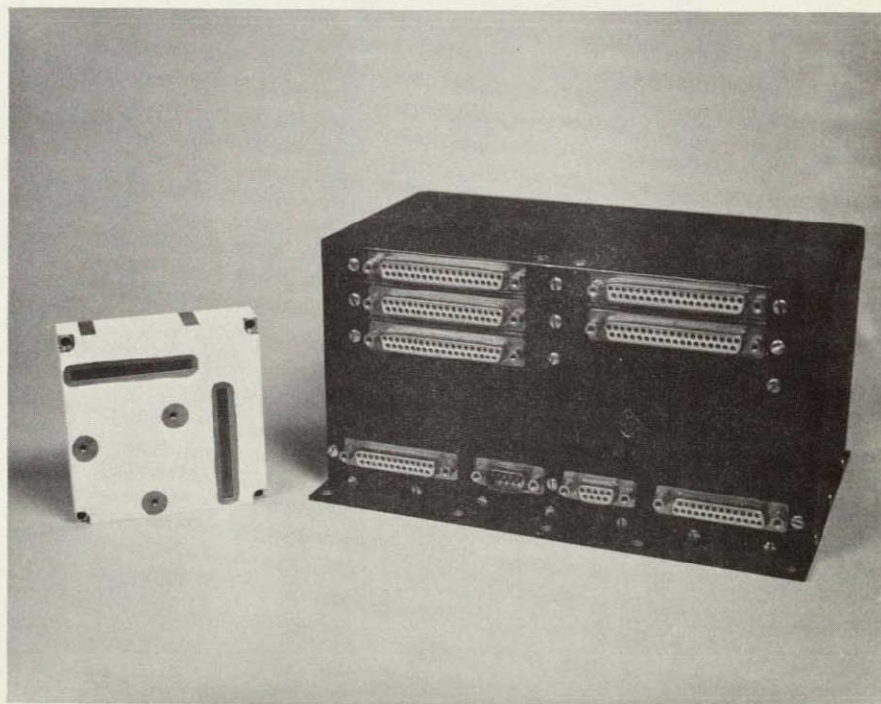


Figure 5-1. Solar Aspect Sensor Electronics (r) and Typical Detector



Figure 5-2. The maximum error with which the sun's direction can be measured with respect to the SAS has been demonstrated to be less than one degree.

The SAS is designed to withstand the typical launch environment and to operate throughout the detector and electronics unit temperature ranges of  $-55^{\circ}\text{C}$  to  $+69^{\circ}\text{C}$  and  $0^{\circ}\text{C}$  to  $+40^{\circ}\text{C}$  respectively, for three years at a 50% duty cycle.

The SAS weighs less than five pounds and consumes about one watt of power at 24 volt dc.

### 5.1.3 PRINCIPLE OF OPERATION

#### 5.1.3.1 Detector

Each SAS detector includes two orthogonally-oriented digital sun sensors. Figure 5-3 presents a pictorial representation of one such sensor, which consists of a Gray-coded reticle and nine individual solar cells (only seven cells are shown in Figure 5-3). Eight of the nine cells provide a 256-bit range, so that the sun's direction can be measured within

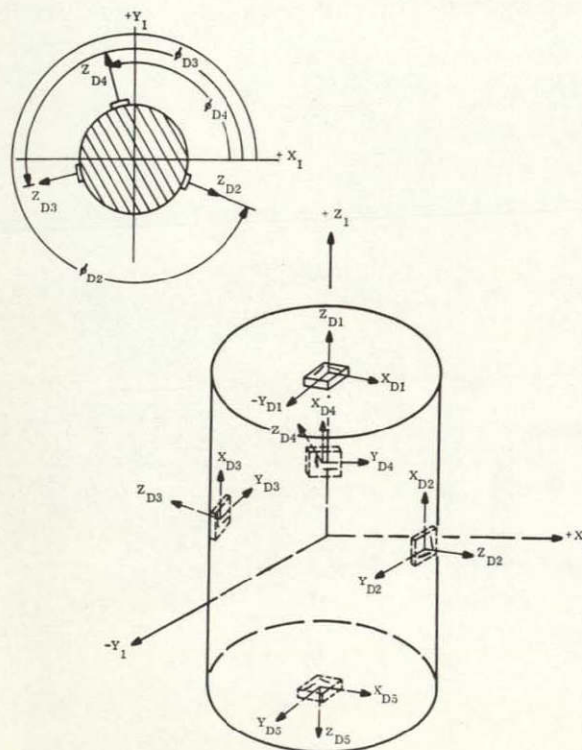


Figure 5-2. SAS Detector Orientation

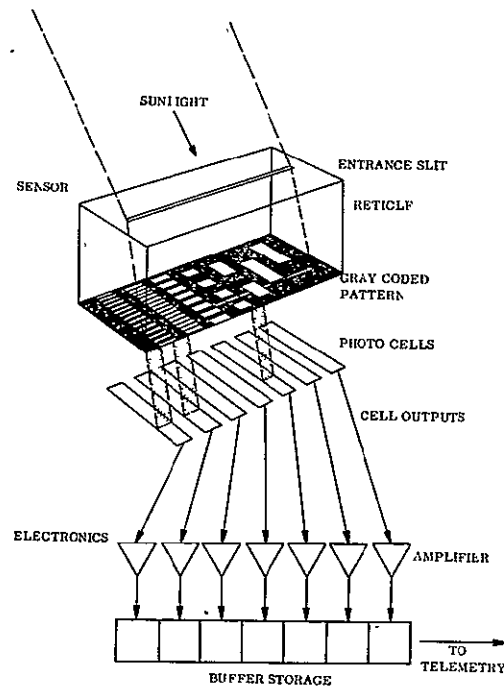


Figure 5-3. Sensor Pictorial Representation

a  $\pm 64$ -degree field-of-view with an accuracy of 0.5-degree (1 bit). The ninth cell, called the AGC cell, is illuminated whenever the sun is within the field of view, and its output is used to determine which of the five SAS detectors is most directly illuminated by the sun.

The Gray coded reticle is a small oblong block of fused quartz with a slit centered along the top surface, and a Gray coded pattern on the bottom surface. Sunlight enters the eye through the slit, casting a narrow band of illumination across the Gray coded pattern. The Gray coded reticle pattern provides for the generation of 8 bits of information. In any given bit, the band of sunlight either will or will not pass through the reticle pattern, depending on the angle of the reticle with respect to the sun.

Because the reticle has a Gray coded pattern, only one bit changes at a time. Where the opaque and clear areas on the reticle arranged in a conventional binary code, with simultaneous changes in more than one bit, there could be catastrophic errors in the determination of the angle if the transitions were not perfectly synchronized. It can be seen that in all eight bits, no two of the transitions are in the same straight line. The width of the

opaque or clear areas in the least significant bit is twice as wide as the resolution of the reticle. If the reticle pattern were in a conventional binary code, the width of the opaque or clear areas of the least significant bit would be equal to the resolution.

However, the Gray coded reticle provides transitions in the more significant bits when the band of sunlight is halfway through an opaque area in the least significant bit.

Each of the eight bits on the Gray coded reticle is superimposed on a photocell. The function of the cells is to detect the light (or note the absence of light) in the apertures at a given angle, and to produce measurable electrical signals correspondingly.

Silicon solar cells are used in the sensor. Their major limitation is the relatively small signal, on the order of 20 to 30 microamperes, which requires amplification. However, their advantage over photoconductive materials is that they can readily withstand space environment, are very uniform, and have a linear relationship of incident light to output. The effects of ultraviolet and Van Allen belt radiation are minimized because the cells have the substantial shielding of the fused quartz block.

An additional wide open bit with a solar cell under it is included on sensors of this type. This is referred to as the AGC bit and is used to compensate for the variation in output of the solar cells under the Gray code bits, which is a function of the angle of incidence.

#### 5.1.3.2 Electronics Unit

The block diagram of the electronics is shown in Figure 5-4 and described below.

The input sample data pulse causes the data register and identification to clear and sets the  $A_1$  flip flop to the "one" state. The  $A_1$  flip flop is used to control the 4 kHz clock pulse generator and eye selection switches. With the  $A_1$  flip flop in the "one" state, clock pulses are generated and the eye selection circuit is activated. Clock pulses cause the identification binary counters  $S_1$  through  $S_3$  to count. The outputs of the binary counter  $S_1$  through  $S_3$  are decoded as shown and thus provide the scan system to select the eye that is most



illuminated. When the counter reaches 110, it is decoded, inverted and used to open the shunt switch of eye number 1. If eye number 1 is the most illuminated eye, the current produced by the AGC bit would flow into the grounded base amplifier (this current had previously been shunted by the closed switch) and cause a pulse to occur at the differential amplifier. If Eye No. 1 is not the most illuminated eye, no current or insufficient current would flow into the grounded base amplifier to cause a pulse to be produced at the differential amplifier. The binary counter will then continue to count and scan each eye until the most illuminated eye produces a pulse at the differential amplifier.

The  $A_2$  flip flop was set to the "one" state when  $S_1$  changed from a "one" to a "zero". In the "one" state the  $A_2$  flip flop enables the threshold switch.

The pulse produced by the differential amplifier when the proper eye is scanned causes the threshold detector switch to close. The negative going step voltage produced by the threshold switch causes the 500  $\mu$ s mono-stable multivibrator to be triggered.

The output of the one shot is inverted and used to drive the NOR gate inputs as shown. This ground level input, together with the ground level input of the decoded identification, will cause all series of the selected eye to close. Current from the illuminated solar cells of the selected eye will flow through the correct data register amplifier.

The output of the inverter connected to the one shot output is also connected to a pulse generator. This pulse generator will produce a set pulse that is coincident with the trailing edge of the 500  $\mu$ s pulse.

Flip flops  $S_4$  through  $S_{19}$  comprise the data register. These flip flops have an AC set (S) input and a gate set (G) input. The G input resistor is used to bias a diode connected to the base of the "one" side transistor of the flip flop. The G inputs of all these flip flops are connected to the appropriate grounded base amplifier as shown. When current from the illuminated solar cells flows into these amplifiers, the output voltage increases. The set pulse is ended with the output of the amplifiers and the data flip flops will be set to a "one" or remain

in a "zero" depending upon the amount of current flowing in each data bit amplifier from the data bit solar cells. The set pulse is also used to reset the A<sub>1</sub> flip flop thus ending the sequence.

S<sub>1</sub>, S<sub>2</sub> and S<sub>3</sub> now contain information to identify the selected sun and S<sub>4</sub> through S<sub>19</sub> contain the required sun angle information. The outputs of S<sub>1</sub> through S<sub>9</sub> is inverted and presented as a parallel output. The data at the output will remain until a new sample data pulse is received.

Total elapsed time in worst case from the end of the sample data pulse is new data at the output is 3.2 ms.

In summary, the SAS determines which of the five detectors is most directly illuminated by the sun, and provides as an output a 19-bit digital word which identifies the detector and the sun's direction with respect to that detector.

## 5.2 ENGINEERING DEVELOPMENT

### 5.2.1 SOURCE SELECTION

The only vendor to respond positively to the requests for quotation on the ATS sun sensor subsystem was the Adcole Corporation. Their basic design has been modified to conform with requirements for Hughes Aircraft Company approved parts, for alignment provisions, and for addition of temperature sensors in each detector and the electronics unit. (GE documents #490106 and 4906107, "Approved Parts List", and "Approved Materials and Processes", respectively was provided to Adcole for compliance.

### 5.2.2 OPERATING CHARACTERISTICS

Three major performance characteristics of the SAS which had not been sufficiently investigated to assure satisfactory performance on the ATS were examined analytically; these include: Crosscoupling, Maximum Error in Sun Detection Measurement and Possibility of False Triggering on Earth-Reflected Sunlight. In addition to the areas discussed below, an error analysis was performed by Adcole which is reprinted as Appendix F of Reference 1. (Section 5.6).

### 5.2.2.1 Crosscoupling

This phenomenon is seen as the dependence of the output of one detector eye when measuring an Angle A on the Angle B measured by the other detector eye in a plane orthogonal to that containing Angle A (See Figure 5-5). The effect is shown in Figure 5-6. Examination of the transfer function,  $f(A, B)$ , has revealed the following:

1. Crosscoupling between the two geometrically orthogonal axes occurs because of the nature of the refraction at the airquartz entrance to the reticle.
2. No crosscoupling occurs at Angles B (or A) = 90°, i. e. , when the incident light is in the X-Z (or Y-Z) plane.
3. Crosscoupling is a maximum when one angle (e.g., A) is at the edge of the field of view (26- to 26.6- degrees) and the other angle (e.g., B) is between 38.7- and 51.3- degrees.

A detailed investigation of crosscoupling is described in Appendix C of Reference 2 (section 5.6).

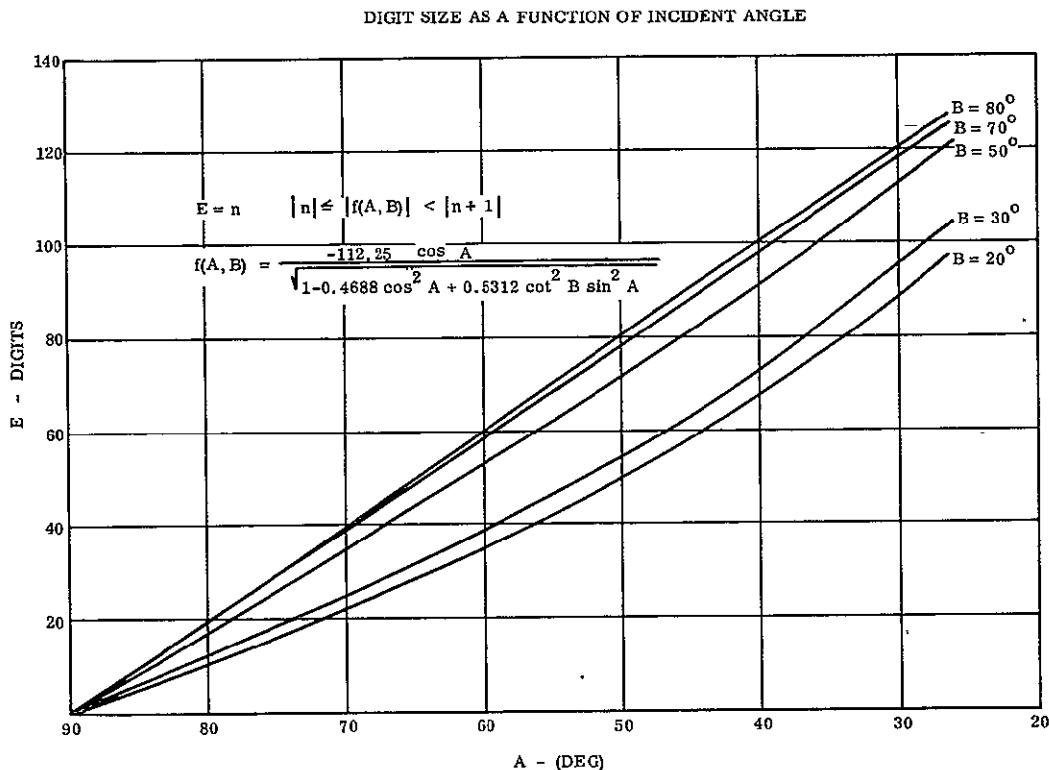


Figure 5-5. SAS Detector Alignment Geometry





The error analysis can be summarized as follows:

1. The maximum error in Angle A is 1.30 degrees when  $A = 50^\circ$  and  $B = 26^\circ$ , which is consistent with the region of maximum crosscoupling as previously discussed.
2. The minimum error in Angle A occurs for  $A = 50^\circ$  and  $B = 90^\circ$ , and is  $0.48^\circ$ . The error in A when it is measured in the X-Z plane, however, is slightly larger than  $0.5^\circ$ . This occurs because, although the output of cell no. 2 is zero, there is an uncertainty of one digit in the reading of Angle B.

#### 5.2.2.3 Possibility of False Triggering on Earth-Reflected Sunlight

A solar aspect system with full spherical coverage will have both the sun and the earth in its field of view at the same time. The system must, therefore, be able to distinguish between the two. The SAS consists of five detector units with overlapping fields. One of these detectors is selected by the electronic unit and its readings are the only information processed. Detector selection is made by comparison of signals from "AGC" cells which are part of each detector. The detection sensitivity is at least 1 degree, which corresponds to 3.3 percent of the signal at 64 degrees.

Interference with sun sensor operation in this case would mean that the flux received from the earth is so nearly equal the flux received from the sun in a worst case arrangement that the detector facing the earth would be selected. Erroneous information would then be presented to the telemetry.

Analysis of the problem, therefore, consists of establishing the magnitude of both the earth-shine flux and the solar flux at the AGC cells. The worst case exists in the lower (6000 nm) orbit and when one detector is oriented parallel to the earth terminator, while the other detector is inclined 64 degrees to the sun. The analysis shows the solar flux received at the AGC cell is eight times the flux received due to earth shine. False detector selection can, therefore, be ruled out.

A detailed analysis on this problem is presented in Reference 1 (Section 5.6).

### 5.2.3 MECHANICAL CONSIDERATIONS

The primary mechanical requirements which must be satisfied by the SAS design are the following:

1. Ability to withstand the expected launch environment (shock, vibration, acceleration, rapidly changing pressure).
2. Ability to operate for extended periods under orbital conditions (vacuum, temperature extremes and transients, radiation).
3. Ability to be aligned on the ATS spacecraft with an accuracy consistent with the measurement capability of the sensor.

The light-weight, simple, mechanical design of both the detectors and the electronics unit assures compliance with the first requirement, a fact which has been repeatedly demonstrated in engineering, qualification and acceptance tests. The final design of the SAS employs magnesium-lithium alloy cases, in place of the manufacturer's standard aluminum construction, for reduced weight.

The insensitivity of quartz- to-thermal and radiation effects, the careful choice of electronic components, and the protection afforded the electronics unit by the frame and surfaces of the spacecraft provide a high degree of confidence that the orbital requirements will be met satisfactorily.

Alignment on the spacecraft is through the use of an intermediate fixture which is attached to reference surfaces on each detector and contains mirrors for optical autocollimation. The SAS manufacturer is required to maintain alignment of the sensitive axes with respect to the reference surfaces.

The size of each of the five detectors is 3.17 by 3.17 by 0.8 inches. The size of the electronics unit is 4.43 by 4.49 by 8.54 inches. The size of the electronics unit is 4.43 by 4.49 by 8.54 inches. Total system weight is less than 5 pounds.

Each of the six major items in the SAS contain resistance-type temperature sensors which will provide useful data in verifying thermal predictions and in establishing requirements for future programs.

#### 5.2.4 ELECTRICAL CONSIDERATIONS

The solar aspect sensor is designed to operate on a 24 vdc power that is regulated to  $\pm 2$  per cent and to consume a maximum of 1.05 watts. Line transients of  $\pm 1.5$  volts with a time duration of 5 milliseconds will not interfere with normal operation of the Solar Aspect Sensor.

The outputs of the Solar Aspect Sensor terminate in a current-limiting resistor followed by two parallel diodes. The outputs are:

1. Three parallel outputs that indicate the detector being read in binary code.
2. Eight parallel outputs for each of the two measurement axes that indicate the angles being read in Gray code.

When the Solar Aspect Sensor is terminated (Figure 5-7) the voltage at points A and B shall be as follows:

For Gray or Binary Code "0"

$$V_a = V_b = 0 \text{ vdc} + .4 \text{ vdc} \\ -2.0 \text{ vdc}$$

For Gray or Binary Code "1"

$$V_a = V_c = +0 \text{ mv} \\ -50 \text{ mv}$$

$$V_b = V_d = +0 \text{ mv} \\ -50 \text{ mv}$$

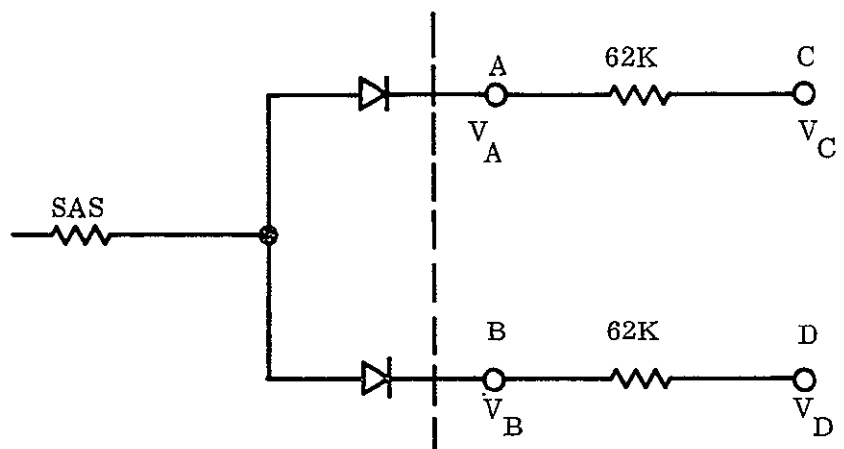


Figure 5-7. SAS Termination Circuit

The Solar Aspect Sensor has a separate test connector for monitoring of the following functions:

1. All internally generated voltages
2. Scan oscillator output
3. Clock pulse
4. Set pulse
5. AGC output

The Solar Aspect Sensor while operating will be provided with a start pulse every three seconds from the spacecraft. This pulse will be a -23 volt pulse with a time duration of 46.4 milliseconds. Seven milliseconds after the receipt of this pulse the Solar Aspect Sensor will present its readings at the outputs and will remain unchanged until receipt of the next start pulse.

#### 5.2.5 ENGINEERING TEST PROGRAM

##### 5.2.5.1 Objectives

The engineering test and evaluation of the SAS was conducted during the period July through December 1965. The objectives of these tests were to demonstrate:

1. Soundness of the SAS design under extreme environmental conditions, particularly solar vacuum
2. Agreement between theoretically predictions and actual performance
3. Agreement of test results from GE and Adcole

##### 5.2.5.2 Test Descriptions, Equipment and Results

In subsequent paragraphs, each phase of the engineering test will be described, the required test equipment noted, and the results summarized. Due to the nature of the SAS, it was appropriate to test the detector individually, the electronics unit, and the detector-electronics combination (system).

#### 5.2.5.2.1 Detector Tests

5.2.5.2.1.1 Philosophy/Description. It has been shown in Appendix C of Reference 1 (Section 5.6) that the sun's direction, as defined by angles measured in two orthogonal planes, can be determined if the digital output of both detector eyes is given. (The expressions are repeated in Appendix 5A of this report.) Furthermore, determination of the detector transition edges\* in the normal planes (Angles A or B =  $90^\circ$  as shown in Figure 5-5) defines the performance of the detectors in all planes according to the expressions referenced above. It therefore remained to measure the transition edge locations with respect to a normal to the detector (the "0" direction). These locations, as well as the actual output of each "bit" cell, were measured for both detector eyes to provide a complete picture of the detector operation.

#### 5.2.5.2.1.2 Test Equipment and Procedure.

The detector was mounted to a fixture on a pair of orthogonally arranged rotary tables (rotabs), as shown in Figure 5-8. The detector face was aligned normal to the beam axis of the xenon arc lamp solar simulator with an alignment mirror fixture and an autocollimator.

The output of the least significant bit and AGC cells were connected as shown in Figure 5-9 and the null condition determined with a John Fluke Differential Voltmeter. The position of the smaller (upper) rotab was readout with an accuracy of  $\pm 1$  arc minute at each null within the  $\pm 64$ -degree field-of-view about each detector sensitive axis. Similarly, the output of each "bit" cell was measured.

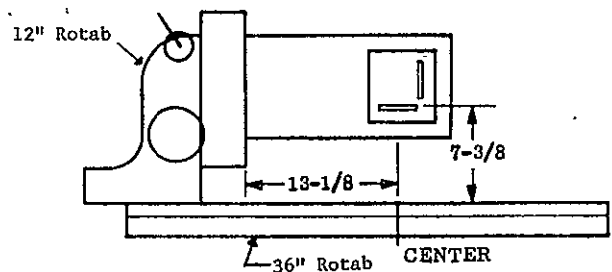


Figure 5-8. Optical Alignment Setup.

---

\*Those angles at which the least significant bit cell current equals the AGC cell current.

These tests were conducted at 25°C and repeated at -107°C and +100°C.

5.2.5.2.1.3 Results. The silicon cell output currents for each of the 8 "bits" were measured and are shown in Figures 5-10 thru 5-13. (For brevity, only single-axis data is shown.)

The errors in transition edge location for each bit, both for the detector and for the SAS System, are shown in Figures 5-14 through 5-17. (System errors will be discussed in a subsequent paragraph.) It is clear that the detector errors are well below the specified maximum error of 1.3 degrees.

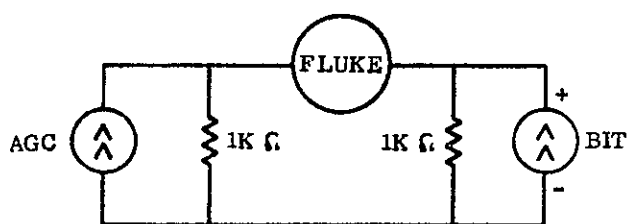


Figure 5-9. Nulling Circuit

#### 5.2.5.2.2 Electronics Tests

All tests of the electronics unit were performed using the ATS-SAS test console, which is described in Appendix 5C to this report. Since the capabilities and operation of the test console are described in detail in that appendix, only those functions directly related to each electronics test will be mentioned in the following discussions.

All tests were conducted at temperatures of -15°C, 25°C, and 55°C.

##### 5.2.5.2.2.1 Minimum Eye Selection Current.

#### 1. Test Description

In this test, the ability of the electronics unit to determine which eye is "most illuminated" is evaluated. The procedure is to shield three of the five detectors (or silicon cells representing their AGC cells) from all illumination so that their current output is zero; to



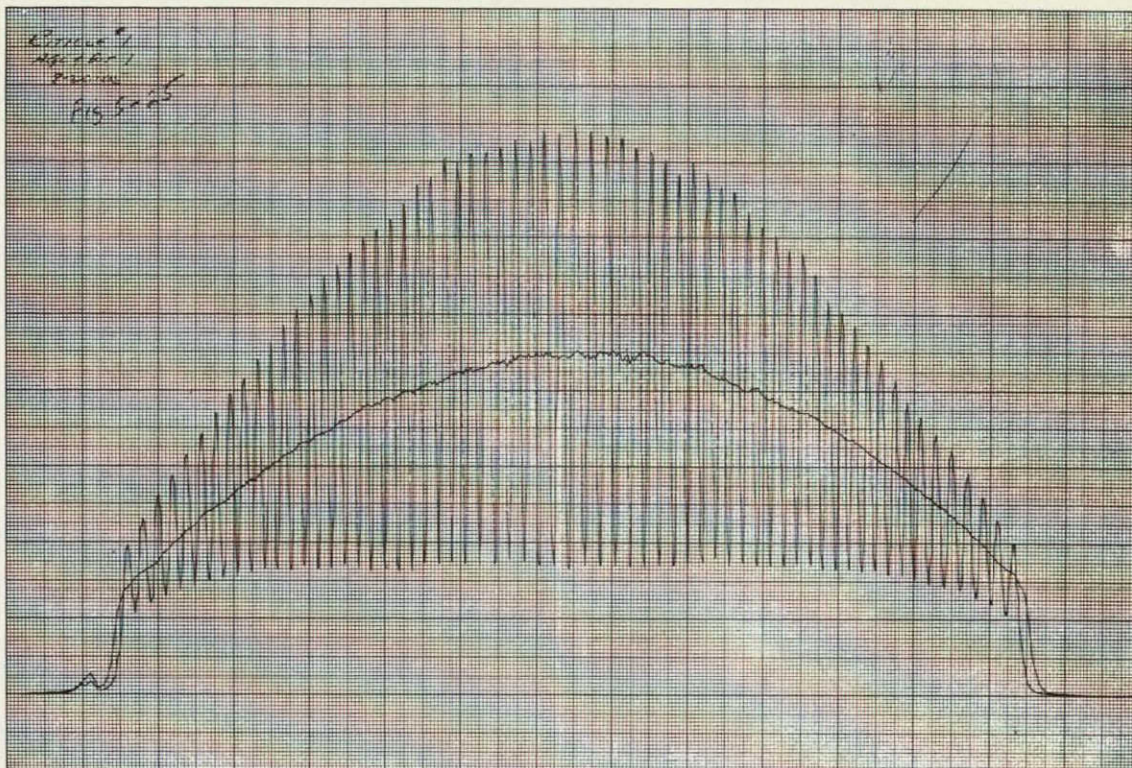


Figure 5-10. Test Results, Recticle 1 AGC and Bit 1

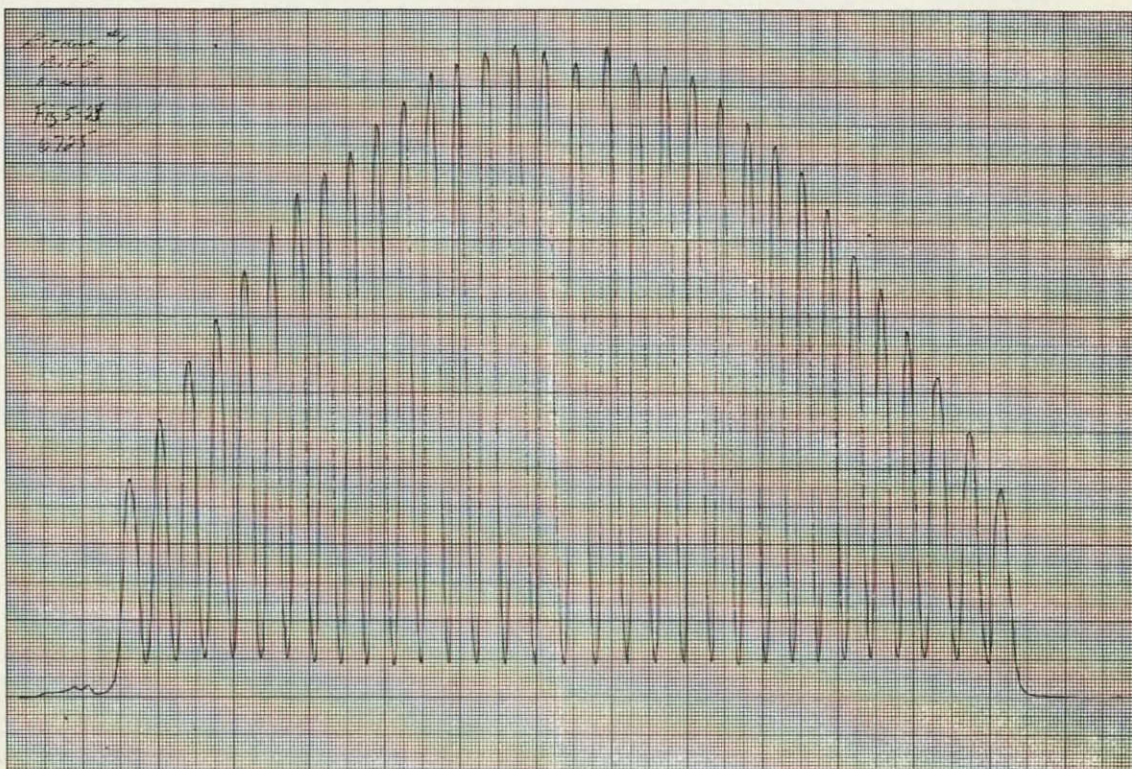


Figure 5-11. Tests Results, Recticle 1 Bit 2



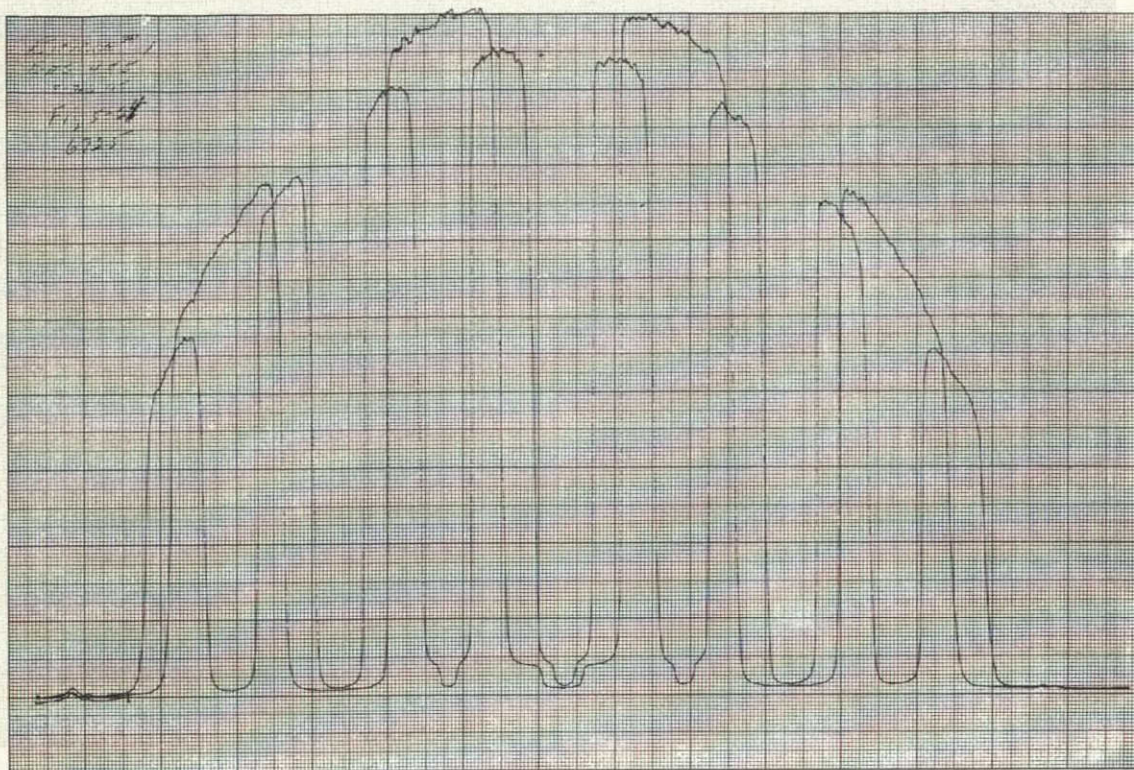


Figure 5-12. Test Results, Reticle 1 Bits 4 and 5

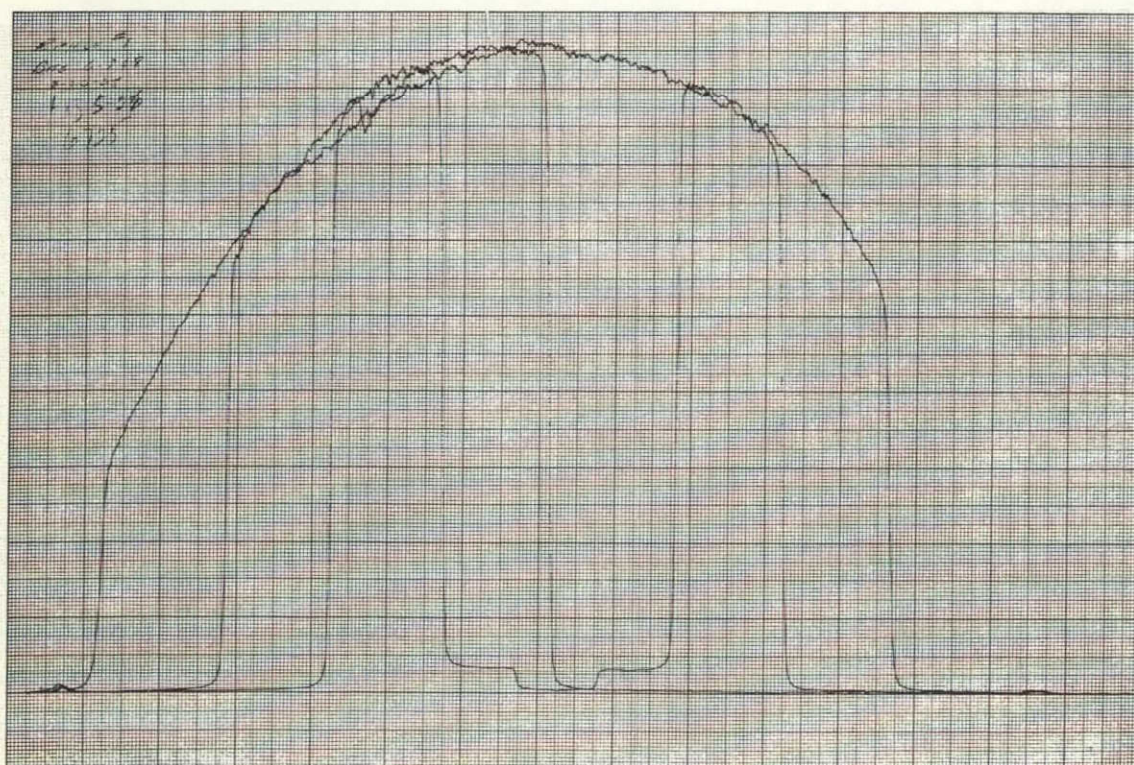


Figure 5-13. Test Results, Reticle 1 Bits 6, 7, and 8



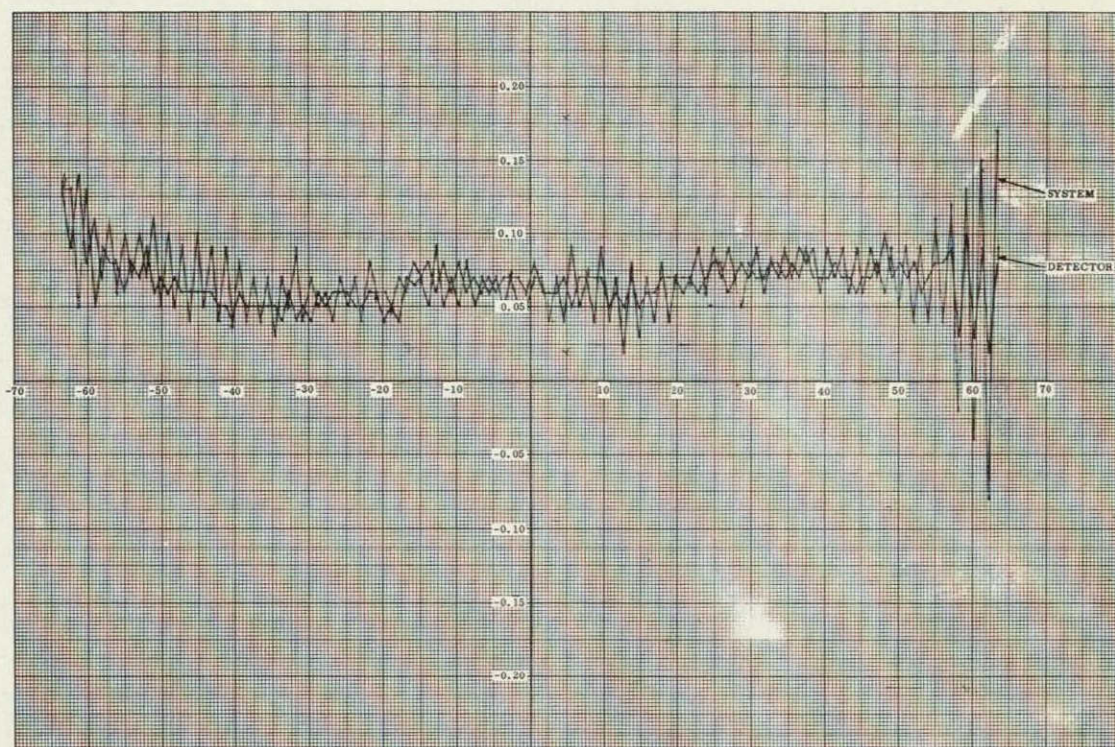


Figure 5-14. Transition Edge Error vs True Transition Position (Reticle 1, Bit 1)

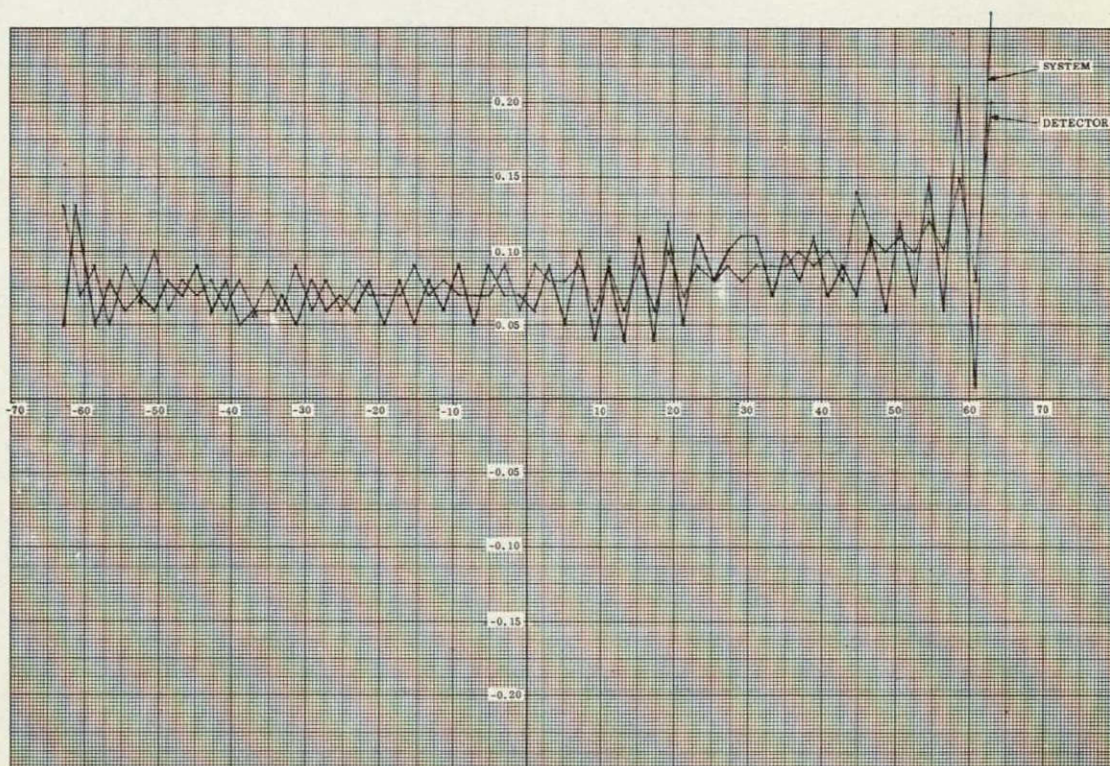


Figure 5-15. Transition Edge Error vs True Transition Position (Reticle 1, Bit 2)



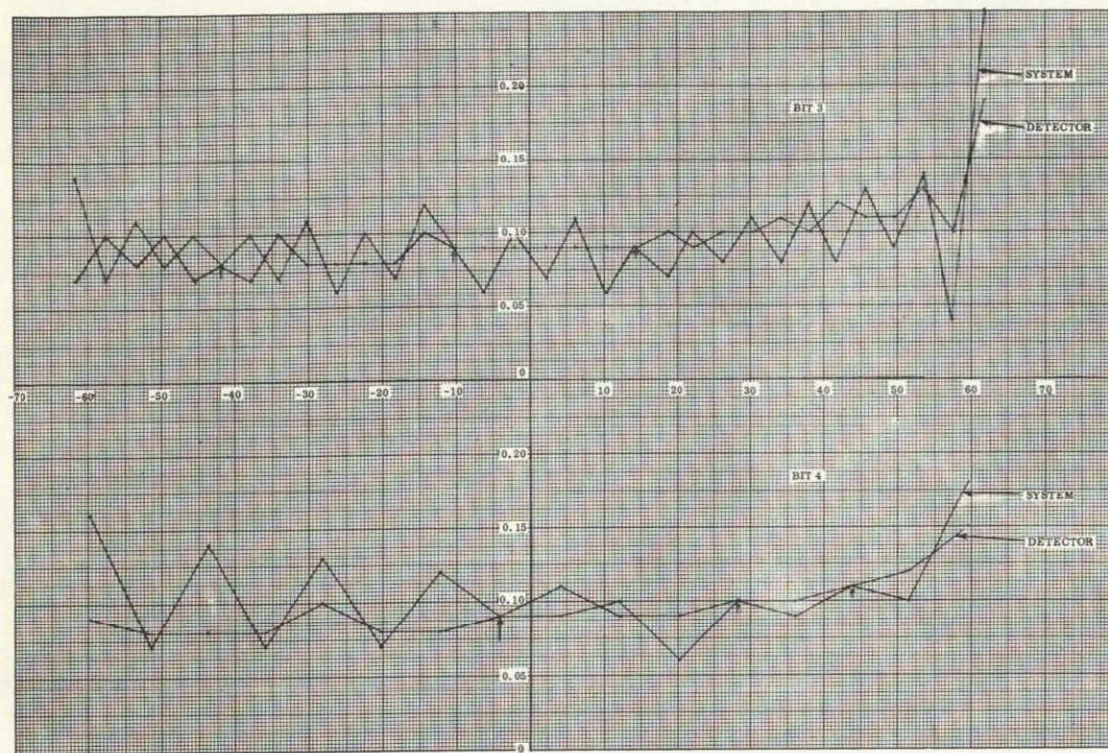


Figure 5-16. Transition Edge Error vs True Transition Position (Reticle 1, Bits 3 & 4)

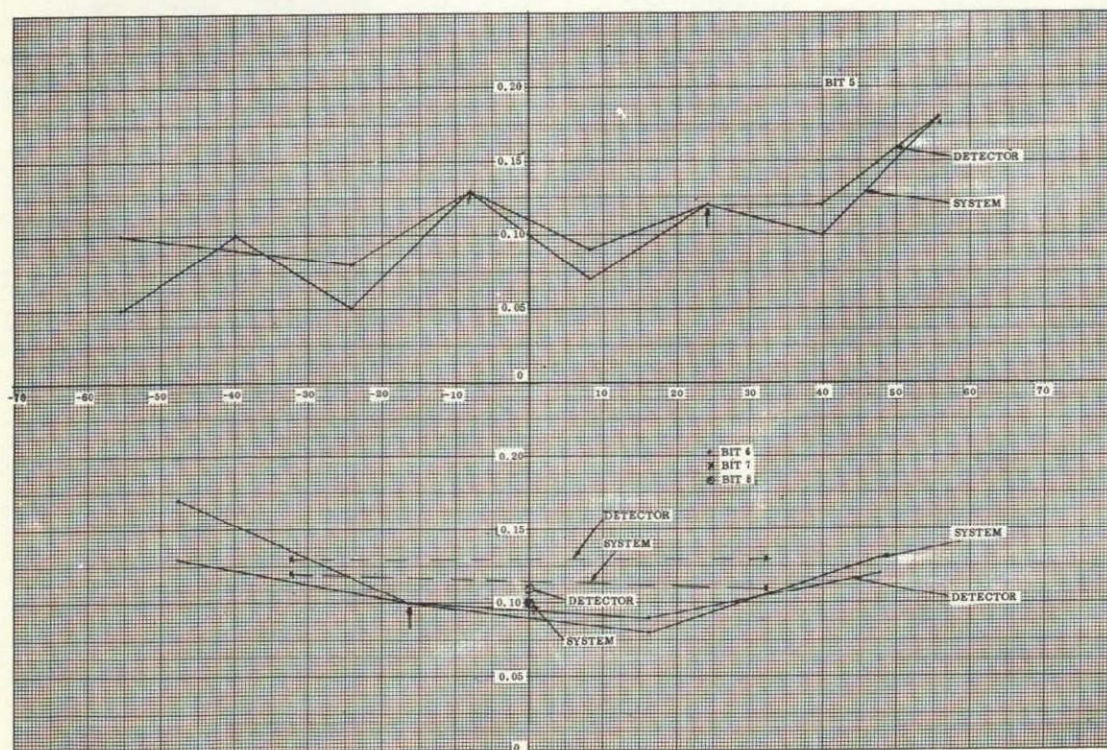


Figure 5-17. Transition Edge Error vs True Transition Position (Reticle 1, Bits 5, 6, 7 & 8)



illuminate a fourth detector so that the AGC cell output current is a particular value (e.g., 10  $\mu$ a); and increasing the output current of the fifth AGC cell (by increasing its illumination) until the unit selects the "fifth" detector as most illuminated.

For each value of "set" current, there are 25 data points. The "set" currents at which these eye selections were investigated were 10, 25 and 43  $\mu$ a. The entire test was conducted at three different input voltage levels: nominal (-24.00 vdc), maximum (-24.48 vdc), and minimum (-23.52 vdc).

## 2. Results

Under the conditions of this test as stated above, the electronics AGC circuitry established a level from the cells of each head and during the scanning selected the most illuminated. The test was performed using the 25 possible permutations of the heads.

With the AGC input set at 10  $\mu$ a, the simulated AGC current from another head was increased. The second head was selected at approximately 2  $\mu$ a greater than the reference head. At 25  $\mu$ a input, the one to cause selection was 3  $\mu$ a and at 4 AGC 3  $\mu$ a, the differential required was approximately 4  $\mu$ a.

### 5.2.5.2.2.2 AGC Linearity

#### 1. Test Description

This test was to establish the linearity between the AGC current and the AGC voltage. The AGC voltage was monitored as the AGC current was increased in 5  $\mu$ a increments from 0 to 60  $\mu$ a. This test was performed on two AGC cells, one from Detector No. 1 and the other from Detector No. 5.

#### 2. Results

Test data showed the linearity to be better than 5 percent.

### 5.2.5.2.2.3 AGC Response

The AGC Response Test was performed to demonstrate the ability of the electronics to respond to changes in AGC current.

The electronics was operated in its normal mode with the exception of the AGC current input. The AGC input had a dc level of 25  $\mu$ a with a sinusoidal peak-to-peak AGC output voltage became distorted. This occurred at approximately 20 cps.

#### 5.2.5.2.2.4 Bit Amplifier Performance.

##### 1. Test Description

The electronics, in its normal mode of operation, had AGC current inputs of 10  $\mu$ a, 25  $\mu$ a and 43  $\mu$ a; the current of the 16-bit information cells was increased until the output of the electronics changed state ("0" to "1"). This test showed the ability of the electronics to detect the threshold level of the bit current.

##### 2. Results

The maximum deviation from the nominal threshold levels and tolerances are:

10 $\mu$ a	+ 0.00 $\mu$ a	- 0.67 $\mu$ a
25 $\mu$ a	+00.20 $\mu$ a	-00.24 $\mu$ a
43 $\mu$ a	+00.65 $\mu$ a	-00.12 $\mu$ a

#### 5.2.5.2.3 System Tests

The purpose of these tests was to verify that the operation of the detector-electronics unit combination met the SAS accuracy requirements.

##### 5.2.5.2.3.1 Transition Edge Locations.

##### 1. Test Description and Equipment

This test was essentially identical to the detector transition edge test (see Section 5.2.5.2.1), except that the change in state of the output bits from the electronics unit was used to sense the transition edges. The test was performed at 25°C with the xenon lamp solar simulator.

##### 2. Results

The error data resulting from this test is plotted on Figure 5-10 through 5-13 (the same sheets which show the detector errors). It can be seen that system operation is well within the allowable error.

### 5.2.5.2.3.2 Compound Angle Measurement in Direct Sunlight

#### 1. Test Description and Equipment

In this test conducted during October 1965, a detector was aligned with a precisely known relation to true south, and the output of the electronics unit monitored every two minutes for comparison with the actual sun direction at that instant. The true south direction was found through observations of prominent landmarks whose positions were well known. The actual sun direction for the latitude and longitude of the test site (the roof of the GE Space Center) was found from data in the 1965 American Ephemeris and Nautical Almanac. A theodolite, alignment mirrors, and a standard time data source were used in the test. To record the output of the electronics unit, a multipoint recorder was used which had a two minute cycling time. This presented a problem since the output of the electronics unit at the beginning of the recorder cycle was not necessarily the output at the end of the cycle, since the electronics might have switched at the middle (anywhere throughout the duration) of the cycle. For this reason, the interrogate oscillator (in the test console) was disabled and the electronics unit was given a readout pulse every 2 minutes. This was accomplished by enabling the interrogate oscillator for approximately 3 seconds every 2 minutes. In this manner, once the recorder started its cycle, the readout was fixed for the duration of the cycle.

#### 2. Data Processing

To simplify the process of data reduction, a computer program was devised. This program employed the sensor transformation equations to determine the orthogonal angles of the sun as measured by the sensor. It then compared the measured angle with the actual as determined from the data on sensor orientation site coordinates and time. The printout displayed the time of the reading, the true angle, the measured angle and the error. The appropriate translation equations and a typical data sheet are given in Appendix 5D to this section.

#### 3. Results

The entire printout for this test was contained in Reference 3 (Section 5.6) and will not be repeated here. An examination of these results, however, clearly indicates entirely satisfactory operation of the SAS in measuring compound angles.

Data was accumulated with the sun in two separate planes, i.e., Angle B varying from 18 to 8 degrees with Angle A varied from -64 to +64 degrees, and at the edge of the field of view with Angle B varying from 61 to 64 degrees and Angle A varying from 64 to 53 degrees. The first 12 readings from the extreme edge of the field show an error of less than 0.6 degree, only about half of the maximum allowable error of 1.3 degrees.

#### 4. Verification of Compound Angle Test Results

In conjunction with the compound angle tests that were conducted on the Solar Aspect Sensor, an additional test was performed to increase the confidence level in the register output.

The detector was mounted to the test fixture as shown in Figure 5-18.

In the initial condition the solar simulator was arranged normal to the detector. The detector was then rotated by the 36-inch rotary table and the output recorded for various table angles.

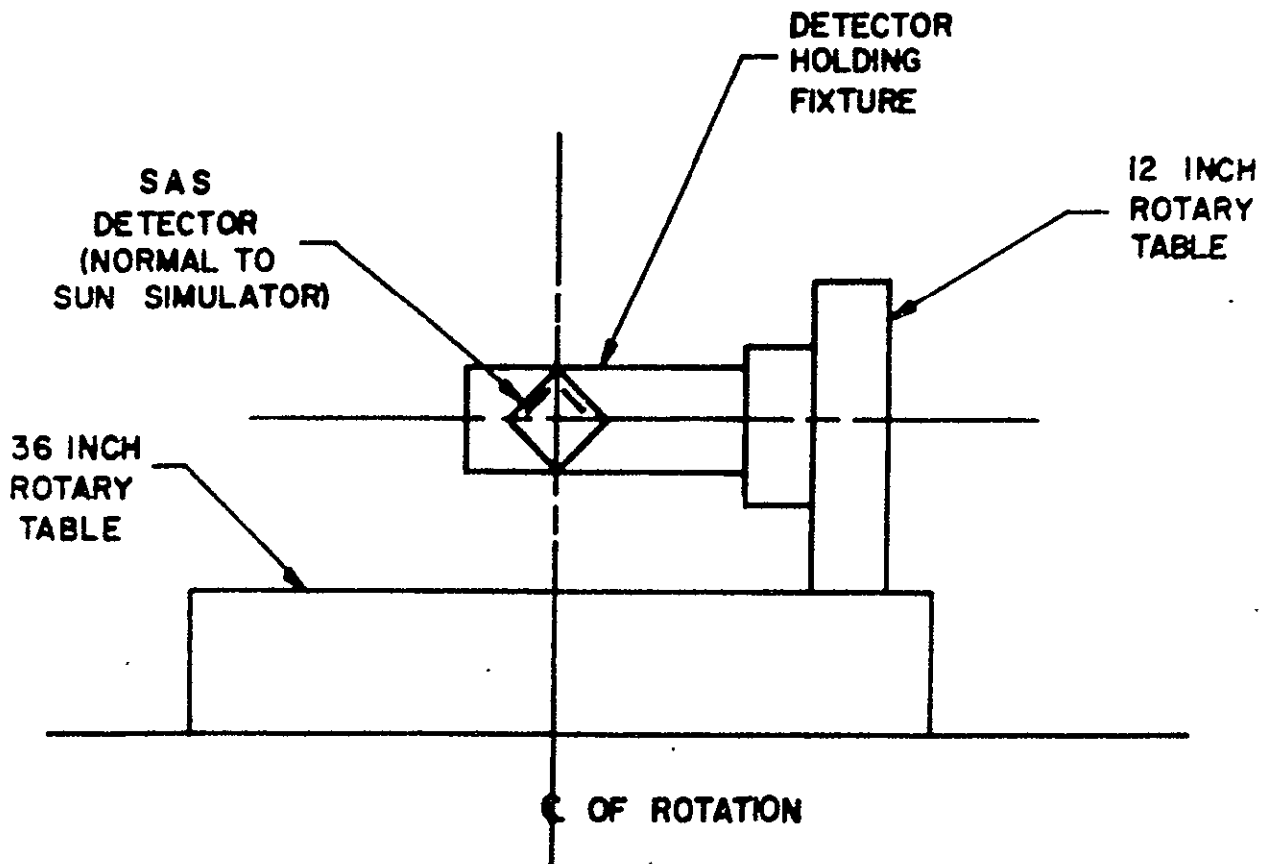


Figure 5-18. SAS Detector and Test Fixture

The output of the register was calculated for given table angles and the effect of this angle on Eye No. 1. Figure 5-19 illustrates the geometry for the calculation of the effective angle sensed by Eye No. 1.

Angle  $\phi$  is defined as the table induced angle about the  $Z' - Z'$  axis. Angle  $B$  is the angle detected by Eye No. 1. Line OE is defined as the normal to the detector face. A typical calculation is as follows:

Induce a table angle of  $25^\circ$ , this will be rotation about the  $Z' - Z'$  axis,

Angle  $\phi = 25^\circ$  Assume  $OE = 1$ ; this can be done without loss of generality.

$$B = \tan^{-1} 0.466$$

$$B = 33.4^\circ$$

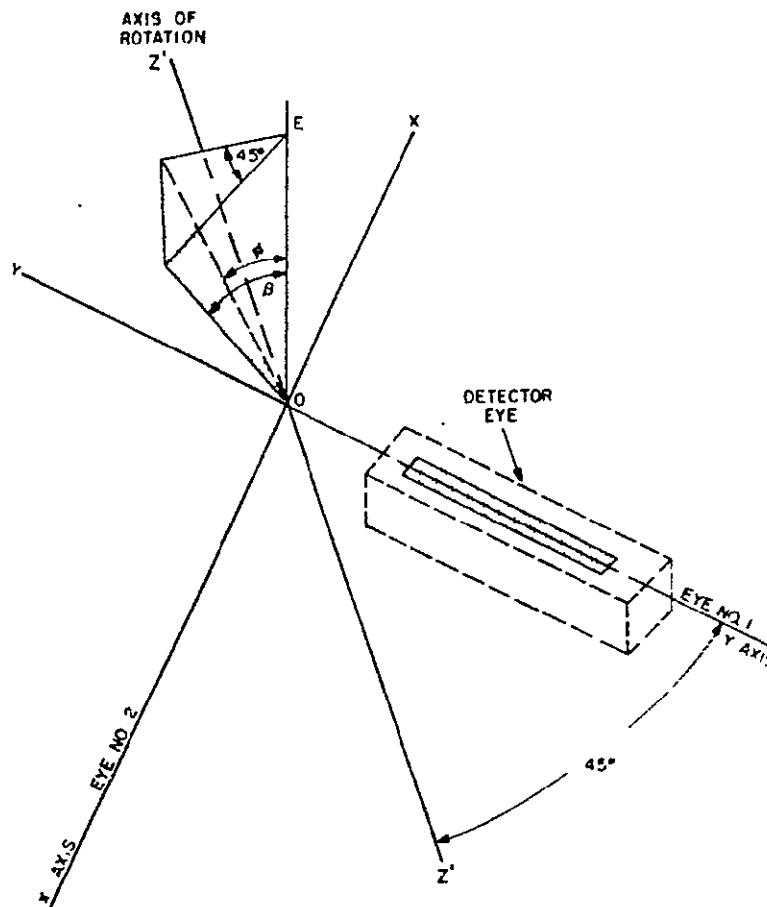


Figure 5-19. Sensed Angle Geometry

This value is the theoretical value of the angle as sensed by Eye No. 1. This was compared to the actual register output.

<u>Actual</u>	<u>Theoretical</u>
32.5°	33.4°

This angular difference is still below the 1.3 band given to compound angles. The curve on Figure 5-20 is a plot of one eye of theoretical value of the angle versus actual readout of that eye.

5.2.5.2.4 Environmental Tests

5.2.5.2.4.1 General

Since the Adcole Solar Aspect Sensor had been previously flight-qualified on earlier space missions, a full environmental test program was not required. It was necessary, however, to qualify the design under those ATS environments which were significantly different from

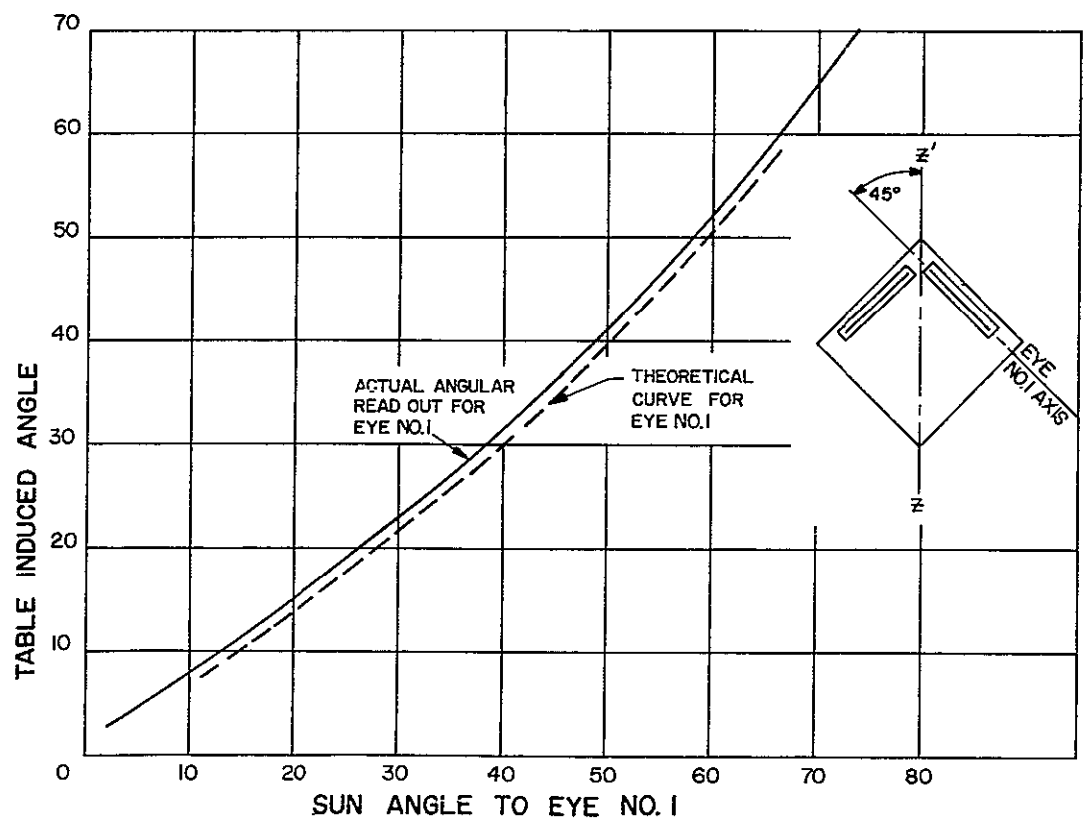


Figure 5-20. Theoretical Value versus Actual Readout



those of the earlier missions. An examination of requirements revealed that the vibration and solar vacuum tests were critical. (It must be understood that this discussion applies only to the engineering test program, and that prototype and flight units are vigorously qualification and acceptance tested.)

#### 5.2.5.2.4.2 Vibration Tests

The vibration test levels used were the qualification levels described in General Electric Specification SVS-7306. These tests were of particular interest since they were required to prove the new light magnesium-lithium cases. The only failure was a broken mounting bracket in the electronics unit. The corrective redesign was shown to be entirely satisfactory in a subsequent test.

#### 5.2.5.2.4.3 Solar Vacuum Tests

##### 1. Purpose

The solar vacuum test was required to determine the temperature extremes which the SAS detectors would "see" in the flight environment and to assure that operation at these temperatures would be satisfactory.

##### 2. Test Setup

An SAS detector was mounted on a fixture in a vacuum chamber so that it could be illuminated by simulated solar radiation. (See Figure 5-21) The fixture was designed to thermally isolate the detector so that the heating and cooling rates were a function only of the detector's thermal qualities. The electronics unit was also placed in the chamber, but was not exposed to the sunlight. (It's temperature was maintained in the range  $70 \pm 50^{\circ}\text{F}$ .) See Figure 5-22.

##### 3. Test Profile

This profile was to be followed for three cycles, however, on the third and final cycle the parabolic reflector of the solar simulator cracked. Thermal analysis concluded that the test need not be completed. The Solar Aspect Sensor responded properly to stimulation at the temperature extremes. The maximum temperature experienced by the detectors was  $+125^{\circ}\text{F}$  and  $-23^{\circ}\text{F}$ , and electronics  $+108^{\circ}\text{F}$  and  $+20^{\circ}\text{F}$ .

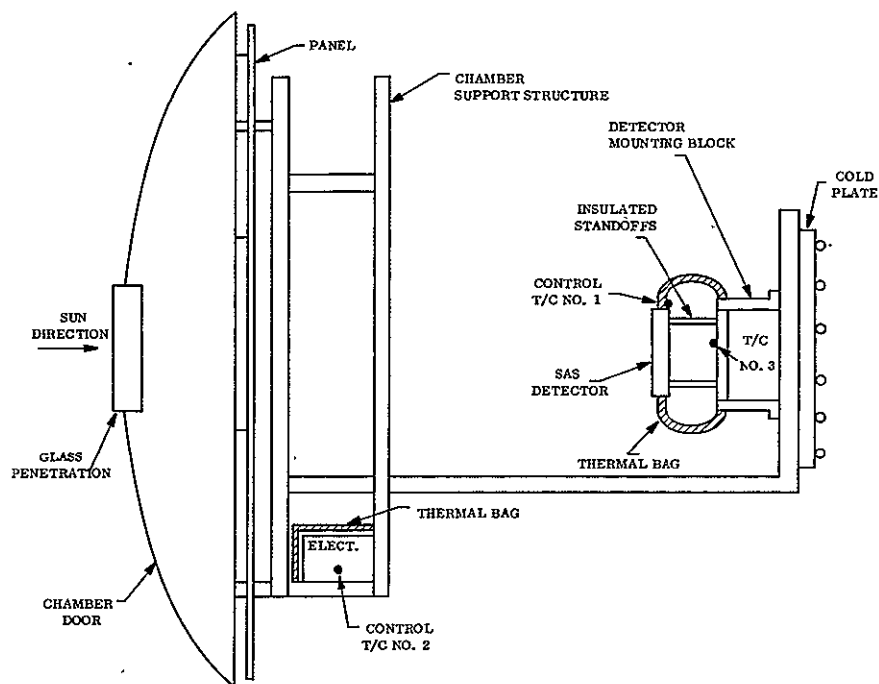


Figure 5-21. SAS Solar - Vacuum Test in 5-By 6-Foot Chamber

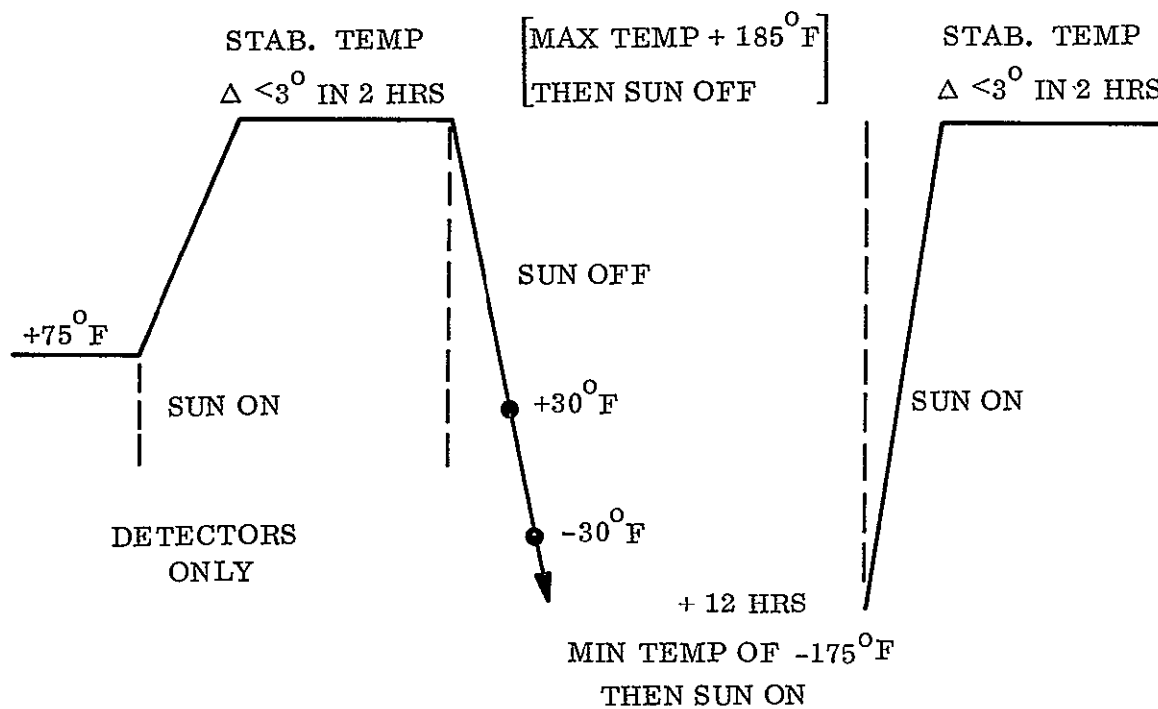


Figure 5-22. Test Profile Temperature Excursion

#### 5.2.5.2.4.4 Magnetic Field Effects on Proper SAS Operation

During system tests of the GGTS Flight vehicle\*, a malfunction of the SAS was discovered. As the vehicle was rotated by the test fixture, the SAS internally-generated voltages began to decay. It appeared that the SAS was sensitive to changes in vehicle attitude. The electronics unit was removed and powered through extender cables from the spacecraft. The electronics unit was then moved through various attitudes, but the malfunction was not repeated.

It was suggested that possibly the magnetic field generated by the damper magnets was affecting the transformer in the power supply assembly of the SAS electronics. The electronics unit was powered on the bench and the magnets placed at their approximate locations near the unit. The malfunction was repeated by rotating the damper magnets and the field strength measured. A flux density of 8 gauss was sufficient to cause the SAS electronics to fail. In orbit, no problem exists since the damper magnets will be deployed on the GGTS vehicle. The magnets of the ATS Combination Passive Damper will remain within the vehicle, so tests were conducted using the SAS electronics and CPD No. 1. Tests proved that the field generated by the CPD is not of sufficient magnitude to hinder proper operation of the SAS in the ATS vehicle, and no further testing of this type was conducted.

#### 5.2.6 CONCLUSIONS BASED ON SAS ENGINEERING TEST PROGRAM

The engineering test program verified that the Adcole Solar Aspect Sensor meets the functional and environmental requirements of the ATS mission.

#### 5.3 QUALIFICATION TESTS

Two prototype Solar Aspect Sensor units (designated as component and system qual.) were subjected to similar environments at more severe levels than the anticipated operating environments in order to establish confidence that the design was valid under extreme operating conditions. Following tests, the component qual unit was not further dispositioned, but the system qual unit was included in the spacecraft qualification tests conducted

---

\*A solar aspect sensor system was also used as a sensor on board the Gravity Gradient Test Satellite.

by the vehicle contractors following the GE tests. A summary of these environments and references to the appropriate test reports are listed below. These documents are on file at GE and will be made available on request of the Contract Administrators for NASA programs.

### 5.3.1 QUALIFICATION

#### 5.3.1.1 Component Qualification

Serial No.	PO3 (electronics) PO31 - PO35 (detector)
Part No.	47D207014P1 (electronics) 47D207013P1 (detector)
Test Reports	4315 - QC - 006 (8/1/66) 4315 - QC - 007 (8/31/66)
Failure Analysis Report	192 - E - 6 (6/9/66)

#### Test Sequence:

1. Functional
2. Temperature
3. Acceleration
4. Humidity
5. Thermal-Vacuum
6. Dipole
7. Weight and CG

Note: Hi Pot and megger test performed at GE

Vibration test performed by Vendor prior to shipment to GE

### 5.4 FLIGHT ACCEPTANCE

Each of the Solar Aspect Sensor flight units was exposed to vibration and thermal-vacuum environments at levels anticipated during flight to verify that the design had not degraded

during manufacture. A summary of these environments and references to the applicable test reports are listed below. These documents are on file at GE and will be made available on request of the Contract Administrator for NASA programs.

#### 5.4.1 ATS-A

Serial No.	F04 (electronics) F041 - F045 (detector)
Part No.	47D207014P1 (electronics) 47D207013P1 (detector)
Test Report	4315 - QC - 012 (9/15/65)
<u>Test Sequence:</u>	
1.	Functional
2.	Thermal-Vacuum
3.	Functional
4.	Dipole
5.	Weight and CG

#### 5.4.2 ATS-D

Serial No.	F05 (electronics) F051-F055 (detector)
Part No.	47D207014P1 (electronics) 47D207013P1 (detector)
Eng. Test Reports	4315 - QC - 233 (2/8/67)
<u>Test Sequence:</u>	
1.	Functional
2.	Thermal-Vacuum
3.	Functional

4. Dipole
5. Weight and CG

#### 5.4.3 ATS-E

Serial No.	F03 (electronics) F031 - F035 (detector)
Part No.	47D207014P1 (electronics) 47D207013P1 (detector)
Test Report	4315 - QC - 026 (4/6/67)

#### Test Sequence:

1. Functional
2. Thermal-Vacuum
3. Functional
4. Dipole
5. Weight and CG

5.4.3.1 Solar Aspect Sensor Detector/Electronic Unit Vibration in ATS-E Power-on Launch Mode.

##### 5.4.3.1.1 Summary

NASA planned to verify critical maneuvers of the Centaur second stage during launch of the ATS-E through data supplied by the Solar Aspect Sensor. Since the SAS was not designed to be turned on until the orbit phase, GE conducted vibration test to acceptance levels to establish a level of confidence that the SAS could be operated during powered flight with no degradation in performance of this sensor.

Vibration of each one of the prototype solar aspect sensor (SAS) detector and electronic units to the sinusoidal and random acceptance levels of specification SVS-7306, REV C, in the X-X, Y-Y and Z-Z axes completed in July, 1969. The detector and electronic units were vibrated separately with 24 vdc applied to the interconnected units at all times during the testing.

Continuous monitoring of SAS signal outputs revealed no abnormal conditions while vibrating in the power-on mode. Pre-and post-vibration insulation resistance tests revealed no degradation. Post vibration detector reticle (eye) output measurements with a simulated sun indicated a two-minute shift in detector reticle field of view angle. This shift is based only on the angle measurements taken when each bit of the Gray code first lit an indication lamp on the test console.

#### 5.4.3.1.2 Discussion

Pre-and post-vibration insulation measurements were performed on the electronics unit with an HP 412B VTVM and ATS SAS shorting box. Measurements were taken only on Head 1 connector and J8 and there was no indication of leakage on RX100 meg. ohms.

Pre-and post-vibration detector reticle angle measurements indicated in Table 5-1 were taken utilizing equipment and procedures specified in Standing Instruction SI 237, 012 for the SAS. Each time one of the eight parallel signal output indication lamps on the SAS test console first lit during rotation of the detector head, the Gray code angle was read regardless of the state of the other seven bits.

Vibration testing was conducted to Specification SVS-7306 REV C acceptance levels utilizing the SAS acceleration mounting plate. Detector unit vibration tests were conducted in addition to the electronic unit vibration tests. During all vibration tests both units were interconnected and power (24 vdc) was applied. The detector output angle indication lamps on the SAS test console were monitored during vibration as well as selected test points being watched on an oscilloscope. No abnormal indications were apparent from this monitoring during vibration.

### 5.5 APPLICABLE DOCUMENTS

1. GE Drawing No. 47D207013, "Outline, Solar Aspect Sensor, Detector Unit"

Table 5-1. Detector Field of View Measurement

Reticle "A" of SAS Detector S/N P035 Connected as Detector Head 1 to  
SAS Electronics S/N P030

	Pre-Vibration (deg-min)	Post-Vibration (deg-min)
All bits off at	+0° 8'	+0° 10'
Bit 1A on at	+0° 50'	+0° 52'
Bit 2A on at	+1° 10'	+1° 12'
Bit 3A on at	+2° 14'	+2° 16'
Bit 4A on at	+4° 18'	+4° 18'
Bit 5A on at	+8° 20'	+8° 22'
Bit 6A on at	+16° 28'	+16° 30'
Bit 7A on at	+32° 18'	+32° 20'
Bit 8A on at	+0° 6'	+0° 8'

Reticle "B" of SAS Detector S/N P035 Connected as Detector Head 1 to  
SAS Electronics S/N P030

	Pre-Vibration (deg-min)	Post-Vibration (deg-min)
All bits off at	0° 0'	0° 0'
Bit 1B on at	-0° 42'	-0° 44'
Bit 2B on at	-0° 58'	-0° 58'
Bit 3B on at	-1° 58'	-2° 0'
Bit 4B on at	-4° 0'	-4° 0'
Bit 5B on at	-8° 4'	-8° 6'
Bit 6B on at	Not Obtainable	
Bit 7B on at	-31° 44'	-31° 48'
Bit 8B on at	+0° 18'	+0° 18'

2. GE Drawing No. 47D207014, "Outline, Solar Aspect Sensor, Electronics Unit"
3. GE Drawing No. 47C207035, "Solar Aspect Sensor Detector Alignment"



Other documents containing data related to the SAS engineering evaluation for ATS are:

1. Quarterly Progress Reports, First thru Eighth, "Gravity Gradient Stabilization System for the Applications Technology Satellite", NASA Contract NAS 5-9042, General Electric Co.
2. "Design and Test Audit", same program data as above, 2 Nov. 1966.
3. "ATS System Reliability Analysis Report", Adcole Corporation, 5 May 1965.
4. Specification SVS-7306, "Solar Aspect Sensor - Applications Technology Satellite", Rev. C, dated 6 June 1966.

#### 5.6 LIST OF REFERENCES

##### Document

1. "Third Quarterly Report, Gravity Gradient Stabilization System for Applications Technology Satellite", Document No. 65SD4266, 20 April 1965
2. "Second Quarterly Report, Gravity Gradient Stabilization System for Applications Technology Satellite", Document No. 65SD4201, 10 January 1965
3. "Sixth Quarterly Report, Gravity Gradient Stabilization System for Applications Technology Satellite", Document No. 66SD4318, 20 January 1966

## APPENDIX TO SECTION 5

### Appendix

- 5A      Detector Transformation Equations
- 5B      Determination of the Effective Index of Refraction to be used for SAS Data Reduction
- 5C      SAS Test Console
- 5D      Transformation Equations for Direct Sunlight Test

# APPENDIX 5A DETECTOR TRANSFORMATION EQUATIONS

Given the index of refraction of the reticle block (quartz), N; and the number of bits read out of the detector reading angles A and B as E<sub>1</sub> and E<sub>2</sub>, the angle may be found directly from:

$$\cot A = \frac{E_1}{[L^2 - (1-N^2)(E_1^2 + E_2^2)]^{1/2}}$$

$$\cot B = \frac{E_2}{[L^2 - (1-N^2)(E_1^2 + E_2^2)]^{1/2}}$$

$$L = \frac{128 [1 - N^2 \cos 26^\circ]^{1/2}}{\cos 26^\circ}$$

## NOTE

The error calculations which have been made assume that the bias error which is present due to the assymetric placement of the pattern around zero is removed. That is, the pattern is placed such that the edge of the "0" digit is directly under the slit, rather than its center. Therefore, 1/2 must be added to each reading E<sub>1</sub> or E<sub>2</sub> from the detector before they are substituted into the equations given above.

(N is the index of refraction of the quartz reticle.)

## APPENDIX 5. B

### DETERMINATION OF THE EFFECTIVE INDEX OF REFRACTION TO BE USED FOR SAS DATA REDUCTION

The transfer function of the SAS was derived for monochromatic incident light. Since the detector contains a block of quartz, the index of refraction of quartz appears in the transfer function. Solar illumination, however, is obviously not monochromatic, and the index of refraction of quartz varies sufficiently over the range of wavelengths of the detector response so that an effective index of refraction must be found and incorporated. Graphs of the solar spectrum in the region of interest, silicon solar cell response and the index of refraction of fused quartz as a function of wavelength, are shown in Figures 5B-1, 5B-2 and 5B-3. From these graphs, it is evident that a monochromatic index of refraction is not satisfactory. Specifically, this is shown by differentiating the transfer function (for simplicity the one valid in the planes of the two slits) with respect to the index of refraction,  $n$ .

$$\sigma = \arcsin \left( \frac{nd}{\sqrt{t^2 + d^2}} \right)$$

where

$\sigma$  = Angle of incidence

$d$  = Distance from the center at the bottom of the quartz vehicle

$t$  = Thickness of the quartz reticle = 0.4480 inch

$$\frac{d\sigma}{dn} = \frac{d}{\sqrt{t^2 + d^2} (n^2 - 1)}$$

Then to the first order:

$$\sigma + \Delta\sigma = \frac{nd}{\sqrt{t^2 + d^2}} + \left[ \frac{d}{\sqrt{t^2 + d^2} (n^2 - 1)} \right] \Delta n$$

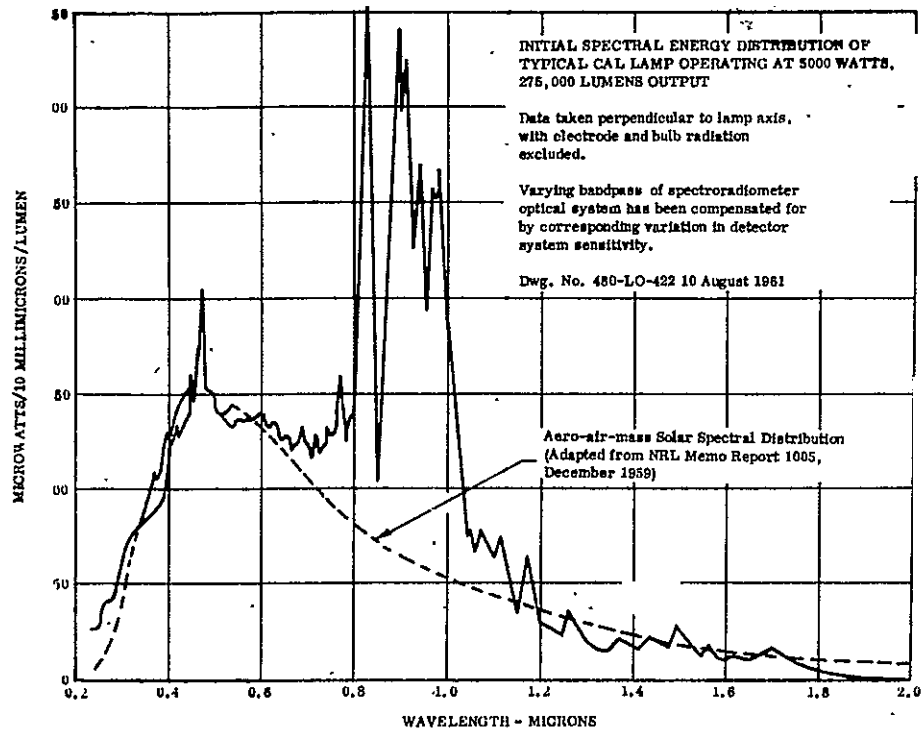


Figure 5B-1. GE 5000 Watt Xenon Compact Arc Lamp

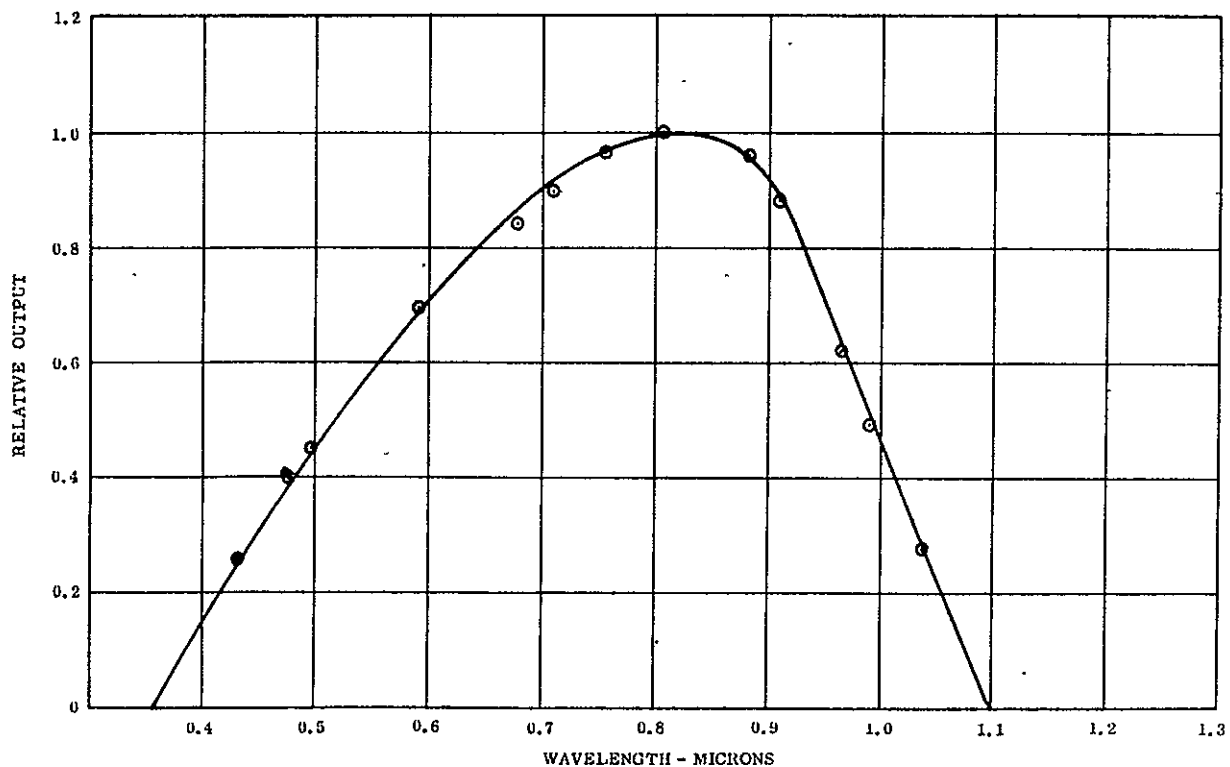


Figure 5B-2. Solar Cell Relative Spectral Response

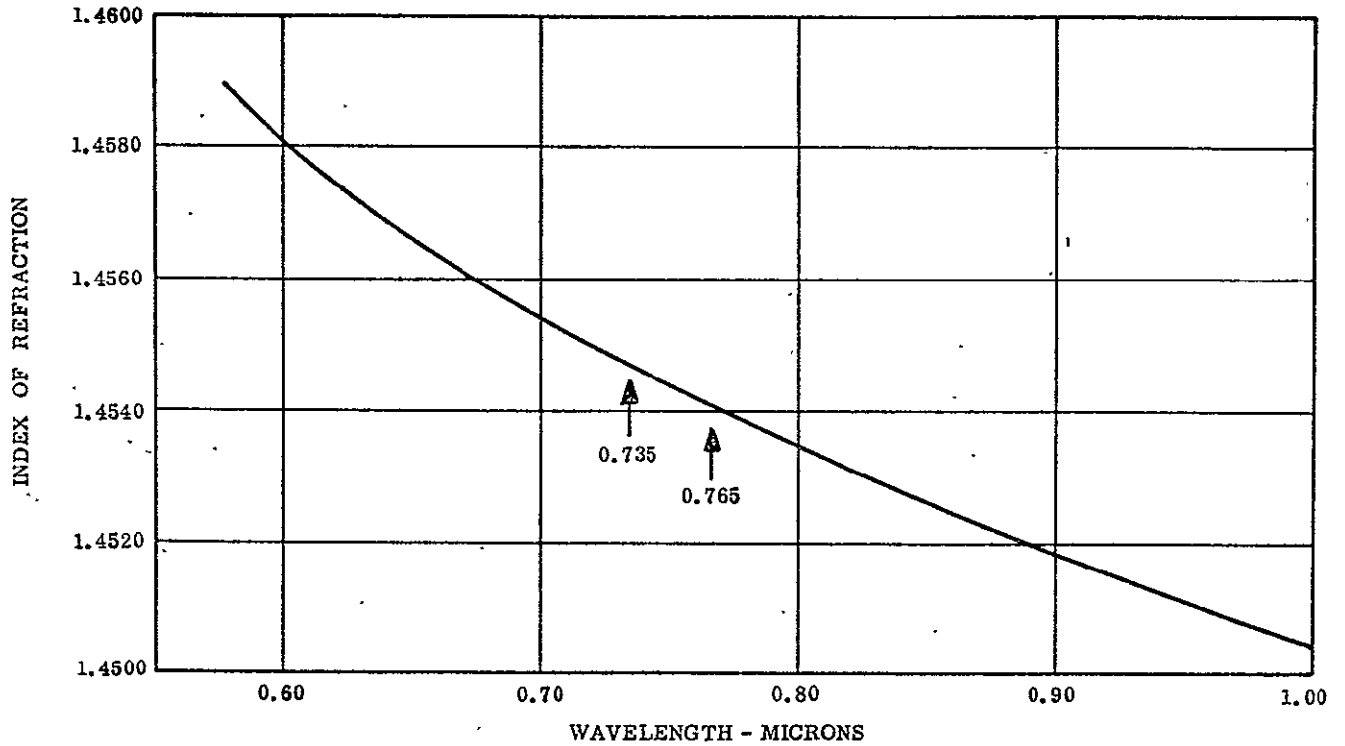


Figure 5B-3. Fused Quartz Index of Refraction

Where  $\Delta \sigma$ ,  $\Delta n$  are small changes in the measured angle of incidence and the index of refraction.

Therefore,

$$\Delta \sigma = \left[ \frac{d}{\sqrt{t^2 - d^2 (n^2 - 1)}} \right] \Delta n \text{ (in radians)}$$

At 63.5 degrees, near the last transition edge of the SAS setector, the term in brackets is approximately equal to 1.44. Therefore,

$$(\Delta \sigma)_{63.5} \approx 1.44 \Delta n \text{ (radians)}$$

or

$$(\Delta \sigma)_{63.5} \approx 82.5' \Delta n \text{ (degrees)}$$

From this, it is evident that the index of refraction can induce considerable error into the SAS outputs. Also, it is clear that the index of refraction used in the transfer function must be different if the SAS is tested with an illumination source which has a spectral distribution different from that of the sun, e.g., an xenon arc lamp with a spectral distribution shown in Figure 5B-1.

Theoretically, the effective index of refraction is the index of quartz at the "median wavelength" of the product of the spectrum of the sun and the response of the detector. The output of the detector is proportional to the area under that product curve and the "median wavelength" is then that point on the abscissa below and beyond which the area under the curve is the same. Figure 5B-4 is a graph of the product of the solar spectrum and the typical silicone solar cell response. The "median wavelength" was determined graphically and equals 0.696 micron.

Figure 5B-5 shows the product of the xenon arc lamp spectrum and silicon solar cell response. The "median wavelength" here equals 0.826 micron. Test data from the SAS taken with an xenon arc lamp, however, shows that a best fit is achieved with an index of

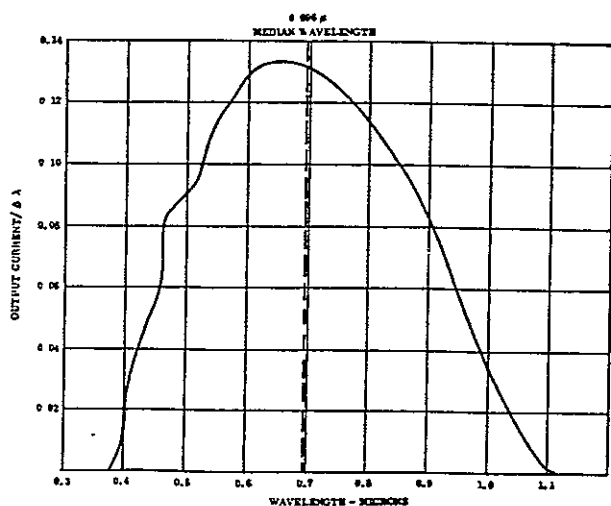


Figure 5B-4. Product of Solar Spectrum and Silicon Solar Cell Response

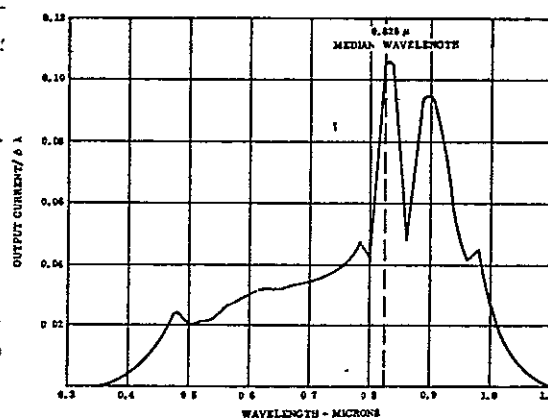


Figure 5B-5. Product of Xenon Spectrum and Silicon Solar Cell Response

refraction of 1.4541. This, according to Figure 5B-3, corresponds to 0.765 micron rather than the predicted 0.826 micron and indicates that the detector response is significantly different from that shown in Figure 5B-2. The xenon arc lamp spectrum is not that of Figure 5B-1 since the SAS detector operation was over-simplified and other factors must be considered in the derivation of a transfer function.

For testing purposes, the problem has been solved empirically. Fifteen different SAS detectors have been tested and an index of refraction of 1.4541 best fits all data taken with the Adcole solar simulator. The magnitude of errors introduced from this source is small in the ATS application (of the order of 0.02 degree) and no corrective action is presently planned. The following analytical and experimental program would allow such errors to be minimized further.

1. Measure the response of the actual solar cells used
2. Measure the spectrum of the Adcole solar simulator
3. Measure the spectrum of a carbon arc solar simulator
4. Test one SAS detector with a carbon arc solar simulator

The data from these experiments would then provide additional confidence in the method used to devise the effective index of refraction or would provide points on a graph of calculated versus measured median wavelength which could be used for interpolation.



## APPENDIX 5C

### SAS TEST CONSOLE

#### 1. TEST CONSOLE SYNOPSIS

The ATS Solar Aspect Sensor Test Console can be used to check the operation of the detector unit, electronics unit, and the combined subsystem.

Specifically the test console has the following functions:

1. Capability of simulating the output of any one bit of the sensor.
2. Simulation of the AGC cells for five detectors.
3. Leakage current measurement of the redundant output-insulation diodes.
4. Measurement of the analog output of the detector bits.
5. Display of the output of the electronics unit as to what detector is being monitored and the state of the bits of that detector.
6. Furnishes a read command to the electronics.
7. Measurement of the power input to the electronics unit.
8. Monitoring of the state of the electronics unit when a transient is present on the power line.
9. Makes available the following points for test purposes.

-18 V	Temperature Sensor 1
-10 V	Temperature Sensor 2
Gated Clock	Temperature Sensor 3
EAGC	Temperature Sensor 4
4KC Clock	Temperature Sensor 5
	Temperature Sensor 6

10. Points internal to the test console which are available:

-24 volts and Interrogate Oscillator Output

## 2. TEST CONSOLE (Complete Description)

The functions described in paragraph 1 are accomplished as follows:

The picture of the Test Console is in Figure 5C-1.

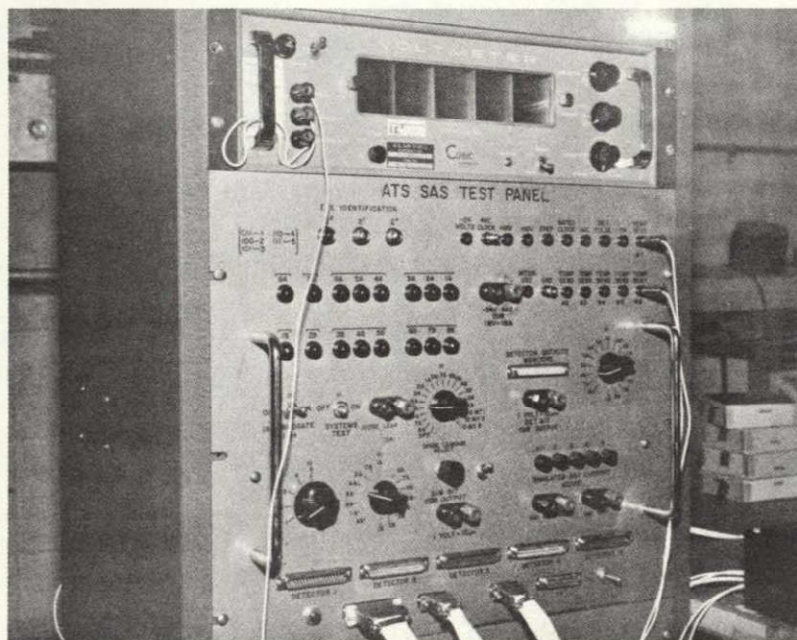


Figure 5C-1. SAS Test Console

1. The test console can simulate any one cell of any detector. This is accomplished by the use of a 45 volt battery across a variable voltage divider. Simulation of the detector is done by an Adcole R4611 solar cell.

The circuit is shown in Figure 5C-2.

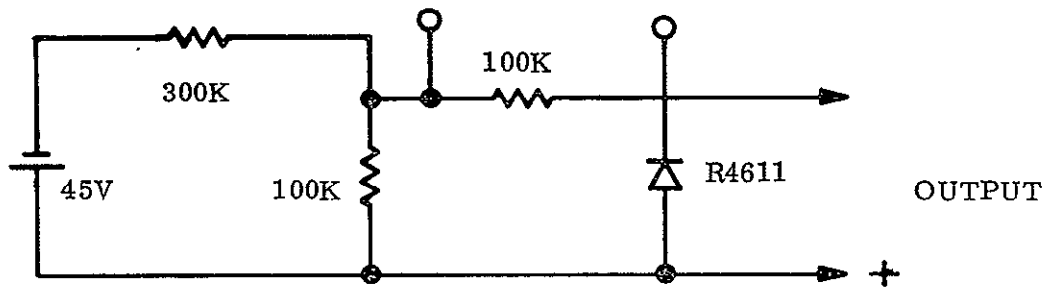


Figure 5C-2. Detector Simulation Circuit

Switching is used to enable the current output to simulate any one of the 16 bits of a detector.

Outputs are also available to measure the simulation current input to the electronics unit.

It was found that an error in this reading resulted from the fact the desired load (detector input to the electronics) was present only 1% of the time. A switch was added to switch the output of the above circuit to an external resistor of the appropriate magnitude, which was found to be one kilo-ohm.

2. Simulation of the output of the AGC cell for five detectors can be done. This is accomplished by using five of the following circuits shown in Figure 5C-3.

The voltage across  $R_1$  is measured to measure the current output of the supply. The capacitor  $C_1$  is used to filter any noise that is present. The capacitor  $C_2$  serves as a coupling of an ac signal put at "A" to the dc output of the supply. In this manner the output can be sine wave with a dc level.

Switching is also used to measure the voltages across the five different  $R_1$ S (one per circuit).

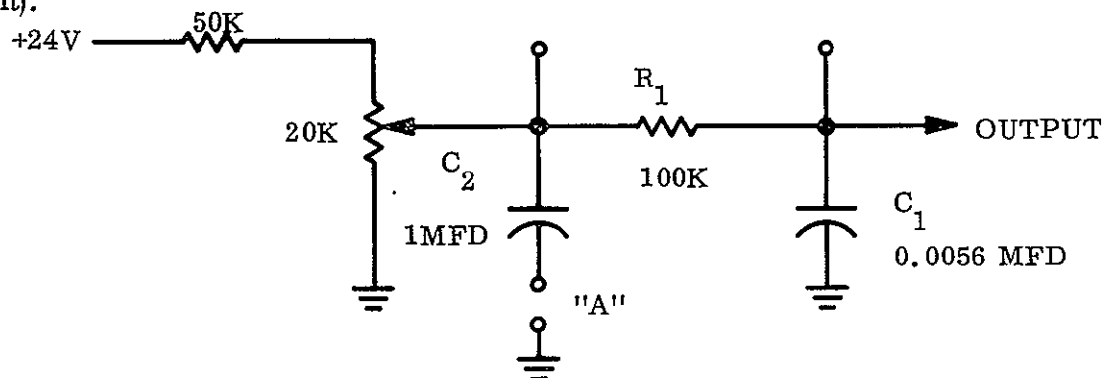


Figure 5C-3. AGC Cell Output Simulation

3. The test console has the facility to measure the diode leakage of the redundant outputs of the electronics units. The circuit used is shown in Figure 5C-4.

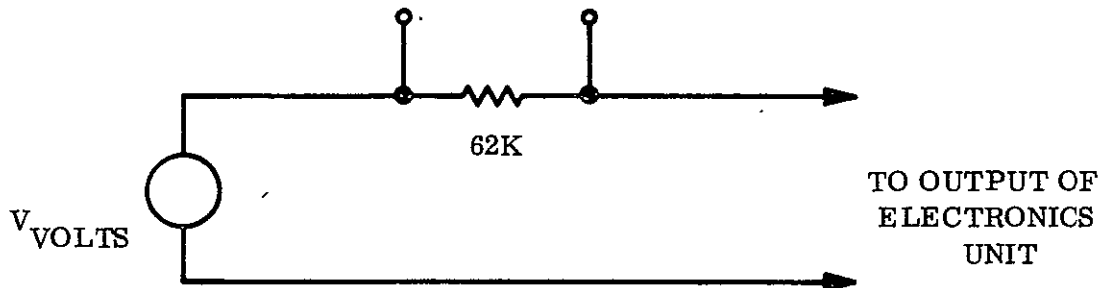


Figure 5C-4. Diode Leakage Measuring Circuit

With  $V$  volts applied, the potential from point A to ground is measured. Switches are used to switch to any one of the nineteen bit outputs of the electronics unit.

4. The test console can also measure the current output of any one detector bit. See Figure 5C-5.

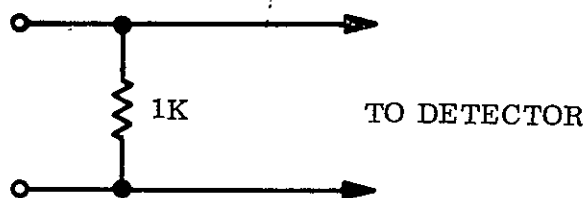


Figure 5C-5. Output Current Measuring Circuit

To measure the current output of the detector, the voltage across the one kilo-ohm load is measured. Switches are used to measure the output of the seventeen bits of the detector.

5. The test console is equipped with a visual readout in the form of lights which indicate the state of the electronics unit as to what detector is being monitored and the state of the bits of that detector. The circuit is as follows.

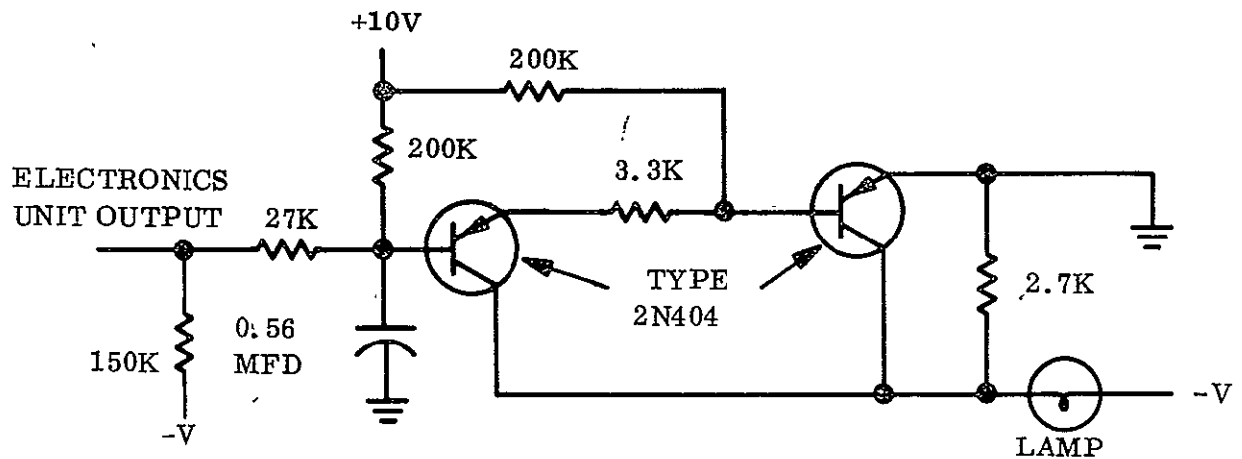


Figure 5C-6. Detector Monitoring Circuit

6. The electronics unit has a built in memory, that is, its output will not change unless given a command to read. The test console furnishes this command by the use of an interrogate oscillator. The test oscillator oscillates at eleven cycles per second with a one percent duty cycle.
7. The test console can monitor the current input of the electronics unit by measuring the voltage drop across a one-ohm resistor which is in series with the power input to the electronics unit.
8. To see if the electronics unit was stable (as far as its output is concerned) to transients on the line; a transient generator was built which has as its output a pulse 5 milliseconds wide. The magnitude is plus or minus 1.5 v with minus 24 volt dc level.
9. The test console makes available certain points from within the electronics unit and detector. These points are simply wired to the panel of the tester.

These points are as follows:

-18 V	Temperature Sensor 1
-10 V	Temperature Sensor 2
Gated clock	Temperature Sensor 3
EAGC	Temperature Sensor 4
4KC Clock	Temperature Sensor 5
	Temperature Sensor 6

10. Points internal to the test console which are available:

-24 volts

Interrogate Oscillator Output



# APPENDIX 5D TRANSFORMATION EQUATIONS FOR DIRECT SUNLIGHT TEST

The transformation equations for a translation from the reference coordinate system to our latitude and longitude are given as follows:

$$\widehat{B} = \widehat{A} \widehat{B}$$

$\widehat{B}$  Represents the direction of the sun in the new system

$\widehat{B}$  Represents the direction of the sun in the reference system

$\widehat{A}$  Is the transformation matrix

The elements of  $\widehat{A}$  and  $\widehat{B}$  are.

$$A (1, 1) = \cos (PL) \sin (PD)$$

$$A (1, 2) = \cos (PD)$$

$$A (1, 3) = \sin (PL) \sin (PD)$$

$$A (2, 1) = \cos (PL) \cos (PD)$$

$$A (2, 2) = \sin (PD)$$

$$A (2, 3) = \sin (PL) \cos (PD)$$

$$A (3, 1) = \sin (PL)$$

$$A (3, 3) = \cos (SL) \cos (SD)$$

$$B (1, 1) = \cos (SL) \cos (SD)$$

$$B (2, 1) = \sin (SD)$$

$$B (3, 1) = \sin (SL) \cos (SD)$$

$$R = A (1, 1) B (1, 1) + A (1, 2) B (2, 1) + A (1, 3) B (3, 1)$$

$$P = A (2, 1) B (1, 1) + A (2, 2) B (2, 1) + A (2, 3) B (3, 1)$$

$$Q = A (3, 1) B (1, 1) + A (3, 3) B (3, 1)$$



$$\text{Angle A} = \left[ \tan^{-1} (-Q/P) \right] \frac{180}{3.14157}$$

$$\text{Angle B} = \left[ \tan^{-1} (R/P) \right] \frac{180}{3.14157}$$

The following symbols were used in the above equations.

PD - local declination

PL - local longitude

SD - sun declination

SL - sun longitude at reference

The transformation equations for the detector for a compound angle are given as follows:

$$A = \frac{E_1 + 1/2}{\sqrt{L^2 - (1-N^2) \left[ (E_1 + 1/2)^2 + (E_2 + 1/2)^2 \right]}}$$

$$B = \frac{E_2 + 1/2}{\sqrt{L^2 - (1-N^2) \left[ (E_1 + 1/2)^2 + (E_2 + 1/2)^2 \right]}}$$

Where

$$L = 128 \sqrt{\frac{1 - N^2 \cos 26^\circ}{\cos 26^\circ}}$$

N = index of refraction

$E_1$  = segment number for sensor A

$E_2$  = segment number for sensor B

## **SECTION 6**

**PCU**

## POWER CONTROL UNIT FACT SHEET

### DESIGNER:

General Electric Company Space Division

### CONTROLLING DOCUMENTS:

Specification	SVS-7307
Outline Drawing	47E209576
Assembly Drawing	47E207948
Standing Instruction	237015

### PERFORMANCE REQUIREMENTS:

Provides interface between the ATS spacecraft and the gravity gradient stabilization system to accomplish these functions:

1. Buffer Command to
  - a. Switch sensors on and off
  - b. Energize motor and solenoid controls
  - c. Fire squibs
2. Supplies reference power supply for temperatures, pressures, events, and position sensors
3. Distribute power and frame grounds
4. Interface distribution of telemetry signals
5. Combine and convert digital event signals for analog telemetry
6. Provide telemetry voltage monitoring
7. Condition power for angle indicator

### Inputs

1. Command pulses
2. Power
3. Telemetry measurements

### Outputs

1. Solenoids
2. Squibs
3. Motors
4. Sensor power
5. Telemetry

Power Consumption 3.5 watts

Weight 8.2 lb

### UNIT DESIGNATION:

5962033	Component Qualification Unit
5962032	Prototype Unit
5962036	ATS-A Flight Unit
5962035	ATS-D Flight Unit
5962035	ATS-E Flight Unit

## SECTION 6

### POWER CONTROL UNIT

#### 6.1 PURPOSE AND FUNCTION

The design of the Power Control Unit centralizes the electrical interface between the ATS spacecraft and the gravity gradient stabilization system. However, several interfaces do bypass the PCU. Because of the high frequency signals involved, it is clearly more reliable and practical to route several telemetry leads directly from the monitor to the two telemetry encoders, such as the TV camera signals.

The PCU accepts power and command signals from the ATS command subsystem. Upon receipt of the proper ground command signal, the PCU is capable of switching on power to any one of the attitude sensing or control devices associated with the gravity gradient stabilization system.

The unit contains the electronic circuits such as power supplies and intelligence converting devices that are necessary for making temperature, voltage, position, and other diagnostic measurement within the system. It also provides a centralized distribution point for telemetry and control signals, which are not processed in the PCU.

To summarize, the functions of the PCU are:

##### Power Switching

- a. TV camera subsystems
- b. Solar Aspect Sensor
- c. Angle Indicator
- d. IR Earth Sensors
- e. Angle Indicator Lamps
- f. Extension and Scissoring Motors

- g. Damper Clutch Solenoid
- h. Squib Firing
  - 1) Damper Boom Shaft
  - 2) Eddy Current Damper Rotor
  - 3) Primary Boom Assembly
- 2. Emergency Relay Reset
- 3. Ground Return Distribution
- 4. Power Distribution
- 5. Telemetry Distribution
- 6. Digital-to-Analog Event Channel
- 7. Digital Event Logic
- 8. Telemetry Reference Voltage
- 9. Telemetry and Power Voltage Monitors
- 10. Frame Sync Distribution

The PCU case is 6.25 inches high by 8.5 inches wide by 9.5 inches long. Parts and modules are mounted on two sided etched printed circuit boards. Power required for the operation is approximately 3.5 watts at -24 and -30 volts dc. The unit's weight is approximately 8.25 pounds. The PCU Prototype is shown in Figure 6-1.

This section presents a detailed technical history of the engineering development and testing that was expended to design and develop the PCU. In addition, a list is presented of the tests that were conducted to qualify and acceptance test the hardware.

## 6.2 ENGINEERING DEVELOPMENT

### 6.2.1 MECHANICAL CONSIDERATION

The electrical packaging design approach to the PCU utilizes standard cordwood modules which were plugged into printed circuit boards. Cordwood modules allow high packaging

### 6.2.2 ELECTRICAL CONSIDERATIONS

Conservative design margins were used in the control function circuitry. For example, the transistors can experience 50 percent degradation in current gain, and leakage current in the common emitter configuration, and still perform satisfactorily. Reliability and worst-case analyses on all circuits in the PCU were performed in order to establish that they will operate satisfactorily when subjected to the temperature, pressure, radiation and life requirements of SVS-7307.

The motors, solenoids, and squib circuits which draw heavy current and function with a wide variation in voltage were operated from the -30 volts unregulated power bus. The sensors and instrumentation circuits, which required a tighter voltage control, were operated from the -24 volts regulated power bus.

Two types of command pulses are used: discrete and proportional. A discrete command pulse were of arbitrary length and used to actuate attitude sensors, operate solenoids, and fire squibs. Proportional commands were used to extend or retract the booms and expand or contract (scissor) the angle of the gravity gradient stabilization booms. The proportional pulse width could be varied, thus controlling the length of time required to perform the desired boom function.

All circuits were tested under various temperature conditions and over a range of resistance and capacitance values. Transistors were selected for various parameters and tested with the circuits for proper circuit operation. All circuits were checked with the unregulated bus set to -21 and -39 volts although actual specifications were 24.3 to 32 volts. A summary of all PCU functions is given in the following paragraphs. Refer to the PCU schematic, Figure 6-3, during this discussion.

#### 6.2.2.1 Command Interface Circuit

The command interface circuit was used as a buffer for all interfaces with the spacecraft command decoders. They were used to drive latching type relays directly or with further amplification to drive motors or solenoid loads.

Design of the circuit was taken from the ATS Interface Document Appendix A supplied by Hughes Aircraft Company. The resistor type was changed in order to facilitate normal welded module construction.

#### 6.2.2.2 Armature Drivers

The motor driver circuit was an extension of the command interface circuit with added stages of amplification. Output drive capability was about 10 amperes. Diodes were connected between ground and the output in order to quench the inductive stored energy in the load. The diodes were sized to take currents on the order of the expected peak load currents. A qualified motor was connected to the design circuit and functionally operated. The diodes proved to be capable of performing the intended function.

The saturation voltage of the output transistors was checked with loads from 5 to 10 ohms to insure that the transistors stayed in saturation through the current range. This test was also used to establish minimum wire size needed to provide sufficient voltage and current to the motors.

Both extension motors could be extended or retracted by a single command or each motor could be operated individually to compensate for any possible differences in driving rates of the two motors. As the scissoring circuits were similar, the scissoring motor could be controlled like the extension motors.

The armature driver has had two identical circuits, one circuit for the extension command and the other for the retraction command. The extension command was received and amplified by a two stage amplifier. The amplified signal was then coupled to two transistor switches. One of the switches controlled a darlington-type power switch that drives the armature winding; the other switch provided one of the two inputs to the field driver. The second input to the field driver was connected to the retraction circuit. Hence, the output of the extension or the retraction circuit determined the polarity of the signal that was applied to the motor field winding. An inhibit circuit was provided to inhibit the retraction circuit if both commands were applied simultaneously.

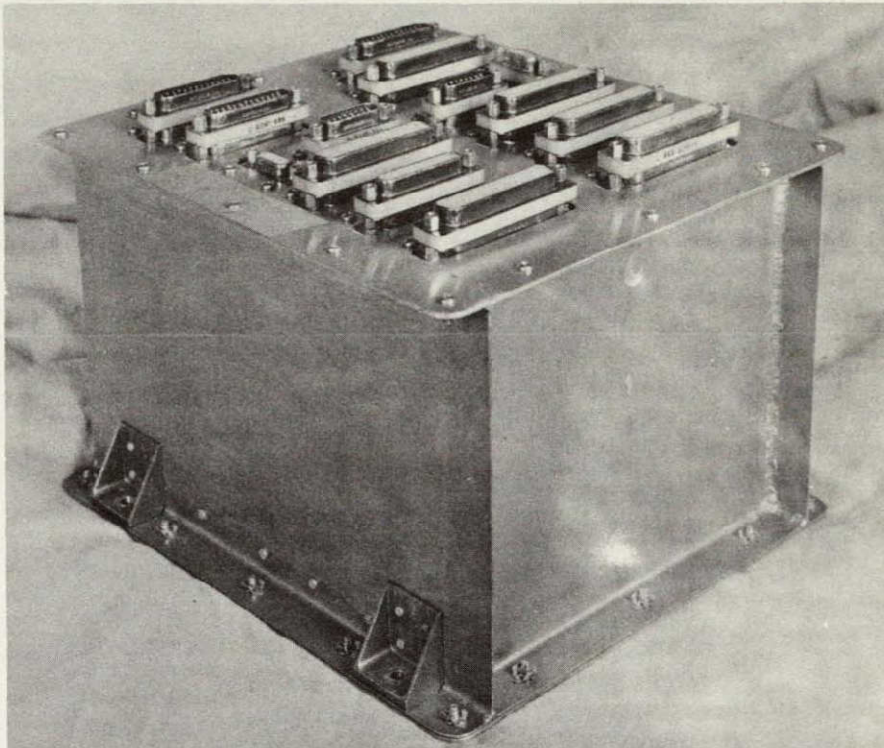


Figure 6-1. Power Control Unit — Prototype

density, and provide protection for electronic parts with high reliability. Manufacturing, testing, and maintenance were performed in discrete logical steps. The module design has been standard at GE for more than five years; over one million failure free hours of module testing have been logged. This record provides a high level of confidence in materials and processes used in the cordwood construction.

Due to the extremely high density of construction in the PCU as well as for light weight, ruggedness, and heat transfer, printed circuits on both sides of the board are used. Parts; such as power transistors, power resistors, and relays that were too large to be conveniently located in modules; were attached directly to the printed circuit board and are hand wired to terminals. Each board had a minimum of two connector modules. These modules were inserted in cut-outs on the cover plate and specially color coded to facilitate mating. The wiring boards for the first flight PCU are shown in Figure 6-2 during construction.



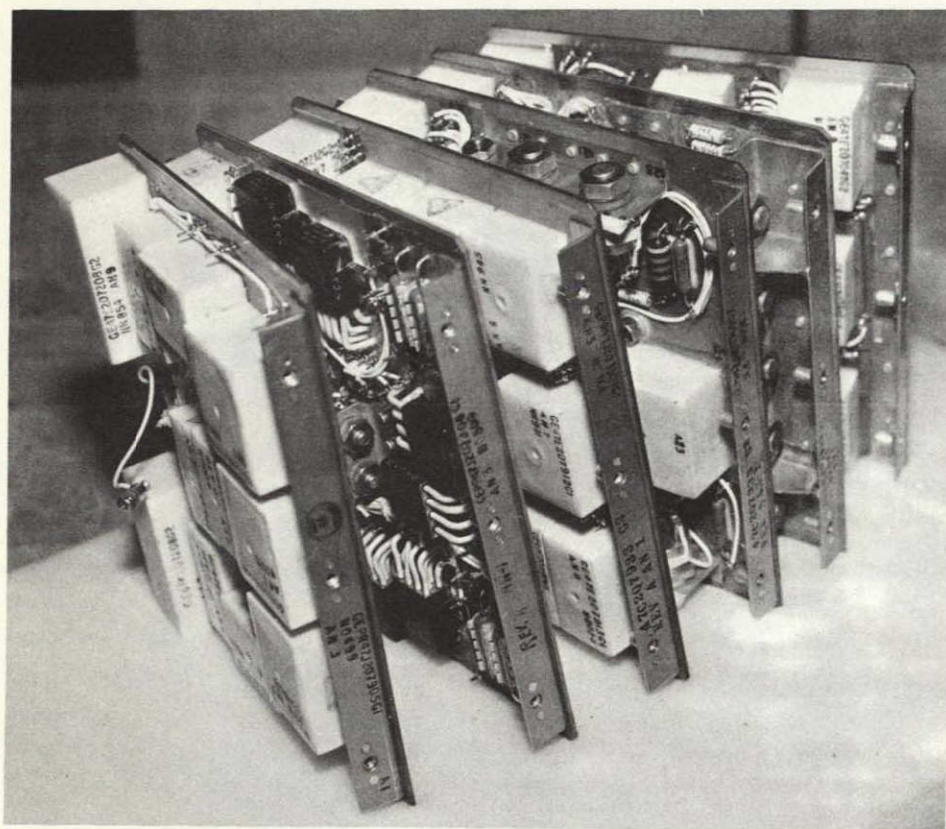


Figure 6-2. PCU Wiring Boards for the First Flight Unit Shown During Assembly

The aluminum box was of welded construction and accessible from top and bottom by means of removable covers. Printed circuit boards were held in place by raceways, fastened to the sides of the box by rivets, and by board-mounted "L" brackets which were secured to the bottom, removable plate by floating anchor nuts and bolts. The box was connected to the spacecraft with four mounting flanges welded to the sides of the box as called out in the PCU outline drawing, PR47E209576. This drawing is available upon request of the GE Contract Administrator for NASA Programs.

Stress and thermal analyses of the unit were performed and found satisfactory. Materials used conformed to the ATS vehicle. The unit was subjected to vibration and acceleration tests which exceeded the levels called out in Specification SVS-7307 (Power Control Unit - Application Technology Satellite) to demonstrate reliable construction. The unit passed all tests without changes or redesign.

#### 6.2.2.3 Field Drivers

Control signals from the armature driver module permitted the field driver module to function. Working as a bi-polar switch, the module controlled the direction of current flow through the field winding. This either extended or retracted the rods, and the scissor motors changed the angle of the rods.

Tests were conducted by applying both simulated and actual (motor) loads to the module. Some of the characteristics measured were delays and saturation voltages. Delays between the input and output signals were within tolerance. The saturation voltage of the drive transistors was within design limits even when the load exceeded specification limits.

#### 6.2.2.4 Digital-to-Analog Converter Network

Four digital events were converted to one analog signal in order to conserve telemetry channels. An error analysis was performed which showed that a four input ladder network always gave unique voltage level readouts at the ground station for any combination of inputs.

The resistor ladder module consisted of four ladder networks, each with four inputs and one output. A switch was connected to each input and a digital voltmeter connected to the output terminals. The input switch applied either -5 volts or ground to the input, hence, the output depended upon the level at each input. If the input level of -5 volts was represented by "1" and an input of ground was represented by "0" the output was determined by the formula:

$$V_{\text{out}} = V_{\text{ref}} (8/15E_1 + 4/15E_2 + 2/15E_3 + 1/15E_4)$$

where:

$$V_{\text{ref}} = -5 \text{ V}$$

$$E_x = \text{Input}$$

<u>E<sub>1</sub></u>	<u>E<sub>2</sub></u>	<u>E<sub>3</sub></u>	<u>E<sub>4</sub></u>	<u>V<sub>out</sub></u>
0	0	0	0	.000 ± 5 mv
0	0	0	1	.333 ± 2%
0	0	1	0	.667 ± 2%
0	0	1	1	1.000 ± 2%
0	1	0	0	1.333 ± 2%
0	1	0	1	1.666 ± 2%
0	1	1	0	2.000 ± 2%
0	1	1	1	2.333 ± 2%
1	0	0	0	2.667 ± 2%
1	0	0	1	3.000 ± 2%
1	0	1	0	3.334 ± 2%
1	0	1	1	3.667 ± 2%
1	1	0	0	4.000 ± 2%
1	1	0	1	4.333 ± 2%
1	1	1	0	4.667 ± 2%
1	1	1	1	5.000 ± 2%

#### 6.2.2.5 Solenoid Drive Circuits

The solenoid driver circuit was an extension of the command interface circuit with added stages of amplification. The circuit accepted the command signal and amplified the signal in a three-stage amplifier that drove a power switch. The output drive capability was approximately 15 amperes maximum with the power transistor in saturation. A diode was placed between ground and the output to quench the inductive stored energy in the solenoid load. The diode was sized to take currents on the order of the expected peak surge current. Using the actual solenoid as the load, tests were conducted to determine if the diode was sufficient. The test showed that there was no inductive delay, inductive "kick", or improper operation.

The loading was varied to determine the saturation of the drive transistor and the minimum wire size necessary for proper operation of the solenoid.

#### 6.2.2.6 Squib Drive Circuit

Two circuits were used to drive the squibs. One circuit is similar to that used by the space-craft contractor. The other was used as a solenoid driver, but due to a change in requirements which eliminated the clutch solenoids in the primary boom assembly, the driver was used to control the squib firing that uncages the boom.

In the first circuit the incoming signal was integrated to cause a time delay of  $1.1 \pm 0.4$  second. The delayed signal was then amplified and differentiated, resulting in an output pulse width of 30 to 100 milliseconds. The processed pulse then drove a power amplifier that had a squib as its load.

The second circuit was a power amplifier consisting of the standard interface circuit with added stages of amplification. It did not have a delay and the pulse width was controlled by ground command.

Various tests were made on these circuits; these tests included testing for load capabilities, testing with various value piece parts and testing for circuit parameter variation such as delay times, with different level input command signals. The tests showed that the circuit functioned properly within the design limits. The second circuit was also checked for load capabilities in excess of the power transistor load current rating. It was found that with pulse operation, the transistor could reliably carry twice the rated current.

#### 6.2.2.7 Telemetry Power Supply

The telemetry power supply circuit utilized a differential amplifier and a zener reference diode to provide a stable, precision -5 volt supply. The voltage was adjusted by means of two selected resistors. Temperature variations were kept to a minimum by means of a temperature stabilized zener reference diode connected to one side of the differential amplifier. Load variations were minimized by the low output impedance of the feedback amplifier.

Various tests were made on this circuit with parts, loads, and voltage variations. The load was varied from 250 to 1500 ohms in 250-ohm steps with the regulated supply set to -24, -25, and -23 volts. Temperature tests were conducted at  $-20^{\circ}\text{C}$ , ambient, and  $+70^{\circ}\text{C}$ . The results satisfied the tolerances set for the circuit.

#### 6.2.2.8 Relay Circuits

There were six latching relays whose main function was to apply power to the sensing circuits. A secondary function of the relay was to drive a telemetry circuit to indicate when power was applied to the sensing circuit. In order to energize or de-energize the sensing

circuits, each relay had two relay drivers, one of which drove the set coil and the other drove the reset coil. The drivers were modified buffer interface circuits with an added stage of amplification. These drivers amplified the command signal so that it would be capable of driving a transistor switch which allowed power to be applied to the relay coil.

#### 6.2.2.9 Relay Reset Circuit

This circuit was a typical interface circuit with an added stage of amplification. Its purpose was to enable the reset of all relays from the unregulated line in case of failure in the -24 volt line.

#### 6.2.3 OPTIMIZATION PROGRAM

There were seven major changes in the design of the Power Control Unit during the course of development. They were as follows:

1. In the Fourth Quarter of 1964, the electrical design of the PCU was considerably simplified. Changes were made in order to reduce weight to the goal established by NASA/GSFC. The functions eliminated from the PCU were:
  - a. Motor starting and stopping control
  - b. Separation timer and automatic boom stops
  - c. Boom motor current sensors and ac power supply
  - d. Video relay and automatic alternator
  - e. Bridge resistors for temperature detectors
  - f. Pulsed power regulator for damper solenoid
  - g. Minus six volt regulated power supply
  - h. Several squib driver circuits
2. The command reset buffer amplifier, working off the unregulated voltage bus, was added in order to provide reset capabilities for all relays in the event that the regulated bus malfunctioned.

3. An inhibit feature in the command buffer amplifier was incorporated. This feature prevents simultaneous input command from turning on the extension and retract circuits at the same time. If this were allowed to happen, the field driver circuit would malfunction causing four transistors to short out. The inhibit circuit allowed the boom extension or expansion commands to over-ride the boom retraction or contraction commands.
4. Two additional transistor buffer amplifiers were added to the motor driver module to provide additional isolation between armature and field driver outputs. This change was considered necessary after testing of the primary boom assembly motor with the PCU breadboard showed evidence that there was feedback to the common amplifier point in conjunction with some transformer action in the motor. The combination of these two characteristics gave a possible instability when the motor was turned off.
5. GE was advised by deHavilland that the motors could draw up to 6.4 amperes when a locked rotor and certain environmental conditions existed. Therefore, it was found necessary to replace the 5-ampere motor drive transistor. The Type MHT 6396 transistors were replaced with a 20 ampere transistor, Type MHT 8001.
6. During system testing at Hughes Aircraft Company, it was found that -30 volt current limiter in the spacecraft would turn off when power was applied. An investigation revealed that all the squib drivers were turning on for 15 microseconds. In order to correct this problem, capacitors were connected to the first stage of the squib driver power amplification circuit, minimizing the turn on pulse.
7. An agreement was reached between NASA/GSFC and GE to modify the tip mass caging system of the primary boom assembly and to provide a positive release through the use of pyrotechnic devices. At the same time, a decision was made which resulted in the removal of the clutching capabilities in the primary boom assembly. This change made available four solenoid driver circuits required for the pyrotechnic devices. These drivers have the capabilities of driving loads of 5 ampere maximum. As the squib required 3 amperes minimum for sure-fire, 5 amperes was sufficient. Current limiting resistors were installed in the Primary Boom in order to prevent the current from exceeding 5 amperes.

A test was performed on 10 of these transistors to determine pulse current capabilities. It was found that a current as high as 10 amperes for a duration of 100 milliseconds would not cause a breakdown in the transistor. The tests were run to determine the capability of the transistors to withstand collector current and power dissipation in excess of the manufacturer's ratings.

The circuit used for this investigation was identical to others used in the Power Control Unit. Driving the power circuit was a monostable multivibrator with a period of 33 seconds, and a 100 millisecond wide pulse. The power circuit output had a high wattage, variable resistance load.

Ten transistors were selected for this test; five were commercial parts, and five were prime parts. Each transistor was pulsed a minimum of 50 times with loads from 5 amperes to 7.5 amperes in 1/2-ampere steps. Five transistors were then selected for further evaluation up to 10 amperes. At the start, middle, and end of the test,  $V_{ce}$  and current were monitored and recorded. (See Table 6-1) The analysis (Table 6-2) shows very little deterioration in the transistors due to this test.

Table 6-1. Power Stress Test Results ( $V_{ce}$  After 50 Pulses)

$V_{ce}$ Sat (Volts)										
Commercial Parts						Prime Parts				
Current (Amperes)	A	B	C	D	E	F	G	H	I	J
5.0	1.6	1.2	1.0	1.2	1.2	1.4	1.3	1.3	1.3	1.2
5.5	1.3	1.2	1.0	1.0	1.2	1.4	1.2	1.2	1.0	1.5
6.0	1.3	1.4	1.2	1.2	1.4	1.4	1.6	1.3	1.3	1.5
6.5	1.6	1.4	1.3	1.3	1.5	1.5	1.8	1.4	1.3	1.5
7.0	1.7	1.7	1.3	1.5	1.5	1.6	2.0	1.6	1.5	1.7
7.5	1.7	2.0	1.4	1.5	1.7	2.0	2.2	1.7	1.7	1.7
8.0	2.2		4.0		4.0		4.2		2.2	2.5
8.5	2.6		5.5		4.8		5.5		3.8	3.0
9.0	2.5		5.8		6.0		6.0		3.5	3.1
9.5	3.2		6.2		6.2		6.2		3.8	3.5
10.0	4.0		7.0		7.6		7.5		4.2	4.8
10.5	5.5									
11.0	5.5									
11.5	6.0									

Table 6-2. Prime Part Test Results

Prime Part	$I_{ce}$ (NA)		$h_{fe}$ (NA)	
	2/12/66	9/22/66	2/12/66	9/22/66
F	0.46	1.0	86	87
G	0.40	1.0	87	90
H	0.09	1.0	89	89
I	0.32	1.0	88	89
J	0.40	1.0	83	90

$I_{ce}$  at  $V_{ce} = 60$  vdc and  $V_{be} = -2$  vdc

$H_{fe}$  at  $V_{ce} = 2$  vdc

$I_{ce} = 1$  amp dc

#### 6.2.4 ENGINEERING TESTS AND RESULTS

##### 6.2.4.1 Objective

The Power Control Unit (Drawing 47J207904 Figure 6-3) was subjected to a series of engineering tests to evaluate its design and its ability to withstand the environments as required by the Power Control Unit Component Specification SVS-7307.

##### 6.2.4.2 Test Procedure

Tests were conducted in accordance with the PCU Engineering Test Plan described in PIR 4172-091. All test levels either meet or exceeded the requirements of SVS-7307. Where these extremes in themselves caused out-of-tolerance readings, the results were extrapolated to the specified limits.

##### 6.2.4.2.1 Temperature Tests

Temperature tests were run at 160°F and -20°F. After the temperature had stabilized, a functional and a continuity test were performed at each temperature level. Thermocouples were attached to the following components and the temperature monitored throughout the test.



<u>Thermocouple</u>	<u>Component</u>
1 . . . . .	Module A1
2 . . . . .	R24 Heatsink
3 . . . . .	Q22 Heatsink
4 . . . . .	Module A18
5 . . . . .	Between A18 and R20
6 . . . . .	On R53

6.2.4.2.1.1 Results of Test. Graphs on Figures 6-4 thru 6-10 show the variations in temperature of the selected components throughout the test. Figure 6-4 shows the thermal change of the chamber during the test. Figure 6-5 through 6-10 illustrate the effect of the chamber temperature and the heat generated by the Power Control Unit at selected points. As can be seen, the temperature did not vary more than 5°F while the unit was operational.

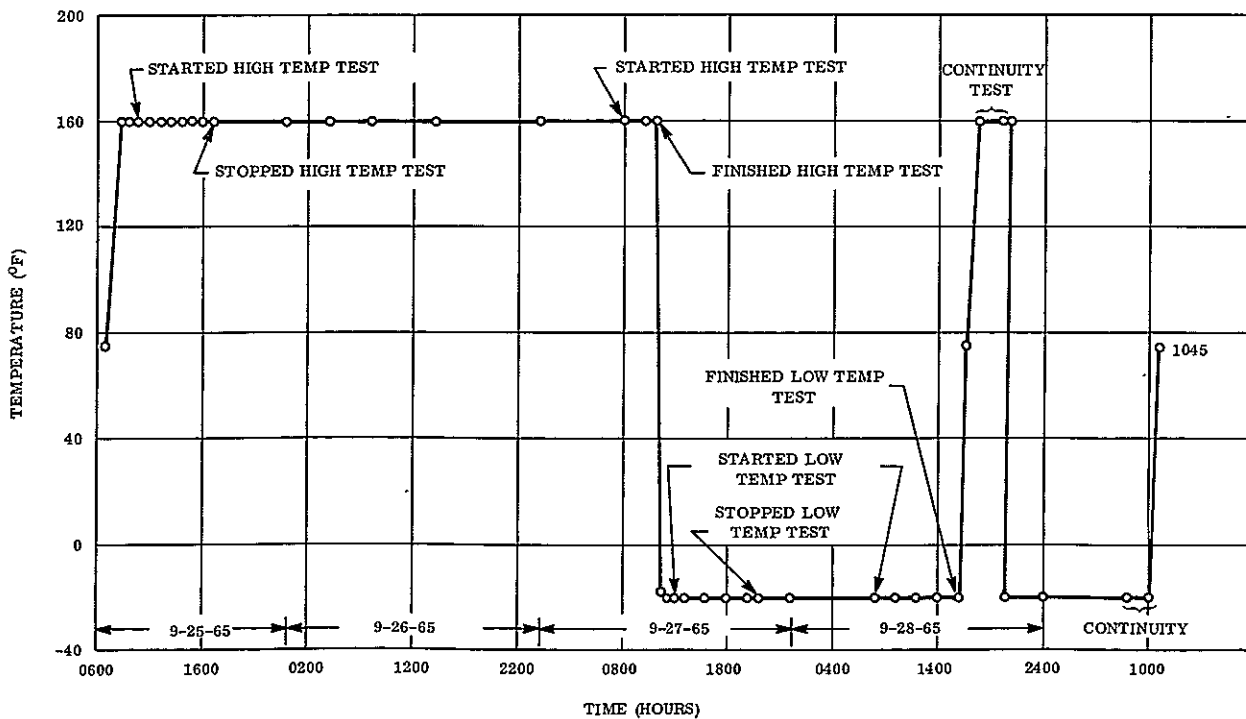


Figure 6-4. Thermal Test Chamber Temperature

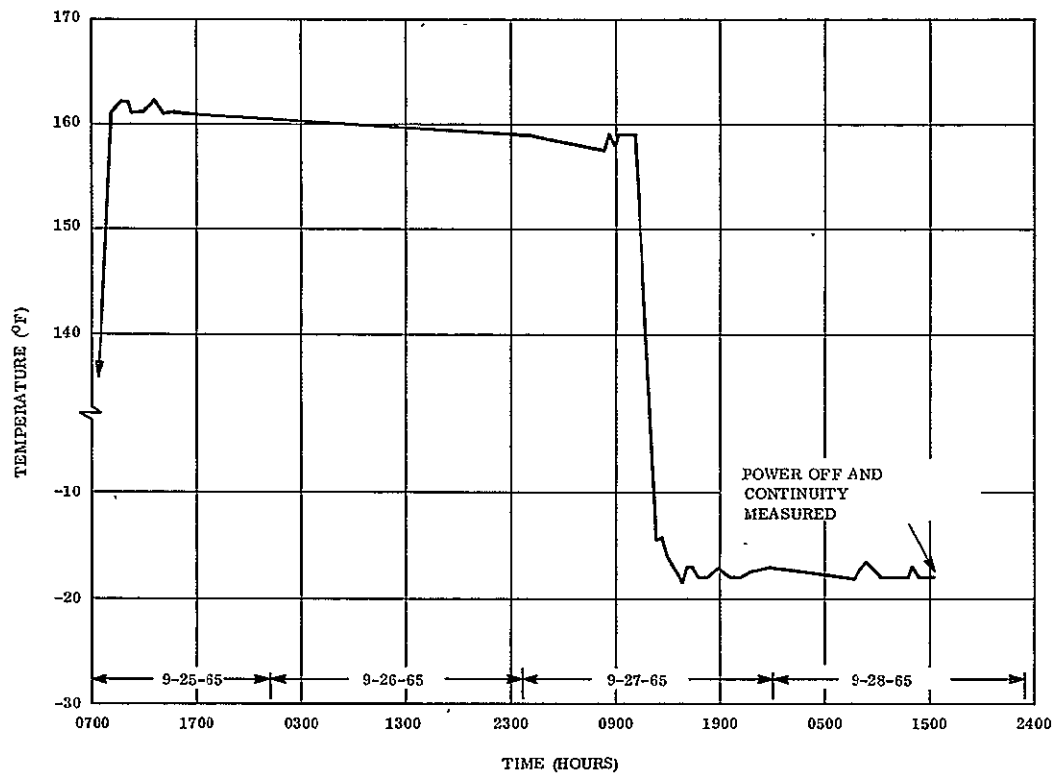


Figure 6-5. Thermal Test Power Supply Module Temperature

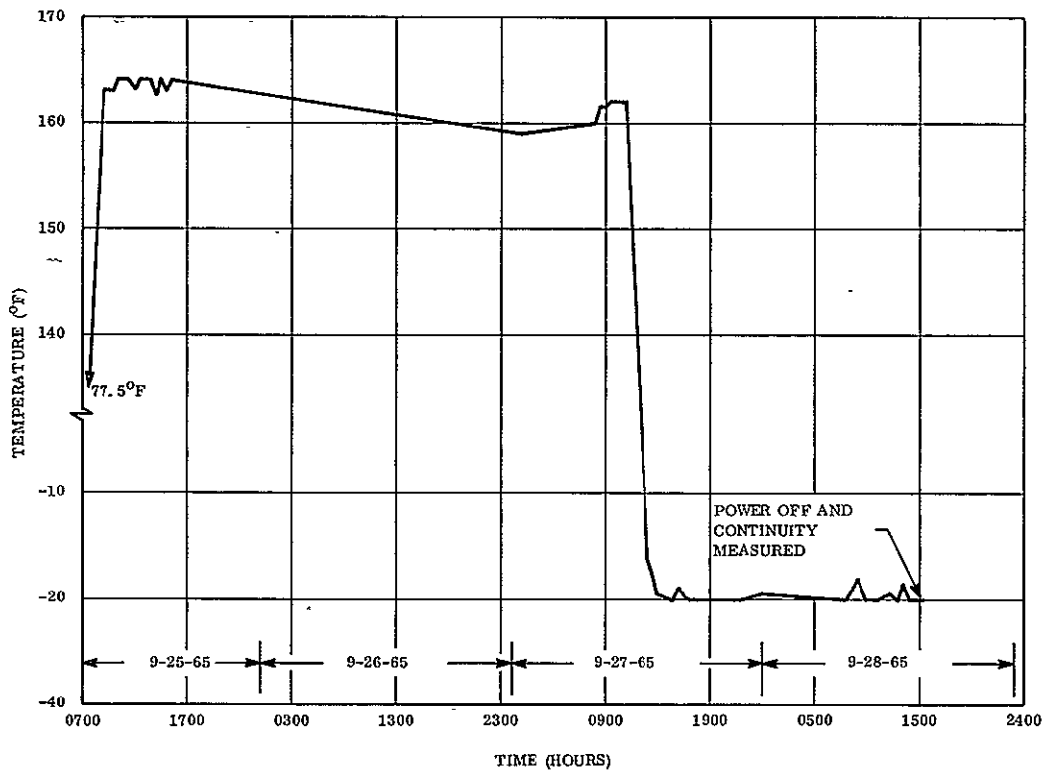


Figure 6-6. Thermal Test, R53 Temperature

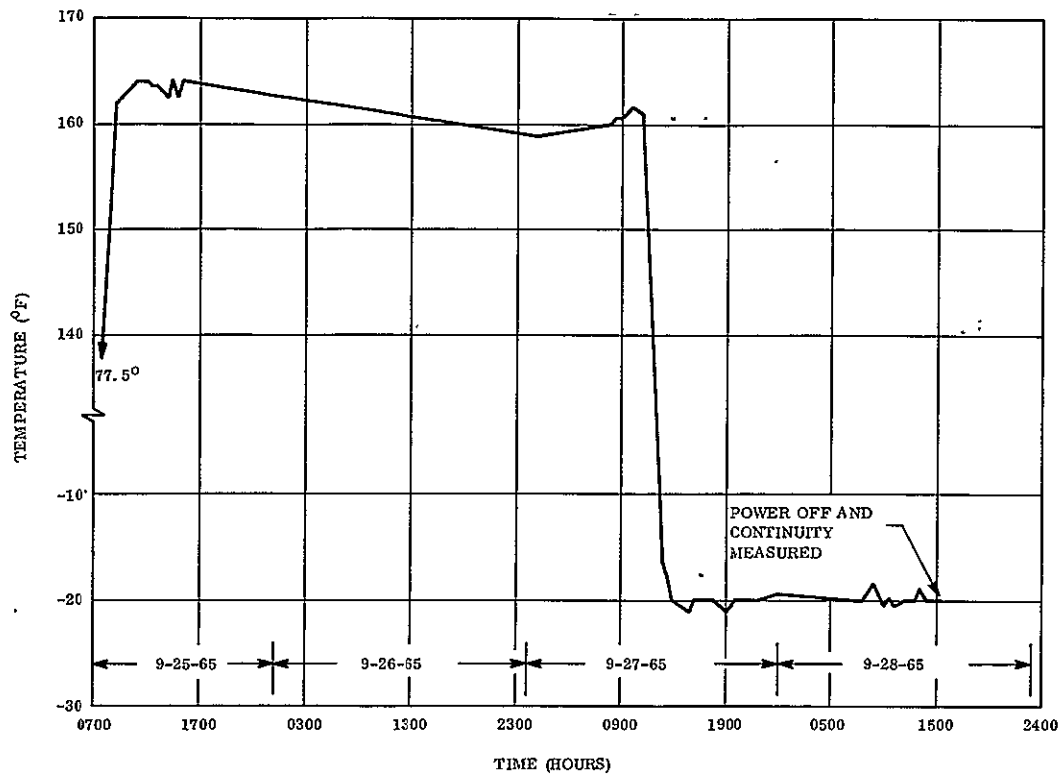


Figure 6-7. Thermal Test, R20 Heat Sink Temperature

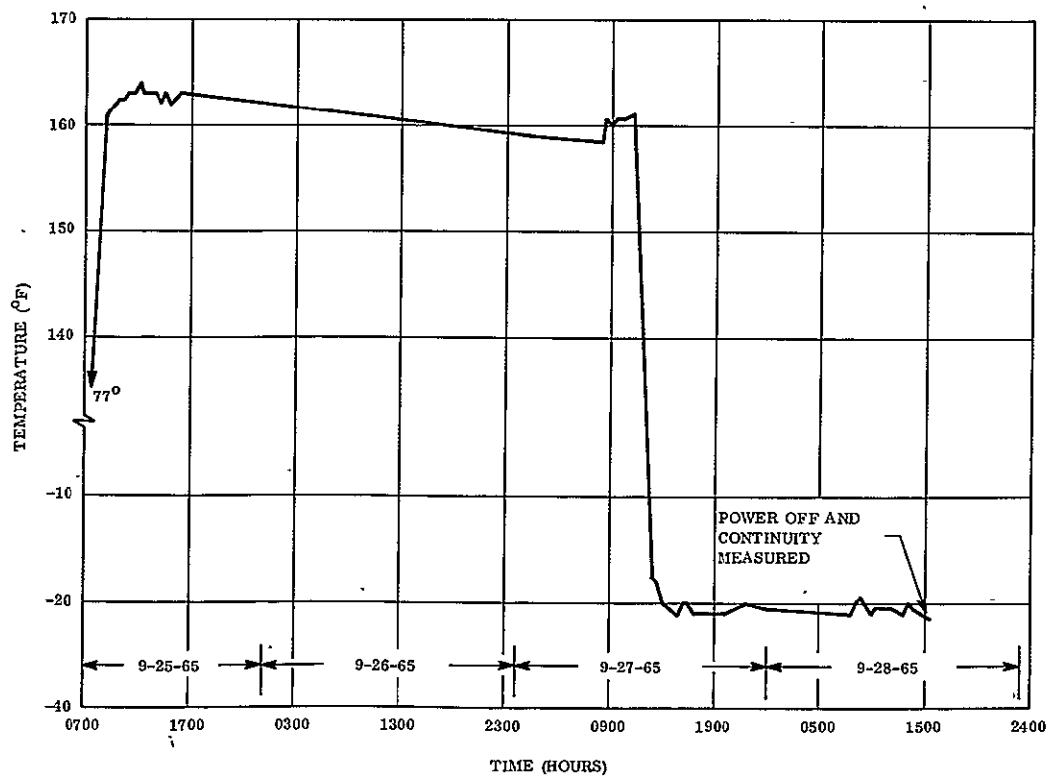


Figure 6-8. Thermal Test, Field Driver Scissor B Temperature

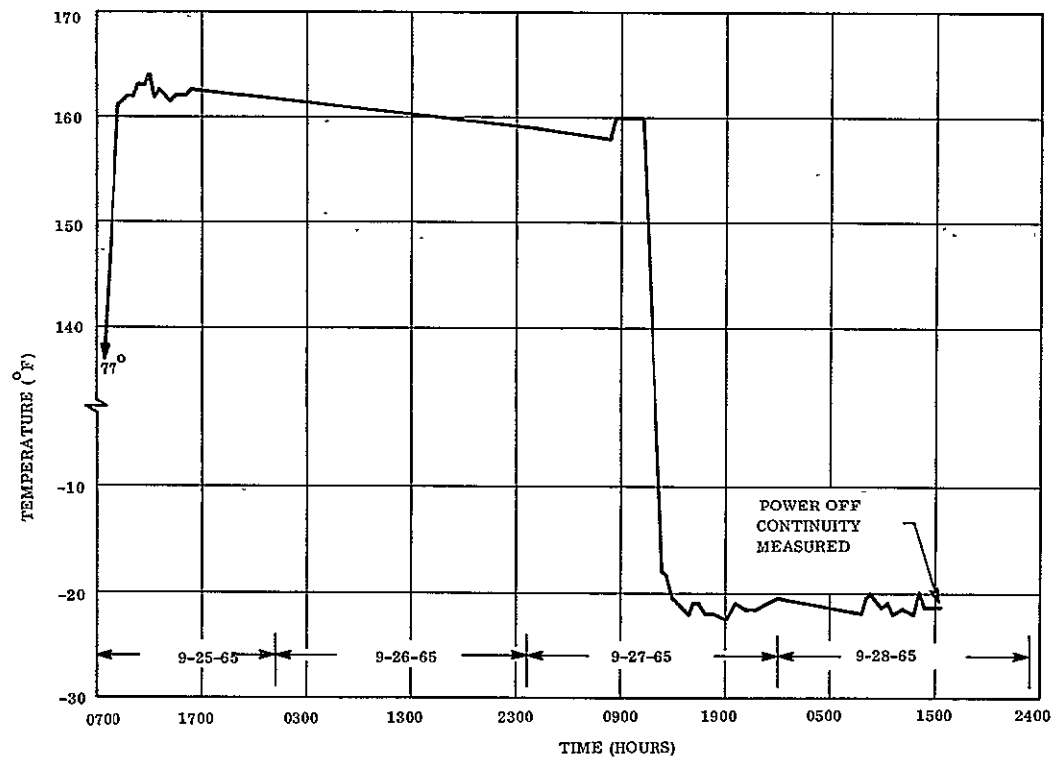


Figure 6-9. Thermal Test, Q22 Heat Sink Temperature (Armature Scissor B)

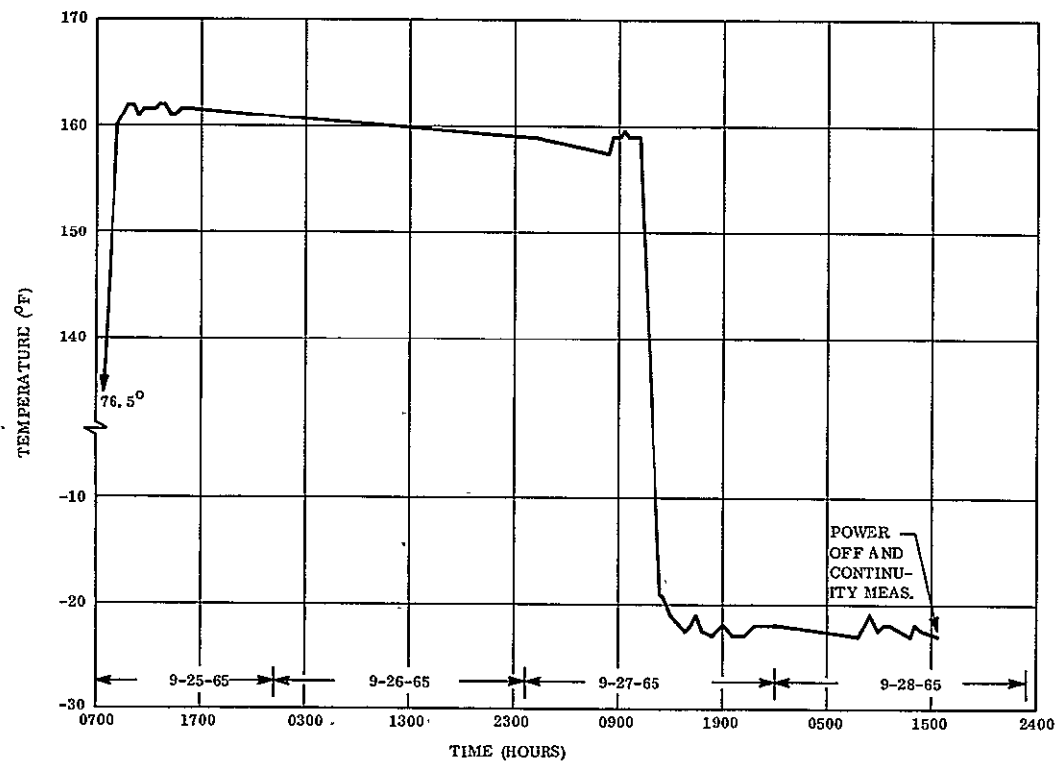


Figure 6-10. Thermal Test, R24 Heat Sink Temperature

#### 6.2.4.2.2 Thermal Vacuum Test

Thermal vacuum tests were run at temperatures of  $-20^{\circ}\text{C}$  and  $+60^{\circ}\text{C}$  and with vacuums in excess of  $1 \times 10^{-5}$  mmHg. Thermocouples were installed at locations that were deemed to be the most vulnerable to rises or changes in temperature. These locations were as follows:

#### LOCATION OF THERMOCOUPLES FOR THERMAL-VACUUM TEST

<u>Recorder</u>	<u>Thermocouple</u>	<u>Location</u>	
A	1	Module A1	
A	2	R24 Heatsink	
A	3	Q22 Heatsink	
A	4	Module A18	
A	5	Between A18 and R20	
A	6	R53	
A	7	Top of box	
A	8	Bottom of box	
A	9	Solenoid Driver, Eddy Current	Q3
A	10	Rod B Normal Solenoid Driver	Q18
A	11	Solenoid Driver, Hysteresis	Q2
A	12	Rod A Emergency Solenoid Driver	Q6
A	13	Solenoid Driver, Eddy Current	Q4
A	14	Solenoid Driver, Rod B Emergency	Q16
A	15	Squib Driver 1B and 2B	Q12
B	1	Solenoid Driver, Hysteresis	Q1
B	2	Squib Driver, Damper Boom A & B	Q14
B	3	Squib Driver, 1A and 2A	Q10
B	4	Solenoid Driver, Rod A Normal	Q8
B	5	Squib Driver, Damper Boom A & B	Q27
B	6	Squib Driver, Damper Boom A & B	Q18
B	7	Squib Driver, 1B and 2B	Q11
B	8	Scissor Motor B Arm	Q22
B	9	Rod Motor B Arm	Q20
B	10	Rod Motor A Arm	Q19
B	11	Squib Driver, 1A and 2A	Q9
B	12	Scissor Motor A Arm	Q21
B	13	Squib Driver, Damper Boom A & B	Q28

6.2.4.2.2.1 Results of the Test. Figures 6-11 thru 6-18 were plotted to display the behavior of the components of the most interest. Various points are indicated to show where changes were made in loading. Figure 6-11 shows the variation in temperature at the

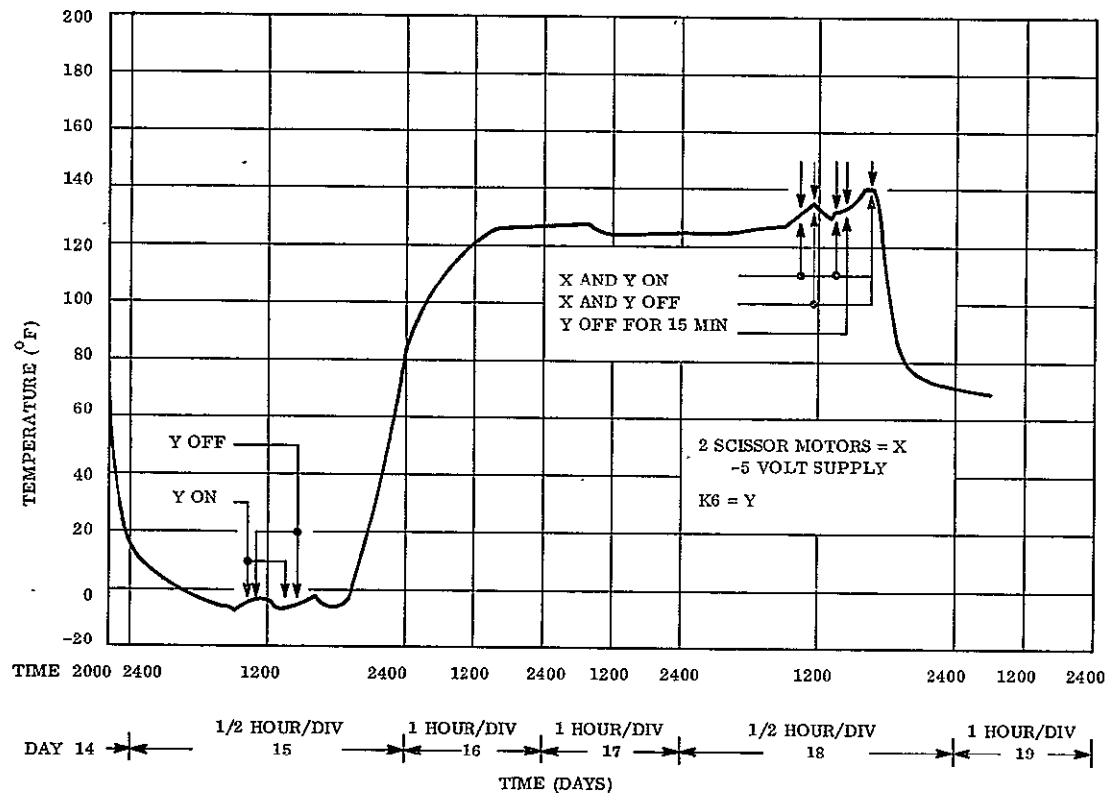


Figure 6-11. .PCU Mounting Surface Temperature vs Time

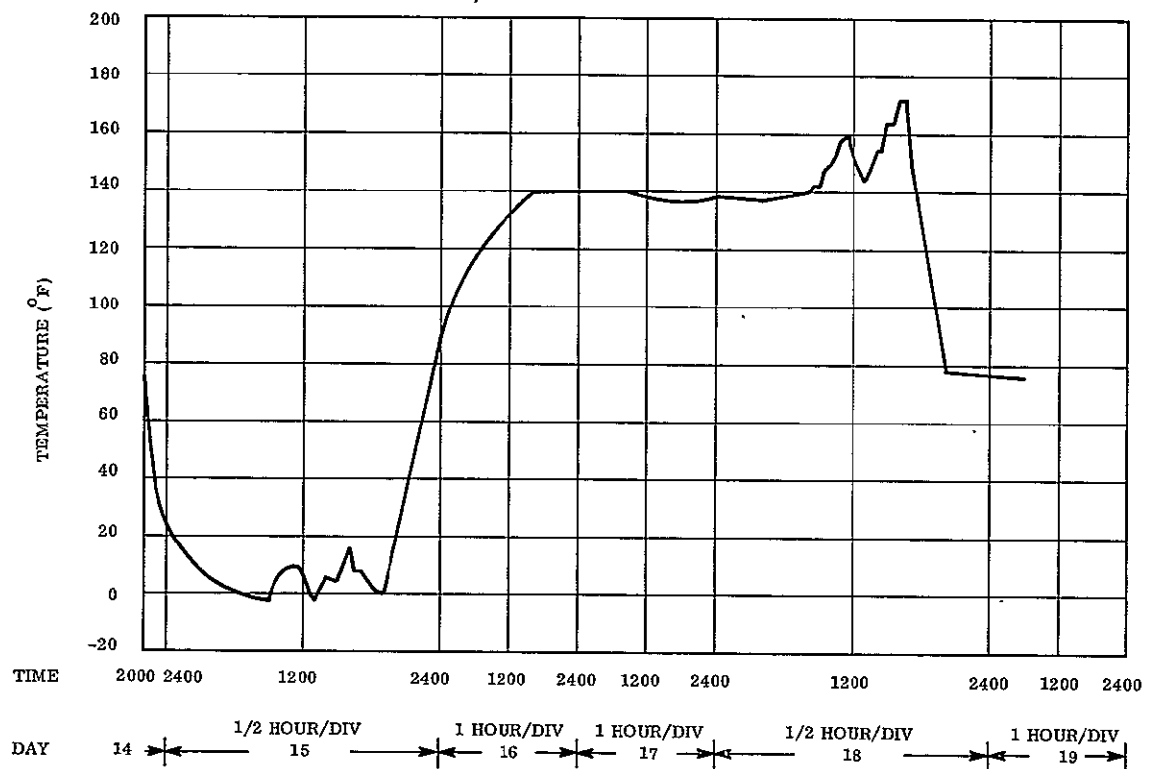


Figure 6-12. Squib Driver A9 Output Transistor Temperature vs Time

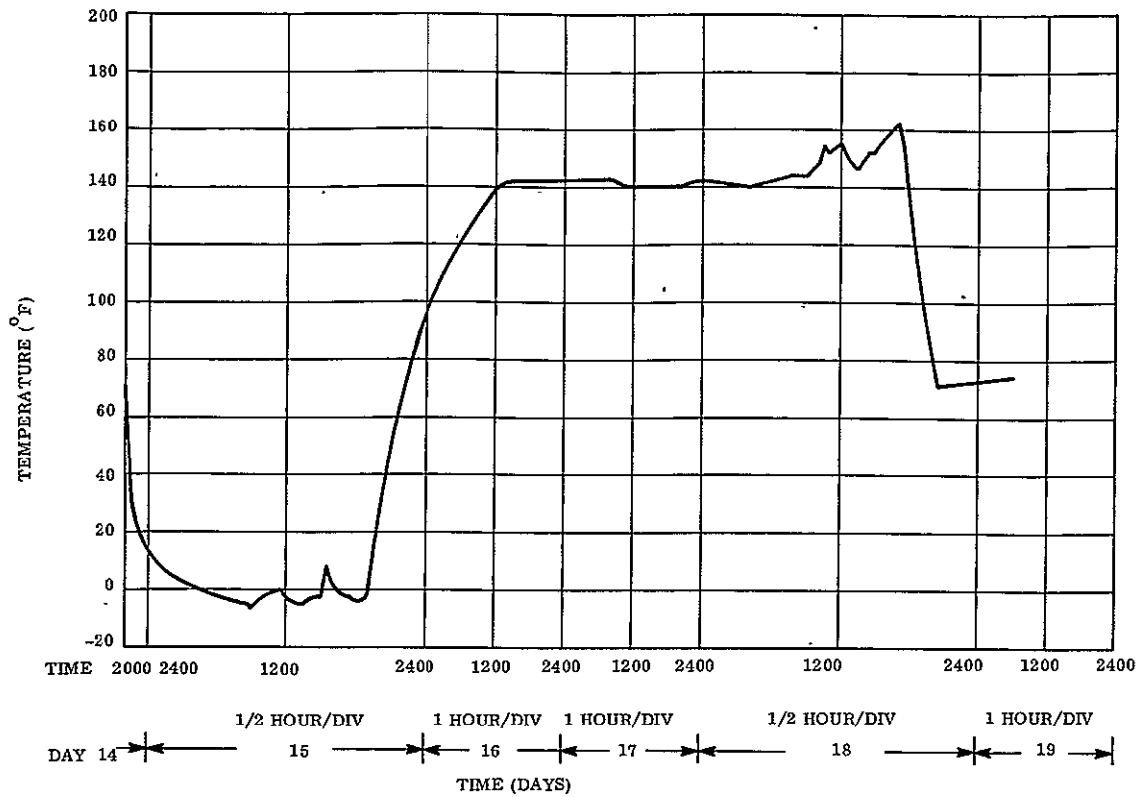


Figure 6-13. Hysteresis Driver Transistor Q2 Temperature vs Time

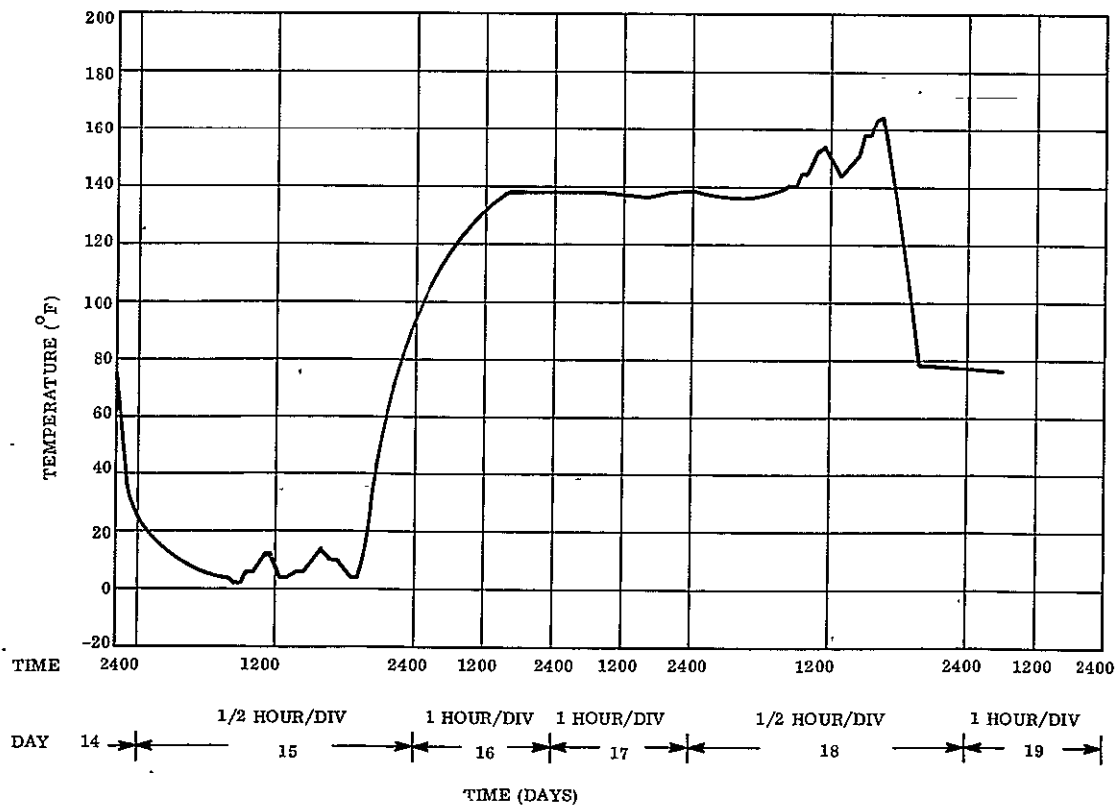


Figure 6-14. Hysteresis Driver Q1 Transistor Temperature vs Time

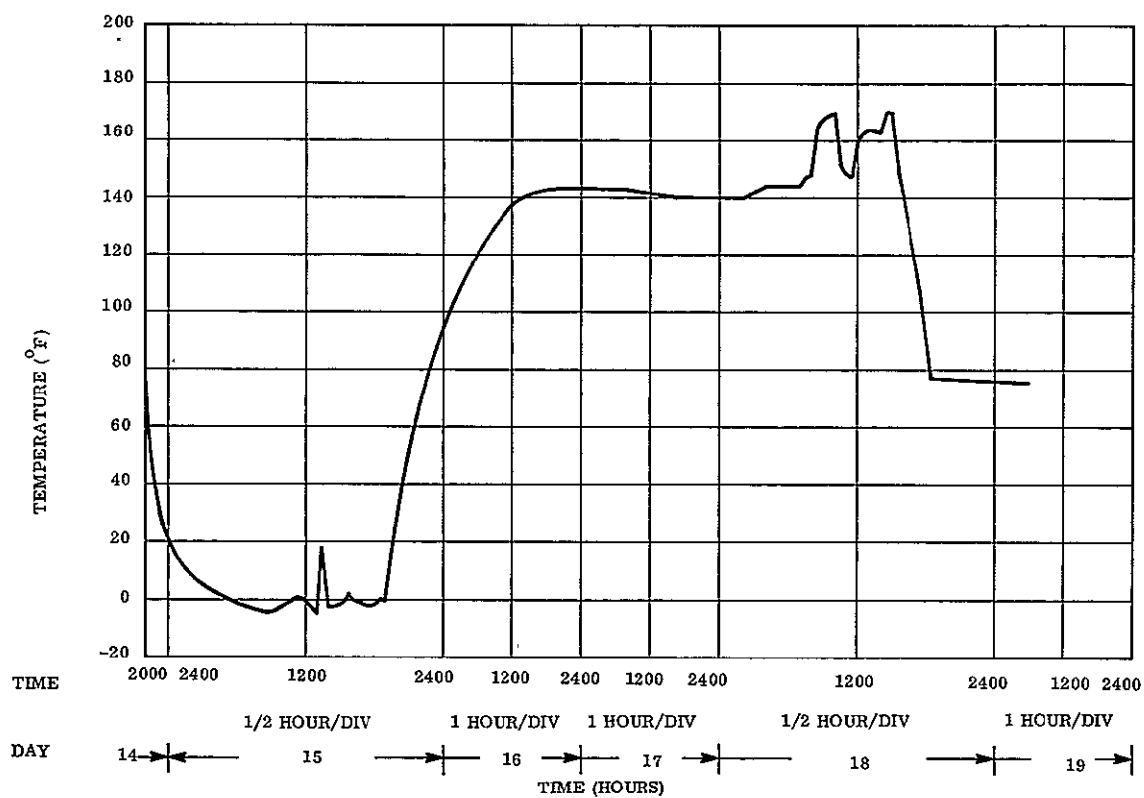


Figure 6-17. A19 Scissor B Armature Driver Transistor Temperature vs Time

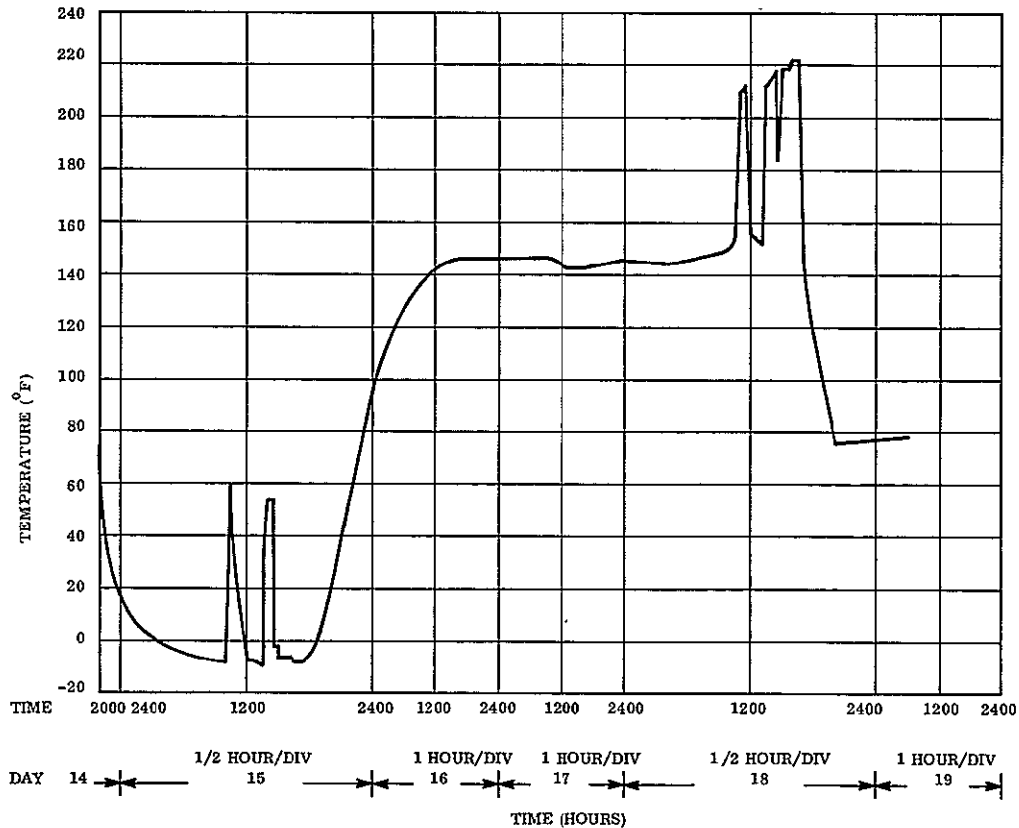


Figure 6-18. R53 (Detector Lamp Circuit) Resistor Temperature vs Time



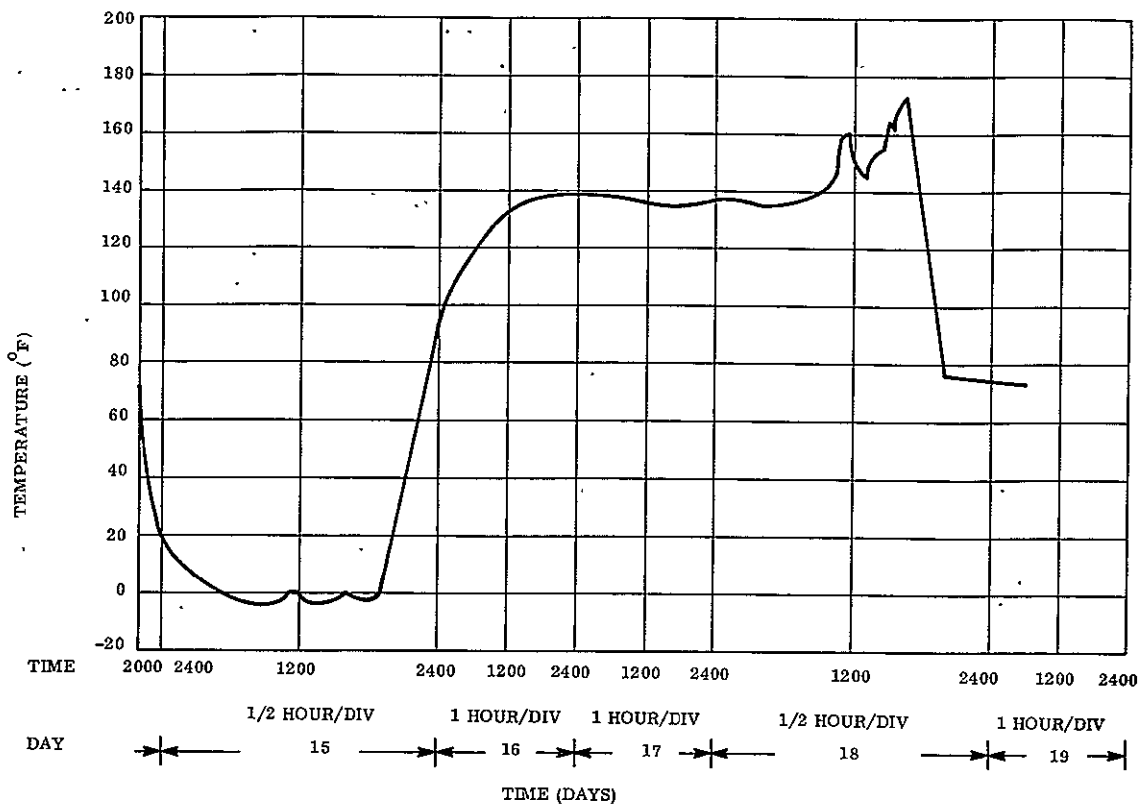


Figure 6-15. A18 Field Driver Scissor B Temperature vs. Time

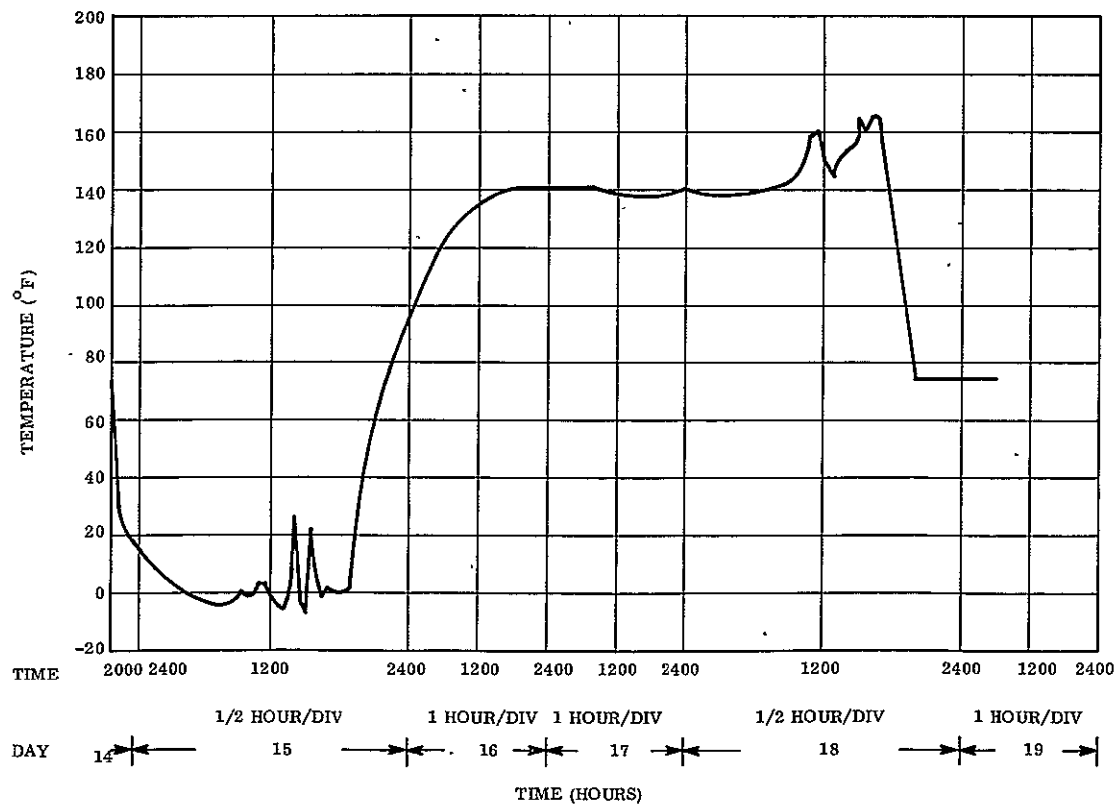


Figure 6-16. Temperature Heat Sink Beside Q22 (Output of Mod A19) vs. Time

mounting surface of the Power Control Unit. Using this graph in conjunction with those of Figures 6-12 and 6-13 will help explain sudden changes in the plots. As an illustration, Figures 6-12, 6-13, and 6-14 seem to follow the curve of Figure 6-18 and the comments on Figure 6-11 indicating that the heating of R53 was felt throughout the unit. At high temperatures the scissor motors were energized resulting in the plots shown on Figures 6-15, 6-16, and 6-17. These graphs show, in general, that the temperature variation followed Figure 6-18 and indicated a slow rise in component temperature due to the activation of the motors.

#### 6.2.4.2.3 Vibration

The Power Control Unit was subjected to qualification level of vibration as specified in SVS-7307. The unit was energized and all relays were monitored.

6.2.4.2.3.1 Results of the Test. The unit operated satisfactorily and an inspection revealed no mechanical or electrical failure. As a result of the vibration test, foam potting is not considered necessary. Post vibration function tests were successful.

#### 6.2.4.2.4 Magnetic Dipole Test

The magnetic dipole test was performed with the Power Control Unit in both the active (with the PCU operating) and the passive state (nonoperating). In order to determine the direction and magnitude of the dipole; the unit was positioned at various angles, vertical and horizontal to the plane of the magnetometer. The position with the largest magnitude was assumed as the direction and magnitude of one component of the dipole. This process was repeated on two other sides.

6.2.4.2.4.1 Results of the Test. Testing showed that the magnitude of the dipole can vary from 25 pole centimeters to 650 pole centimeters, depending on a given command. The lowest reading was obtained when the unit was in the passive state. The highest reading was obtained when the Eddy Current Damper driver was activated.

#### 6.2.4.2.5 EMI Test

The EMI test procedure and the results are described in PIR 4172-127.

#### 6.2.4.2.6 Acceleration Test

The unit was subjected to the qualification levels of acceleration per SVS-7307. The unit was not energized during this test.

6.2.4.2.6.1 Results of the Test. The unit was inspected for mechanical or electrical failures and no defects were found. Post-acceleration tests were successful.

#### 6.2.4.3 Functional Test

##### 6.2.4.3.1 Voltage Monitor Test

The voltage monitor module conditions the -5, -24, and -30 supply voltages to values below -5 volts by means of resistor dividing networks for telemetry processing.

6.2.4.3.1.1 Results of the Test. The results of the test showed that in all cases the outputs were well within tolerances.

##### 6.2.4.3.2 Ladder Module Test

6.2.4.3.2.1 Results of the Test. The outputs of the three ladder networks were within specification for all tests performed. On Event 4 (the fourth ladder) Input 4 was not used and the output resulted in values that did not agree with the formula. However, this condition did not exist on the prototype or flight units.

##### 6.2.4.3.3 Solenoid Driver Modules

The Power Control Unit contains six similar constructed solenoid driver modules, controlling two 1.6-ohm loads and four 8-ohm loads. One of each type was selected for evaluation. These two units showed the greatest variation in output with changes in temperature and voltage.

6.2.4.3.3.1 Results of the Test. Figure 6-19 is a plot of power supply input voltage versus the power transistors saturation voltage ( $V_{ce}$ ) recorded on Table 6-3. Figure 6-20 is a plot of input voltage versus the power transistor saturation voltage ( $V_{ce}$ ) recorded on Table 6-4. All readings were within the limits called out in the specification even though the power voltage was 4 volts higher than specified. Several discrepancies however were apparent.

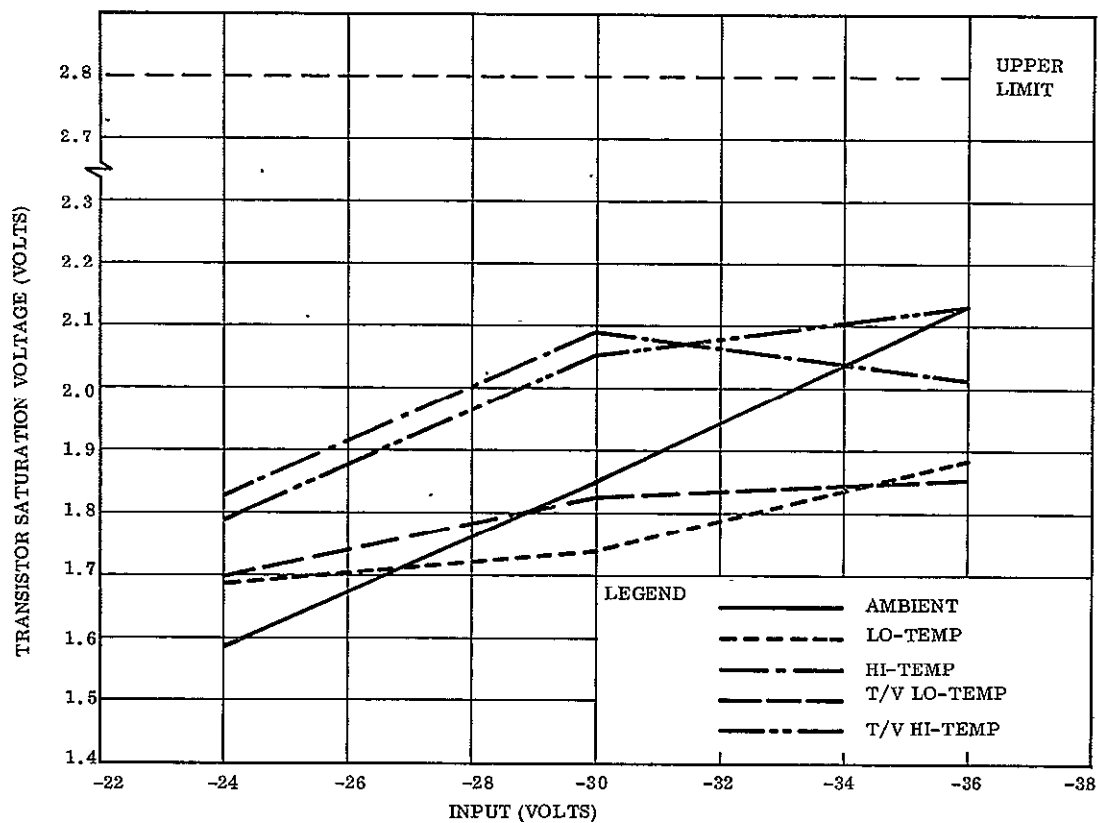


Figure 6-19. Solenoid Driver Transistor Saturation Voltage vs Input Voltage Hysteresis Damper

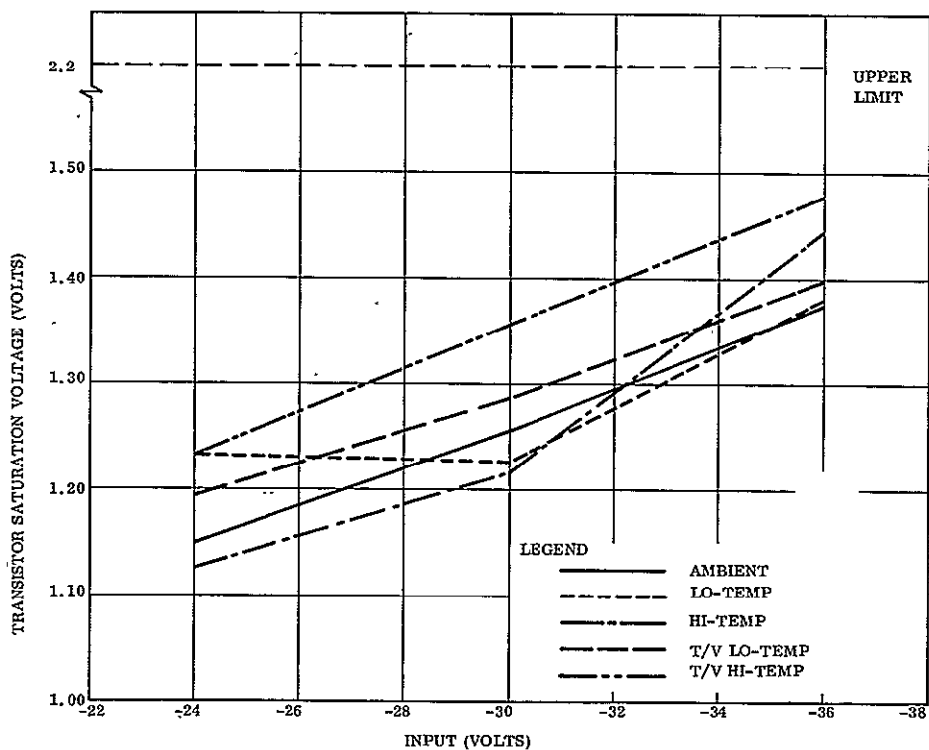


Figure 6-20. Solenoid Driver Transistor Saturation Voltage vs Input Voltage, Rod B Emergency

Table 6-3. Solenoid Driver, Hysteresis Damper

Environment	Input Volts	$R_L$ (ohms)	Volts $V_L$	Amperes $I_L$	A PS Volts	B 1R PCU Load	C 1R PS PCU	B + C	B+C+ $V_L$	$V_{ce}$
Ambient	NOM	1.6	-26.5	16.5	-29.50	.825	.32	1.145	27.645	1.855
	Lo-V	1.6	-21.2	13.2	-23.70	.66	.256	.916	22.116	1.584
	Hi-V	1.6	-32.02	20	-35.53	1.0	.388	1.388	33.400	2.130
Lo-Temp	NOM	1.6	-26.7	16.7	-29.60	.835	.324	1.159	27.859	1.741
	Lp-V	1.6	-21.16	13.2	-23.76	.66	.256	.916	22.076	1.684
	Hi-V	1.6	-31.38	19.6	-34.62	.98	.380	1.360	32.74	1.880
High-Temp	NOM	1.6	-26.44	16.55	-29.68	.828	.32	1.148	27.588	2.092
	Lo-V	1.6	-21.04	13.2	-23.78	.66	.256	.916	21.956	1.824
	Hi-V	1.6	-31.02	19.5	-34.50	.975	.378	1.353	32.373	2.127
Post Vibration No. 1	NOM	1.6	-26.3	16.45	-29.58	.823	.32	1.143	27.443	2.137
Post Vibration No. 2	NOM	1.6	-26.68	16.7	-29.70	.835	.324	1.159	27.839	1.861
Thermal/Vacuum	NOM	1.6	-25.50	16.0	-29.70	1.75	.62	2.370	27.870	1.83
Low	Lo-V	1.6	-20.26	12.2	-23.76	1.33	.472	1.802	22.062	1.698
Temp	Hi-V	1.6	-27.5	17.2	-31.89	1.88	.666	2.546	30.046	1.844
Thermal/Vacuum	NOM	1.6	-25.24	15.8	-29.64	1.72	.614	2.334	27.574	2.056
High	Lo-V	1.6	-20.10	12.6	-23.74	1.37	.488	1.858	21.958	1.782
Temp	Hi-V	1.6	-26.22	16.4	-30.78	1.79	.636	2.426	28.646	2.134
Post Thermal/Vacuum	NOM	1.6	-26.60	16.6	-29.72	.83	.322	1.152	27.752	1.968
Post Acceleration	NOM	1.6	-26.6	16.6	-29.68	.83	.322	1.152	27.752	1.928

Table 6-4. Solenoid Driver Rod "B" Emergency

Environment	Input Volts	R <sub>L</sub> (ohms)	V <sub>L</sub>	I <sub>L</sub>	A PS Volts	IR(B) PCU-Load	IR(C) PS-PCU	B+C	B+C+V <sub>L</sub>	V <sub>ce</sub>
Ambient	NOM	8	28.06	3.51	29.88	.495	.068	.563	28.623	1.257
	LO-V	8	22.34	2.8	23.94	.395	.055	.450	22.79	1.15
	HI-V	8	33.83	4.23	35.88	.595	.082	.677	34.507	1.373
Low Temp	NOM	8	28.10	3.52	29.92	.496	.069	.565	28.665	1.225
	LO-V	8	22.30	2.79	23.98	.394	.054	.448	22.748	1.232
	HI-V	8	33.86	4.24	35.92	.598	.083	.681	34.541	1.379
High Temp	NOM	8	28.10	3.51	29.88	.495	.068	.563	28.663	1.217
	LO-V	8	22.42	2.81	24.00	.396	.055	.451	22.871	1.129
	HI-V	8	33.80	4.23	35.92	.595	.083	.678	34.478	1.442
Post Vibration No. 1	NOM	8	27.98	3.50	29.88	.494	.068	.562	28.542	1.338
Post Vibration No. 2	NOM	8	28.00	3.50	29.94	.494	.068	.562	28.562	1.378
Thermal/Vacuum Low Temp	NOM	8	27.64	3.46	29.92	.860	.134	.994	28.634	1.286
	LO-V	8	21.96	2.74	23.94	.680	.107	.787	22.747	1.193
	HI-V	8	33.40	4.18	36.00	1.004	.162	1.202	34.602	1.398
Thermal/Vacuum High Temp	NOM	8	27.56	3.44	29.90	.850	.133	.983	28.543	1.357
	LO-V	8	21.90	2.74	23.92	.680	.107	.787	22.687	1.233
	HI-V	8	33.28	4.16	35.95	1.03	.162	1.192	34.472	1.478
Post Thermal/ Vacuum	NOM	8	28.10	3.51	29.96	.495	.068	.563	28.663	1.297
Post Acceleration	NOM	8	28.10	3.51	29.92	.495	.068	.563	28.663	1.257

They were caused by misreadings, inaccurate test equipment, or in one case, by having the current limiting control set too low on the power source. Another source of error is in the calculations of the line voltage drops with low value resistance and high value current.

Several failures occurred during the test in this section of the Power Control Unit. At high temperature, the transistor switch in Rod A Emergency mode solenoid circuit started to operate without a command signal. This trouble was caused by a faulty transistor (2N2906) in the module. Also, at high temperature, the output transistor for the Rod A Normal mode solenoid was accidentally shorted to ground causing the power output transistor to open.

**6.2.4.3.3.1 Sample Calculation for Solenoid Driver.** A sample calculation of transistor saturation voltage with input voltage is shown in Figure 6-21 for the hysteresis damper solenoid driver module. The test circuit used for determining the line voltage drops and the voltage drops across the output transistor is shown together with the calculations for determining  $V_{ce}$ .

**6.2.4.3.3.1.1 Ambient Test**

$A$  = Power Supply Voltage = -29.50 volts

$V_L$  = Voltage Across Load = -26.50 volts

$V_L$  = Load Resistance = 1.6 ohm

Line A consists of two parallel wires with an equivalent resistance of .05 ohm.

Line B consists of two parallel wires with an equivalent resistance of .0194 ohm.

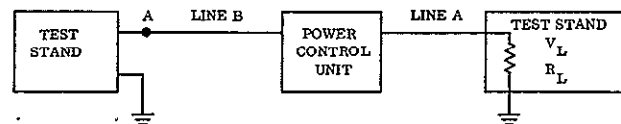


Figure 6-21. Hysteresis Damper Solenoid Driver Test Circuit

Table 6-5. Field Driver, Rod "B"

Environment	Input Volts	$R_L$ (ohms)	$V_1$	$V_2$	$V_{in}$	$V_3 =$ $V_{in} -$ $V_L$	A $V_3 + V_1$
Ambient	NOM	80	1.10	29.60	30.0	.40	1.50
	LO-V	80	1.00	23.7	24.0	.30	1.30
	HI-V	80	1.10	35.58	36.0	.42	1.52
Low Temp	NOM	80	1.10	29.6	30.0	.40	1.50
	LO-V	80	1.10	23.56	24.0	.44	1.54
	HI-V	80	1.2	35.60	36.0	.40	1.60
High Temp	NOM	80	1.04	29.64	30.0	.36	1.40
	LO-V	80	.97	23.77	24.0	.23	1.20
	HI-V	80	1.08	35.58	36.0	.42	1.50
Post Vibration No. 1	NOM	80	1.08	29.64	30.0	.36	1.44
Post Vibration No. 2	NOM	80	1.06	29.66	30.0	.34	1.40
Thermal/Vacuum Low Temp	NOM	80	1.16	29.60	30.0	.40	1.56
	LO-V	80	1.10	23.70	24.0	.30	1.40
	HI-V	80	1.20	35.60	36.0	.40	1.60
Thermal/Vacuum High Temp	NOM	80	1.08	29.58	30.0	.42	1.50
	LO-V	80	1.0	23.65	24.0	.35	1.35
	HI-V	80	1.10	35.57	36.0	.43	1.53
Post Thermal/Vacuum	NOM	80	1.1	29.68	30.0	.32	1.42
Post Acceleration	NOM	80	1.06	29.68	30.0	.32	1.38



$$\begin{aligned}\text{Current through } R_L &= \frac{V_L}{R_L} \\ &= \frac{26.5 \text{ V}}{1.6} = 16.5 \text{ amps} = I_L\end{aligned}$$

$$\text{Drop in Line A} = 16.5 \text{ amp} \times .05 = 0.825 \text{ volts} = B$$

$$\text{Drop in Line B} = 16.5 \text{ amp} \times .0194 = 0.32 \text{ volts} = C$$

$$\text{Drop across Output Transistor} = A - V_L - B - C = V_{ce}$$

$$V_{ce} = -29.5 - (26.5 - 0.825 - 0.32)$$

$$V_{ce} = -29.5 + 27.645$$

$$V_{ce} = 1.855 \text{ volts}$$

6.2.4.3.3.1.2 Thermal Vacuum Test. Cables used during thermal/vacuum test had the following impedances.

Line A consisted of two cables in a series with a combined resistance of 0.109 ohm.

Line B consisted of two cables in a series with a combined resistance of 0.0388 ohm.

#### 6.2.4.3.4 Field Driver Module

The Power Control Unit has four similarly constructed field driver modules that controlled the rotation of the four motors associated with the Gravity Gradient Boom System. Because these modules are identical, the one that exhibited the widest variation when subjected to temperature, thermal vacuum and voltage changes was selected for evaluation.

6.2.4.3.4.1 Results of the Test. Table 6-5 lists the environment, power supply input voltage, load and calculated data derived from the test on Rod B Field Driver. A set of sample calculations is given showing how calculated data was derived.

Figure 6-22 is the graph of the power supply voltage versus the saturation voltage of the two transistors in series with the field winding. The plot shows the low temperature low voltage reading to be in error. Sources of error are:

1. Test equipment
2. Reading meters

All other readings are well within the specification. Several failures were encountered in the field driver modules. The failures were all due to shorted transistors. The faults were caused by either applying the wrong load or an inadvertent ground. Steps were taken to help eliminate the application of the wrong load by moving the loads closer to the field driver output test terminals and plugging output test terminals when not used.

#### 6.2.4.3.4.2 Sample Calculation

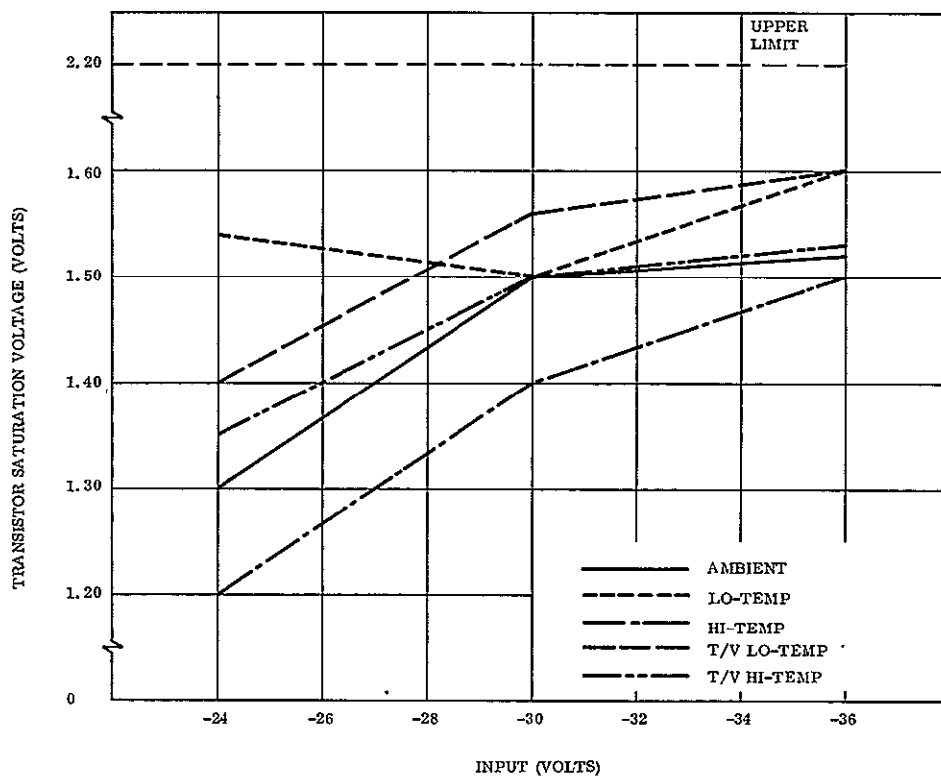


Figure 6-22. Motor Field Driver Transistors Saturation Voltage vs Input Voltage, Rod B Field Driver

6.2.4.3.4.2.1 Sample Calculation, Field Driver. A sample calculation of transistor saturations voltage with input voltage for the field driver module and the test circuit used for determining the line voltage drops and the voltage drops across the output transistors is shown in Figure 6-23.

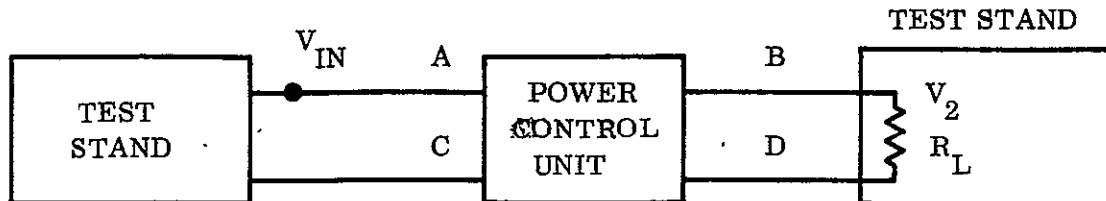


Figure 6-23. Field Driver Test Circuit

Voltage drop in Line A and B plus drop in one transistor

$$= V_{in} - V_2 = V_3$$

$$= 30 - 29.60 = 0.40 \text{ V}$$

Voltage drop in Line C and Line B plus drop in one Transistor

$$= V_1 = 1.10 \text{ V}$$

Total drop =  $V_3 + V_1$

$$= 0.40 + 1.10 = 1.50 \text{ V}$$

Line A = .0194 ohms

Line B = 0.1502 ohms

Line C 3 wire = .0257 ohms

Line D = 0.1507 ohms

$$I_{RL} = \frac{V_2}{R_L} = \frac{29.60}{80} = 0.37 \text{ ampere}$$

The voltage drop in the cables is small and was omitted from the calculations.

#### 6.2.4.3.5 Motor Driver Module and Armature Driver

There are four identical motor driver modules in each Power Control Unit. Each one performs two functions simultaneously. One function is to activate the motor's armature and the second function is to apply the correct control signal to the field driver module. As the

motor driver modules are alike in all respects only one was selected for evaluation and that one exhibited the widest variations when subjected to temperature, thermal-vacuum, and voltage changes.

6.2.4.3.5.1 Results of the Test. Table 6-6 has a complete set of data on motor driver for Rod A. Some of the data was taken during the test and some was computed from the test data. All testing was performed with a resistive load of 6.3 ohms to simulate the motor armature. Figure 6-25 shows the graph of the Power Supply Voltage (Input Voltage on Table 6-6) versus the Saturation Voltage ( $V_{ce}$ ). All readings were within tolerance and no troubles were experienced during the test. The graph shows that several readings were probably in error.

6.2.4.3.5.2 Sample Calculations for Motor Driver Rod A. The test setup for determining the line voltage drops and the voltage drops across the output transistor is shown in Figure 6-24. together with the calculations necessary for determining  $V_{ce}$ .

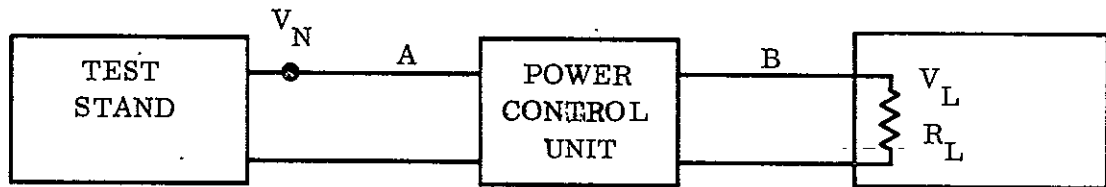


Figure 6-24. Line Voltage Drop Determining Circuit

$V_N$  = Power Supply Voltage = 29.88 volts

$V_L$  = Voltage across  $R_L$  = 27.59 volts

$R_L$  = Load Resistance = 6.3 ohms

Line A consists of four wires with a total resistance of .0194 ohm.

Line B consists of one wire with a resistance of 0.1507 ohm.

$$I_L = \frac{V_L}{R_L} = \frac{27.59 \text{ V}}{6.3} = 4.38 \text{ amperes}$$

Column B = IR drop in Line B =  $4.38 \cdot 0.1507 = .68$  volt

Column C = IR drop in Line A =  $4.38 \cdot .0194 = .085$  volt

Drop across output transistor =  $V_N - V_L - B - C$

$$= 29.88 - 27.59 - 0.68 - .085 \quad V_{ce} = 1.525 \text{ volt}$$

Table 6-6. Motor Driver, Rod "A"

Environment	Input Volts	R <sub>L</sub> (ohms)	V <sub>L</sub>	I <sub>L</sub>	V <sub>n</sub> PS Volts	IR(B) PCU Load	IR(C) PS PCU	B+C	B+C+V <sub>L</sub>	V <sub>ce</sub>
Ambient	NOM	6.3	27.59	4.38	29.88	.68	.085	.765	28.355	1.525
	LO-V	6.3	22.06	3.51	23.94	.544	.068	.612	22.672	1.268
	HI-V	6.3	33.38	5.3	35.88	.822	.103	.925	34.305	1.575
Low Temp	NOM	6.3	27.66	4.40	29.90	.683	.0853	.7683	28.428	1.472
	LO-V	6.3	21.78	3.46	23.84	.536	.067	.603	22.383	1.457
	HI-V	6.3	33.39	5.3	35.92	.822	.103	.925	34.315	1.605
High Temp	NOM	6.3	27.64	4.40	29.88	.683	.0853	.7683	28.408	1.472
	LO-V	6.3	22.08	3.51	23.94	.544	.068	.612	22.692	1.248
	HI-V	6.3	33.28	5.28	35.90	.82	.103	.923	34.203	1.697
Post Vibration No. 1	NOM	6.3	27.69	4.40	29.88	.683	.0853	.7683	28.458	1.422
Post Vibration No. 2	NOM	6.3	27.77	4.41	29.94	.683	.0855	.7685	28.538	1.402
Thermal/Vacuum Low Temp	NOM	6.3	27.26	4.33	29.92	1.152	.168	1.320	28.58	1.34
	LO-V	6.3	21.66	3.45	23.95	.920	.134	1.054	22.714	1.236
	HI-V	6.3	32.98	5.22	36.00	1.39	.202	1.592	34.572	1.428
Thermal/Vacuum High Temp	NOM	6.3	27.20	4.32	29.90	1.152	.168	1.320	28.52	1.38
	LO-V	6.3	21.64	3.45	23.95	.920	.134	1.054	22.694	1.256
	HI-V	6.3	32.79	5.2	35.95	1.39	.202	1.592	34.382	1.568
Post Thermal/ Vacuum	NOM	6.3	27.78	4.41	29.96	.683	.0855	.7685	28.548	1.412
Post Acceleration	NOM	6.3	27.78	4.41	29.92	.683	.0855	.7685	28.548	1.372

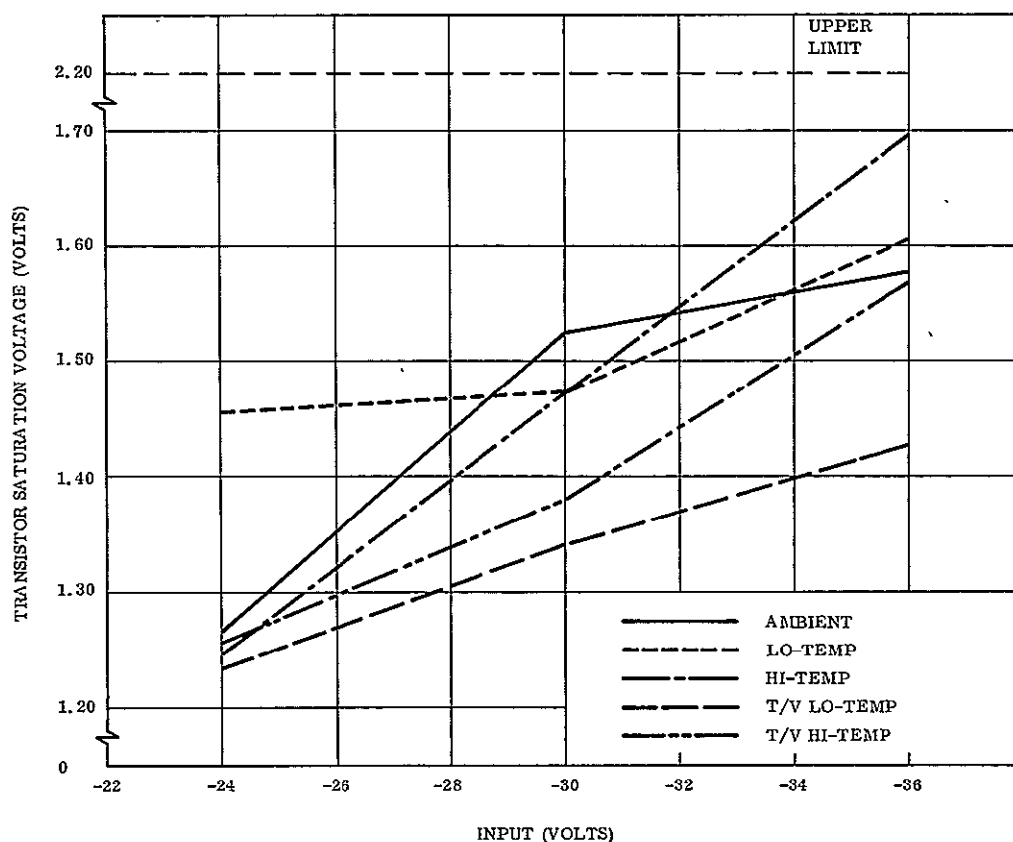


Figure 6-25. Motor Armature Driver Saturation Voltage vs Input Voltage, Rod A Motor Armature Driver

Thermal-vacuum test cables used during thermal-vacuum test had the following impedances.

1. Line B consists of two cables in series with a total resistance of 0.2627 ohm
2. Line A consists of two cables in series with a total resistance of .0388 ohm.

#### 6.2.4.3.6 Telemetry Power Supply Module

6.2.4.3.6.1 Results of the Test. Within the design range of loading, the circuit worked well throughout the engineering test. Using the data from Table 6-7 the graphs on Figure 6-26 and 6-27 were plotted. Figure 6-26 shows the plot of the supply's output versus the load at nominal voltage. Figure 6-27 shows the plot of the supply's output versus the change in -24 volts with a constant load. Taking -5.010 volts as the mean, the upper and lower specification limits were drawn. All readings were within tolerance.

Table 6-7. -5 Power Supply.

Environment	Output with Different Loads			
	Input Volts	1300 Ohms	650 Ohms	300 Ohms
Ambient	NOM	5.012	5.006	4.992
	LO-V	5.010	5.010	5.000
	HI-V	5.014	5.012	5.006
Low Temp	NOM	5.020	5.020	5.018
	LO-V	5.020	5.020	5.014
	HI-V	5.029	5.026	5.020
High Temp	NOM	5.008	5.006	5.002
	LO-V	5.007	5.004	4.999
	HI-V	5.010	5.009	5.004
Post Vibration No. 1	NOM	5.010	5.010	5.006
Post Vibration No. 2	NOM	5.010	5.010	5.004
Thermal/Vacuum Low Temp	NOM	5.020	5.020	5.010
	LO-V	5.020	5.017	5.009
	HI-V	5.026	5.022	5.016
Thermal/Vacuum High Temp	NOM	5.010	5.008	5.002
	LO-V	5.010	5.008	5.000
	HI-V	5.015	5.010	5.006
Post Thermal/Vacuum	NOM	5.010	5.010	5.006
Post Acceleration	NOM	5.013	5.011	5.006

#### 6.2.4.3.7 Squib Driver Module

A Power Control Unit has four identical squib driver modules which have the one function of controlling the firing of the four squibs. The modules are paired and the paired modules are connected to form two redundant circuits, then each one drives two squibs. As the circuits in the modules are similar, the one that exhibited the widest variations when subjected to temperature, thermal-vacuum and voltage changes was selected for evaluation.

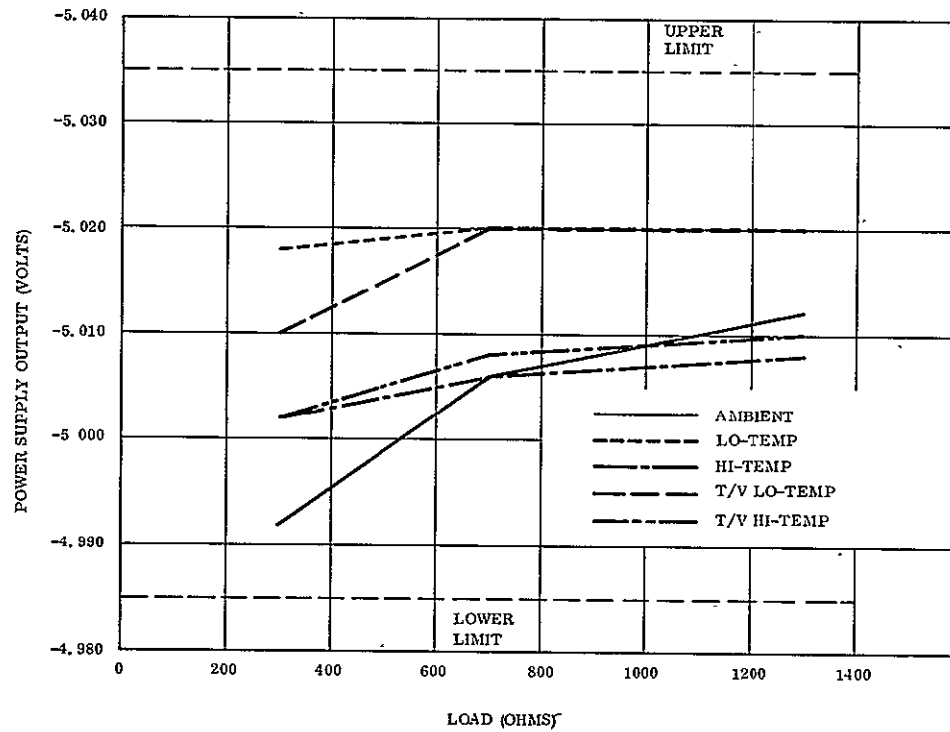


Figure 6-26. -5 Volt Power Supply vs Load at Nominal Voltage

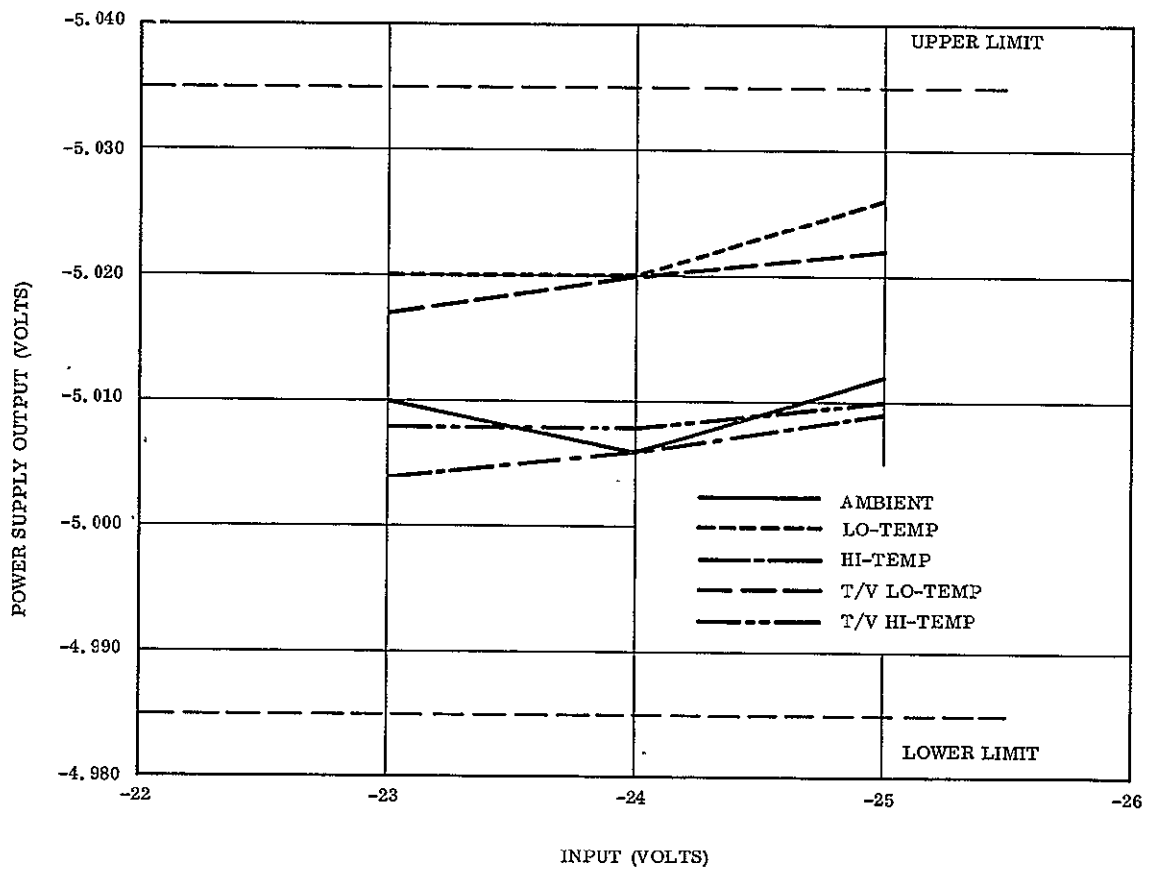


Figure 6-27. -5 Volt Power Supply Output vs Input Voltage (650-ohm Load)



6.2.4.3.7.1 Results of the Test. Table 6-8 has a compiled set of data that was taken during the engineering test. From this table the graphs on Figures 6-28, 6-29 and 6-30 were plotted. Figure 6-28 is the plot of pulse width versus the power supply voltage. This graph shows that all readings, even though the power supply voltage was higher than called out, were within specification. Figure 6-29 is the plot of load current versus supply voltage. Some of the readings exceed the upper specification limit because the load and voltage were out of specification limits. Figure 6-30 is a plot of delay time versus supply voltage. In this plot many readings were out of tolerance. The deviations resulted because the command signal voltage was set lower than specified.

Table 6-8. Squib Drivers (Typical):

Environment	Input Volts	DT Sec.	PW MS	Volts	Load (ohms)	Amperes IL
Ambient	Nom	1.08	72	3.9	.5	7.8
	Lo-V	1.4	62	3.2	.5	6.4
	Hi-V	1.48	82	4.8	.5	9.6
Low Temp	Nom	1.08	59	4.2	.5	8.4
	Lo-V	1.44	50	3.2	.5	6.4
	Hi-V	1.36	68	5.0	.5	10.0
High Temp	Nom	1.04	81	3.5	.5	7.0
	Lo-V	1.4	72	3.0	.5	6.0
	Hi-V	1.48	90	5.1	.5	10.2
Post Vibration No. 1	Nom	1.04	70	4.1	.5	8.2
Post Vibration No. 2	Nom	1.04	70	3.8	.5	7.6
Thermal/Vacuum Low Temp	Nom	1.0	60	3.6	.5	7.2
	Lo-V	1.44	49	2.9	.5	5.8
	Hi-V	1.44	68	4.2	.5	8.4
Thermal/Vacuum High Temp	Nom	1.04	78	3.6	.5	7.2
	Lo-V	1.4	68	2.8	.5	5.6
	Hi-V	1.5	86	4.2	.5	8.4
Post Thermal/Vacuum	Nom	1.04	69.5	3.8	.5	7.6
Post Acceleration	Nom	1.06	70	4.0	.5	8.0

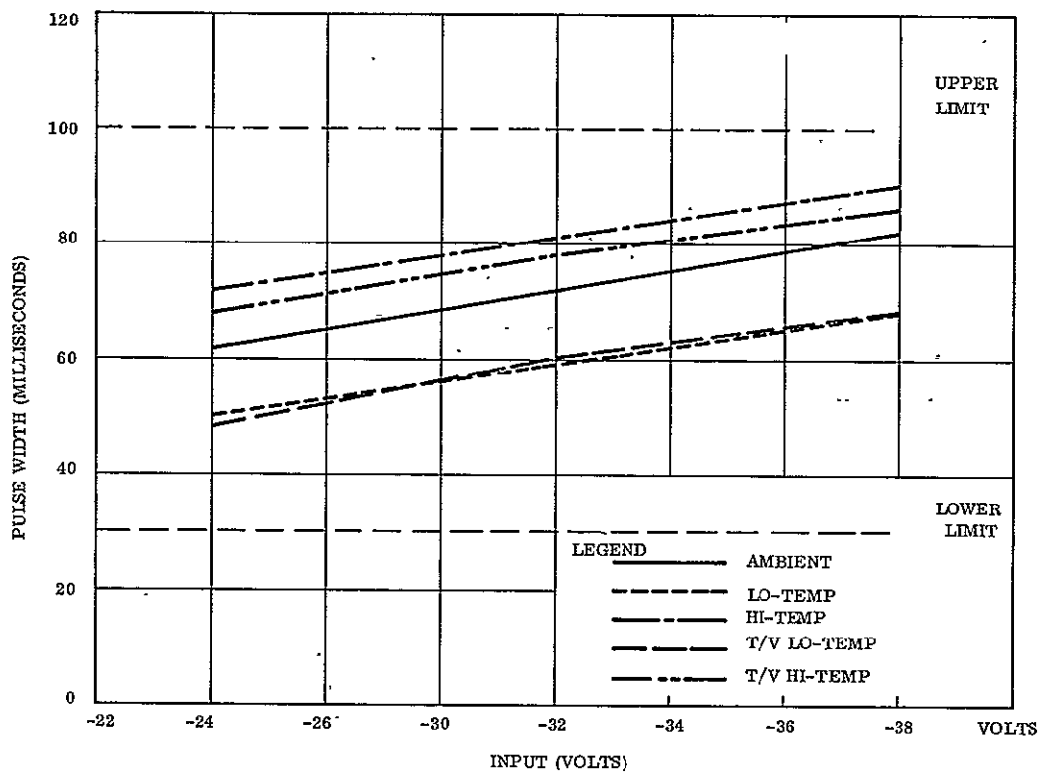


Figure 6-28. Squib Driver Pulse Width vs Input Voltage

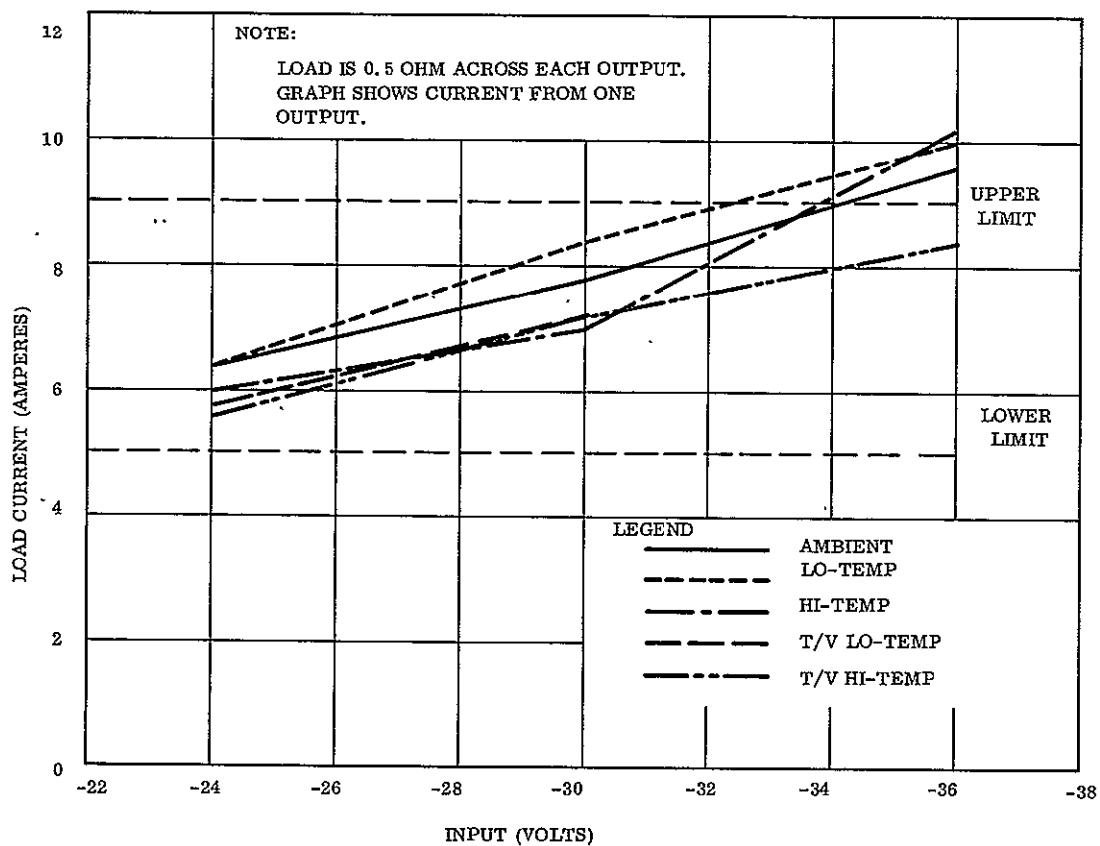


Figure 6-29. Squib Driver Load Current vs Input Voltage

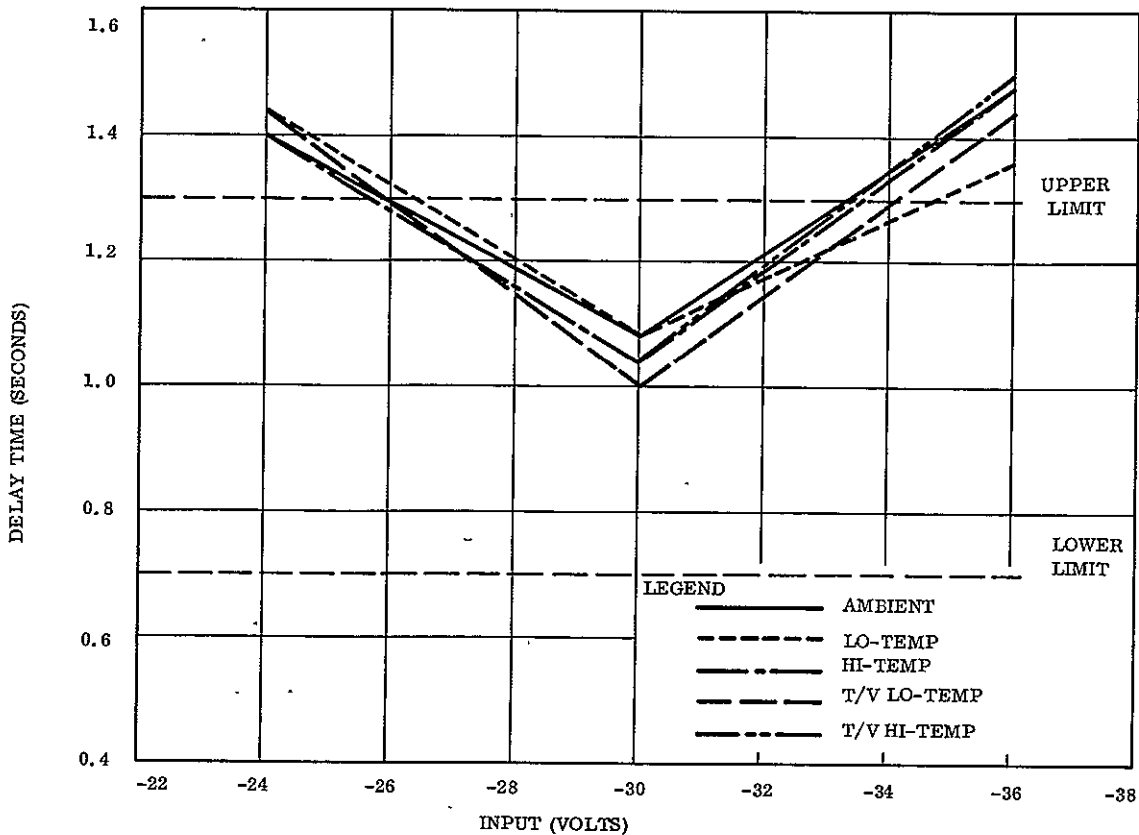


Figure 6-30. Squib Driver Delay Time vs Input Voltage

#### 6.2.4.3.8 Relays and Relay Drivers

6.2.4.3.8.1 Results of the Test. Throughout the test, all outputs were loaded and voltage checks were made to determine that the voltage drop across the relay was negligible. Checks were also made to determine that the telemetry outputs were working correctly. A power dropping resistor (R53) used in conjunction with the CPD angle indicator light bulb on the output of one of the relays, was monitored for temperature rise (Figure 6-30) and at no time did it exceed the design goal limit of 100°C. No troubles were experienced during the test and the test proved successful.

### 6.3 QUALIFICATION TEST

Two prototype Power Control Unit (designated a component and system qual) were subjected to similar environments at more severe levels than the anticipated operating environments in order to establish confidence that the design was valid under extreme operating conditions. Following tests, the component qualification unit was not further dispositioned, but the

system qualification unit was included in the spacecraft qualification tests that were conducted by the vehicle contractor. A summary of these environments and references to the appropriate test reports are listed below. These documents are on file at GE and will be made available on request of the Contract Administrator for NASA programs.

#### 6.3.1 COMPONENT QUALIFICATION

Serial No. 5962033

Part No. 47E207948

Test Report 4315-QC-011 (9/2/66)

Test Sequence:

- |               |                     |
|---------------|---------------------|
| 1. Functional | 6. Acceleration     |
| 2. Humidity   | 7. Functional       |
| 3. Functional | 8. Thermal-Vacuum   |
| 4. Vibration  | 9. Functional       |
| 5. Functional | 10. Magnetic Dipole |

#### 6.3.2 System Qualification

### 6.4 FLIGHT ACCEPTANCE

Each of the PCU flight units was exposed to vibration and thermal-vacuum environments at levels anticipated during flight to verify that the design had not degraded during manufacture. A summary of these environments and reference to the applicable test reports are listed below. These documents are on file at GE and will be made available on request of the Contract Administrator for NASA programs.

#### 6.4.1 ATS-A

Serial No. 5962036

Part No. 47E207948G2

Test Report 4315-QC-020 (11/23/66)

Test Sequence:

- |                     |                        |
|---------------------|------------------------|
| 1. Confidence Check | 5. Thermal-Vacuum      |
| 2. Performance      | 6. Post Thermal-Vacuum |
| 3. Vibration        | 7. Magnetic Dipole     |
| 4. Post Vibration   |                        |

#### 6.4.2 ATS-D

Serial No. 5962035

Part No. 47E207948G2

Test Report 4315-QC-015 (10/4/66)

Test Sequence:

- |                     |                        |
|---------------------|------------------------|
| 1. Confidence Check | 5. Thermal-Vacuum      |
| 2. Performance      | 6. Post Thermal-Vacuum |
| 3. Vibration        | 7. Magnetic Dipole     |
| 4. Post Vibration   |                        |

#### 6.4.3 ATS-E

Serial No. 5962034

Part No. 47E207948G2

Test Report 4315-QC-010 (8/11/66)

4315-QC-014 (10/5/66)

4315-QC-004 (9/4/68)

Test Sequence:

- |                     |                        |
|---------------------|------------------------|
| 1. Confidence Check | 5. Thermal-Vacuum      |
| 2. Performance      | 6. Post Thermal-Vacuum |
| 3. Vibration        | 7. Magnetic Dipole     |
| 4. Post Vibration   |                        |

**SECTION 7**  
**RF ATTITUDE SENSOR**

## RF ATTITUDE SENSOR FACT SHEET

### DESIGNER:

General Electric Company Space Division

### SUBCONTRACTOR:

General Electric Radio Guidance Operation; Utica, New York

### CONTROLLING DOCUMENTS:

Specification	SVS-7305
Work Statement	9750-002WS
Outline Drawing	47E207012

### PERFORMANCE REQUIREMENTS:

#### Function

Measure angle of arrival at the satellite of an electromagnetic wave transmitted from the ground to an accuracy of one degree

#### Life

3-year life at 50% duty cycle

#### Frequency

6212 mHz

#### Power

5 watts max.

#### Weight

8 lb max.



## SECTION 7

### RF ATTITUDE SENSOR

#### 7.1 INTRODUCTION

An RF Attitude Sensor was included as one of the attitude sensors in the original concept of the gravity gradient system design, but it was deleted by a NASA/Goddard change order to the Contract (Modification No. 5, dated January 1, 1965). The RF Attitude Sensor would have measured the angle of arrival of an electromagnetic wave transmitted from the ground up to 25 degrees off the sensor boresight with an accuracy of one degree. The angle of arrival was to be determined by measuring this angle with respect to two orthogonal axes (designated as pitch and roll axes) which were perpendicular to the boresight. Telemetry signals that were related to these angles were to be transmitted to the ground and processed into spacecraft position with respect to the local vertical. A design specification (SVS-7305) and Work Statement 9750-002 WS (both dated October 1, 1964) were the controlling documents and they were used as a basis for competitive bidding among six qualified subcontractors. Based on price and proven ability to fabricate the sensor, the GE Radio Guidance Operation of Utica, N. Y., was placed under Contract. Preliminary designs had just begun when the effort was cancelled. This section describes the sensor functions and the progress that was made up to the point of cancellation.

The sensor would have received a signal at 6212.094 mHz and measured its angle of arrival to within one degree. This attitude data would have been presented to an on-board telemetry system in digital form with eight bits of data for each of the measured (pitch and roll) channels.

The design goal for the equipment reliability over a three-year operating life was to be 80 percent, with a 50 percent operating duty cycle. This goal was to be met through the use of high reliability components and extensive component derating.

The RF Attitude Sensor was to have consumed five watts maximum from the spacecraft power supply and weighed no more than eight pounds. The physical size of the equipment (Figure 7-1) was to be six inches by six inches by six inches excluding connectors and mounting feet. The antenna face of the unit included a boresight mirror for alignment with the spacecraft structure.

## 7.2 ELECTRICAL DESIGN

The RF Attitude Sensor is based upon three receiver channels and a data processor as shown in Figure 7-2. The central receiver is used to feed phase detectors, referenced by a locally generated 10-kHz signal. The output of the quadrature phase detector is used, via a dc amplifier and stabilizing filter, to control a voltage tuned crystal oscillator. The 18.94 MHz output of the crystal oscillator is multiplied by 324 and 328 to generate two signals at 6136.4 MHz and 6212.1 MHz. The 6136.4 MHz signal serves as a LO signal to mix with the received signal to produce a 75.76 MHz IF signal. When the loop is locked the 6212.1 MHz signal (pilot tone) will be 10 kHz away from the received signal and mix with it in the detector to produce a 10 kHz video output from the receiver. This output 10 kHz carries the phase angle information of the received signal. Both the received signal and the pilot tone signal are processed through many common stages; as a result the phase delays of these stages affect both signals. Due to the common effect of these phase delays they are removed as errors from the system.

The in-phase phase detector output is used as a "lock on" signal for telemetry purposes and as a sweep inhibit to assure lock on of the pilot tone on the proper side of the received signal. A video signal proportional to received amplitude (minimum expected signal) is taken from the limiter and used as a sweep stop signal. Thus advantage is taken of the good received signal-to-noise-ratio to allow a relatively fast acquisition search rate. This same video is sent, from each of the three receivers, to a summer where they are combined to telemeter receiver video level to the ground.

Upon receipt of a read pulse from the vehicle telemetry subsystem (TMSS) a data collection process in the attitude sensor is started. Power is applied to the digital circuits and the next positive going zero crossing of the pitch video starts an eight bit counter counting the 2.56 MHz signal from which the 10 kHz reference signal is derived. The first positive going zero crossing of the central video stops the



Figure 7-1. RF Attitude Sensor Mockup

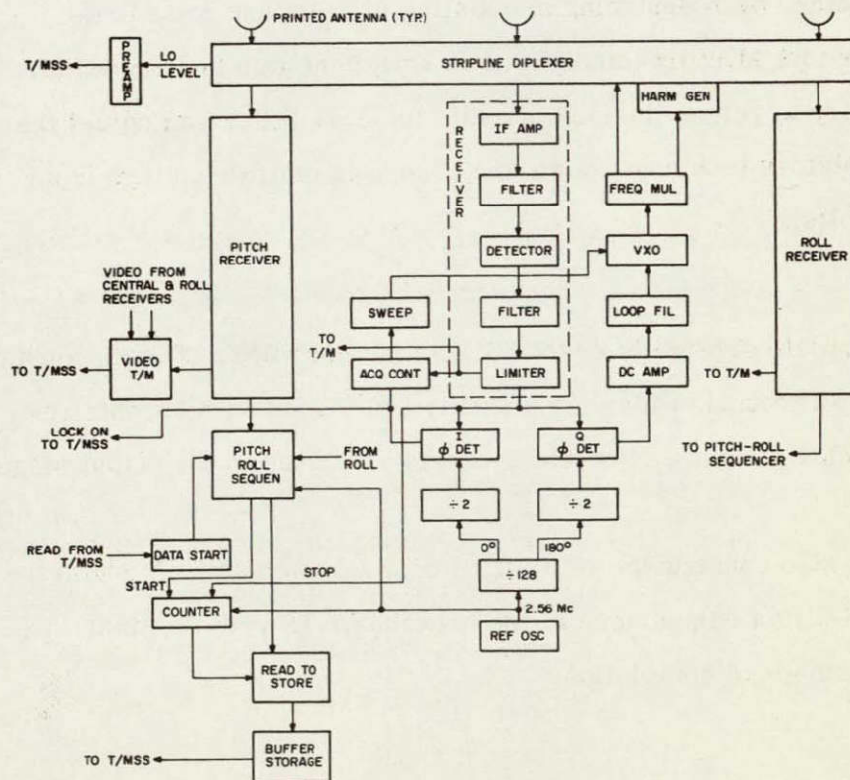


Figure 7-2. RF Attitude Sensor Block Diagram



counting process. The resultant count accumulated is a digital representation of the spacecraft pitch axis attitude with respect to the received phase front. This signal is then read to buffer storage where it is presented to the telemetry subsystem.

This process is then repeated for the roll channel after which power is removed from all digital processing circuits (except the buffer storage) until the next read pulse. In the data collection area there are two approaches under consideration. If the noise generated by the ground and sensor oscillator-multipliers proves to be such as to degrade the data seriously the data sample will be taken over 128 cycles (of the 10 kHz) in each channel. This will reduce the noise errors by more than ten. This area is discussed in more detail in Appendix G.

#### 7.2.1 75.76 MHZ IF AMPLIFIER

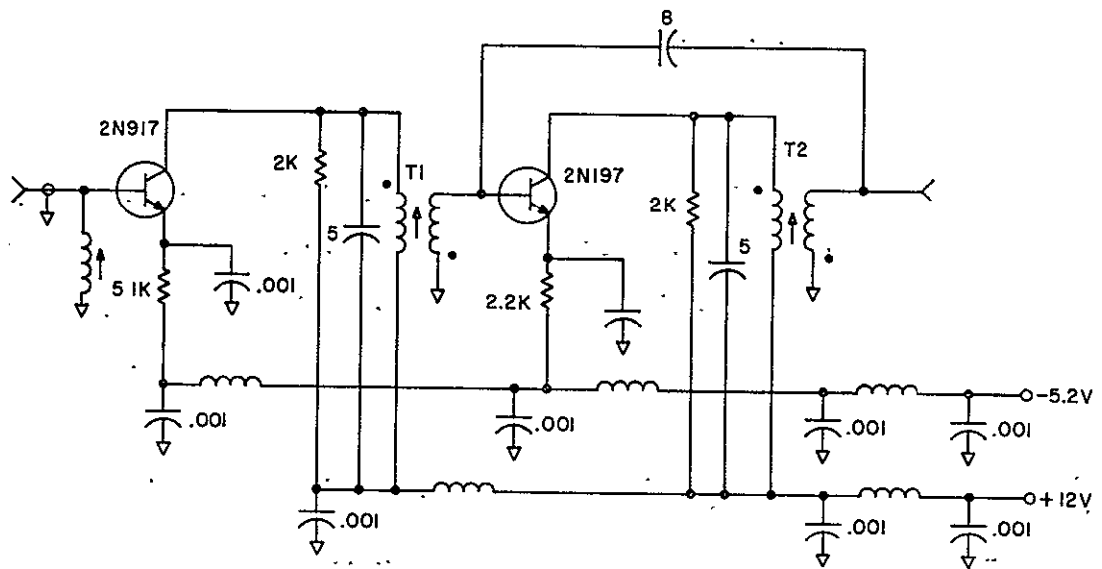
In an effort to reduce design time to a minimum, and use proven circuitry, the 75 MHz IF was obtained by redesigning an existing 68 MHz low noise pre-amplifier. Since the 68 MHz pre-amplifier had sufficient gain and bandwidth it was only necessary to retune the tank circuits to 75.76 MHz, and adjust the emitter biasing resistors to accommodate the change in emitter voltage from -12 volts to -5.2 volts.

Figure 7-3 is a complete schematic of the 75 MHz IF amplifier. The IF consists of two stages of amplification, which for stability are loaded with 2K ohm resistors in the collector circuits. Neutralization is also used in the output stage.

The 75 MHz IF was also constructed in its final configuration using Modular Weldment. Table 6-1 is a comparison of the breadboard IF with the final package in several stages of completion.

Table 7-1. 75 MHz IF Measurements

Breadboard		Final Configuration		Cover
		Pre Potting	Post Potting	
Gain	30 db	29 db	28 db	30 db
Bandwidth	10 mHz	11 mHz	10.3 mHz	10.3 mHz
Input Saturation Level	-37 dbm	-35 dbm	-35 dbm	-35 dbm



ALL CAPS EXPRESSED IN WHOLE NO. ARE IN PF

ALL OTHERS IN  $\mu$  F

L1 7T #32 WIRE SPACEWOUND WITH 1 WIRE DIA BETWEEN EACH TURN CORE 0.21" OD

T1, T2 PRI 7 1/2 T SEC 1 1/2 T #34 WIRE CORE 0.16" OD

Figure 7-3. 75.76 MHz IF Schematic

As can be seen from Table 7-1 there is very little difference between the breadboard, and the final module with cover. However, comparing the breadboard with the pre- and post-potting stage, there are slight differences in both gain and bandwidth.

No temperature testing was done on either the breadboard or the final module before the project was halted. No difficulty is expected in temperature since the 68 MHz pre-amplifier was designed and tested to operate over the temperature range of  $-35^{\circ}\text{C}$  to  $+125^{\circ}\text{C}$ .

### 7.2.2 IF FILTER

The signal-to-noise ratio for the minimum expected signal must be positive prior to the detector to avoid signal suppression by the noise. With the expected overall noise figure of 10 db and a minimum expected signal of -84 dbm the signal-to-noise ratio in a 10 MHz bandwidth should be +10 db. Thus, to provide a safe design that guards against signal suppression, it appears that an IF bandwidth of 10 MHz is a convenient upper bound.

To achieve a better signal-to-noise ratio a filter for the IF was designed. This filter (Figure 7-4) was a direct adaptation of one used on another program. The bandwidth (3 db) of the filter was 1.5 MHz and the filter had an insertion loss of approximately 6 db.

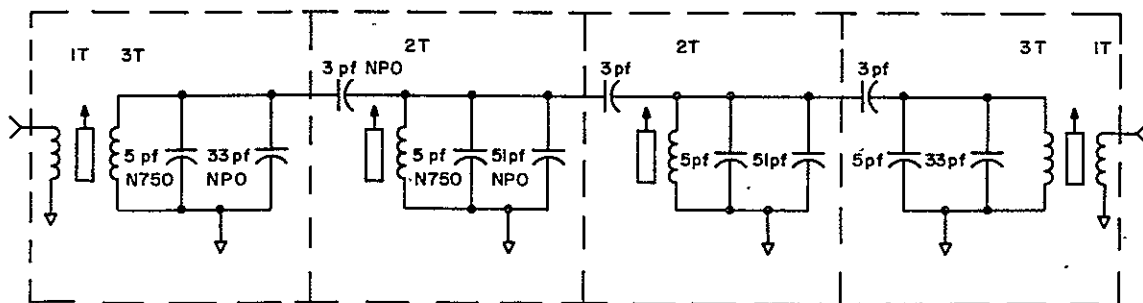


Figure 7-4. Receiver IF Filter

The breadboard filters were built in final module configuration. The resultant size was 1/2 by 1/2 by 2-1/2 inches. The construction of filters in a form factor such as this, has shown to have large effects upon operation. It was for this reason that the first breadboard module was made in the final module form factor.

### 7.2.3 IF AMPLIFIER - DETECTOR

The last IF amplifier and detector circuit is shown in Figure 7-5. The amplifier is a simple tuned stage incorporating a 2N917. The transistor is biased to allow the amplifier to remain linear up to and including the largest signal level encountered. With this system of signal processing this maximum "signal" is the pilot tone which remains constant. The amplifier is coupled to a simple diode detector which is in turn ac coupled to an emitter follower. The 10 kHz tone being the signal of interest in the system, the dc level of the detector is unimportant. Over the entire range of circuit and signal dynamics the output level of this detector ranges between 10 and 300 millivolts peak-to-peak. Considerable care must be taken with stray signals - especially the 10 kHz - to prevent spurious modulation in the system. The chokes and capacitors shown on the +12 volt supply line are to assure good filtering over the frequency range of 10 kHz to 76 MHz.

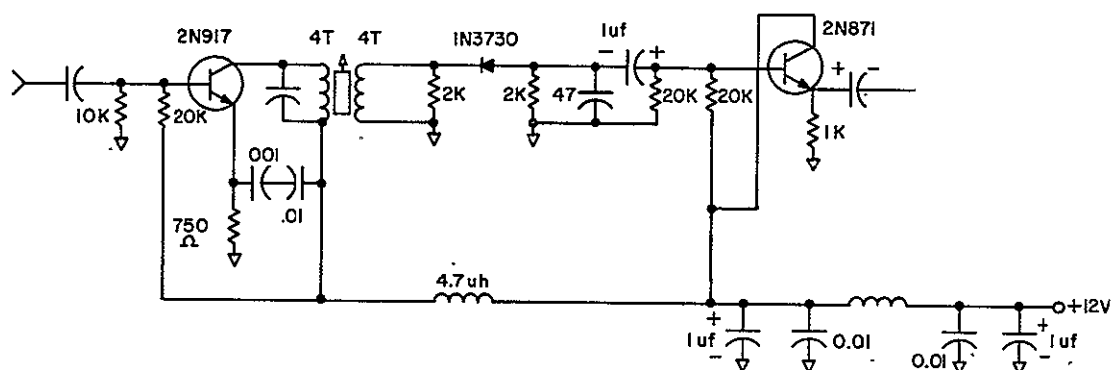


Figure 7-5. Last IF Amplifier-Detector

#### 7.2.4 VIDEO FILTER

The video filter following the detector in the receiver should meet an interesting set of conditions. In order to preserve the phase angle of the signal received by the antennas, the filters in all three channels should be nearly identical. A reasonable tolerance to allow for phase differential between the three filters is one degree. The easiest way to assure meeting such a specification would be to keep the bandwidth wide. If a wide-band filter is used, however, the signal-to-noise ratio at the input of the limiter-phase measuring system may not be high enough to get accurate data. Another drawback to a wide filter is the harmonic distortion arising from the detection process on the single sideband type of signal from the IF amplifier. To hold harmonic distortion errors down in the system it is desirable to have all harmonics 50 db or more below the carrier.

From the phase-angle viewpoint it would be simple and desirable to use a low pass filter to get rid of thermal noise. Indeed if thermal noise of the receiver front end were the predominant noise in the system, from a noise viewpoint this would be sufficient. For the breadboard evaluation of the IF and the data processing concept this is the type of filter that was used. For the final system however, the second harmonic distortion begins to dominate the filter picture. To achieve 20 db filtering of the second harmonic relative to the 10 kHz fundamental it is necessary to utilize a bandpass type of filter. Thus, phase tracking and control of this filter must be handled with care.

If a 10 kHz filter with a bandpass of two kHz were used, it would be expected to exhibit a phase slope on the order of 0.15 degree per cycle per second change in frequency. With a one percent drift in filter frequency due to temperature, a phase error in the order of 0.75 degree would be expected per channel, or worst case 1.5 degrees error per measurement. With ten percent tracking, filter-to-filter, the error should be held to 0.15 degree per measurement. Thus, while care is required, the requirements are within the state of the art.



A type of filter that appeared attractive for this application was the twin tee feedback amplifier. Figure 7-6 shows a schematic diagram of the circuit tried. The feedback resistor ( $R_f$ ) controls the bandwidth of this amplifier and for the values shown the bandwidth was 2 kHz at the three db points. Two units were built utilizing one percent resistors and five percent capacitors. The center frequency of the two units differed by five percent. A group of capacitors were then matched to one percent or less on a bridge and all circuit capacitors were replaced. The frequency difference, filter-to-filter, was now less than one percent.

An unfortunate characteristic of this type of filter was discovered, however. The output terminal of the micrologic amplifier looks at a point that is essentially wide-band. As a result there is no filtering of internally generated noise by the overall circuit. For a weak signal case then, the noise generated in the filter amplifier becomes limiting. Enough work was not done to determine if this could be cured by a following low pass filter. If this type of filter should prove to be unusable

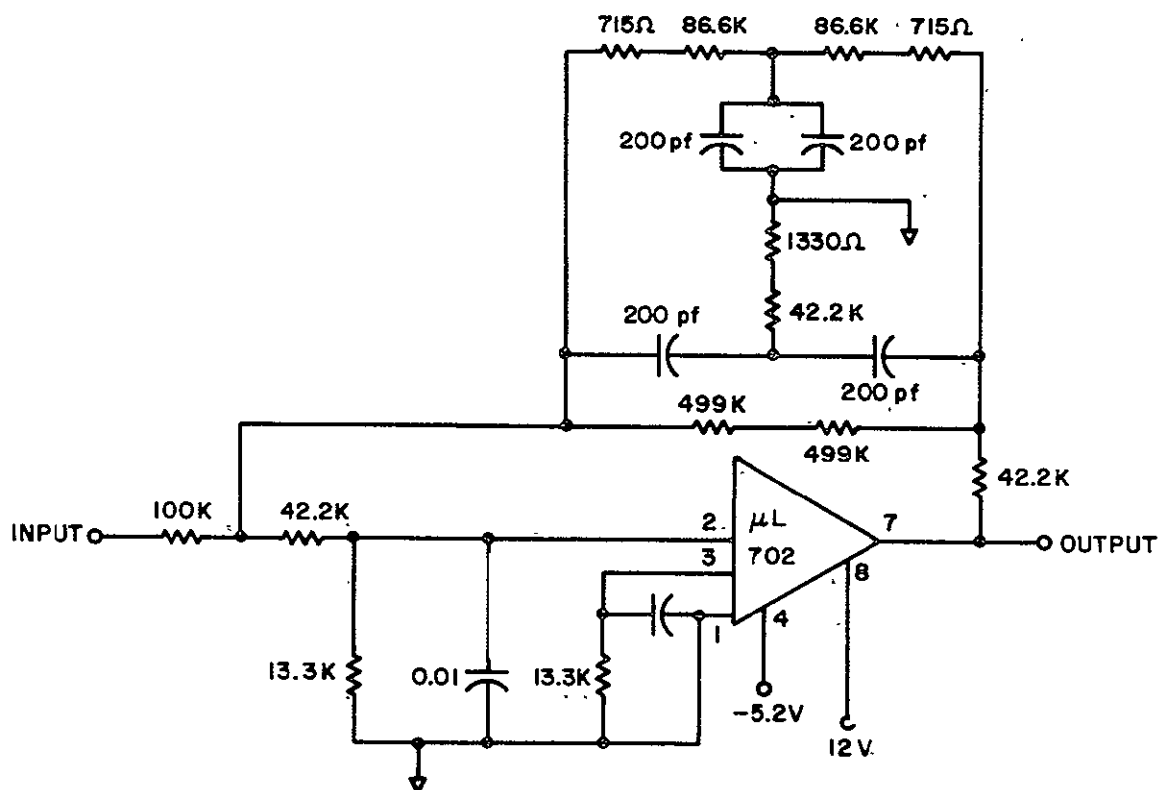


Figure 7-6. 10 kHz Filter

an L-C tuned circuit could be used with some increase in size. Vendor data indicates frequency drifts with temperature of 0.1 percent can be achieved over the entire temperature range of interest.

#### 7.2.5 LIMITERS

Since the received signal amplitude varies over a dynamic range of 30 db, some form of amplitude control is necessary. With a good signal-to-noise ratio existing prior to detection the simplest form of control is one of video limiting. The circuit of Figure 7-7 is currently used in the breadboard. This circuit is designed to carefully control clipping levels throughout the dynamic range to minimize zero crossing phase shifts. The gain of the amplifiers up to the point where the telemetry video output is taken, is controlled to remain linear up to minimum expected signal. At the minimum expected signal level the limiting action is just beginning. Therefore, this point is a valid signal for the telemetry verification of received signal and for acquisition sweep-stop purposes.

By selecting diodes as matched pairs it is found that the symmetry of clipping can be achieved by the circuit at the output end of the limiter as well as the circuit at the input end. To simplify the design (as well as to eliminate the same noise problem discussed in the video filter section) the final equipment would not incorporate the micrologic amplifier approach to the limiter.

#### 7.2.6 ACQUISITION CONTROL

The acquisition control circuit (Figure 7-8) for the attitude sensor has two inputs. A 10 kHz signal from the limiter is fed to an emitter follower detector. This detector is designed to give a single pulse to a Schmitt trigger circuit as the received signal is swept into the bandpass of the loop. The Schmitt trigger (utilizing a Fairchile  $\mu$  L 702 amplifier) is used to stop the sweep circuit. The 10 kHz signal input will only stop the sweep momentarily as the signal approaches. If the VXO frequency is such that the pilot tone is on the proper side of the received signal

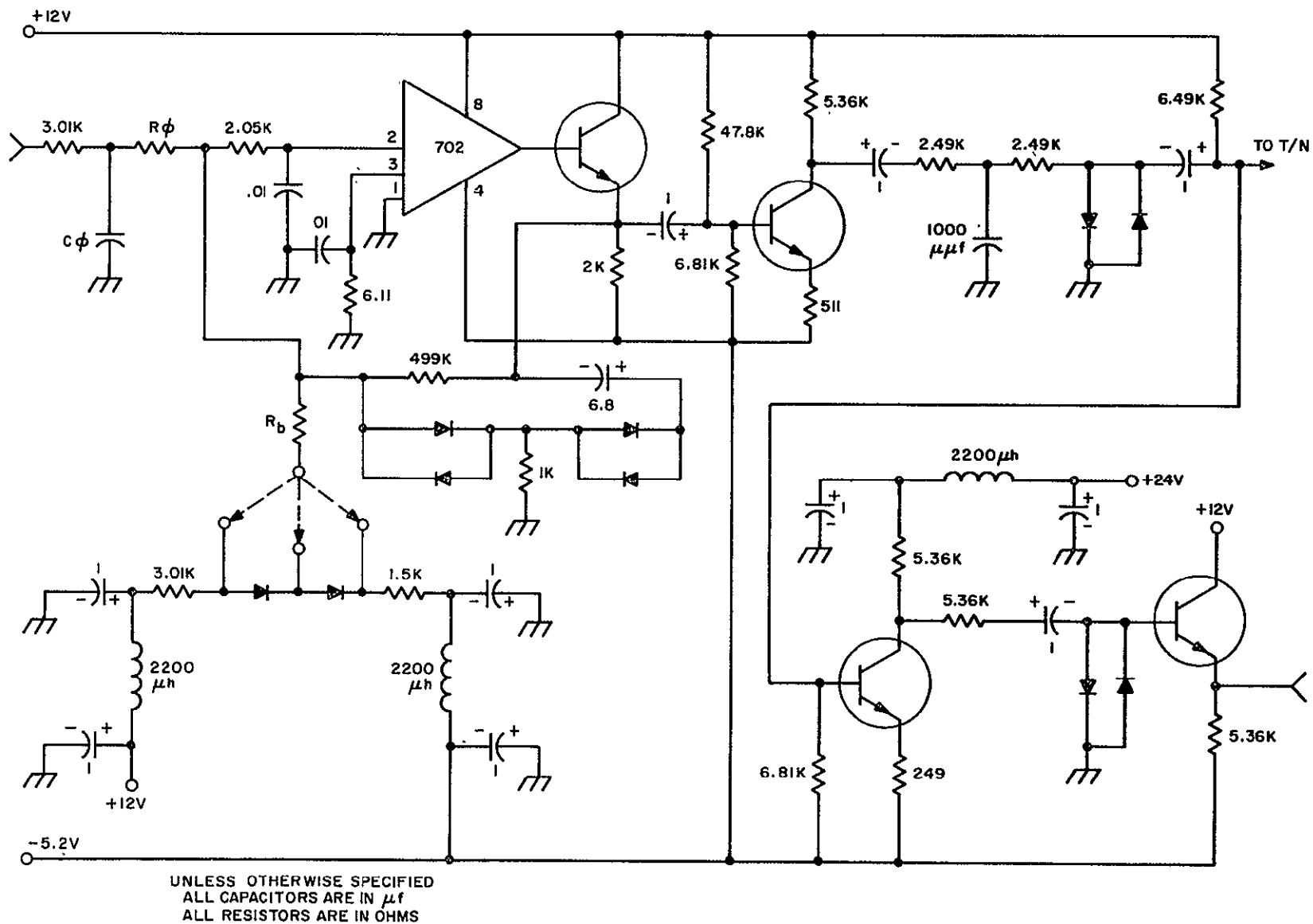


Figure 7-7. Limiters Schematic

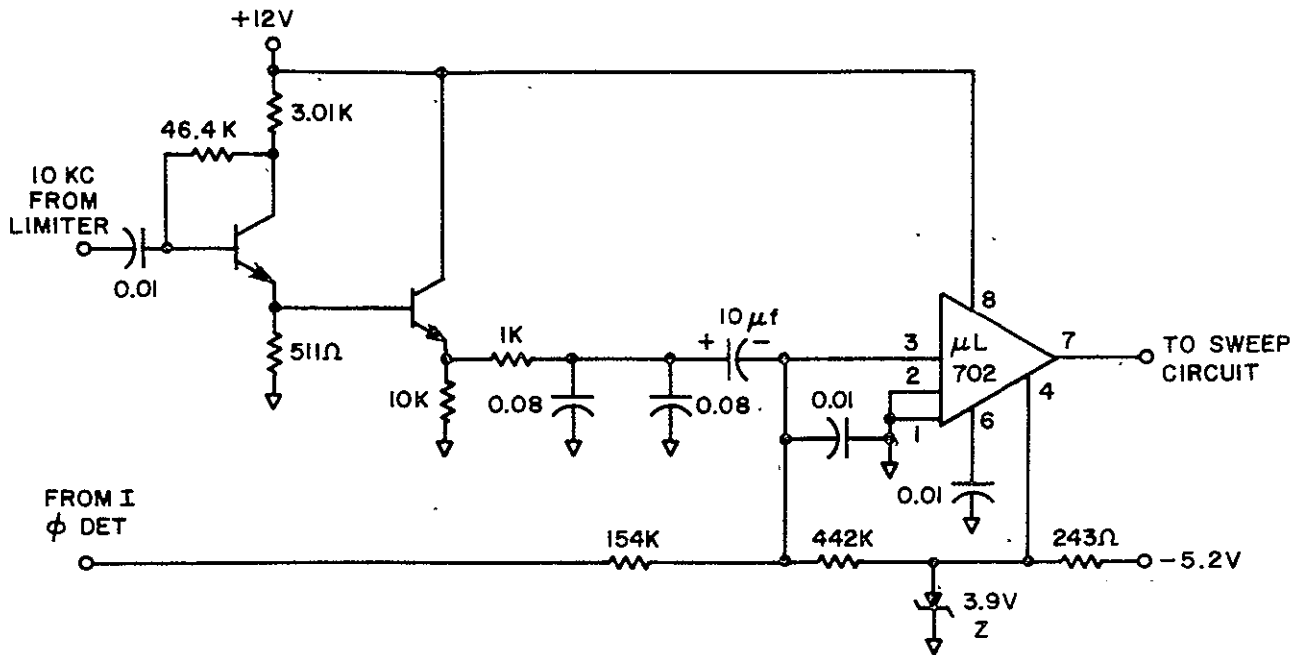


Figure 7-8. Acquisition Control

the input from the "I" phase detector rises as lock occurs. This then permanently triggers the Schmitt trigger to keep the sweep stopped.

### 7.2.7 SWEEP CIRCUIT

To meet the specification for acquisition time for the attitude sensor, a sawtooth type of sweep circuit was designed. This waveform will "waste" the least time in searching at an acquirable rate. A requirement of the sweep is to stop-and-hold when the received signal is in the bandpass of the phase-locked loop. A perfect stop-and-hold is not possible so the sweep rate under the "stopped" condition must be low enough to allow the phase locked loop to respond and acquire the signal. Due to the maximum acquirable rate of the loop, the search rate must be in the order of one search every two seconds. A rate as low as this dictates dc coupling as the only practical approach. With the sweep directly coupled to the VXO it was

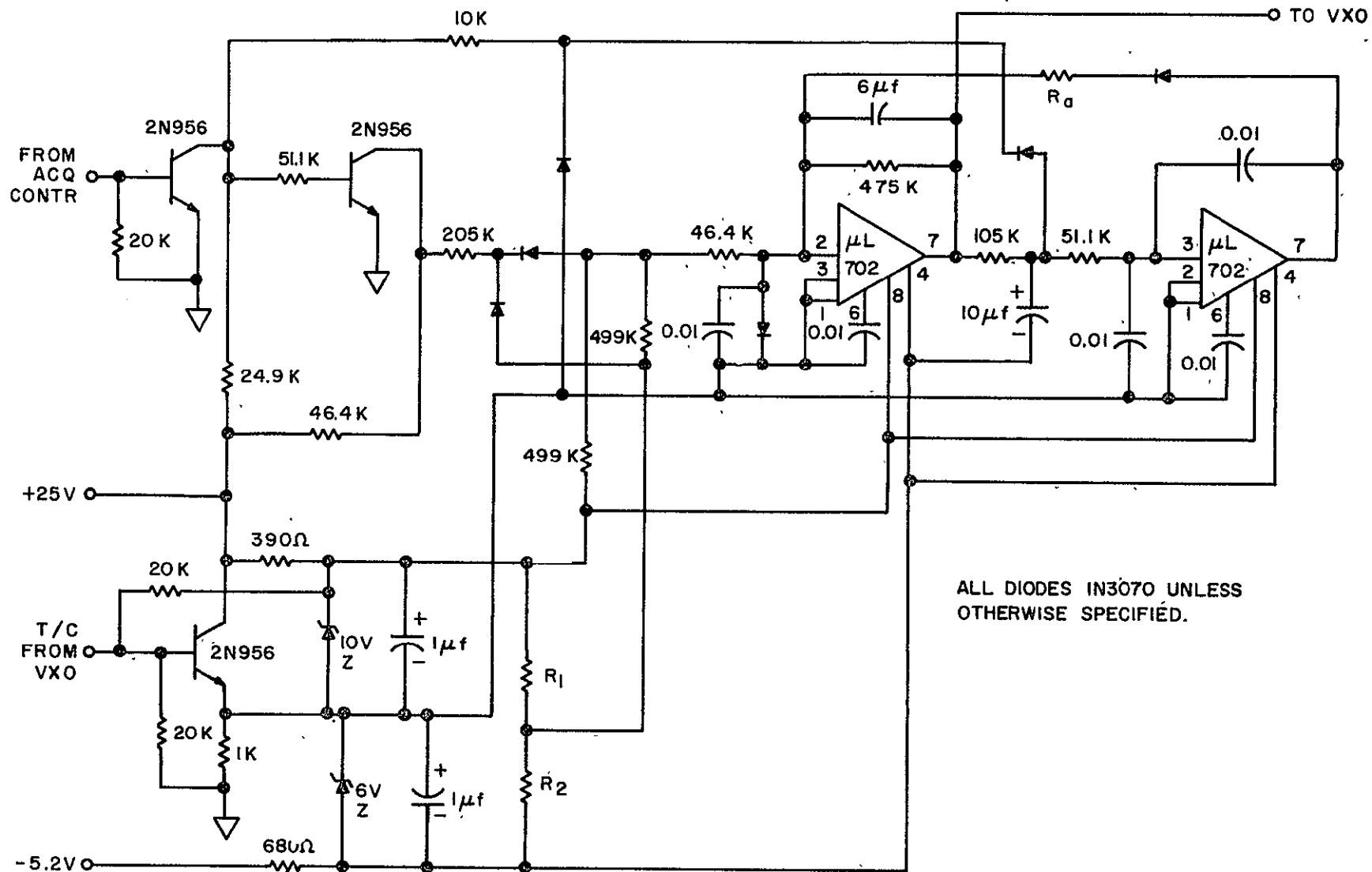


Figure 7-9. Sweep Circuit

decided to have the sweep circuit provide the bias for the varicap in the oscillator circuit. In addition, provision was made for a temperature compensation (T/C) network in the VXO to be coupled to the sweep, to control the varicap bias level. Temperature compensation of the entire circuitry involved in frequency control is therefore accomplished through a bias voltage. The circuit for this bias control can be seen at the lower left of the sweep circuit schematic Figure 7-9.

The acquisition control circuit gives out a positive level whenever the received signal is in the bandpass of the phase locked loop. This signal is applied to two cascaded inverter circuits to provide the proper control levels to "stop" the sweep circuit, control the rate after "stop" and prevent flyback under lock conditions.

The sweep voltage proper is generated by an integrating amplifier utilizing a  $\mu L$  702 micrologic operational amplifier. A second  $\mu L$  702 is used as a Schmitt trigger to sense when the sweep has reached a preset value and generate a flyback pulse. This pulse is coupled through a diode and  $R_a$  to reset the integrating capacitor ( $6\ \mu f$  non polar). Selecting the value of  $R_a$  controls the amplitude of the sweep by determining reset or flyback excursion. The diode between pins one and two on the integrating  $\mu L$  702 prevents overdrive and "hang-up" from the reset pulse. Adjustment of the values of  $R_1$  and  $R_2$  controls the sweep rate of the circuit. The circuit will operate over a range of rates from 0.07 to 10 cps. The amplitude can be adjusted from four to eight volts peak-to-peak. Operation is satisfactory over a temperature range of  $-35^\circ C$  to  $+85^\circ C$ .

### 7.2.8 FREQUENCY MULTIPLIER

The frequency multiplier is required to provide sufficient power at eight and 12 times the oscillator's frequency to drive the harmonic generator and varactor chain, with a minimum of side band interaction.

Table 7-2 shows the specification to which the multiplier was designed.

Table 7-2. Frequency Multiplier Specification

$f_0$	18.94 MHz
Input level	-10 dBm
Output frequencies	$8 f_0$ and $12 f_0$
Output levels	$8 f_0$ at $+13 \pm 1-1/2$ dBm $12 f_0$ at $+16 \pm 1-1/2$ dBm
Side Band Suppression	-70 dB min. below output
Input, Output Impedance	50 ohms
Temperature Range	-35°C to + 85°C
Line Voltage Variation	$V_c \pm 3\%$

Other conditions imposed on the design of the frequency multiplier were: 1) the use of approved types of components, 2) component derating to 25% of maximum rating value, and 3) designing the circuit such that it could be split into modules whose length would not exceed 5 inches.

Figure 7-10 is a block diagram of the multiplier showing each block as a module and the function of each block.

Figure 7-11 is a schematic of the X2 module. It consists of a transistor doubler followed by a double tuned bandpass filter and finally a 37.88 MHz amplifier. The output of the X2 circuit is split and fed to the X4 and X6 modules.

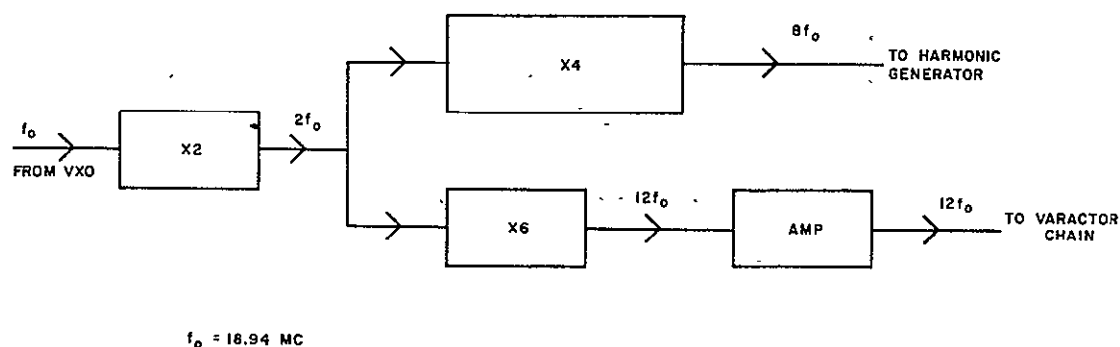
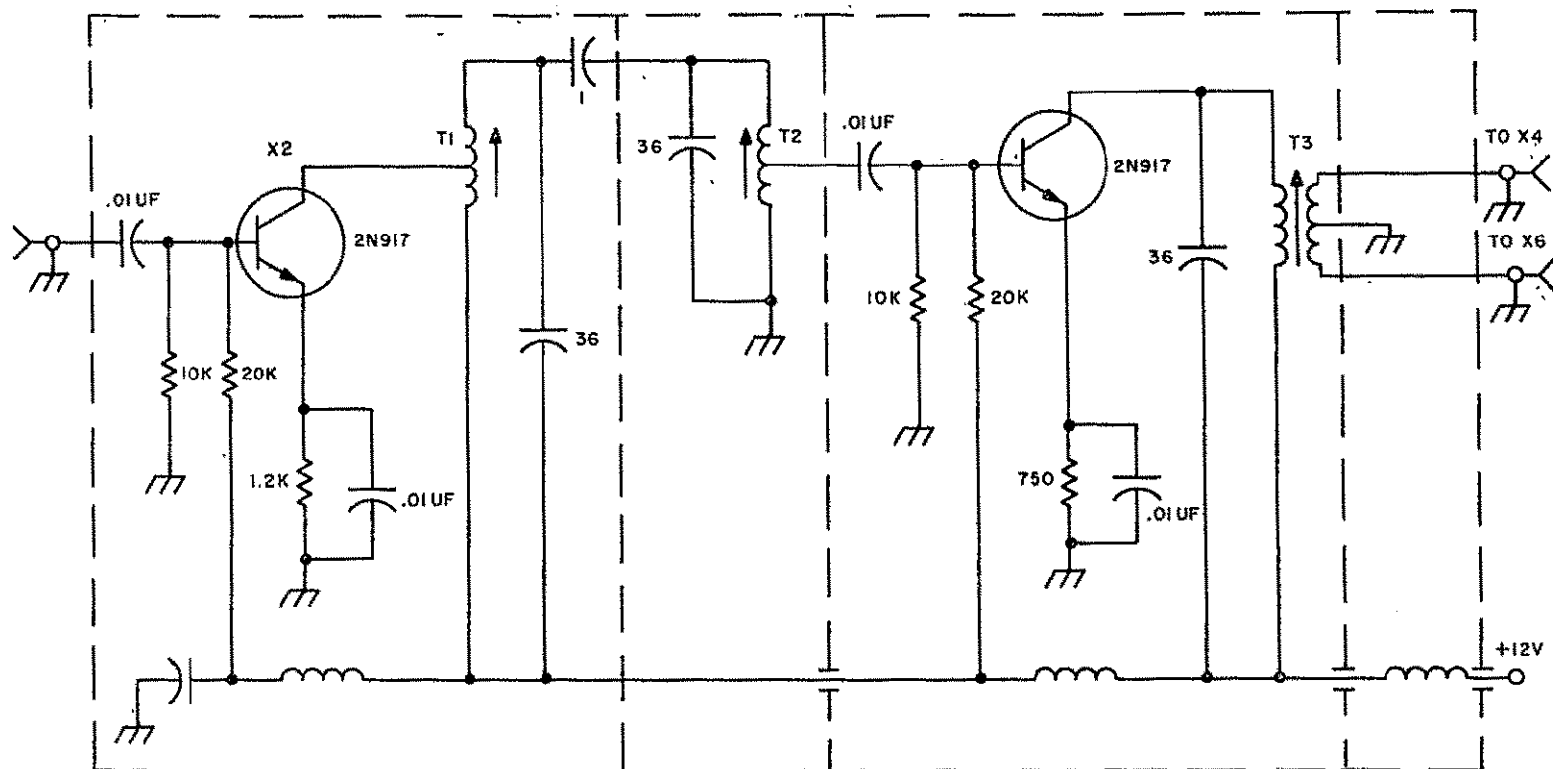


Figure 7-10. Multiplier Block Diagram



UNLESS OTHERWISE SPECIFIED  
ALL CAPACITORS ARE IN UUF  
ALL RESISTORS ARE IN OHMS

T1 & T2 - 8 TURNS TAPPED AT 2 TURNS  
NO. 32 WIRE, CORE 0.16 INCH O.D.  
T3 - PRIMARY 7 TURNS NO. 32 WIRE  
SECONDARY 1 TURN NO. 32 BIFILAR WIRE  
CORE 0.16 INCH O.D.

Figure 7-11. X2 Circuit Schematic



Table 7-3 lists the measured parameters of the X2 module.

Table 7.3 Specification of X2 Module

Gain	16 dB
Bandwidth	1.12 MHz
Side Band Suppression $f_o$	84 dB below output
$3f_o$	84 dB below output
$4f_o$	24 dB below output

The X4 schematic is shown in Figure 7-12. In this circuit the first stage is a quadrupler and the following stages are used to provide filtering and amplification. L-type coupling is used at the higher frequencies in preference to transformer coupling due to better control in matching and higher Q's in the L-type. Due to the limitation that no variable capacitors were available, matching is limited by the range of inductance tuning, which is limited due to the number of turns used. To obtain the required sideband suppression, a sacrifice was made in gain.

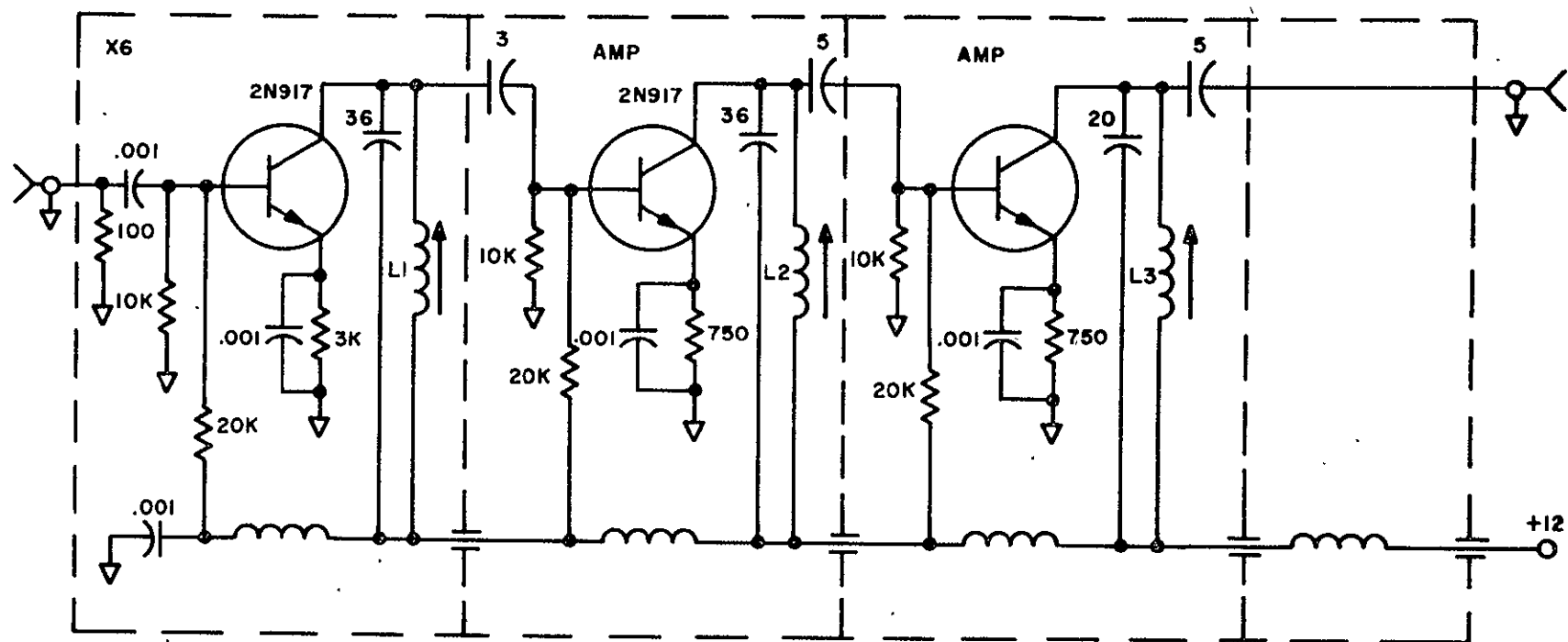
Table 7-4 lists the measured parameters of the X4 circuit.

Table 7.4 X4 Circuit Specification

Gain	13 dB
Bandwidth	3.2 MHz
Sideband Suppression	All sideband 80 dB or more below output

Figure 7-13 shows the schematic of the X6 circuit. The multiplying is done in the first stage with the remaining stages providing gain and filtering. In Figure 7-14 the circuit of the 227.28 MHz amplifier is shown. It was necessary to match the input of the amplifier to the 500-ohm coaxial cable used, since the mismatch produced too much loss of gain. Variable capacitors would have been particularly helpful in this circuit to obtain better matching conditions at the output.





ALL CAPS EXPRESSED IN WHOLE NO. ARE IN PF  
ALL OTHERS IN  $\mu F$

L1, L2 2T NO. 14 WIRE CORE 0.21" O.D.  
L3 1T NO. 14 WIRE CORE 0.21" O.D.

Figure 7-13. X6 Circuit Schematic

Difficulty is anticipated when the transition from breadboard to final package of the X6 and X6 amplifier circuit is made, since at 227 MHz lead lengths and grounding can become significant problem areas. Trouble was encountered in the breadboard in both these areas.

Table 7-5 shows the measured parameters of the breadboard X6 and X6 amplifier.

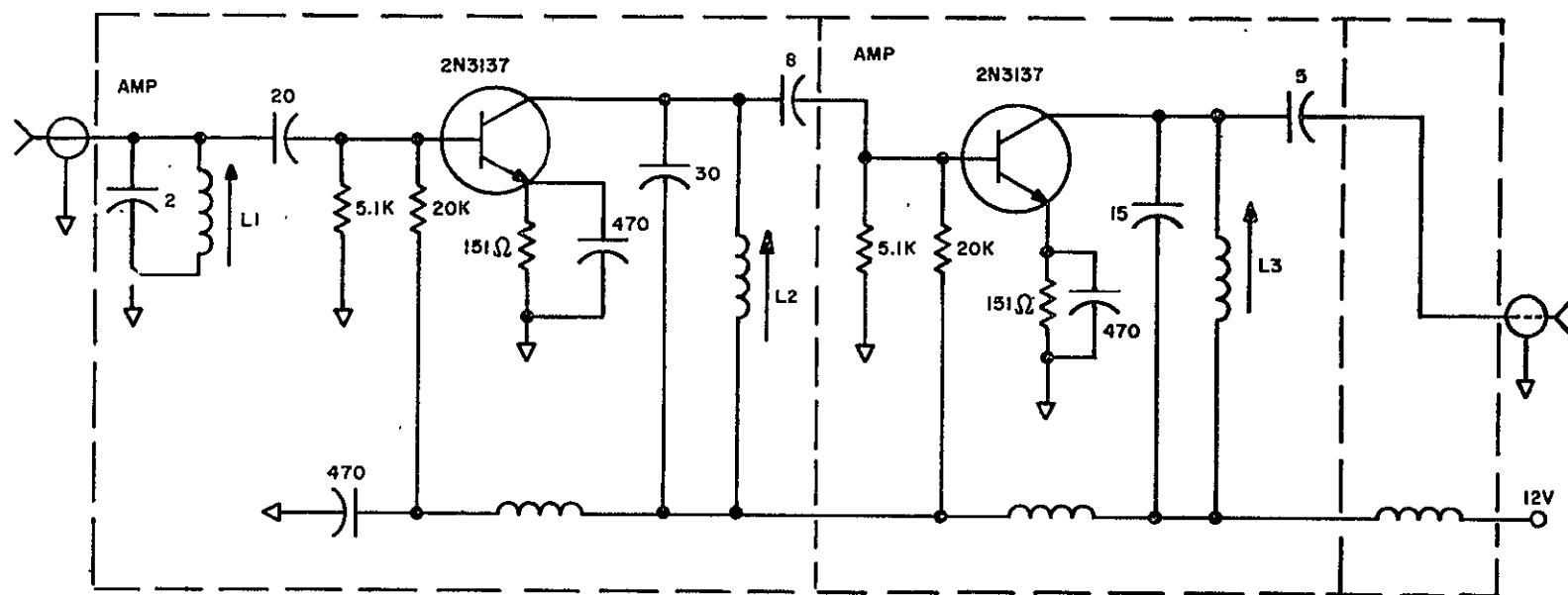
Table 7.5 X6 and X6 Amplifier Specifications

Item	Range
Gain	13 dB
Bandwidth	7.8 MHz
Sideband Suppression	All sidebands down 75 dB below output

With all modules interconnected with coaxial cable not exceeding 4 inches and all outputs measured into 50 ohms, the parameters of interest of the complete multiplier were measured and the results are shown in Table 7-6.

Table 7.6 Multiplier Specification

Item	Range
Input (at 18.94	-10 dBm
Output	
at 151.52 MHz	22 mw (+13.4 dBm)
at 227.28 MHz	42 mw (+16.2 dBm)
Bandwidth	
at 151.52 MHz	3.2 MHz
at 227.28 MHz	7.8 MHz
DC Dissipation	624 mw
Sideband Rejection	
at 151.52 MHz output	All sidebands are 77 dB or more below output
at 227.28 MHz output	All sidebands are 72 dB or more below output



ALL CAPS IN Pf  
 L1  $1\frac{1}{2}$  T NO. 14 WIRE CORE 0.21 IN. OD  
 L2  $\frac{1}{2}$  T NO. 14 WIRE CORE 0.21 IN. OD  
 L3 1 T NO. 14 WIRE CORE 0.21 IN. OD

Figure 7-14. 227.9 Mc Amplifier Circuit Schematic

A comparison of Table 7-2 with Table 7-6 shows that with the exception of line variation and temperature the multiplier meets the initial requirements.

With a constant input of -10 dbm at 18.94 MHz the output power variation for  $\pm 3\%$  line variation was from 22 to 27.5 mw for the X8 output and from 37 to 44 mw for the X12 output, which is within the specification. If the input is also allowed to vary  $\pm 3$  db along with the line voltage then the extremes in output power variation becomes 20 to 29 mw for the X8 output, while the X12 output remained unchanged at 37 to 44 mw.

Over the temperature range of 25°C to 85°C the output power of the X8 output decreased over 3 db, from 24 mw to 10.5 mw, while with line voltage variation the X8 output drops further to 8.5 mw at 85°C. The X12 output power remained a constant 40 mw to 85°C and decreased 5 mw with the line voltage variation.

The main reason for the X8 output dropping with temperature is that the X8 portion of the multiplier is operated as a linear device for minimum noise output, and no temperature compensation is included. In the X12 circuitry a portion is operated in saturation thus providing some temperature compensation. No further work was done on improving the temperature responses of the multiplier since the program was halted.

To finish the design of the frequency multiplier there are two major areas which require further work. One is to temperature compensate the X8 circuitry while still maintaining a low noise output. The other area is in going from breadboard to final package configuration of the X6 and X6 amplifier.

#### 7.2.9 2.56 MHZ OSCILLATOR

The 2.56 MHz signal for the 10 kHz reference divider is generated by a crystal oscillator as shown in Figure 7-15. The series resonant mode for the crystal is used in the feedback loop of the oscillator to assure crystal-controlled



7-23

oscillation. The output of the oscillator is capacitively coupled to a video buffer which amplifies the signal and shapes it into a series of pulses for use in the eight bit divider.

#### 7.2.10 DIGITAL PROCESSING

The following describes pertinent characteristics and design considerations of the digital circuitry contained in RF Attitude Sensor. About 75% of the circuits discussed in this report were breadboarded and tested at room temperature; therefore, the details contained in the enclosed schematic diagrams can be considered quite firm. While size restrictions dictated the use of integrated circuits to perform all logic functions, due to input power limitations, conventional circuits had to be used in some cases.

The digital portion in this unit can be divided in two major sub-groups:

1. The pitch/roll counter and associated storage
2. The divider (by 256) and phase detector

The pitch/roll counter subassembly, the block diagram of which is shown in Figure 7-16, is by far the larger of the two and it consists of:

1. One 8-bit counter time-shared by the roll and pitch channels
2. Sixteen buffer storage stages, eight for each channel
3. Miscellaneous switching and steering circuits

In order to keep the power consumption to a bare minimum, the dc voltage necessary to energize this subassembly, except the storage stages, is turned on for two milliseconds out of every three seconds by a pulse generated by the leading edge of the "READ" command. These two milliseconds are used as shown in Figure 7-17.



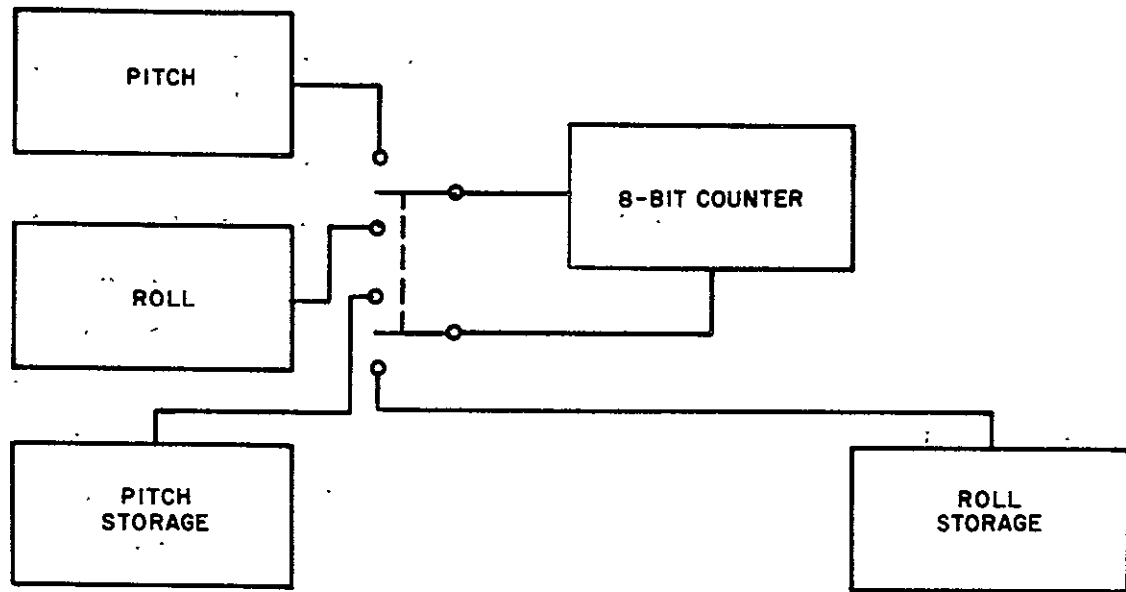


Figure 7-16. Digital Data Collection

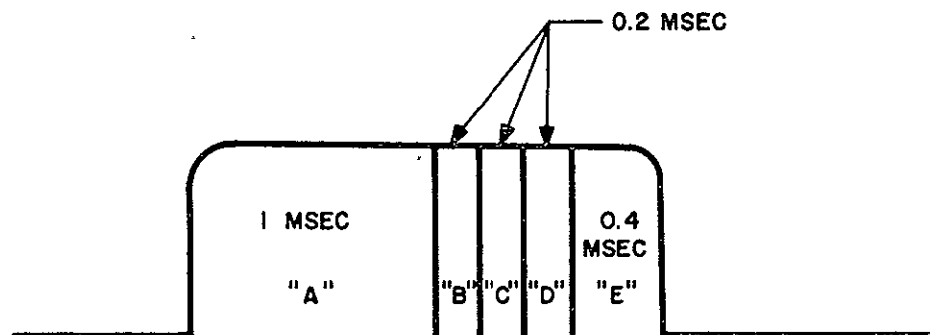


Figure 7-17. Data Timing Diagram

Where:

- "A" and "E" - Time allowed for the rise and fall respectively of the power supply
- "B" - Time utilized to count and store the quantized phase of the pitch channel

- "C" - ~~Inoperative~~ time between pitch and roll counts
- "D" - Time utilized to count and store the quantized phase of the roll channel.

Figures 7-18 and 7-19 show the complete logic diagrams for the data collection circuits of the attitude sensor. During time "B" the pitch and the central signals are allowed to set and reset respectively, the flip-flop A-5, thus opening the gate A-6 and letting through a burst of 2.56 MHz pulses for a period equal to the time difference between the two signals. This burst of pulses is counted and then stored in binary form in the "pitch" buffer storage stages. Flip-flop A-11 ensures that one and only one burst of pulses is allowed through, while the one shot A-14 allows for the counter's trickle time before generating the "STORE PITCH" pulse. A reset pulse of very small duration ( $.25 \mu\text{sec}$  or less) is generated at the beginning of time "B" and "D" to empty out the counter just prior to the arrival of the burst of pulses to be counted.

Nothing happens during time "C", and at time "D" the Roll information goes through the same sequence as the pitch information did at time "B". The information stored in both the pitch and roll registers is available for almost three full seconds before being erased by the clear pulse which occurs when the next "READ" command is received.

#### 7.2.11 256 DIVIDER AND PHASE DETECTOR

This subassembly (Figure 7-20) consists of an eight stage straight divider and a quadrature phase detector using half adders.

The 2.56 MHz signal is divided by 256 and then it is compared with the signal coming from the central channel. The 90 degrees phase shift is obtained by paralleling the eighth stage of the divider with an additional flip-flop which is triggered by the "FUNCTION" output of the seventh stage rather than the "FUNCTION."

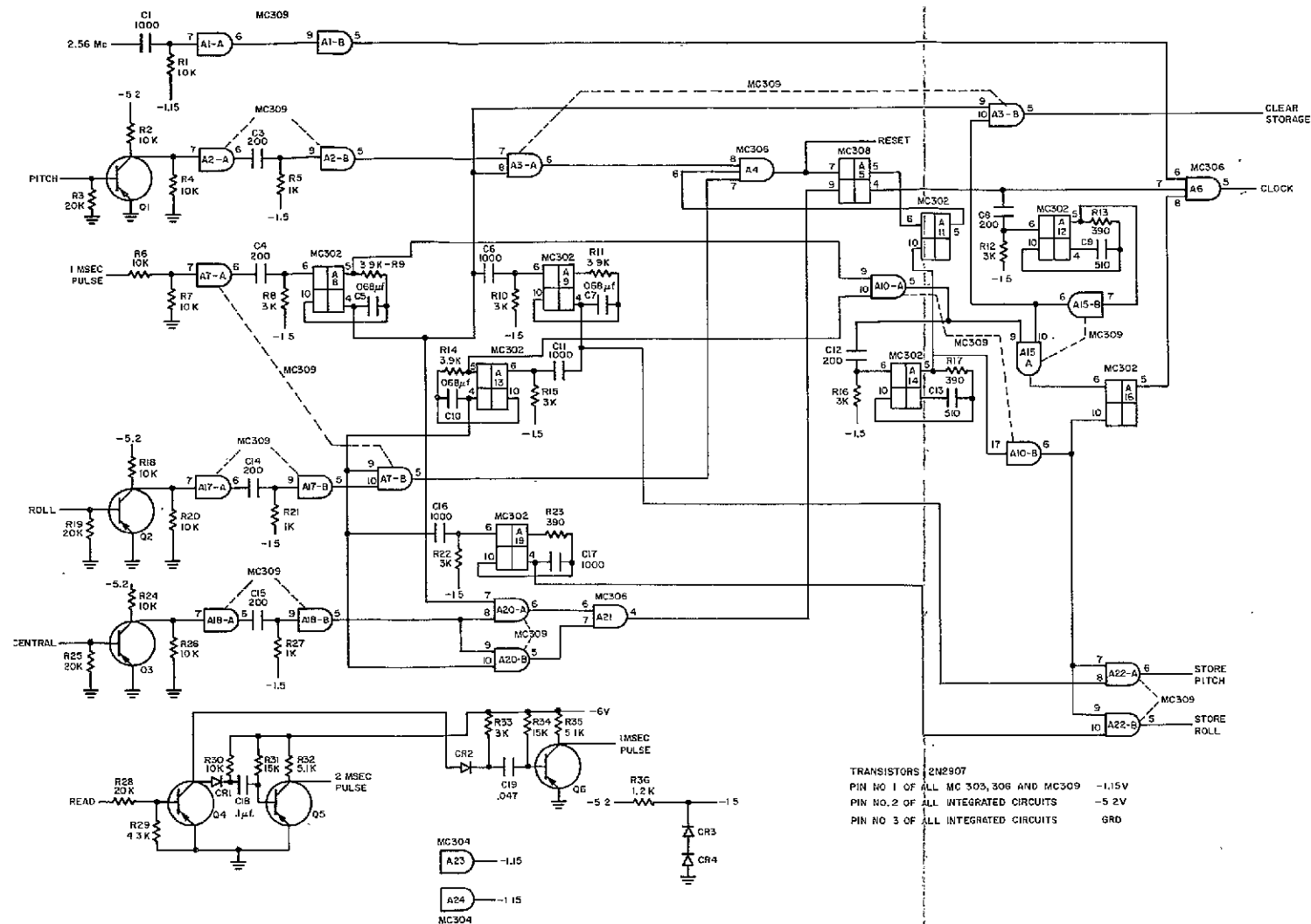


Figure 7-18. 8 Bit Counter Schematic

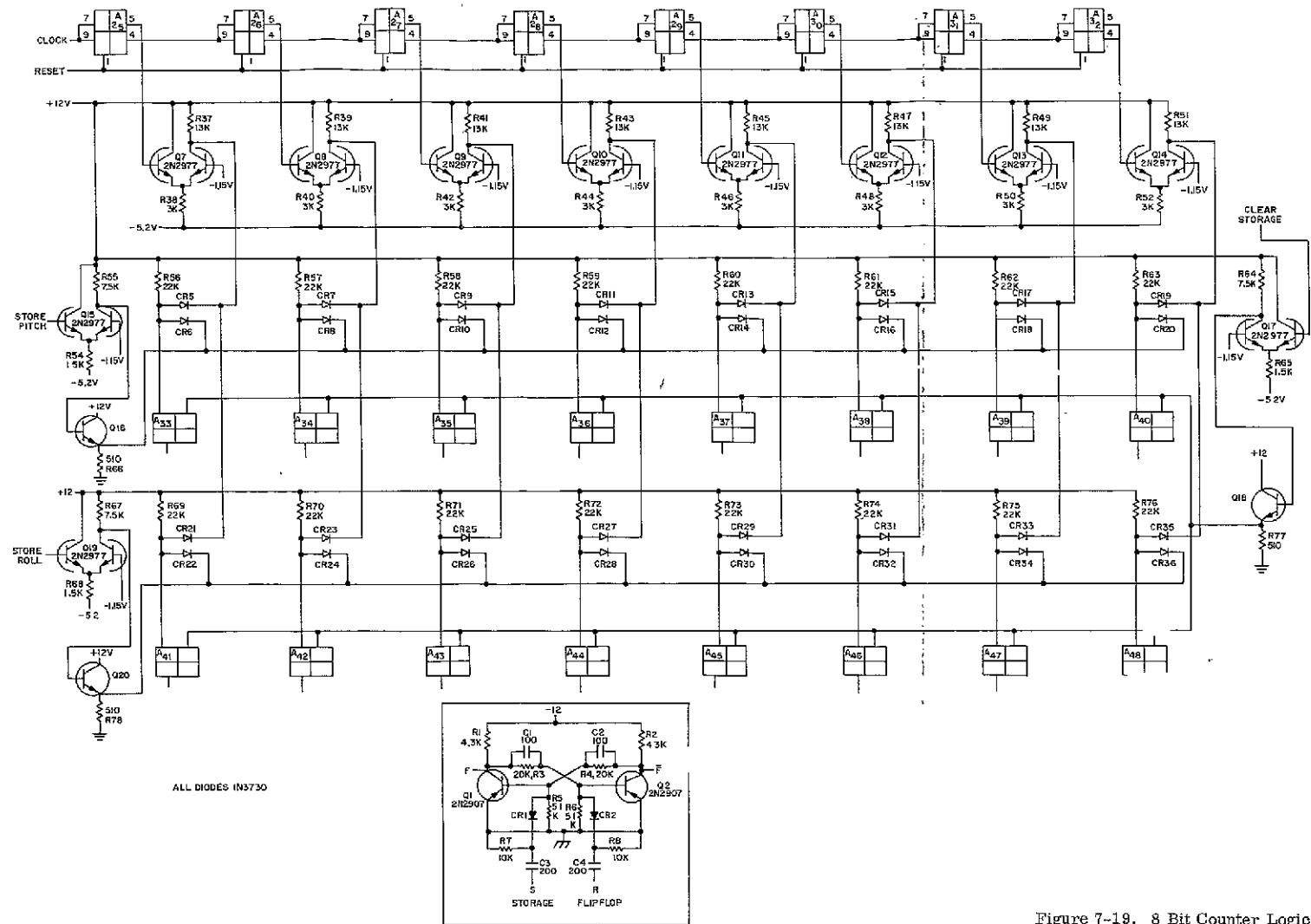


Figure 7-19. 8 Bit Counter Logic

Differential amplifier level translators are used in all cases for the transition from integrated to conventional circuitry in order to minimize temperature effects.

#### 7.2.12 VIDEO TELEMETRY CIRCUIT

The purpose of the video telemetry circuit was two fold. It was desired to have a summer circuit which would have three discrete output levels as a function of three discrete inputs, and it was necessary to convert these to outputs having a separate ground from the Attitude Sensor circuits.

The pitch, roll, and central signals are fed to emitter followers of the 3-channel summer (See Figure 7-21)  $Q_1$ ,  $Q_3$ , and  $Q_5$ . The signals are then coupled to amplifiers  $Q_2$ ,  $Q_4$ , and  $Q_6$ . The signals are half wave rectified and summed across the 2.05K resistor. The summer output is fed to  $D_1$  of the chopper amplifier. The input, feeding the base of  $Q_1$  of the chopper amplifier, (see Figure 7-22) is a square wave proportional to the summer output signal. The output of  $Q_1$  is then fed to the  $Q_2$ ,  $Q_2$  combination which is a Darlington circuit phase-splitter.

The square wave outputs on the emitter and collector of  $Q_3$  are coupled to the full wave bridge network. The full wave bridge converts its inputs to dc voltages and the output is applied to the 2  $\mu$ f 10K filter combination which is terminated to the second ground plane.

The output levels of the video telemetry circuit remained distinct as a function of the temperature as indicated in Table 7-7. As the temperature was varied between the extremes ( $-35^{\circ}\text{C}$  to  $+85^{\circ}\text{C}$ ) the output voltage varied linearly.

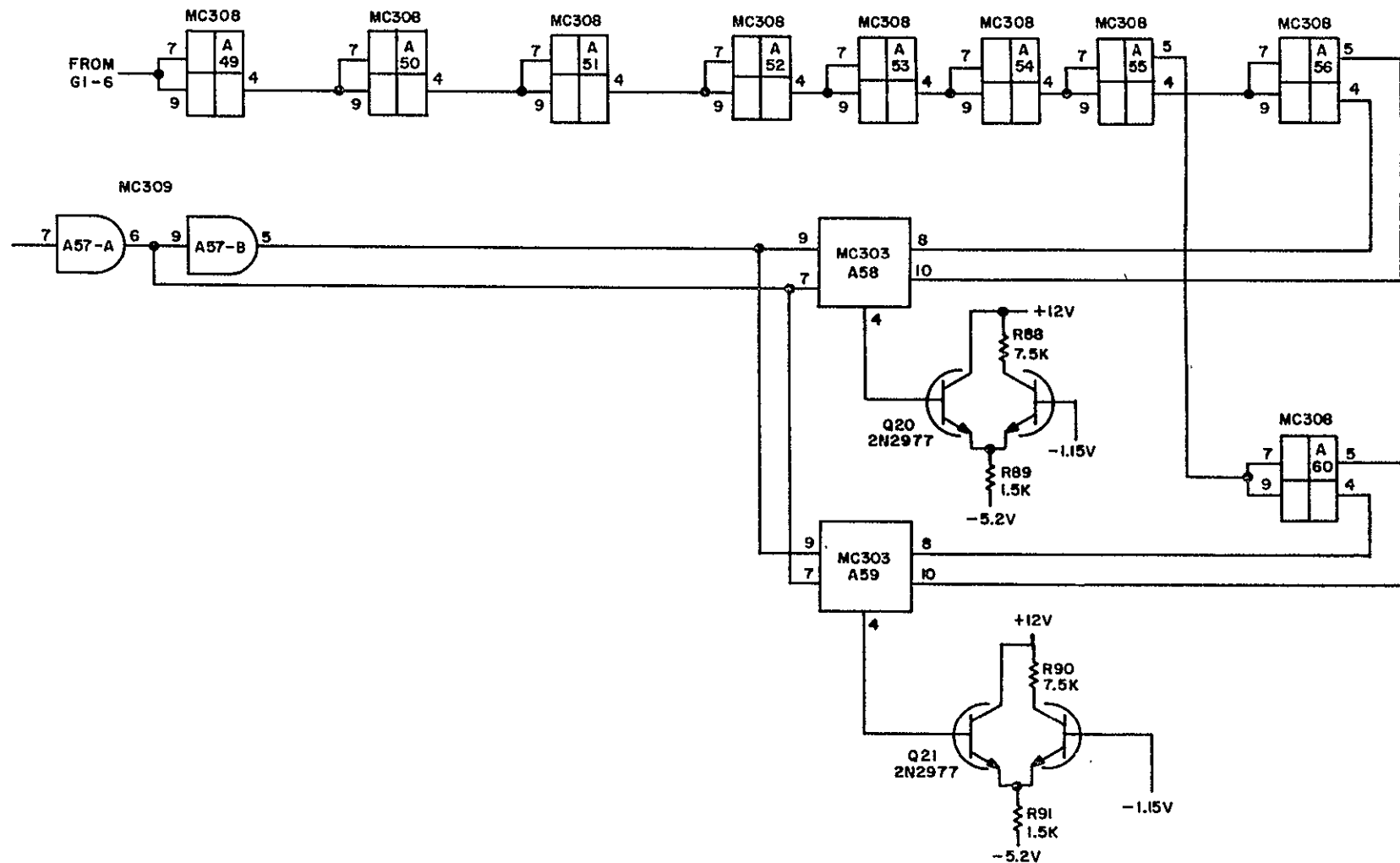


Figure 7-20. 256 Divider and Phase Detectors

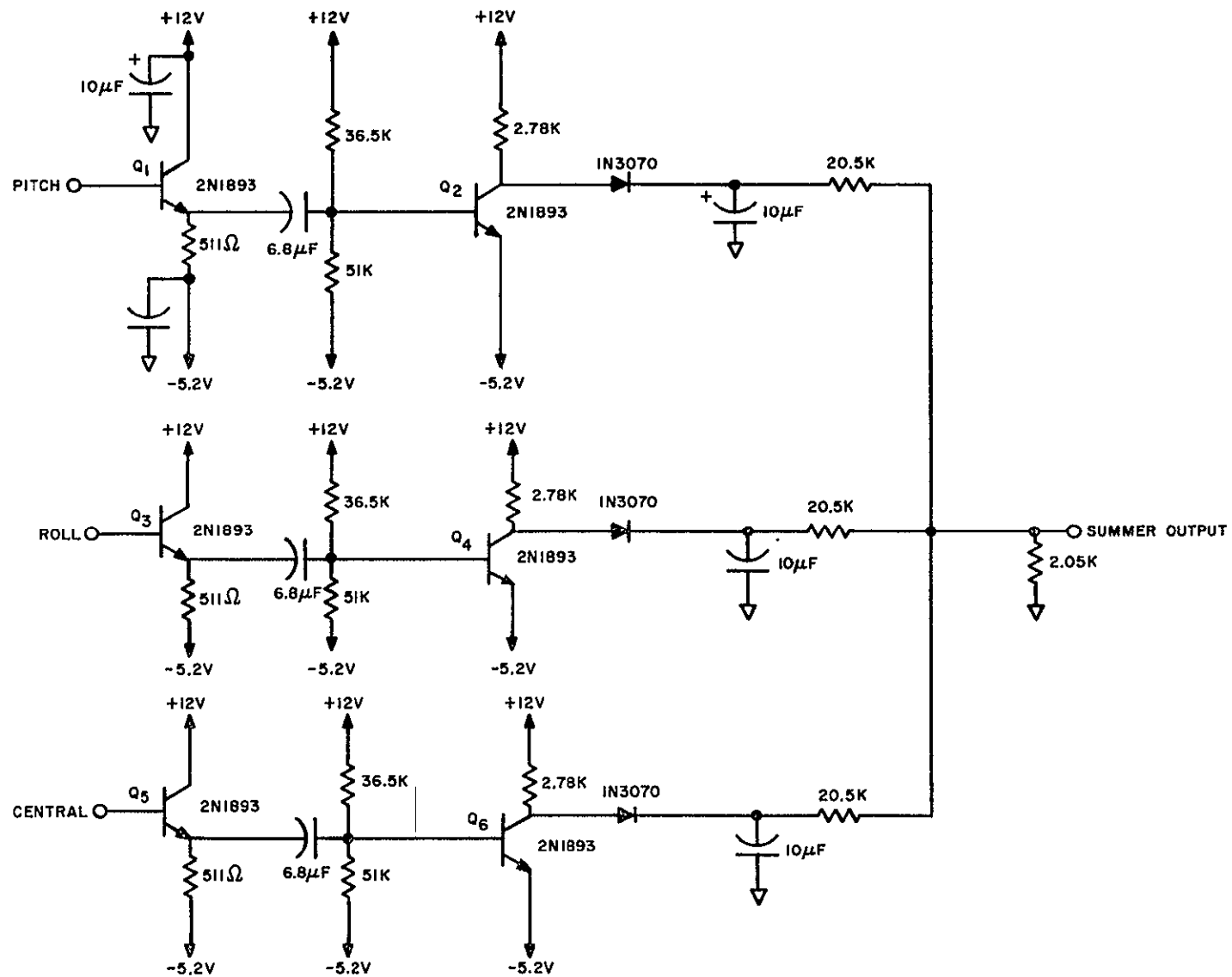


Figure 7-21. 3-Channel Summer

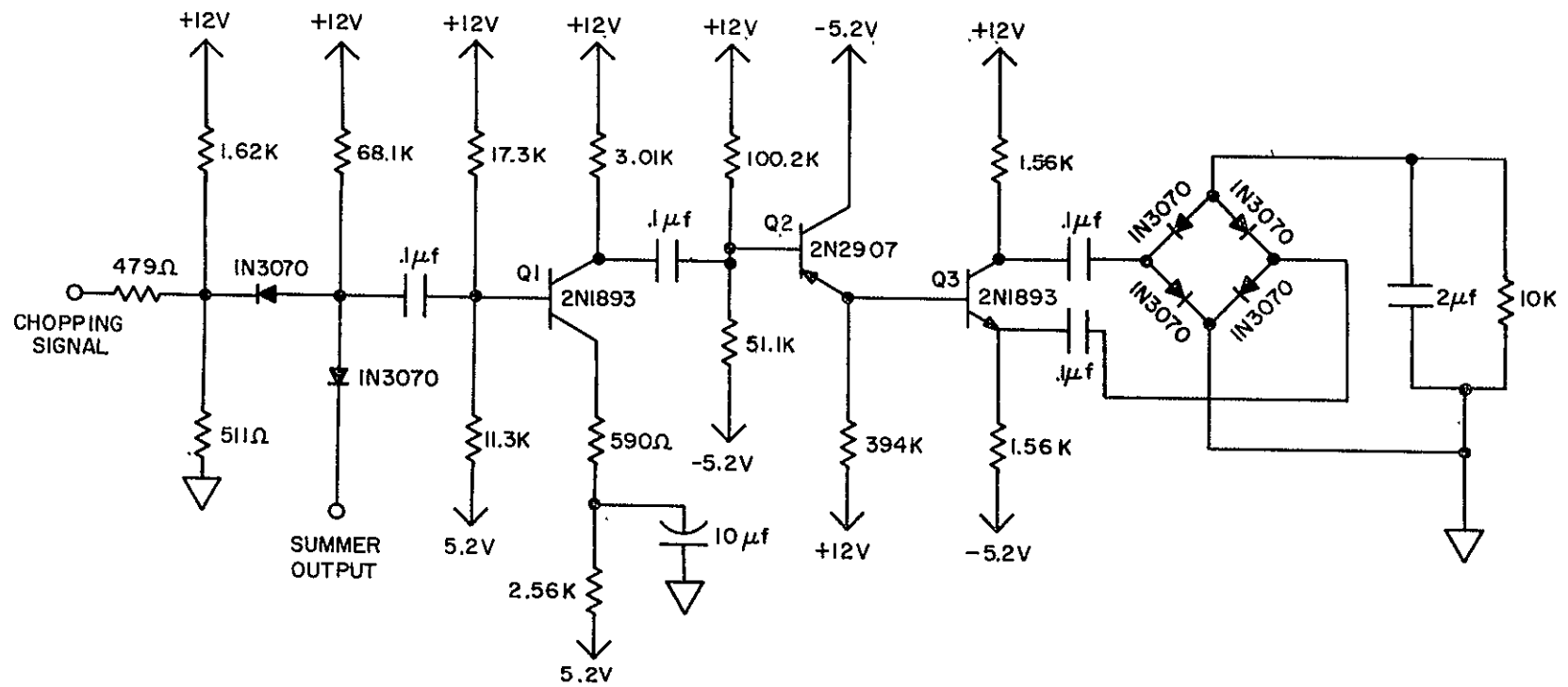


Figure 7-22. Chopper Amplifier



Table 7-7. Output Voltage vs Number of Channels ON as a Function of Temperature

Channels On.	Temperature		
	-35°C	25°C	+85°C
1	-0.75V	-0.9V	-1.3V
1&2	-2.9V	-3.2V	-3.8V
1&2&3	-4.5V	-4.8V	-5.1V

### 7.2.13 POWER SUPPLY.

The requirements for low power consumption and very efficient voltage conversion are recognized as a strong requirement for satellites. Just as important are the requirements for small size and weight. With these in mind it was decided that a square wave dc-to-dc converter was the most acceptable. An attempt was made to do without a regulator, since the spacecraft power source nominal voltage is reasonably constant except for occasional voltage transients. These transients are to be filtered with input and output filters to within tolerable limits.

It was estimated that the following voltage and power levels would be required:

<u>Voltage</u>	<u>Current</u> <u>(milliamperes)</u>	<u>Power</u> <u>(watts)</u>
+25.0	20	.500
+12.0	150	1.800
-5.2	1,170	6.100
-12.0	50	300

In order to obtain a small and efficient power supply it was necessary to employ a conversion frequency in the neighborhood of 20 kHz. This frequency allows the use of small filters as well as the use of Permalloy tape-wound cores for the transformer instead of Orthonol which is normally used at lower frequencies. In addition, Permalloy power loss is an order of magnitude less than the Orthonol material.

The design is a basic square wave converter which employs a saturating, current limited drive transformer to provide base drive for power transistors which switch a nonsaturating power transformer. The drive transformer is a tape wound bobbin core which is current limited by a resistor when the core goes into saturation. The power transistor has a very low saturation resistance, high current gain, high voltage breakdown, and a reasonably fast switching speed. The wire size for the power transformer was chosen as large as possible to minimize the IR drops. Since no regulating scheme was anticipated, it was extremely important to minimize voltage drops in the transistor switches, transformer and lead wire. Thus, with temperature and load fluctuations the output voltage change can be minimized. The greatest anticipated effect on output voltage is due to the output rectifiers which have a temperature coefficient of about 1.8 millivolts per degree and thus a maximum change over temperature environment of about 216 millivolts. This effect can partially be compensated by the change due to the copper conductor IR drop.

A scheme for reduction of power consumption in the logic circuitry has been devised. This scheme switches power to the logic circuitry for two milliseconds and then the logic circuit is turned off for three seconds. Thus, the instantaneous logic power of about 5 watts, averages out to about 10 to 20 milliwatts. However, the switching transistors, diodes, etc., must still be capable of the peak current demand. Switching the logic load was tried on the breadboarded power supply. This produced transients of several tenths of volts on the other output voltages as was expected. Additionally, this limits the input source impedance to a very low value. This then limits the amount of input filtering which can take place.

Since the duty cycle of this load is very low, the final design would incorporate a separate converter for the logic circuitry. This will eliminate the transient problems, and if necessary a voltage regulator can be used because of the low duty cycle involved. Time did not permit the design of this circuitry.

A schematic of the power supply which supplies all but the logic circuitry is shown in Figure 7-23. The efficiency obtained for a power input of 5.0 watts was 78%. Thus, the power loss was about 1.1 watts. Approximately 400 mw is attributed to rectification. The transformer magnetizing current of 20 ma accounts for another 560 mw. The remaining 160 mw is attributed to transistor, copper, drive, and stray losses.

The input filter will be a combination RLC filter. This will account for an additional 3 to 5 percent loss in efficiency. The power supply for the logic circuitry can be as inefficient as 50 percent and still not affect the overall efficiency because of the low duty cycle. Thus, an overall efficiency of 72 percent is expected, requiring about 5.25 watts of input power.

### 7.3 MECHANICAL DESIGN

Specifications for the RF Attitude Sensor package included dimensions of 6 by 6 by 6 inches and a design-goal weight of 8 pounds. The mechanical design approach to accomplish the packaging of the equipment shown in Figure 7-24 is described in detail in the sections that follow. Basically, all items utilized in the package are necessary to the design, and where possible are required to share functions.

No primary structure is provided. The circuit modules are mounted to equipment plates, and these in turn serve as the structural link between the RF assembly and the package base (or mounting) plate.

The RF assembly, equipment plates, and base plate are tied together with thin rigid covers. The covers are forced to take stress loading and are in reality a strong link in the package structure.

The equipment plates provide mounting for the circuit modules, house the dc and signal inter-module cabling (thus eliminating haywire) provide functional circuit

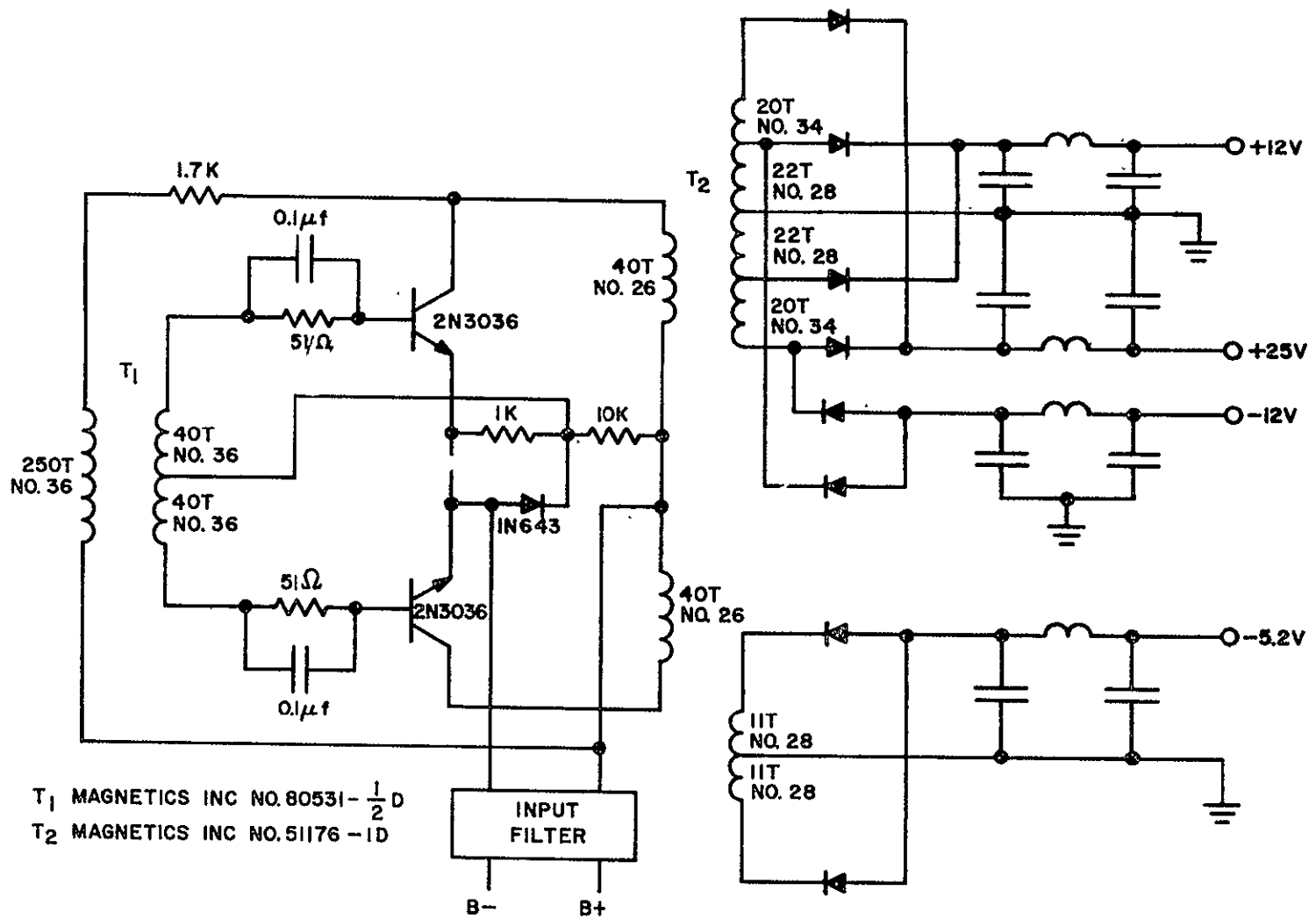


Figure 7-23. Power Supply

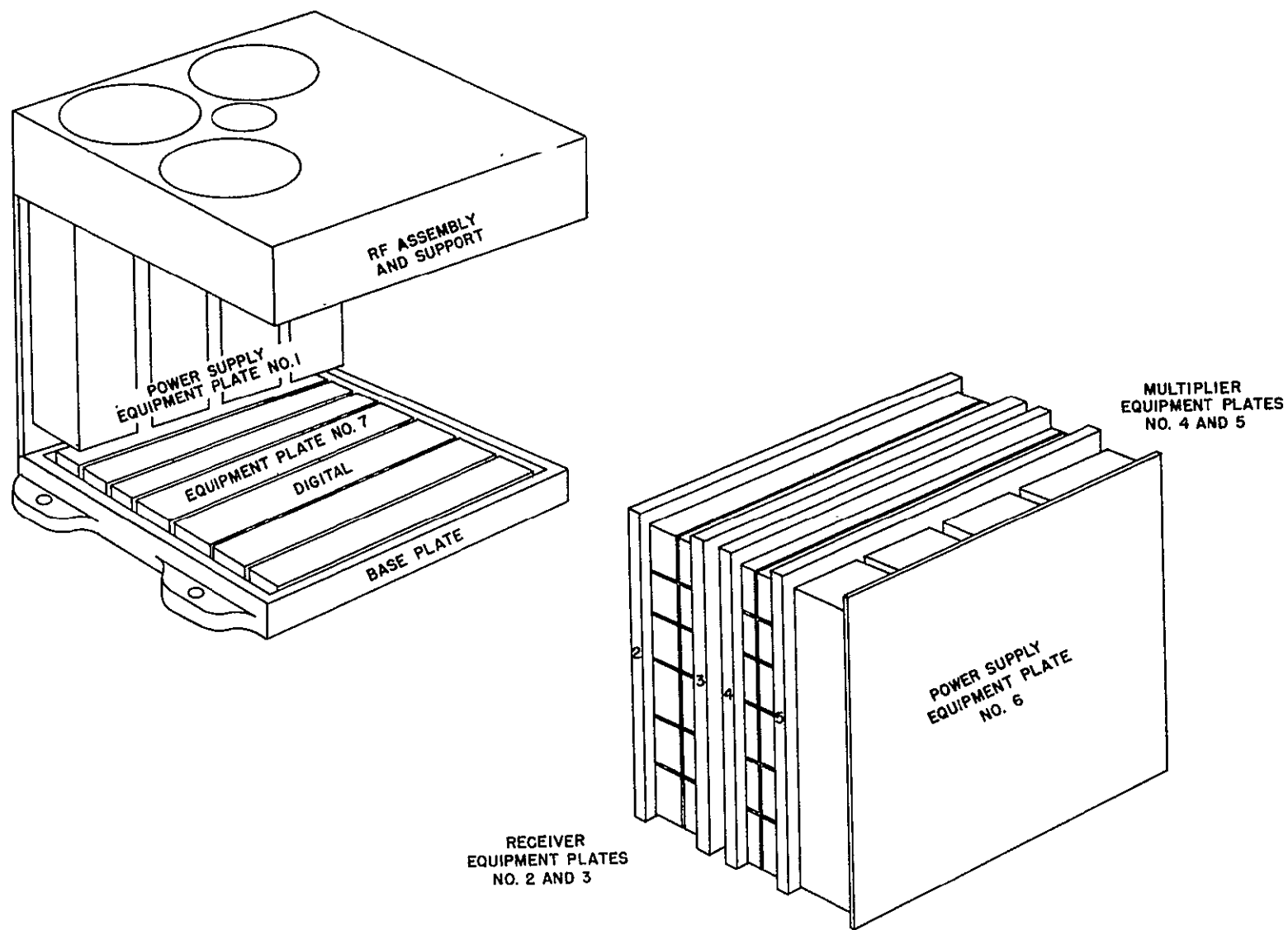


Figure 7-24. RF Attitude Sensor Packaging.

grouping to reduce interconnection, provide structural integrity for both package and modules, and provide heat transfer paths for both modules and other package elements.

The package was divided into the following functional areas:

1. RF assembly
2. RF support
3. Equipment Plates
  - a. No. 1-Power Supply
    - Filters
    - Power Transformer
  - b. No. 2-Receiver
    - Modules for IF loops
  - c. No. 3-Receiver
    - Modules for IF loops
  - d. No. 4-Multiplier
    - Modules for Multiplier Chain
  - e. No. 5-Multiplier
    - Modules for Multiplier Chain
    - Varactor Chain Assembly
  - f. No. 6-Power Supply
    - Filters
    - Power Transformer
  - g. No. 7-Digital
    - Modules for Data Processing and Readout
4. Base Plate
5. Covers

For purposes of this report the work was itemized under the following headings:

1. RF Assembly
2. RF Support
3. Varactor Chain
4. Base Plate
5. Covers
6. Modules
7. Equipment Plates

### 7.3.1 RF ASSEMBLY

The RF assembly was to be purchased as a tested unit with coaxial IF outputs, LO output, varactor chain input, and test points for each antenna.

The unit was designed to bolt directly into the RF support element.

RFI shielding was provided at the interface between the RF unit and package mating parts.

### 7.3.2 RF SUPPORT

The RF support was designed as a welded and machined part. The upper section mated directly with the RF unit, while the lower section mated with the equipment plate subassemblies.

Vibration and thermal loading was distributed by the section design. Two sides of the support accepted removable covers, the other two sides accepted the cover plates for power supply equipment plates (No. 1 and No. 6). All four cover surfaces were grooved to accept rectangular RFI mesh. Stress load was directed through the equipment plate subassemblies (No. 1 through No. 6) to the base plate. Thermal paths from the RF unit were provided by the RF support into the equipment plate subassemblies, and then into the base plate.

### 7.3.3 VARACTOR CHAIN

The varactor chain was to be purchased as a tested unit with coaxial output and input connectors.

The unit was to be mounted to equipment plate No. 5, which also contained the multipliers required to drive the unit.

Equipment plate No. 5 provided a solid heat sink into which the varactor chain unit was mounted. Thermal paths were provided through the equipment plate frame and into the base plate.

#### 7.3.4 BASE PLATE

The base plate was designed as a welded, machined part to accept the equipment plate subassemblies, package covers, and house equipment plate No. 7.

The base plate section contained four package mounting lugs. Grooves for RFI shielding at the cover junctions and equipment plate No. 7 periphery were also provided in the section.

#### 7.3.5 COVERS

Two removable package covers were provided to allow for connection of the IF outputs of the RF assembly to equipment plates No. 2 and No. 3. The covers also facilitated connections from the various equipment plates to the power supply equipment plates and telemetry connectors.

Both power supply equipment plates were designed such that the outer plates of each assembly acted as package covers. Thus, it was possible to remove four covers, making the receiver and multiplier equipment plates more accessible. Equipment plate No. 6 contained the access port for connection of RF coaxial cables for external RF test.

#### 7.3.6 MODULES

Module design for RF Attitude Sensor utilized plug-in functional modules. The system is called MODULAR WELDMENT.

During the initial stages of design effort the modules were defined functionally as follows:



1. IF
2. Detector
3. Filter-Limiter
4. Digital No. 1
5. Digital No. 2
6. Digital No. 3
7. Digital No. 4
8. Digital No. 5
9. Digital No. 6
10. Digital No. 7
11. Digital No. 8
12. Digital No. 9
13. Digital No. 10
14. Digital No. 11
15. Telemetry Amplifier
16. DC amplifier
17. Sweep
18. Power amplifier No. 1
19. Power amplifier No. 2
20. X6 Multiplier No. 1
21. X6 Multiplier No. 2
22. X4 Multiplier
23. X2 Multiplier
24. VCO
25. VXO
26. Input/RFI filter
27. Chopper
28. +24 Filter
29. +12 Filter
30. -12 Filter No. 1
31. -12 Filter No. 2
32. -5.2 Filter

Preliminary layouts for modules Nos. 1, 2, 22, and 23 were essentially completed at the time the RF Attitude Sensor was cancelled. Preliminary layouts for modules Nos. 4 through 14 were in process but involved considerable inter-connection to complete.

Enough general information about module function and complexity was available to allow for preliminary equipment plate assignment.

All module tooling was in place and ready for implementation in the building phase.

#### 7.3.7 EQUIPMENT PLATES

Module assignments are as indicated in the introduction. Equipment plate design is as follows:

1. Provision is made on the top cover plate for mounting dc plugs, passage of coaxial and dc cabling and connectors where applicable.
2. DC wiring is accomplished from an edge-connector to the various dc plugs.
3. Coaxial cables are run to interconnect modules and provide intra-equipment plate connections.
4. An edge frame is provided to space the top and bottom cover plates and rigidize the assembly. As described previously, the frame also distributes stress and thermal loads.
5. After mechanical and electrical tests the unit is assembled, placed in a retaining fixture, and the space between the cover plates filled with hard foam potting compound.
6. Modules are assembled to the dc plugs and the RF cables are attached.
7. The equipment plate can now be checked electrically for proper operation within limits of its modules' functions.

#### 7.3.8 EQUIPMENT PLATE SUBASSEMBLIES

Modules are mounted to the power supply equipment plates with screws. These modules are one inch by one inch cross section and are quite heavy. The individual screw mounting is required for electrical and mechanical integrity.

Digital modules are one half inch by one half inch cross section and are plugged directly into a receptacle to distribute their many interconnecting wires. The modules are mounted through the receptacle with mounting screws.

Receiver and multiplier modules are one half inch by one half inch cross section and are installed on dc plugs mounted in the equipment plate. Both receiver equipment plates are bolted together as an assembly and both multiplier equipment plates are bolted together as an assembly. Both assemblies require coaxial connection to the RF assembly and must be connected to power supply equipment Plate No. 1 and digital Plate No. 7. Signal interconnection must also be provided between these assemblies but most coaxial runs remain within the equipment plates.

**SECTION 8**  
**QUALITY CONTROL AND TEST**

## SECTION 8

### QUALITY CONTROL AND TEST

The GE quality control plan for design and development of the ATS gravity gradient stabilization system was consistent with NASA document NPC 200-2, "Quality Program Provisions for Space Systems Contractor." A detailed QC Program Plan was published as GE Document No. 66SD4246 after a review of all its provisions with NASA/Goddard. This QC plan was integrated with all affected functions at GE to ensure that the quality requirements set forth in the program plan were satisfied through all phases of Contract performance. The system was implemented through such procedural GE documents as:

1. GE Space Division Policies and Instructions (Quality Control and Test)
2. QC Operating Procedure Manual
3. Standing Instructions

A Quality Control Project Engineer was assigned to the ATS Program to integrate all quality assurance activities in accordance with the requirements of the ATS Program Manager. The QC Project engineer established a QC organization to support the ATS program. The organization included engineers and technical personnel who supported the areas of interface, planning, integration, schedule and cost control. QC personnel participated in all design reviews to assure that specifications and drawings satisfied quality control standards. These meetings also afforded opportunities for early identification of potential test problems.

One of the principal responsibilities of QC was vendor surveillance. The surveillance included all major subcontractors and their vendors.

A chief concern of vendor surveillance was the maintenance of calibrated standards at GE which could be relied upon to measure the supplier's product. These standards were calibrated regularly against certified measuring standards which were traceable to national standards.

Another important QC function was the regular requirement (established by Space Division instructions) for collecting and analyzing QC data resulting from test and inspection operations. Trouble, failure and quality data were published in such QC oriented reports as:

- Monthly Quality Status Reports
- Laboratory and Experimental Data Reports
- Quality Data Reports
- Narrative End-Item Reports
- Operational Data Reports

Preliminary reviews of all failure data were made. A failure analysis function was established to determine the need for failure analysis meetings or teardown analysis and to recommend corrective action when required. Action items were assigned to the individuals responsible for effecting the required correction. All failure analysis reports produced during design and development of the ATS Gravity Gradient Stabilization System are on file and can be reviewed upon request of the GE Contract Administrator for NASA Programs.

Qualification (using prototype equipment) and acceptance testing (of flight hardware) were conducted by QC personnel against a set of step-by-step directions published as Standing Instructions. These instructions were prepared by QC test engineers to implement the Quality Assurance Provisions of each subsystem specification. Results of the tests were recorded item by item, accepted by a NASA resident representative, and the completed standing instruction became a certified record of test results. GE published these results in ATS Historical Logbooks for the applicable prototype or flight units. A list of these documents is shown in Table 8-1. The ATS Historical Logbooks can be made available upon request of the GE Contract Administrator for NASA programs.

QC support of the ATS project continued after the gravity gradient systems were accepted by NASA and delivered to the vehicle contractor. There were QC engineering and technical

Table 8-1. ATS Historical Logbooks

Prototype 1	TV Camera System (Qual Unit) 2/13/67 Power Control Unit, 7/27/66 Power Control Unit (Post Rework), 9/27/66
Prototype 2	Primary Boom, 5/13/66 Primary Boom SN-11 P2A, 8/9/66 Primary Boom Half System P2B, 11/2/66 Combination Passive Damper, 5/4/66 Power Control Unit, 5/2/66 Power Control Unit, 6/8/66 TV Camera, 5/13/66 Solar Aspect Sensor, 5/3/66
Flight 1	Combination Passive Damper, 10/25/66 Primary Boom Assembly, 12/24/66 TV Camera System, 11/7/66 Power Control Unit, 9/20/66 Solar Aspect Sensor, 8/25/66 Calibration Curves, 10/21/66 Calibration Curves, TV Camera, 11/8/66 Calibration Curves, Primary Boom, 12/28/66
Flight 2	Combination Passive Damper, 8/28/67 TV Camera System, 6/22/67 Primary Boom, 4/21/67 Solar Aspect Sensor, 8/25/67 Power Control Unit, 12/13/66 Calibration Curves, TV Camera; 7/11/67 Calibration Curves, Primary Boom, 9/27/67 Calibration Curves, CPD, 8/28/67 Calibration Curves, SAS, 8/25/67
Flight 3	Primary Boom (Vol 1 and 2), 11/6/68 Combination Passive Damper, 9/18/68 Calibration Curves, Primary Booms, Calibration Curves, PCU Calibration Curves, TV Camera TV Camera, 9/17/68

people assigned to Hughes Aircraft during system tests of the three flight systems. These individuals provided consultation during those phases of testing that involved the gravity gradient system. These representatives continued to provide technical council during system tests at NASA/Goddard and Cape Kennedy.



## **SECTION 9**

### **RELIABILITY**

## SECTION 9

### RELIABILITY

#### 9.1 INTRODUCTION AND SUMMARY

This section presents the final reliability report on the ATS program. It serves two principal purposes: to present a final reliability assessment of the ATS Gravity Gradient Stabilization System, and to demonstrate that all requirements of the ATS Reliability Program Plan (Document number 66SD4312) have been met.

#### 9.2 SUMMARY OF SIGNIFICANT ACTIVITIES AND ACCOMPLISHMENTS

The following is a quarter-by-quarter summary of the significant activities and accomplishments of the Reliability Engineering Analysis component during the ATS program. The majority of these activities are documented by PIR. A list of all the PIR's published by Reliability Engineering, with a precis of each, will be found in Appendix 9A. Additional documentation will be found in appropriate monthly and quarterly progress reports published during the life of the ATS contract.

##### 9.2.1 FIRST QUARTER (PROGRAM GO-AHEAD THROUGH SEPTEMBER, 1964)

A first draft of the reliability program plan was written. A first apportionment of reliability goals was made based on an assumed component GG subsystem goal. Inputs to the reliability sections of all specifications and work statements were prepared.

##### 9.2.2 SECOND QUARTER (OCTOBER, 1964 THROUGH DECEMBER, 1964)

The reliability program plan was revised and updated. The CPD configuration was evaluated and a recommendation made for a backup mode for the clutch. A search was made for life data on solenoids. A preliminary design reliability analysis of the PCU was performed. Procedures and schedules were established for design reviews.

##### 9.2.3 THIRD QUARTER (JANUARY, 1965 THROUGH MARCH, 1966)

A first reliability analysis of the boom subsystem was prepared; the impact of the backup mode of operation on the electrical subsystem was investigated; the effect and probability of

occurrence of an inadvertent clutching command during boom deployment was evaluated. Critical reliability areas in the CPD and PCU were reviewed: the application of dimple motors to the CPD release mechanisms was investigated; the question of single vs dual squib bridge-wires was also studied. The impact of using a single cable cutter for release of the damper boom mechanism was evaluated, and a cable cutter test plan was generated. A test plan and testing philosophy for the sealed drive unit were also formulated; tradeoffs between part-level and subassembly-level tests were resolved. The part qualification program risk was assessed, based on a study of part histories and mission criticalities.

#### 9.2.4 FOURTH QUARTER (APRIL 1965 THROUGH JUNE 1965)

Participated in design reviews on the Boom Subsystems, PCU, PHD, TVCS, and CPD Angle Indicator. A reapportionment of reliability goals for the gravity gradient subsystem components was prepared. Procedures were established for the Integrated Test Program Board (ITPB) and the Failure Analysis Review Board (FARB). Part qualification requirements were updated, and the impact of various funding levels assessed. The final draft of the reliability program plan was prepared and submitted for review; final contract negotiations were completed. Adcole's reliability analysis of the SAS, and TRW's analysis of the PHD were reviewed. Alternate squib-driver configurations were studied in support of the PCU weight-reduction effort - a sequential-operation backup scheme was recommended. Testing requirements for the PHD torsion wire were defined. Ground rules for the TVCS life test were established. GE reliability effort and the GE/HAC data exchange program were reviewed with NASA's West Coast reliability representative.

#### 9.2.5 FIFTH QUARTER (JULY 1965 THROUGH SEPTEMBER 1965)

A piece-part level failure mode/effects analysis was performed on the PCU; a review of interfaces with other elements of the system was included. A study was begun of system "idiot modes" - catastrophic failures that could be induced by erroneous commands or command sequences. A tradeoff study was made of the CPD clutch transient suppression circuit. The desirability of wiring redundancy in the primary boom assembly was evaluated, and an analysis was made of the boom limit-switch wiring configuration. Switch-contact redundancy in the boom clutch rotary solenoid was studied. A visit to deHavilland was made to review

progress of their failure mode/effects analysis of the boom system. A standard list of piece-part failure rates was established for use in reliability assessments of ATS components.

#### 9.2.6 SIXTH QUARTER (OCTOBER 1965 THROUGH DECEMBER 1965)

A tradeoff analysis was made on the question of adding emergency mode limit switches to the primary boom system. A preliminary reliability assessment on the CPD angle indicator was completed. A failure mode/effects analysis on the CPD itself was initiated. The risk of various boom subsystem failure modes was assessed. Lear-Siegler's reliability analysis of the TVCS and their TVCS life-test plan were reviewed - meetings were held with LSI representatives to resolve discrepancies. An investigation was made of the feasibility and desirability of redundant contacts for sensor on-off relays in the PCU. Followup action was initiated on deHavilland's boom subsystem failure mode/effects analysis. A proposed test plan for the damper boom ball lock release mechanism was evaluated. A response was prepared to NASA's comments on the draft of the reliability program plan.

#### 9.2.7 SEVENTH QUARTER (JANUARY 1966 THROUGH MARCH 1966)

Work was begun on the orbit test plan optimization study (an effort to establish the optimum sequence of gravity gradient experiments, based on mission value of the experiments and the risks of components failure associated with each). A preliminary version of the Flight Malfunction Analysis/Corrective Action Plan was issued. The FMA/CAP is a listing of possible flight malfunctions during the gravity gradient experiment, along with estimated probabilities of occurrence, telemetry indications, effects on the system and on subsequent experiment capability, and contingency plans, where applicable. In conjunction with this above activities, a summary of operating times and duty cycles for all ATS components was prepared and issued. A revised version of LSI's TVCS life test plan was reviewed, and a another meeting held with LSI representatives to resolve questions. Another test plan for the damper boom release mechanism was evaluated. A functional circuit-level failure mode/effects analysis on the SAS was published with some changes from Adcole's original analysis. Reliability estimates for the SAS and TVCS were prepared and issued. A test plan was prepared for the in-house portion of the TVCS life test.

#### 9.2.8 EIGHTH QUARTER (APRIL 1966 THROUGH JUNE 1966)

The final version of the Flight Malfunction Analysis/Corrective Action Plan was issued. A CPD risk assessment was published, listing failure modes versus estimated probability of occurrence. The squib firing circuit utilized for the CPD uncaging mechanism was re-evaluated, and the original choice of configuration was justified. A technique was developed for optimizing the orbit test sequenced on the basis of experiment value and risk - the currently proposed sequence was evaluated and an alternative sequence proposed. An analysis of the life requirements for the angle indicator lamp was performed, and a draft life test plan submitted to Engineering Standards. Integrated Test Program Board activity was supported by Reliability.

#### 9.2.9 NINTH QUARTER (JULY 1966 THROUGH OCTOBER 1966)

Comments were issued on the reliability demonstration data obtainable from a revised damper boom release mechanism test plan. The effect of adding capacitors to PCU squib driver circuits was assessed. Reliability analyses of various tip maas release pyrotechnics circuits were performed an analysis and assessment of the final configuration was published. ITPB activity was supported by Reliability.

All elements of the Reliability Program Plan (Document No. 66SD4312) were complied with - where documentation was involved, the applicable paragraph number is indicated with the appropriate PIR number(s) in Appendix 9A.

As a review of Appendix 9A will indicate, a large proportion of the reliability effort during the ATS program was devoted to what might be termed engineering support tasks, i. e., tasks that did not fall into one of the formalized task areas defined in the program plan.

Some additional work that was requested by the customer but that did not fall within original program scope was performed on CCN funding - the flight malfunction analysis/corrective action plan and the Orbit Test Plan Optimization Study, in particular.

Although some reliability effort - engineering support in particular - was never formally documented, the listing of PIR's in Appendix 9A gives a fair approximation of the way the total program effort was expended on a task-area basis:

Task Area	No. of PIR's	% of Total
Apportionment & Prediction	8	15
Failure Modes and Effects Analysis	11	22
Test Planning Support	19	37
Design Configuration Support	10	20
Part Program & Miscellaneous	3	6
Total	51	100

Note that this distribution of effort differs significantly from the conventional reliability program because the emphasis was on Engineering and Program Office support rather than on "classical" reliability tasks.

### 9.3 SYSTEM RELIABILITY ASSESSMENT.

The following reliability assessment of the ATS gravity gradient stabilization system is based on two mission requirements: (1) stabilization of the vehicle for a nominal three-year mission; and (2) completion of the gravity gradient experiment in accordance with the orbit test plan.

The reliability model established for the basic gravity gradient stabilization mission is shown in Figure 9-1.\*

A basic assumption in this model is that once initial deployment and stabilization have been achieved, and a nominal configuration established, no significant failure mechanisms will

---

\*NOTE: to save space and increase clarity, slightly unconventional notation is used in Figures 9-1 and 9-2: the exponent "2" on a block indicates that two like blocks are in series; an exponent on a parenthesis surrounding a group of blocks likewise indicates two groups in series. This notation is consistent with the mathematical equivalent of the reliability model.

exist for the design life of the vehicle. In the case of the dampers, particularly, it is assumed that the probability of damper survival is essentially the probability of surviving launch and initial engagement - the elements required to clutch in the PHD are therefore considered to be required for the first few hours of the mission. The probability of a catastrophic ECD failure is considered to be remote in any event. The probability of success for each element of the model is indicated in Figure 9-1 above the element. The probability of success for the basic stabilization mission is estimated to be 0.916.

The reliability model for the gravity gradient experiment (ATS-A) is shown in Figure 9-2. As noted, this model assumes that initial stabilization has been accomplished successfully. The principal contributors to unreliability in the model are the two TV camera systems; the system estimate is computed for two cases: both cameras surviving, and at least one of two cameras surviving. These estimates are respectively 0.661 and 0.876.

#### 9.4 DISCUSSION OF TEST FAILURE HISTORY

All significant failures occurring during the ATS test program have been analyzed, and formal failure analysis reports were issued.

Considering all components together, manufacturing defects and test problems (both procedural errors and test equipment malfunction) appear to have been the chief causes of failure, occurring with about equal frequency. To a lesser degree, failures have been caused by design deficiencies, which have been subsequently identified and corrected. With the possible exception of the TVCS, the failure analyses published during the program indicate no inherent reliability weaknesses beyond normal exception in any of the ATS components. TVCS problems which have arisen due to the use of an essentially off-the-shelf commercial component are discussed in detail in Section 4 of this volume.

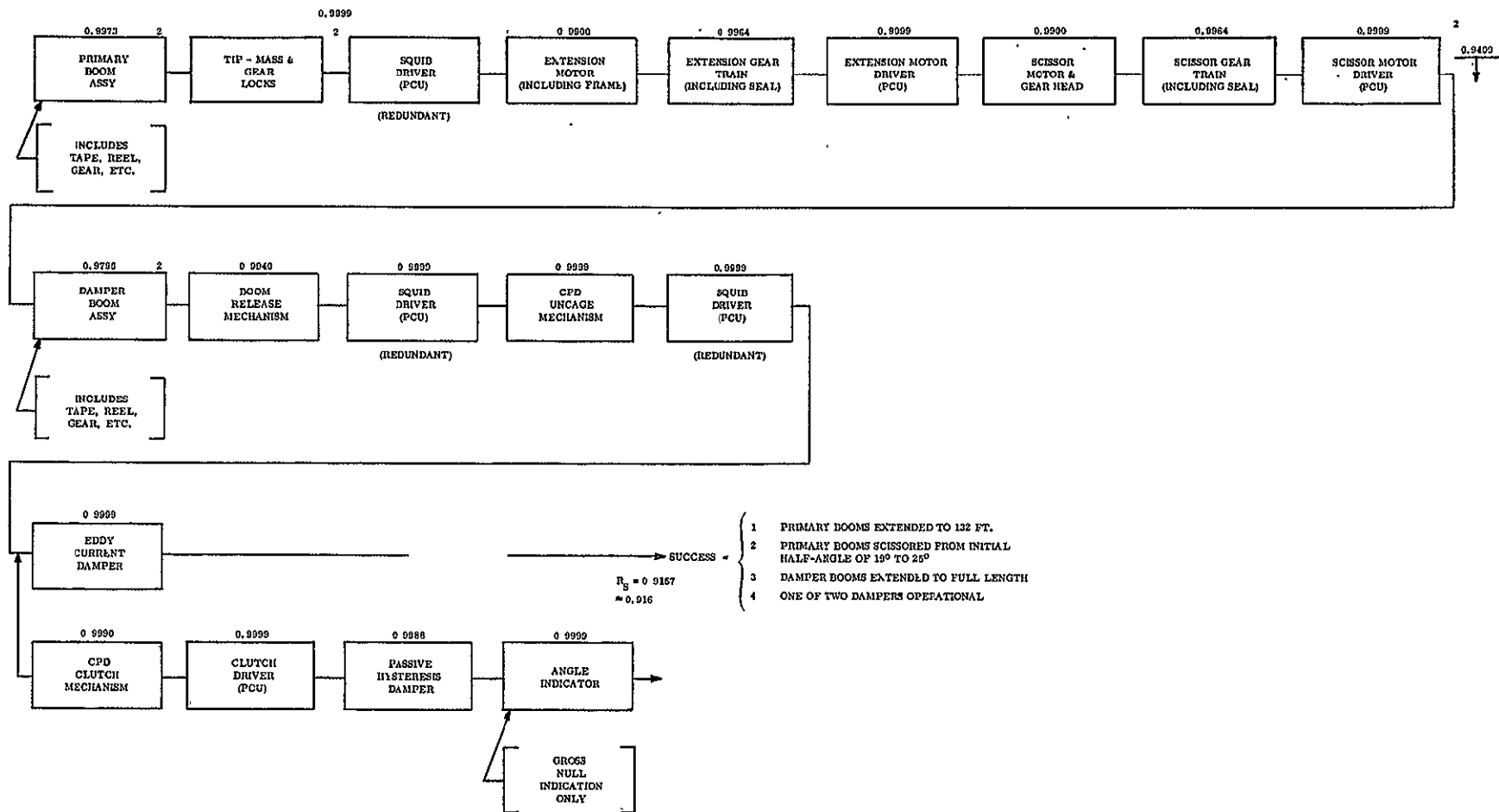


Figure 9-1. Mathematical Model - Basic Gravity Gradient Stabilization Mission



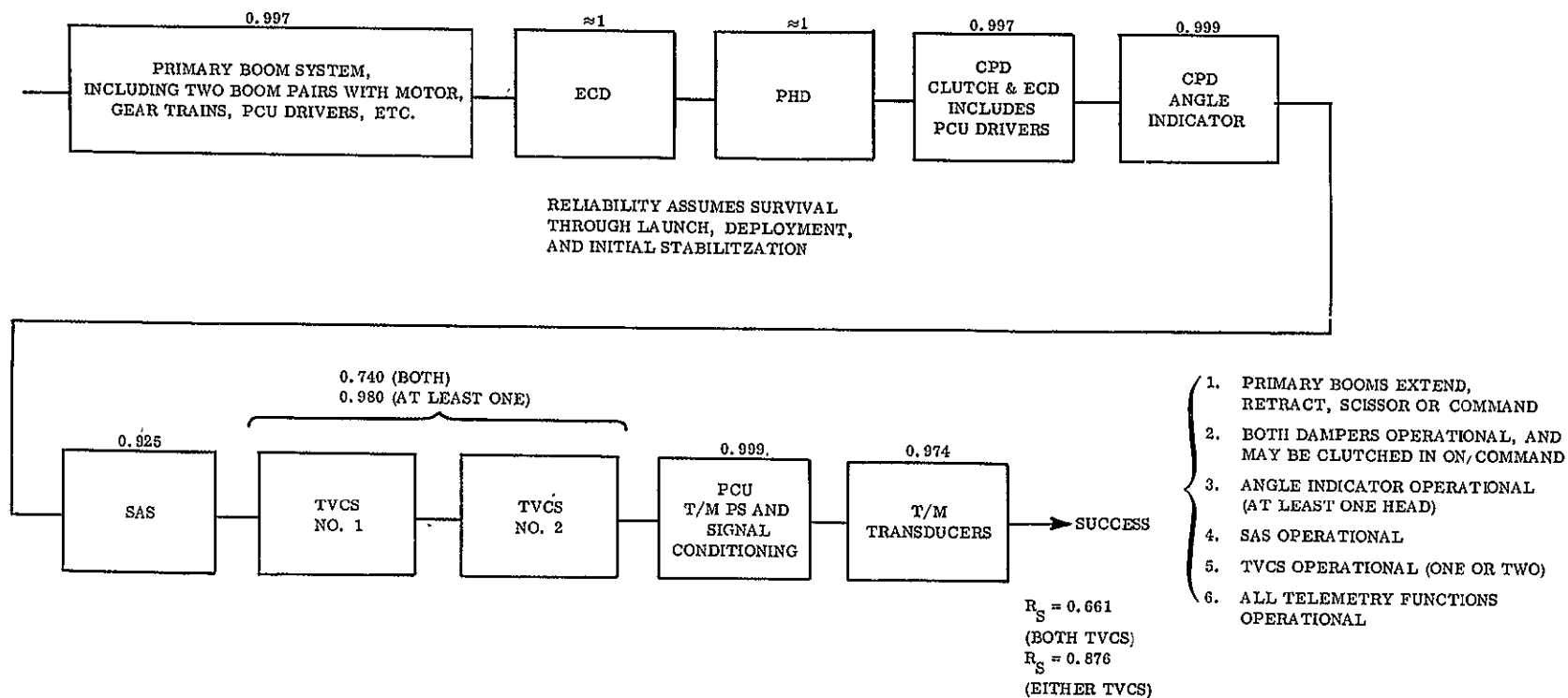


Figure 9-2. Mathematical Model - Gravity Gradient Experiment (ATS-A), Initial Stabilization Assumed

## APPENDIX TO SECTION 9

- 9A RELIABILITY ENGINEERING ANALYSIS PIR'S
- 9B FAILURE ANALYSIS REPORT SUMMARY.

APPENDIX 9A  
RELIABILITY ENGINEERING ANALYSIS PIR'S

PIR No.	Date	Content
4144-103	1-13-65	Reliability testing philosophy
4144-106	1-25-65	Reliability critique, DeHavilland boom system; information on cable-cutter test sample sizes
4144-115	2-17-65	Comparison of proposed test plans for sealed drive assembly
4144-127	3-9-65	Evaluation of dimple motors for CPD uncaging
4144-147	4-9-65	Data on number of trails vs demonstrated reliability (reference CPD test plan)
4144-162	5-5-65	Summary of parts qualification program
4144-171	5-19-65	Updated reliability apportionment
4144-183	5-21-65	Discussion of Adcole's reliability prediction on SAS-errors pointed out
4144-185	5-25-65	Discussion of funding cutback impact on part qualification program
4144-187	5-25-65	Test cycles vs demonstrated reliability for PHD torsion wire tests
4144-188	5-25-65	Approval of STL's reliability program plan (PHD)
4144-200	6-8-65	Ground rules for TVCS life test
4144-203	6-14-65	Further discussion of SAS reliability prediction- reassessment considering duty cycle
4144-219	7-13-65	Recommendation against redundant wiring in boom assembly; concurrence with proposed wiring change in switches
4144-237	8-17-65	Failure mode/effects analysis - PCU
4144-238	8-16-65	GG experiment "Idiot" modes
4144-264	2-29-65	GG equipment failures modes (cover PIR)
4144-266	10-1-65	Tradeoff analysis, CPD solenoid transient suppres- sion circuit
4144-267	10-1-65	List and discussion of part failure rates used in reliability analyses

PIR No.	Date	Content
4144-268	10-4-65	Comment on LSI's TVCS life test plan
4144-270	10-5-65	Evaluation of proposed redundancy in boom clutch solenoid switch contacts - recommendation to drop requirement
4144-271	10-8-65	Analysis of boom limit switch wiring configuration
4144-274	10-11-65	Comments on LSI's TVCS reliability analysis - request for more data
4144-275	10-19-65	Comments on LSI's TVCS life test plan
4144-276	10-25-65	Analysis of emergency-mode limit switching (boom assembly) - recommendation against
4144-277	10-21-65	Discussion of desirability of redundant contacts for sensor on-off relays - found not essential
4144-281	10-28-65	Review of LSI's reliability analysis of TVCS, with comments
4E20-1	11-11-65	Evaluation of damper boom (ball lock) release mechanism test plan, including reliability demonstration information obtainable
4E20-3	11-17-65	Minutes of meeting with LSI on TVCS life-test plan and reliability analysis
4E20-4	11-20-65	Follow-up on deHavilland's boom system FMEA-status of action items
4E20-8	12-15-65	Estimates of risk of various boom system failure modes
4E20-12	1-14-66	Summary of operating times/duty cycles for ATS components
4E20-14	1-17-66	Minutes of meeting with LSI on TVCS life test plan
4E20-15	1-28-66	Preliminary reliability assessment on angle indicator, including circuit FMEA
4E20-17	1-19-66	Comments on reliability demonstration data obtainable from damper boom release mechanism test plan
4E10-3	2-4-66	Comments on revised TVCS life test plan submitted by LSI
4E10-5	2-11-66	Minutes of meeting on in-house portion of TVCS life test
4E10-9	2-15-66	Circuit-level FMEA on SAS with some change from Adcole's original analysis

PIR No.	Date	Content
4E10-12	2-28-66	Flight malfunction analysis/corrective action plan (preliminary) - possible flight malfunctions during GG experiment, est. P (occur.), T/M indication, effects on system and/or subsequent tests, contingency plans
4E10-15	3-12-66	TVCS life-test plan (in-house portion)
4E10-19	3-28-66	Reliability estimate - SAS
4E10-20	3-29-66	Reliability estimate - TVCS
4E10-22	4-27-66	CPD failure mode risk assessment (principal failure modes vs P { occur } )
4E10-25	5-13-66	Final version of FMA/CAP (see PIR 4E10-12 above)
4E10-37	5-11-66	Evaluation of squib firing circuit utilized in CPD uncaging mechanism - choice of configuration just justified
4341-1	5-26-66	Method established for optimizing sequence of tests during gravity-gradient experiment on basis of failure risk and consequences
4341-17	8-1-66	Comments on reliability demonstration data obtainable from proposed damper boom release mechanism test plan
4341-19	8-5-66	Reliability evaluation of tip-mass (pyro) release circuit
4341-23	8-29-66	Analysis of effect of adding capacitors to PCU squib driver circuits
4341-36	11-11-66	Evaluation of damper boom release mechanism test results

APPENDIX 9B  
FAILURE ANALYSIS REPORT SUMMARY

<u>Failed Item</u>	<u>Failure Analysis No.</u>	<u>Date</u>	<u>Failure Description - Cause Category</u>
Primary Boom Assembly	183-E-2	5-16-66	Extension motor polarity reversed. Clutch failure - manufacturing error. Booms jammed--operator error. Numerous other manufacturing and assembly defects, design deficiencies identified and corrected.
	193-E-7	6-24-66	Extension and scissoring motors failed during life test - performance found satisfactory in view of reduced life requirements
	212-E-11	8-2-66	Scissor mechanism failures - test console malfunction. Boom damage - operator error.
	223-E-14	8-18-66	Tip mass failed to uncage - manufacturing defect
	224-E-15	8-18-66	Scissor drive failure - assembly error
	225-E-16	8-18-66	Boom failed to extend - tolerance buildup; design corrected
	247-E-23	10-7-66	Booms scissored past limit switches - test error
	249-E-25	10-7-66	Failure to uncage - test equipment problem
	255-E-26	10-10-66	Failure to uncage - test equipment problem
	256-E-27	10-17-66	Retraction failure - manufacturing defect
	264-E-30	11-9-66	Retraction failure, leakage failure - manufacturing defect
	266-E-31	11-15-66	Boom jammed during deployment - assembly error
	268-E-32	11-17-66	Failure to deploy - tolerance buildup, design corrected.
	269-E-33	12-12-66	Failure to retract - manufacturing errors identified; failure still under investigation
	277-E-37	12-13-66	Failure to uncage - design deficiency/manufacturing defect.

<u>Failed Item</u>	<u>Failure Analysis No.</u>	<u>Date</u>	<u>Failure Description - Cause Category</u>
Damper Boom Assembly	205-E-10	11-16-66	Explosive actuation ruptured due to over-stress - steel bodies now used
	228-E-17	9-13-66	Torn elements, drum bearing failure - failed to deploy. Causes included assembly and test errors, overtesting.
	229-E-18	8-20-66	Torn tape, slow deployment - assembly and test problems
CPD	191-E-5	6-30-66	Squib failed to fire - test equipment problem Lamp filament broken in vibration - no cause identified. Rotor draf - contamination and/or assembly error. Clutch solenoid failure tolerance buildup.
	220-E-13	8-12-66	Mode switch failure - assembly error.
	237-E-20	9-2-66	Hi-Pot failure - improper test procedure.
	238-E-21	8-24-66	Magnet brackets failed in vibration - strength inadequate; bracker redesigned.
	257-E-28	10-24-66	ECD damping coefficient out of spec - assembly error, test equipment problems.
	271-E-34	12-6-66	Out of spec conditions, cleanliness problem cause of anomaly not determined.
PCU	180-E-1	4-27-66	Failed transistors - improper Hi-Pot test procedure.
PCU	186-E-3	6-20-66	Failed transistors -test error.
PCU	199-E-9	9-15-66	Failed transistors - test error.
PCU	244-E-22	9-27-66	Failed transistors - test error.
TVCs	190-E-4	6-14-66	Several out-of-spec conditions - numerous design and process changes introduced.
TVCs	218-E-12	8-12-66	Hi-Pot test failure - test requirement deleted.

**SECTION 10**  
**MATERIALS AND PROCESSES**



## SECTION 10

### MATERIALS AND PROCESSES

An important consideration in the development of the gravity gradient system was a review of requirements for special materials and processes. Initial efforts in the design of components for the gravity gradient system were supported by consultation with GE engineers specialized in the many disciplines required for effective materials and process decisions. A representative of GE's Materials and Processes organization was assigned as liaison engineer. This representative attended all design reviews and assisted in the selection of such items as lubricants for the CPD. Tarnish of silver and the effect it would have as a finish material on the primary booms was an item of study and test. Other investigations by the materials technologist were in response to problems encountered by the requirements engineers who were responsible for specific subsystems. Such a request precipitated an investigation of the CPD angle indicator to determine the effect on its performance due to its relatively exposed location within the ATS spacecraft. Recommendations were made for selection of ports in the angle indicator electronics unit that were reflected in a subsequent parts requirements for resistors, diodes, transistors and phototransistors.

The materials technologist reviewed all design drawings for materials and finishes and his signature was required before the drawing was released.

Materials reporting to NASA complied with the general provisions of the ATS contract. Each GE monthly progress report from 1965 to 1967 contained a section on materials and processes activities; a thorough technical discussion of materials investigations was included in each quarterly report published during the same period. In addition to these reports, five semi-annual reports were published. The range of topics and extent of effort that was expended is evident from a review of the contents of these semi-annual reports. Copies of these reports are on file at the GE Space Division and can be made available upon request of the Contract Administrator for NASA programs. The following pages provide the Table of Contents for these reports.

TABLE OF CONTENTS  
MATERIALS REPORT NO. 1  
DOCUMENT NO. 65SD4221

<u>Section</u>	<u>Page</u>
1 INTRODUCTION . . . . .	1
2 THERMAL CONTROL . . . . .	2
3 COMBINATION PASSIVE DAMPER . . . . .	6
3.1 Materials Considerations for the Bistable Clutch . . . . .	6
3.2 Non-Magnetic Mating Material for the Bellville Washer Spring . . . . .	8
4 GRAVITY GRADIENT ROD MATERIAL CONSIDERATION . . . . .	9
5 LUBRICATION AND MECHANICAL COMPONENTS OF LUBRICATION SYSTEMS . . . . .	14
5.1 General . . . . .	14
5.2 Lubrication Requirements . . . . .	14
5.2.1 Liquid Lubrication . . . . .	14
5.2.2 Self-Lubricating Materials . . . . .	15
5.2.3 Dry Film Lubricants . . . . .	15
5.2.4 Other Approaches . . . . .	15
5.2.5 Recommended Lubricants . . . . .	15
6 ATTITUDE SENSOR SUBSYSTEM. . . . .	18
6.1 TV Camera Boom Targets . . . . .	18
6.2 Adhesive Bonding of Mirrors Aligned to Component Surfaces . . . . .	18
6.3 Recommendations . . . . .	19
7 MATERIALS QUALITY PROVISIONS . . . . .	21

TABLE OF CONTENTS  
MATERIALS REPORT NO. 2  
DOCUMENT NO. 65SD4442

<u>Section</u>	<u>Page</u>
1 INTRODUCTION . . . . .	1-1
1.1 Purpose . . . . .	1-1
1.2 Scope . . . . .	1-1
1.3 ATS Approved Parts List . . . . .	1-1
2 BOOM SUBSYSTEM . . . . .	2-1
2.1 Materials Review of Boom Subsystem . . . . .	2-1
2.2 TV Target Material . . . . .	2-1
2.3 Boom Erection Mechanism Bearings . . . . .	2-2
2.4 Silver Tarnishing Study - Interim Report . . . . .	2-4
2.5 Evaporation of Silver Sulfide Tarnish from Silverplate in Space . . . . .	2-5
2.6 Lubrication . . . . .	2-7
3 COMBINATION PASSIVE DAMPERS . . . . .	3-1
3.1 Bistable Clutch - Life Test Evaluation . . . . .	3-1
3.2 Caging Pin Stop Material Design . . . . .	3-2
3.3 Physical Properties of Rubber Impact Absorber . . . . .	3-3
3.4 Corrosion of Dissimilar Metals - Humidity Tests . . . . .	3-6
3.5 Copper Blackening Method - Angle Indicator . . . . .	3-7
3.6 Adhesive Evaluation - Angle Indicator . . . . .	3-9
4 ATTITUDE SENSOR SUBSYSTEM . . . . .	4-1
4.1 Thermal-Vacuum Testing of Solar Aspect Sensor Reticles . . . . .	4-1
5 GENERAL MATERIALS INVESTIGATIONS . . . . .	5-1
5.1 Considerations for Stainless Steel Springs . . . . .	5-1
5.2 Magnesium Alloy . . . . .	5-1
5.3 Thermal Properties of Aluminum Alloys and Surface Coatings . . . . .	5-3
5.4 Raychem Wire Problems . . . . .	5-5
5.5 Bonding Gold to Gold and Copper to Magnesium - Low Strength Requirements . . . . .	5-5

TABLE OF CONTENTS  
MATERIALS REPORT NO. 3  
DOCUMENT NO. 66SD4225

Section	Page
1 INTRODUCTION . . . . .	1-1
1.1 Purpose . . . . .	1-1
1.2 Scope . . . . .	1-1
2 BOOM SYSTEM . . . . .	2-1
2.1 Tarnishing of Silver Plated Booms . . . . .	2-1
2.1.1 Evaporation Rate of Silver Sulfide from a Silver Surface in Space . . . . .	2-1
2.1.2 Tarnishing of Silver Rod When Coiled . . . . .	2-4
2.2 Primary Boom Motor Gear . . . . .	2-6
2.3 Fracture Analysis of Berylco 25 Overlap Tubes . . . . .	2-8
2.3.1 Part Description . . . . .	2-8
2.3.2 Description of the Failures . . . . .	2-9
2.3.3 Conclusions . . . . .	2-9
2.4 Examination and Analysis of Primary Boom Tape Bearing . . . . .	2-12
3 COMBINATION PASSIVE DAMPER. . . . .	3-1
3.1 Physical Properties of Rubber Impact Absorber. . . . .	3-1
3.2 Effects of Outgassing on Angle Indicator Optics . . . . .	3-4
3.3 Analysis of Radiation Effects on Angle Indicator Components . . . . .	3-5
3.4 Encoder Disc Thermal Coupling . . . . .	3-8
3.5 Preparation of PRC 1538 for Lamp Cushions . . . . .	3-8
3.6 Thermal Cycling of Angle Indicator Phototransistors and Bulbs . . . . .	3-9
3.6.1 Experimental Procedure . . . . .	3-10
3.6.2 Results and Conclusions . . . . .	3-11
3.7 Development of a High Viscosity Low Temperature Curing Adhesive . . . . .	3-12
3.7.1 MPC-100-A High Viscosity Adhesive Produced by GE . . . . .	3-12
3.7.2 Epon 815 and Tetra Made Thixotropic Using PbW Cab-o-Sil . . . . .	3-12
3.7.3 Conclusion . . . . .	3-13
3.8 Bonding of CPD Caging Pin Shock Absorber . . . . .	3-13
4 ATTITUDE SENSING SUBSYSTEM . . . . .	4-1
4.1 Failure Analysis of Power Control Unit Transistor Q1 . . . . .	4-1
4.2 Failure Analysis of Power Control Unit Transistor Type MHT 6334 . . . . .	4-1
APPENDIX A. REFERENCES . . . . .	A-1

TABLE OF CONTENTS  
MATERIALS REPORT NO. 4  
DOCUMENT NO. 66SD4479

Section	Page
1 INTRODUCTION . . . . .	1-1
1.1 Purpose . . . . .	1-1
1.2 Scope . . . . .	1-1
2 BOOM SYSTEM . . . . .	2-1
2.1 Reflectance of Boom Samples . . . . .	2-1
2.2 Vacuum Test of Boom Drive Assembly . . . . .	2-1
2.3 Leak Check of Boom Drive Assembly . . . . .	2-2
2.4 Evaluation of Possible Contamination by Weld Splatter . . . . .	2-2
2.5 Improved Paint . . . . .	2-3
2.6 Epoxy for Sealant . . . . .	2-3
2.7 Use of Stycast 1090 . . . . .	2-3
3 COMBINATION PASSIVE DAMPER . . . . .	3-1
3.1 Clutch Cold Weld Test . . . . .	3-1
3.2 Inspection of Miniature Incandescent Lamps for Angle Indicator. . . . .	3-2
3.3 Removal of Anodizing During Ultrasonic Cleaning . . . . .	3-3
3.4 Bonding to Teflon . . . . .	3-3
4 ATTITUDE SENSING SYSTEM . . . . .	4-1
4.1 Humidity Test of Epoxy Paint . . . . .	4-1
4.2 Tip Targets . . . . .	4-1
4.3 Evaluation of Transistors . . . . .	4-1
5 TELEVISION CAMERA SYSTEM . . . . .	5-1
5.1 Gold Plated Connectors . . . . .	5-1
5.2 Material on TV Camera Window . . . . .	5-1

TABLE OF CONTENTS  
MATERIALS REPORT NO. 5  
DOCUMENT NO. 4233

Section	Page
1 INTRODUCTION. . . . .	1-1
1.1 Purpose . . . . .	1-1
1.2 Scope . . . . .	1-1
2 BOOM SYSTEM . . . . .	2-1
2.1 Post Thermal - Vacuum Reflectance Values . . . . .	2-1
2.2 Post Humidity Reflectance Values . . . . .	2-1
2.3 Reflectance Values at Opposite Ends of a Tape . . . . .	2-1
2.4 Ring Standoffs . . . . .	2-1
2.5 X-Ray of Sealed Units . . . . .	2-2
2.6 Micrometeorite Tests of Rods . . . . .	2-2
3 COMBINATION PASSIVE DAMPER . . . . .	3-1
3.1 Inspection of Miniature Lamps for Angle Indicator . . . . .	3-1
3.2 Inspection of CPD Parts . . . . .	3-2
4 ATTITUDE SENSING SYSTEM . . . . .	4-1
4.1 Tip Targets . . . . .	4-1
5 TELEVISION CAMERA SYSTEM . . . . .	5-1
5.1 Vacuum Test of Shutter Lens . . . . .	5-1
APPENDIX A. Micrometeorite Test of Be Cu Gravity Gradient Rods . . . . .	A-1

**SECTION 11**  
**MANUFACTURING**

## SECTION 11

### MANUFACTURING

Manufacturing participation in the gravity gradient program for ATS was divided into support during the development phase and fabrication of prototype and flight equipment during the production phase. During development, Manufacturing was called upon to construct breadboards of gravity gradient components under engineering investigation. Dynamic and thermal models (Figures 11-1 and 11-2) were also fabricated during this period.

Some of the specialized Manufacturing areas and facilities used on ATS are a controlled environmental assembly area, a materials laboratory, an electronics and electrical shop, and a machine shop.

#### 11.1 CONTROLLED ENVIRONMENTAL ASSEMBLY AREA

Contamination control facilities were used extensively during assembly of the CPD. Portable ultraclean areas were erected in the assembly area that featured a recirculating, self-cleaning air system that eliminated contaminants down to a size of one micron. Personnel working in this area were required to wear sterilized white coveralls and bonnets, gloves, and protective coats. Figure 11-3 shows assembly of the Flight 2 CPD in the clean area.

#### 11.2 MATERIALS LABORATORY

This laboratory provided the capability for teardown analysis and evaluation of mechanical, electrical and electro-mechanical parts. The lab is equipped with standard measuring and calibrating equipment.

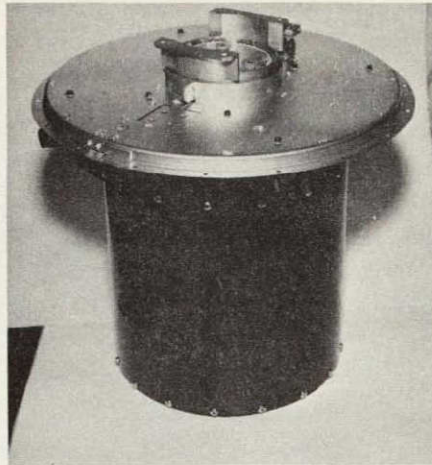
#### 11.3 ELECTRONICS SHOP

The electronics shop assembled the Power Control Unit and provided support for evaluating the performance of the Solar Aspect Sensor and TV Camera Systems. Assembly was performed by certified wiremen who were qualified to perform soldering operations in accordance

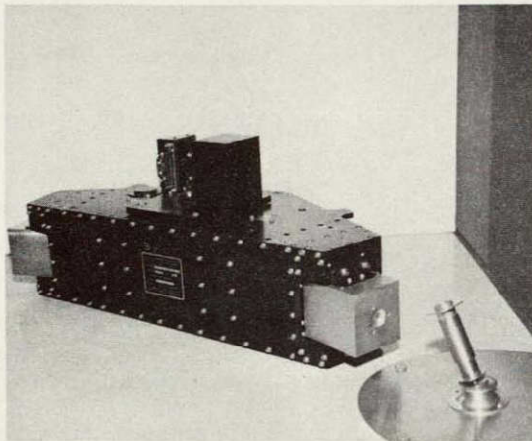
with NASA/Goddard Specification NPC 200-3. Typical of the tasks performed in the Electronics Shop is the PCU wiring board shown in Figure 11-4. The wiring boards were built up of cordwood modules that were interconnected by printed circuits.

#### 11.4. MACHINE SHOP

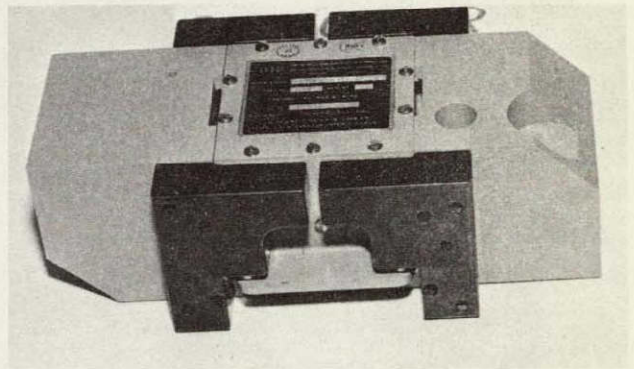
The Machine Shop is a well equipped area containing 78 major pieces of machine tool equipment. Facilities include various sizes and capabilities of lathes, drill presses, milling machines, jig borers and grinders. There were enough pieces of machine tool equipment available that scheduling of parts fabrication was seldom in conflict with any other program requirements. A working model of the CPD uncaging mechanism, shown in Figure 11-5, is typical of components turned out by the Machine Shop during development of gravity gradient hardware. The booms designated for use on the ATS-E system were edge interlocked in this Machine Shop. An Elox machine was used to form the interlocking edges by means of an electrical discharge process.



Combination Passive Damper



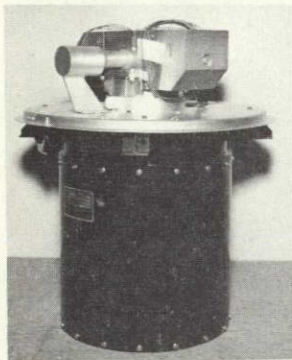
Primary Boom Package



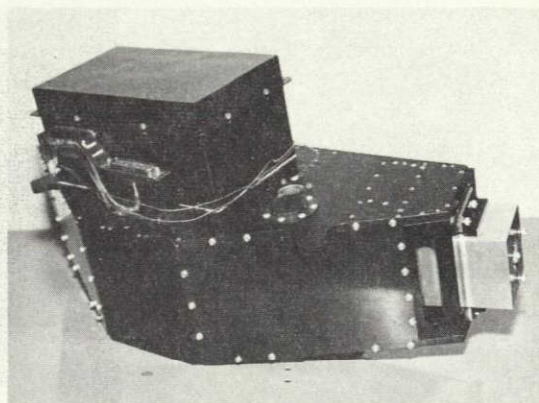
Damper Boom

Figure 11-1. Typical Dynamic Model Units

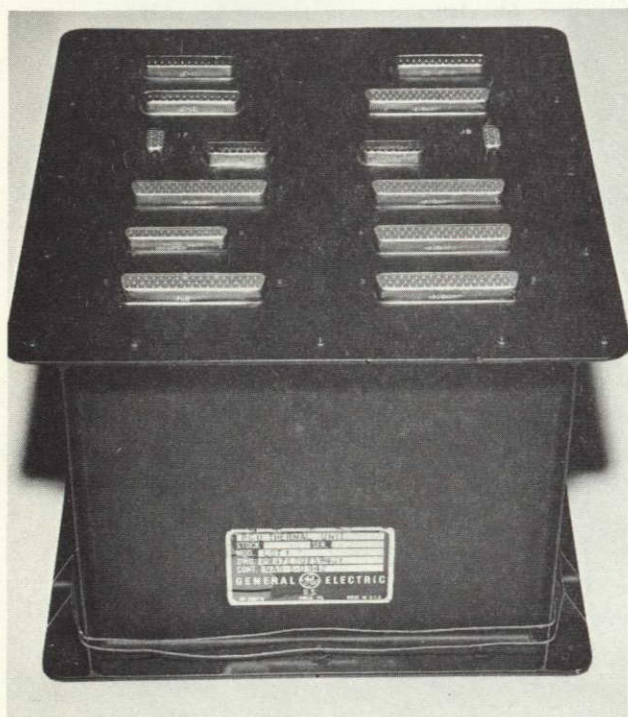




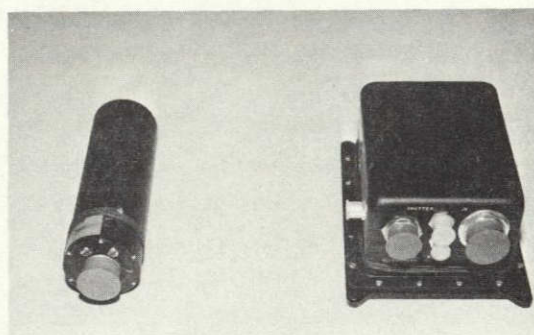
CPD Damper Boom



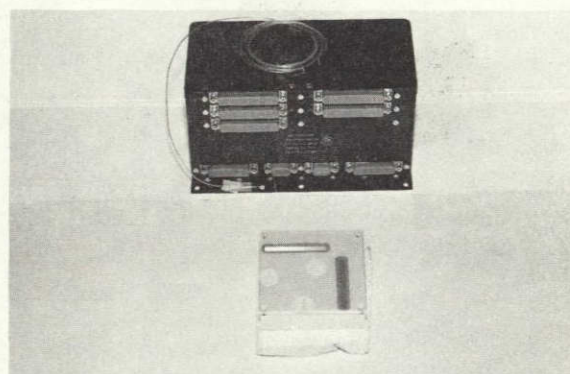
Primary Boom Package



Power Control Unit



TV Camera and Electronics



SAS and Detector

Figure 11-2. Thermal Model Units



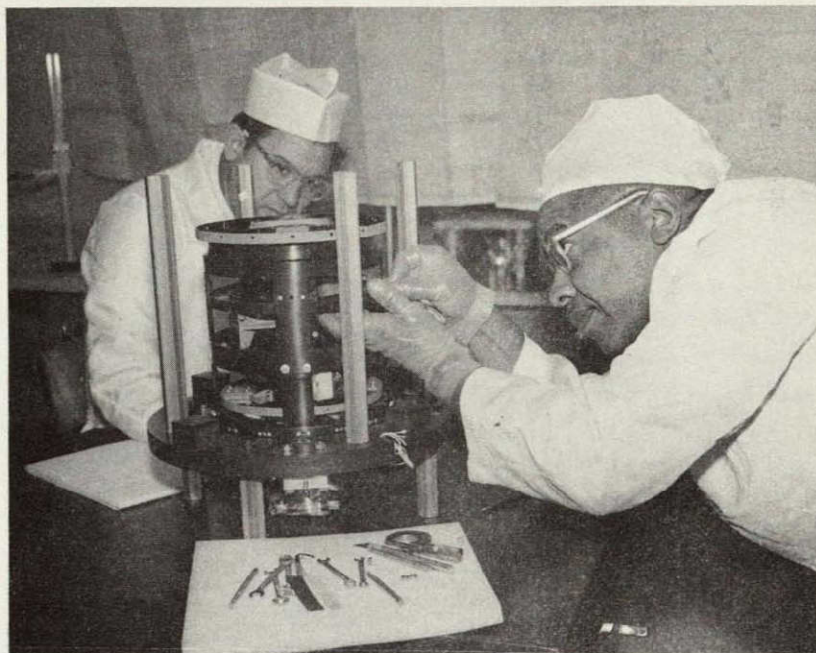


Figure 11-3. Assembly of Flight 2 CPD in Clean Area

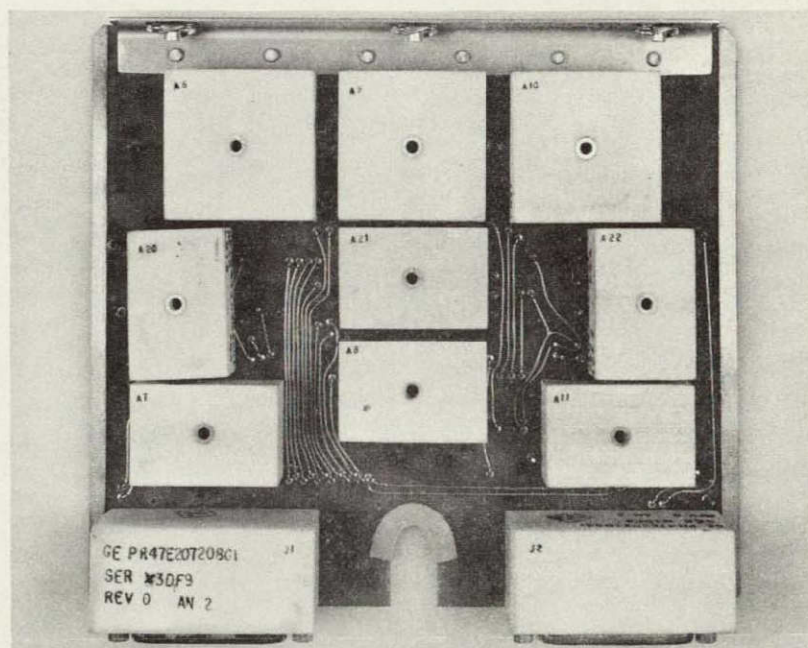


Figure 11-4. Typical PCU Wiring Board Featuring Cordwood Modular Construction



Figure 11-5. Working Model of CPD Caging Arrangement

**SECTION 12**  
**PARTS PROGRAM**

## SECTION 12

### PARTS PROGRAM

The ATS parts program was built around the Approved Parts List 490L106 and Specification SVS-7325, Use of Standard Parts, Materials and Processes. The plan of the program was to use parts that had the highest probability of failure-free operation during the life of the ATS spacecraft. Major provisions of the program, as agreed to by NASA in October 1964, included:

1. Selection of the most reliable types of parts
2. Selection of the best suppliers as determined by past performance and vendor survey in accordance with NASA Specification 200-3
3. Performance of sound electrical and environmental screening tests
4. Selection of those parts that exhibited the most stability as a result of a power aging period.

Parts to be selected for use in the gravity gradient system were divided into two groups (A and B). Group A parts were those with no history to indicate that the parts could survive. These parts were qualified through a series of environmental tests. Group B parts, on the other hand, had been previously qualified for spacecraft applications. This last group was functionally tested before certification for use on the ATS program. The following list summarizes each of the qualification tests and includes reference documents.

#### 12.1 TRANSFORMER, INVERTER

Identification Number: R4610P1

Manufacturer: EG&G  
Boston, Massachusetts  
FSCM 92678

Manufacturer's Identification Number: T1241

Date of Manufacture of Parts: May through December, 1965

Parts Supplied By: Adcole Corporation  
Waltham, Massachusetts

Purpose of Test: Qualification for ATS Program

Test Conducted By: Associated Testing Laboratories, Inc. (ATL)  
Burlington, Massachusetts

Quantity of Parts Tested: 10

Date Test Completed: July 5, 1966

Documentation: a) GE Drawing No. R4610, Rev. A, AN-2  
b) Adcole Specification No. 8161, Rev. C  
c) ATL Test Procedure No. TP-2589-11, Rev. 1  
d) ATL Test Report No. NT-2589-11

Comments: Test was started on five transformers. Whenever a unit failed, it was replaced by one which had been subjected to all previous tests up to that point. One piece failed sealing. One piece was incorrectly tested by error during the Dielectric Withstanding Voltage Test and was replaced. Three pieces failed the Thermal Shock Test, because of physical deformation. This was found to be caused by a processing error in the manufacturing of the transformers. Corrective action was implemented on all existing and replacement parts as described in the test report. The five transformers in the final lot met all requirements.

Disposition: The transformers were qualified for ATS flight use.

## 12.2 SOLAR CELL ASSEMBLY

GE Identification Number: R4611P1

Manufacturer: Hoffman Electronics Corporation  
El Monte, California  
FSCM 99942

Manufacturer's Identification Number: S-3406

Date of Manufacture of Parts: December, 1965

Assemblies Supplied By: Adcole Corporation  
Waltham, Massachusetts

Purpose of Test: Qualification for ATS Program

Test Conducted By: Associated Testing Laboratories, Inc. (ATL)  
Burlington, Massachusetts



Quantity of Assemblies Tested: 5

Date Test Completed: April 12, 1966

Documentation: a) GE Drawing No. R4611, Rev. A, AN-2 and AN-3  
b) Adcole Specification No. 8182, Rev. D  
c) ATL Test Procedure No. TP-2662-11  
d) ATL Test Report No. NT-2661-11

Comments: Each solar cell assembly consisted of nine individual cells. Performance was measured by forward current and reverse leakage current for each cell. The assemblies were subjected to environmental tests of Thermal Shock, Vibration, and Acceleration. All cells and assemblies met all requirements.

Disposition: The solar cell assemblies were qualified for ATS flight use.

### 12.3 TWO-WAY SOLENOID

GE Identification Number: R4612P1

Manufacturer: Koontz-Wagner Electric Company  
South Bend, Indiana  
FSCM 02250

Manufacturer's Identification Number: KW13927

Date of Manufacture of Parts: October, 1965

Purpose of Test: Qualification for ATS Program

Test Conducted By: Koontz-Wagner Electric Company  
South Bend, Indiana

Quantity of Parts Tested: 6

Date Test Completed: June 10, 1966

Documentation: a) GE Drawing No. R4612, Rev. B  
b) Koontz-Wagner Test Plan No. KES-0241  
c) GE PIR No. 4323-FM-260  
d) Koontz-Wagner Test Report No. KES-0241 (3 sections)

Comments: As specified in the test plan, two pieces (Group I) were subjected to a series of environmental and stress tests. The failure of both samples because of broken shafts in vibration resulted in a redesign which was incorporated in all test samples. Four pieces (Group II) were subjected to extensive life tests at temperature extremes of -23 and +66°C, following Vibration and Armature Motion Tests. A deviation from the test plan resulted in two solenoids being operated for 15,000 strokes and two for 23,000 strokes. See PIR 4323-FM-260.

As a result of loosened pole pieces after 10,000 strokes, the solenoids were reworked during the life test. However, the number of successful strokes of each of the solenoids is very large compared to the flight requirement which is in the order of 100 strokes.

Disposition: The two-way solenoids were qualified for ATS flight use.

#### 12.4 CABLE CUTTER ASSEMBLY

GE Identification Numbers: 895D724P1 (cartridge)  
115C7516P1 (guillotine)

Manufacturer: Hoxex, Inc.  
Hollister, California  
FSCM 10640

Manufacturer's Identification Number: Model 5401 (cartridge)  
Model 5402 (guillotine)

Date of Manufacture of Parts: July, 1965

Purpose of Test: Qualification for ATS Program

Test Conducted By: Hoxex, Inc.  
Hollister, California

Quantity of Items Tested: 33 cartridges  
28 guillotines

Date Test Completed: August 27, 1965

Documentation: a) GE Drawing No. 895D724, Rev. B.  
b) GE Drawing No. 115C7516, AN-1  
c) GE Specification No. SVS 5292, AN-1  
d) GE Propulsion Engineering Report No. PER 4182-15

Comments: The Hoxex Model 3956 guillotine with Model 3600 cartridge were formerly qualified to sever a 3/32 inch cable. The function on the ATS Program is to sever a 1/8 inch 7 x 19 stranded stainless steel cable. The assembly was upgraded by substituting cartridge Model 5401 (formerly Model 3700) and other changes. Environmental tests were performed on the redesigned cartridge and guillotine (Models 5401 and 5402) at qualification test levels per Table I of GE Specification SVS-5292. Load level determination tests and pressure versus time tests were performed. The redesigned models met all requirements.

Disposition: The cable cutter assemblies were qualified for ATS flight use.



## 12.5 EXTENSION MOTOR (BRAKE MOTOR)

deHavilland Identification Number: 5398L10

Manufacturer: Globe Industries  
Dayton, Ohio  
FSCM 25140

Manufacturer's Identification Number: 106A161

Date of Manufacture: January, 1966

Purpose of Test: Qualification for ATS Program

Test Conducted By: GE Spacecraft Department  
Valley Forge, Pennsylvania

Quantity of Parts Tested: 2

Date Test Completed: June 6, 1966

Documentation: a) deHavilland Drawing No. 5398L10, Rev. B  
b) deHavilland Specification No. DHC-SP-SG. 63, Issue A  
c) deHavilland Specification No. DHC-SP-ST. 48, Issue A  
d) GE Test Plan No. ETP-4165-2, Rev. D  
e) GE PIR No. 4383-ATS-102, Qualification Test Report, Brake Motor

Comments: Qualification testing was initiated on the two samples - S/N 106 and S/N 107. Initial parameters, which were out-of-spec are considered acceptance items rather than qualification items. S/N 107 exhibited changes in commutation characteristics during low pressure functional testing at high temperature (+59°C) and at low temperature (-17°C). Vibration and Acceleration Tests were successfully performed per the test plan. In the Life Test, the motor successfully completed the required 14-hour portion, and the Life Test was continued. At 40 hours in the Life Test, S/N 107 ceased to operate due to an open brush connection. Analysis of the motor by the manufacturer did not reveal any cause of the open brush.

S/N 106 had received preliminary measurements only and, although the motor was in like-new operating condition and met all requirements, it was returned to the vendor with S/N 107, which was delivered for analysis of the open brush. Nothing abnormal was found in the teardown and analysis by the manufacture.

Note that, with a duty cycle of 14 percent, the Life Test duration of 40 hours represents motor operating time in mission environment of 5.6 hours. This is 8 times the total required operating time for 40 minutes, and 34 times the required mission time of 10 minutes. In addition, to preclude the use of motors containing insipient faults, all motors are being monitored for armature current signature during component testing of the Primary Boom assemblies.

Disposition: The motors were qualified for ATS flight use.

## 12.6 SCISSOR MOTOR (GEARHEAD MOTOR)

deHavilland Identification Number: 5398L11

Manufacturer: Globe Industries  
Dayton, Ohio  
FSCM 25140

Manufacturer's Identification Number: 114A152

Date of Manufacture: January, 1966

Purpose of Test: Qualification for ATS Program

Test Conducted By: GE Spacecraft Department  
Valley Forge, Pennsylvania

Quantity of Parts Tested: 2

Date Test Completed: June 28, 1966

Documentation: a) deHavilland Drawing No. 5389L11, Rev. A.  
b) deHavilland Specification No. DHC-SP-SG. 64, Issue A  
c) deHavilland Specification No. DHC-SP-ST. 48, Issue A  
d) GE Test Plan No. ETP-4165-3, Rev. C  
e) GE PIR No. 4383-ATS-011, Qualification Test Report, Gearhead Motor

Comments: Qualification testing was initiated on the two samples - S/N 110 and S/N 111.

Initial parameters which were out-of-spec are considered acceptance items rather than qualification items. S/N 110 developed audible noise after ten hours of operation at room ambient conditions during functional checkout and test. Although the motor was still in operating condition and met all requirements, it was returned to the vendor for analysis. Nothing abnormal was found in the teardown and analysis by the manufacturer.

S/N 111 was subjected to tests of Thermal Vacuum, Vibration, Acceleration, and Life per the test plan and met all requirements. In the Life Test, the motor successfully completed the required 24-hour portion. The test was continued per the test plan. At 60 hours, armature current had become electrically noisy and load current was observed to increase. These changes apparently were minor and did not affect performance. At 440 hours in the Life Test, the motor ceased to operate due to an open brush connection. Analysis of the motor by the manufacturer did not reveal any cause of the open brush.

Note that, with a duty cycle of 8 percent, the Life Test duration of 440 hours represents motor operating time in mission environment of 35 hours. This is 40 times the total required operating time of 53 minutes, and 100 times the required mission time of 21 minutes. In addition, to preclude the use of motors containing insipient faults, all motors are being monitored for armature current signature during Component Testing of the Primary Boom Assemblies.

Disposition: The motors were qualified for ATS flight use.

## 12.7 LINEAR ACTUATOR ASSEMBLY

GE Identification Numbers: 895D724P1 (cartridge)  
47C209579P- (linear actuator)

Manufacturer: Hoxex, Inc.  
Hollister, California  
FSCM 10640

Manufacturer's Identification Number: Model 5626 (thruster)

Date of Manufacture of Parts: March, 1966

Purpose of Test: Qualification for ATS Program

Test Conducted By: Hoxex, Inc.  
Hollister, California

Quantity of Assemblies Tested: 38

Date Test Completed: May 18, 1966

Documentation: a) GE Drawing No. 895D724, Rev. B  
b) GE Drawing No. 47C209579, Rev. E  
c) GE Specification No. SVS 7428, AN-1 and AN-2  
d) GE Reaction and Actuation Equipment Report No. PER 41M5

Comments: The Hoxex Model 562601 Thruster is a version of the Hoxex Model 2900 Linear Actuator with a Hoxex Model 5401 Cartridge replacing the original pressure cartridge. The original model tested (47C209579P2) failed to meet requirements. The linear actuator was redesigned changing the piston material from aluminum to stainless steel. Environmental tests were performed on the redesigned models at qualification test levels per Table I of GE Specification SVS-7428. The redesigned models (47C209579P3) met all requirements.

NOTE. Since completion of the testing reported herein, a case of body rupture was encountered, even though the actuator never failed to function. The linear actuator was redesigned, changing the body material from aluminum to stainless steel. The redesigned and requalified unit is model 47C209579P4.

Disposition: The linear actuator assemblies (model 47C209579P4) were qualified for ATS flight use.

## 12.8 DAMPER BOOM RELEASE ASSEMBLY

GE Identification Number: 1) 47D209594A2 (Ball Lock Release Assembly)  
2) 895D724P1 (Cartridge, Pressure, Electro-explosive)  
3) 47D209579P3 and P4 (Linear Actuator)

Manufacturer: 1) Avdel, Inc.	2 and 3) Hoxex, Inc.
Burbank, California	Hollister, California
FSCM 84256	FSCM 10640

Manufacturer's Identification Number: 1) Avdel No. 51419  
2) Halex Model 5401  
3) Halex Model 5626

Purpose of Test: Qualification and Reliability Demonstration for ATS Program

Test Conducted By: GE Spacecraft Department and Halex, Inc.  
Valley Forge, Pennsylvania Hollister, California

Quantity of Items Tested: 1) 36  
2) 145  
3) 33 (P3) and 43 (P4)

Date Test Completed: October 20, 1966

Documentation: a) GE Drawing No. 47D209594, Rev. A  
b) GE Drawing No. 47C209579, Rev. E  
c) GE Drawing No. 895D724, Rev. B  
d) GE Specification No. SVS-7428  
e) GE Test Procedure Per No. 4182-SPTP-0016, Rev. C  
f) GE PIR No. 4TK2-ATS-IV-26  
g) GE PIR No. 4145S-266  
h) GE PIR No. 4363-KCL-329  
i) GE PIR No. 4341-ATS-36  
j) GE Test Report No. 41M3-001

Comments: Testing of the Damper Boom Release Assembly and its components was carried out in accordance with test procedure 4182-SPTP-0016. The testing was intended to demonstrate the reliability of the assembly and to affirm qualification. An evaluation of the test results showed an effective demonstrated reliability of 0.994 at a 50 percent confidence level.

Although the linear actuator performed its required function in all cases, the rupture of the bodies which occurred in the pyrotechnic actuation tests led to a redesign (from model P3 to Model P4) and a full requalification test. The redesigned model of the linear actuator met all requirements.

Disposition: The damper boom release assemblies were qualified for ATS flight use.

## 12.9 TRANSISTOR, SILICON, NPN

GE Identification Number: R4343P1

Manufacturer: Texas Instruments, Inc.  
Semiconductor Components Division  
Dallas, Texas  
FSCM 01295

Manufacturer's Identification Number: 2N2432

Date of Manufacture: August, 1965  
September, 1965

Purpose of Evaluation: Qualification for ATS Program

Evaluation Conducted By: GE Spacecraft Department  
Valley Forge, Pennsylvania

Quantity of Parts Evaluated: 9

Date Evaluation Completed: March 18, 1966

Documentation: a) GE Drawing No. R4343  
b) GE PIR No. 4493-033  
c) GE PIR No. 4494-042  
d) GE PIR No. 4493-048

Comments: The evaluation was initiated on five samples per PIR No. 4493-033. Results are reported in PIR No. 4493-042. As the result of an error during the Burn-In Test, three samples were damaged. A second evaluation was then performed on four new samples. See PIR No. 4493-048. Physical examination revealed no defects or deficiencies in the design or processing of the transistors. The electrical measurements were quite stable and indicated the ability to survive prolonged voltage and thermal stresses.

Disposition: The transistors were qualified for ATS flight use.

## 12.10 RELAY

GE Identification Number: R2313P11

Manufacturer: General Electric Company  
Waynesboro, Virginia  
FSCM 01526

Manufacturer's Identification Number: 3SAM1320A2

Date of Manufacture: September, 1965

Purpose of Evaluation: Qualification for ATS Program

Evaluation Conducted By: GE Spacecraft Department  
Valley Forge, Pennsylvania

Quantity of Parts Evaluated: 5

Date Evaluation Completed: July 29, 1966

Documentation: a) GE Drawing No. R2313  
b) Military Specification MIL-R-5757C  
c) GE PIR No. 4494-057  
d) GE PIR No. 4494-074, Rev. A

Comments: The evaluation was conducted on five samples in accordance with the evaluation plan - PIR No. 4494-057. The details and the results of the test and evaluation are reported in PIR No. 4494-074. All measurements met specification requirements. All design and construction details of the relay appeared to be sound, and the workmanship was good. The narrow spread of measurements of most parameters demonstrates product uniformity.

Disposition: The relays were qualified for ATS flight use.

**SECTION 13**  
**NEW TECHNOLOGIES**

## SECTION 13

### NEW TECHNOLOGIES

In compliance with the provisions of the NAS-5-9042 New Technologies clause, the Space Division of the General Electric Company maintained surveillance for the life of the contract over the design and development of the gravity gradient system for inventions, discoveries, improvements and innovations. Early in the effort, representatives from the New Technologies Agency at NASA/Goddard conducted a briefing on what constituted new technologies, the reason for reporting new technologies and the publications used by Goddard to disseminate these disclosures throughout NASA and into industry. This information was made available to all GE organizations at MSD engaged in the ATS gravity gradient design and the groups were monitored each month in quest of new technologies. Several candidate items were defined during the active period of design and development, and these were included as part of the quarterly progress reports. All disclosures defined during the year were published in the annual new technologies reports. These reports include:

- First Annual New Technologies Report, GE Document No. 65SD4471, dated July 31, 1965
- Second Annual New Technologies Report, GE Document No. 66SD4439, dated July 1966.

The most fruitful period in which new technologies were uncovered was during the engineering development phase of the contract. These activities were completed in 1966 and no new technologies were discovered since, even though all ATS activities at GE continued to be monitored for inventions or new uses for existing processes. Negative reports were issued each year by letter from the GE Contract Administrator for NASA programs. A summary of the more significant disclosures made during the ATS contract follows:



### 13.1 ANGLE INDICATOR

The angle indicator was incorporated into the CPD to sense the relative angle of the damper boom and provides a digital output of that angle in relation to the spacecraft center body through a possible arc of  $\pm 45$  degrees. A continuous 5-bit Gray code readout is provided. As a new technology, the device should have applications where a requirement exists to monitor angular motion.

Angle detection is accomplished with the system shown in Figure 13-1. A coded disc (1) is mounted to the damper boom shaft through which light is passed from one of two light sources (2) (3) onto phototransistors (4). The disc code utilizes an expanded Gray code and by taking advantage of the increasing allowable error of angle detection going away from null (as dictated by the requirements of the system), it is only necessary to use five bits. Typical outputs for any one shaft position would consist of three, 10-bit digital words, all of which are unique to that one position. The multiple words at each position are due to radial excursions of the damper boom shaft. The digital words will be catalogued and can be read directly or fed into a computer to give direct angular readout.

The light supply consists of a fiber optic bundle (5), one end of which is divided into ten small bundles (6); each fiber optic is aligned to a phototransistor (4). The other end is divided into two bundles (7) and (8) each of which is placed in the field of a collimated light beam coming from a tungsten filament lamp (9). The fiber optic bundle consists of approximately 5000 individual fibers that are scrambled in such a manner that one-half of the individual fibers opposite each phototransistor go to each light source. Each lamp is capable of supplying the required light intensity for all ten phototransistors; thus, the two lamps provide a redundant light source. Only one lamp is used at a time in the ATS application; switching to the other lamp is done by command. Depending on which lamp is selected, an average life of the lamps is from 10 to 15 thousand hours.

### 13.2 ANGLE INDICATOR READOUT DEVICE

The encoder in the boom angle indicator provides an angular position readout which is independent of small displacements of a rotating member in relation to a fixed member. Fundamentally, the device is a simple Gray-code encoder which has a slit pattern on a thin disc. The disc is attached to the rotating member (damper boom) that is to be monitored. The disc is shown in Figure 13-2. A collimated slit-beam of light either passes through or is interrupted by pattern lines on the disc; the light is detected by photodetectors which are located below the disc. Use of the Gray code pattern provides digitized readout while minimizing error at the code change point.

### 13.3 CPD CLUTCH MECHANISM

The diaphragm spring device and the associated clutch arrangement was designed for use in the Combination Passive Damper. The CPD contains two dampers -- an eddy current damper and a hysteresis damper. These dampers are alternately coupled to a single damping boom shaft (Figure 13-3) in orbit to test the relative merits of the two dampers to damp the libratory diaphragm spring (1), and faces (11) and (12) form a spool on the end of the actuator shaft which contact the surface of the diaphragm spring during actuation only.

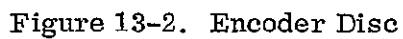
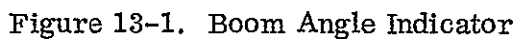
The coned diaphragm spring (1), has two stable positions, and is used as an over-center toggle. The diaphragm spring is coned so that it exerts a force on shaft one (6) such that the V-groove (7) contacts the lower clutch face (5) of the output shaft (3). The mating of these surfaces under the compressive load provided by the diaphragm spring (1) produces a friction coupling torque which allows shaft one (6) to drive the output shaft (3) rotationally with no restraining external force present. The V-shape of the engaging surfaces ensures that the mating shafts will be properly aligned axially and radially.

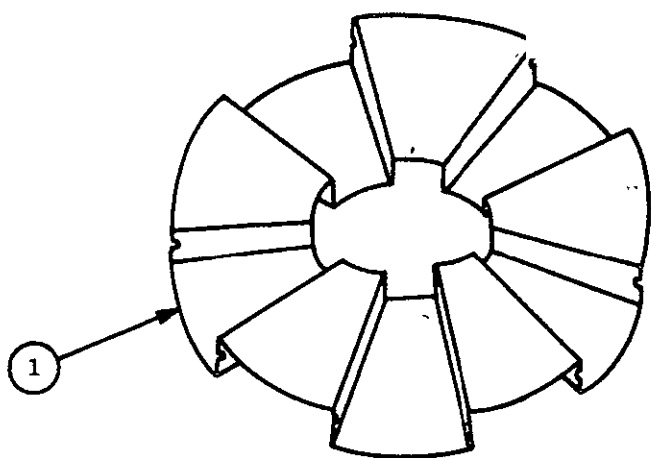
In transferring the output shaft (4) to shaft two (8), the actuator 10 is displaced linearly upward. This displacement causes spool face (11) to contact the surface of the diaphragm spring, driving it flat and then over-center so that the diaphragm spring (1)

back to the position shown in Figure 13-3b, where shaft one (6) is again coupled to the output shaft (3). Note in Figure 13-3b and c, that the inoperative shaft has a nominal clearance to the output shaft V-surface. Because of this clearance which is necessary to isolate the inoperative shaft, the output shaft (9) is displaced axially this same distance during switchover.

The novel features of the new technology are as follows:

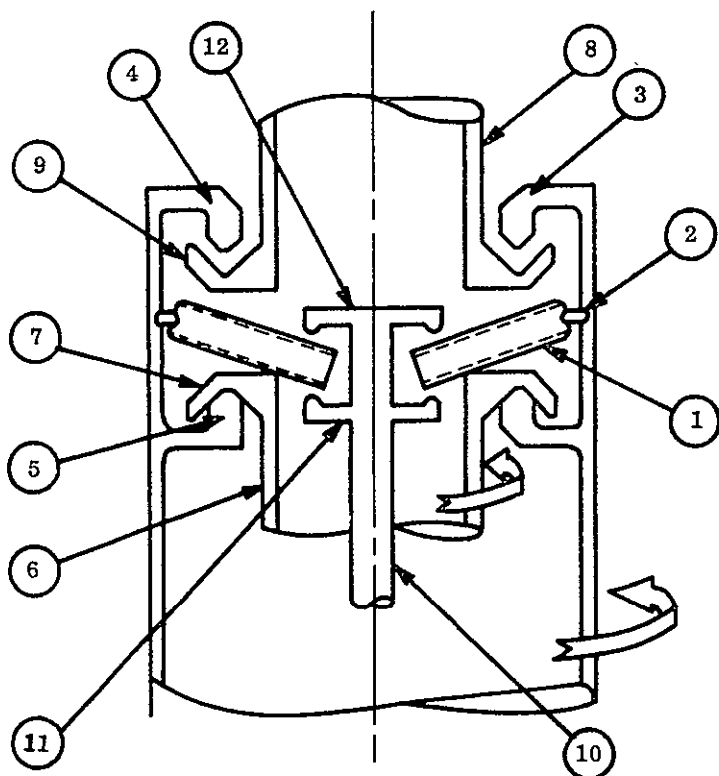
1. The overall clutch mechanism provides in a compact package a dual coupling method which eliminates all external forces that would tend to retard rotation or cause axial displacement. When the clutch is engaged in one direction, it is essentially floating and is completely free from the actuator and the disengaged component parts.
2. The fluted configuration (Figure 13-3a) of the diaphragm spring lends itself to a wide range of load-deflection combinations which are readily predictable. The spring, in combination with the pivot ring, has the properties of an over-center toggle device but with fewer parts. The spring has a larger "throw" than a plain Belleville washer, plus the advantage of having essentially equal force/deflection characteristics in each of the two operating directions. It also occupies less space than other similar over-center devices. The spring is formed in a flat (on-center) position, and is coned at assembly by the fact that the diameter of the holding ring is smaller than the free diameter of the flat spring. The deformation of the spring during coning and during subsequent over-center actuations is accounted for through simple bending of the sides and faces of the flutes. Stresses and loads resulting from such bending are readily calculable and any calculable and any desired load-deflection characteristics can be easily obtained. Load-deflection characteristics of other similar devices (i. e., Belleville washer and variations thereof) are more restrictive and less amenable to accurate prediction. Another advantage of the fluted configuration of the spring is that it can be manufactured without resorting to exotic manufacturing techniques.
3. The self-centering feature of the V-groove clutch surfaces as forced together by the spring is an integral advantage of the overall design. The V-groove arrangement ensures that the mating parts will repeatedly engage in the concentric position and with parallel faces for any location of clamping force within the engagement circle.



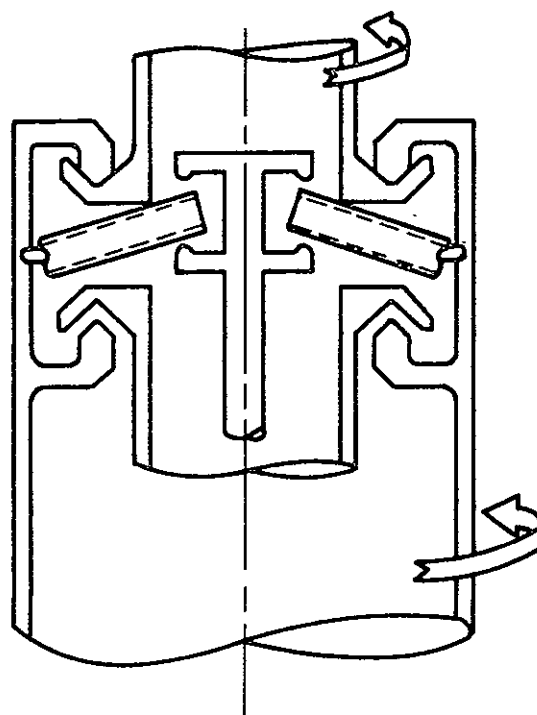


(a) DIAPHRAGM SPRING

- |                      |                      |
|----------------------|----------------------|
| 1. Diaphragm spring  | 7. Circular V-groove |
| 2. Ring              | 8. Shaft two         |
| 3. Output shaft      | 9. Circular V-groove |
| 4. Upper clutch face | 10. Actuator         |
| 5. Lower clutch face | 11. Lower spool face |
| 6. Shaft one         | 12. Upper spool face |



(b) EDDY-CURRENT DAMPER MODE



(c) HYSTERESIS DAMPER MODE

Figure 13-3. CPD Clutch Mechanism

